A. MAQBOOL, 2024

DOCTOR OF PHILOSOPHY THESIS

NİĞDE ÖMER HALISDEMİR UNIVERSITY
GRADUATE SCHOOL OF NATURAL AND APPLIED SCIENCES

T.R.
NİĞDE ÖMER HALİSDEMİR UNIVERSITY
GRADUATE SCHOOL OF NATURAL AND APPLIED SCIENCES
DEPARTMENT OF AGRICULTURAL GENETIC ENGINEERING

INTEGRATIVE AGRONOMIC AND GENETIC APPROACHES TO UNDERSTAND IRON AND COPPER DEFICIENCY RESPONSES IN SOYBEAN (*Glycine max* (L.) Merr) AND *Arabidopsis thaliana*

AMIR MAQBOOL

AUGUST 2024

T.R.

NİĞDE ÖMER HALİSDEMİR UNIVERSITY
GRADUATE SCHOOL OF NATURAL AND APPLIED SCIENCES
DEPARTMENT OF AGRICULTURAL GENETIC ENGINEERING

INTEGRATIVE AGRONOMIC AND GENETIC APPROACHES TO UNDERSTAND IRON AND COPPER DEFICIENCY RESPONSES IN SOYBEAN (*Glycine max* (L.) Merr) AND *Arabidopsis thaliana*

AMIR MAQBOOL

Doctor of Philosophy Thesis

Supervisor

Asst. Prof. Emre AKSOY

August 2024

The study entitled "**Integrative agronomic and genetic approaches to understand iron and copper deficiency responses in soybean (*Glycine max* (L.) Merr) and *Arabidopsis thaliana***" and presented by **Amir MAQBOOL** under the supervision of **Assist. Prof. Emre AKSOY** has been recognized as a Doctor of Philosophy thesis by the jury at the **Agricultural Genetic Engineering of Niğde Ömer Halisdemir University, Graduate School of Natural and Applied Sciences**.

Head: Prof. Ufuk DEMİREL, Niğde Ömer Halisdemir University

Member: Prof. Musa KAVAS, Ondokuz Mayis University

Member: Assoc. Prof. Ceyhun KAYIHAN, Başkent University

Member: Assist. Prof. Emre AKSOY, Middle East Technical University

Member: Assist. Prof. Ayten Kübra YAĞIZ, Niğde Ömer Halisdemir University

CONFIRMATION:

This thesis has been approved by the above jury members designated by the Board of Directors of the Graduate School of Natural and Applied Sciences on …/…/2024 and has been confirmed with the resolution of the Board of Directors on …/…/2024 and decision number…….

...../...../2024

Prof. Dr. Mustafa KARATEPE

DIRECTOR

THESIS CERTIFICATION

I certify that the thesis has been written by me and that, to the best of my knowledge and belief. All information presented as part of this thesis is scientific and in accordance with the academic rules. Any help I have received in preparing the thesis, and all sources used, have been acknowledged in the thesis.

Amir MAQBOOL

SUMMARY

INTEGRATIVE AGRONOMIC AND GENETIC APPROACHES TO UNDERSTAND IRON AND COPPER DEFICIENCY RESPONSES IN SOYBEAN (*Glycine max* (L.) MERR) AND *Arabidopsis thaliana*

MAQBOOL, Amir
Niğde Ömer Halisdemir University
Graduate School Of Natural And Applied Sciences
Department Of Agricultural Genetic Engineering

Supervisor Asst. Prof. Emre AKSOY

August 2024, 290 pages

Calcareous-alkaline soil-induced iron (Fe) deficiency chlorosis (IDC) impairs crop growth, yield, and nutritional quality. This thesis investigates agronomic and genetic strategies to enhance the productivity and seed nutrient content of soybean (*Glycine max* (L.) Merr.) and *Arabidopsis thaliana* under IDC conditions. IDC-tolerant and sensitive soybean cultivars were analyzed, showing that tolerant cultivars responded better to Fe fertilization, increasing seed Fe concentration, protein content, and size, while reducing seed phytate levels. Genetic analysis identified specific genes within quantitative trait loci (QTL) associated with IDC tolerance, and bioinformatic analysis of *Arabidopsis* orthologs identified a novel transcription factor, *GATA12*, involved in iron homeostasis in plant roots. Transcriptomic analysis of IDC-tolerant soybean cultivars showed differential expression of key transcription factors and transporters, including *UMAMIT28* from the UMAMIT amino acid transporter family, which plays a crucial role in iron and copper homeostasis. Functional characterization of *UMAMIT28* in Arabidopsis confirmed its involvement in maintaining Fe and Cu balance. This thesis highlights the importance of combining agronomic and genetic approaches to enhance crop yield, nutritional quality, and resilience under IDC stress, addressing global food

security and malnutrition. Additionally, the discovery of GATA12 and UMAMIT28 advances the understanding of transmetal homeostasis in plants.

Keywords: Calcareous-alkaline soil, IDC tolerance, GATA, genotypic variation, UMAMIT, yield

ÖZET

SOYA (*Glycine max* (L.) MERR) VE *Arabidopsis thaliana*'DA DEMİR VE BAKIR EKSİKLİĞİ TEPKİLERİNİ ANLAMAK İÇİN ENTEGRATİF TARIMSAL VE GENETİK YAKLAŞIMLAR

MAQBOOL, Amir
Niğde Ömer Halisdemir Üniversitesi
Fen Bilimleri Enstitüsü
Tarımsal Genetik Mühendisliği Anabilim Dalı

Danışman Dr. Öğr. Üyesi Emre AKSOY

Ağustos 2024, 290 sayfa

Kireçli-alkali topraklarda gözlenen demir (Fe) eksikliği klorozu (IDC), bitki gelişimi, verim ve besin kalitesini olumsuz etkiler. Bu tez, soya (*Glycine max* (L.) Merr.) ve *Arabidopsis thaliana*'nın IDC koşullarında verim ve tohum besin içeriğini artırmak için tarımsal ve genetik stratejileri birleştirmektedir. IDC'ye toleranslı ve hassas soya çeşitleri incelenmiş, toleranslı çeşitlerin Fe gübrelemesine daha iyi yanıt vererek tohum Fe konsantrasyonu, protein içeriği ve tohum boyutunu artırdığı, fitat seviyelerini ise azalttığı gözlemlenmiştir. Soyadaki genetik analizlerle IDC toleransı ile ilişkili kantitatif özellik lokusları (QTL) içinde spesifik genler tanımlanmış ve bu genlerin *Arabidopsis* ortologlarının biyoinformatik analiziyle Fe homeostazında rol oynayan yeni bir transkripsiyon faktörü olan GATA12 keşfedilmiştir. IDC'ye toleranslı soya çeşitlerinin transkriptomik analizi, önemli transkripsiyon faktörleri ve taşıyıcıların farklı şekilde ifade edildiğini ortaya koymuş; özellikle UMAMIT amino asit taşıyıcı ailesinden UMAMIT28'in demir homeostazında kilit rol oynadığı belirlenmiştir. Arabidopsis'te UMAMIT28'in fonksiyonel karakterizasyonu, bu genin demir ve bakır homeostazındaki rolünü doğrulamıştır. Bu tez, tarımsal ve genetik yaklaşımların birlikte kullanılmasının, gıda güvenliği ve yetersiz beslenme sorunlarına çözümde önemini vurgulamaktadır.

Ayrıca, bitkilerde transmetal homeostazı için gerekli olan yeni bir transkripsiyon faktörü ve taşıyıcıyı tanımlanmıştır.

Anahtar Kelimeler: Kireçli-alkalin toprak, demir eksikliği kloroz toleransı, GATA, genotipik varyasyon, UMAMIT, verim

ACKNOWLEDGEMENTS

First, I would like to thank Almighty for giving me the courage to complete this doctoral thesis. I would like to thank my beloved supervisor Assistant Professor Emre Aksoy who has taught me everything, starting from the very first day of the thesis and guiding me properly and providing a chance to work on several experiments in his lab. I would like to thank Professor Sebastien Thomine CNRS, University of Paris Saclay, France, who provided me a chance to work in his lab for a part of the PhD thesis. I would like to thank the jury members Professor Ufuk Demirel, Professor Musa Kavas, Associate Professor Ceyhun Kayıhan and Assistant Professor Ayten Kübra Yağız for their precious time for the evaluation of thesis and progressive reports.

I would like to dedicate this thesis to my beloved parents and brothers who supported me throughout the journey.

I would like to thank Ayhan Sahenk Foundation for providing me with the monthly stipend for four years.

I would like to thank Middle East Technical University, Ankara, Turkey for providing me the lab space to conduct the experiments related to doctorate thesis.

I would like to thank the University of Paris Saclay and European COST ACTION "Trace metals metabolism in Plants" (CA19116) for providing me with the funding for my stay at CNRS Gif Sur Yvette via two STSMs.

I would like to thank the Niğde Omer Halisdemir University for partially funding the doctorate thesis under the project number TGT 2020/16-LÜTEP.

I would like to thank TUBITAK (The Technological and Scientific Research Council of Turkey) for providing the funding for the thesis work with project numbers 119Z149, 216Z153, 122Z968, 123N986 and 122Z428.

SYMBOLS AND ABBREVIATIONS

Symbols	Description
cm	Centimeter
℃	Degrees Celsius
µg	Microgram
µL	Microliter
µmol	Micromole
mmol	Millimole
g	Gram
L	Liter
mM	Millimolar
M	Molar
µM	Micromolar
min	Minutes
rpm	Rounds Per Minute
nm	Nanometer
sec	Seconds
h	Hour

Abbreviations	Description
WHO	World Health Organization
IDC	Iron Deficiency Chlorosis
PCR	Polymerase Chain Reaction
qRT-PCR	Quantitative Real Time PCR

TABLE OF CONTENTS

LIST OF FIGURES

LIST OF TABLES

CHAPTER I

INTRODUCTION

According to the World Health Organization (WHO), iron (Fe) deficiency is one of the major problems affecting more than a billion people worldwide. As plants are the primary source of food, deficiency of Fe in plant edible parts leads to Fe deficiency in both animals and humans, which results in growth defects and several diseases (Markova et al., 2019). Fe is the key factor involved in fundamental biological processes in all living organisms. In plants, iron is required for essential biological processes including respiration, photosynthesis, and chlorophyll biosynthesis, and serves as a cofactor of enzymes involved in oxygen and electron transport, and many others (i.e., iron-sulfur and redox enzymes) (Zheng et al., 2010). However, deficiency of Fe leads to hampered plant growth and development in all plant stages which results in poor nutritional value and yield of the crop (Rajniak et al., 2018). Iron is the fourth most abundant element in the Earth's crust. However, despite its high prevalence, its bioavailability is limited because most of the iron in soils exists as oxides and hydroxides, which are poorly soluble and therefore not easily accessible for plant uptake. Additionally, calcareous soils resulting from high carbonate and bicarbonate concentrations lead to insufficient Fe uptake by plants (Lucena et al., 2007). High soil pH is a painstaking challenge for researchers because according to an estimate, about 30% of the world’s arable soils are calcareous with low Fe bioavailability. Thus, high pH conditions are attributed to voluminous areas of Fe-deficient soils for the plants (Takahashi, 2003). The inability of plants to uptake sufficient Fe from the soil results in iron deficiency chlorosis (IDC), visible in the interveinal tissues of young leaves. Species that are poorly adapted to calcareous soils, including crops like fruit trees and soybeans, as well as taxa from acidic environments, often develop lime-induced (high pH condition) chlorosis. This condition arises due to inadequate uptake, improper distribution, or immobilization of iron (Fe) (Zohlen and Tyler, 2004: Gautam et al., 2021).

To fulfill the iron demand plants have evolved different strategies to uptake Fe from the soil and translocate it from the roots into the shoots and/or seeds (Aksoy et al., 2018). According to iron uptake mechanisms plants are divided into two classes Strategy I plants

and Strategy II plants (Kobayashi et al., 2012). The main difference between the two strategies is the iron form taken up from the rhizosphere: Strategy I plants can uptake Fe in the form of Fe^{2+}, while Strategy II plants have evolved mechanisms to uptake the Fe^{3+}. Dicots and non-gramineous monocots mobilize Fe from the soil by Strategy I. In this strategy, Fe is taken up by the plant roots in three steps, i.e., 1) the acidification of rhizosphere by proton extrusion mediated by H+-ATPASE (AHA), 2) the reduction of non-soluble $Fe3^{+}$ into Fe^{2+} by the action of FERRIC CHELATE REDUCTASE/FERRIC REDUCTION OXIDASE (FCR/FRO), and 3) the uptake of Fe2+ by a divalent metal transporter, IRON-REGULATED TRANSPORTER1 (IRT1). To maintain Fe homeostasis, plants must sense the bioavailable Fe in the growth medium and fine-tune their transcriptome accordingly. Fe uptake and long-distance translocation are primarily regulated by bHLH transcription factors (Gao et al., 2019). These factors fall into two major signaling groups centered on the FER-LIKE IRON DEFICIENCY INDUCED TRANSCRIPTION FACTOR (FIT) and the POPEYE (PYE) networks (Kobayashi, 2019). The FIT network, localized in the root epidermis, regulates Fe uptake from the rhizosphere, while the PYE network, specific to the root vasculature, is involved in Fe transport into and out of the vascular tissues (Mari et al., 2020). Although these two networks are proposed to function synchronously (Kobayashi et al., 2019), their interconnection has not been demonstrated yet. Apart from the bHLH transcription factors, different transcription regulators also play a role in the control of Fe uptake and distribution mechanisms. The studies conducted in recent years have demonstrated the interaction of different transcription factors with the bHLH regulatory network to control the pathways involved in hormonal regulations, abiotic stress responses, and even plant growth and development (Gao et al., 2019; Kobayashi, 2019).

Soybean (*Glycine max* (L.) is an important leguminous crop having high protein and oil content (Singh et al., 1999) and is highly affected by Fe deficiency. Soybeans follow the reduction-based strategy of iron uptake from the soil. However, soybean comes under the category of those crops which are highly affected by iron deficiency. Like other plants, low Fe availability leads to hampered chlorophyll synthesis, shorter plant stature, and poor yield in soybean (Vasconcelos et al., 2014). In soybean, yield losses due to Fe deficiency chlorosis (IDC) are estimated at millions of tons annually (Naeve, 2006). Several practices have been performed to solve IDC, including expensive fertilizer applications and tedious agronomic practices. These agronomic practices need to be

repeated every year and increase the production cost. However, the identification of tolerant soybean genotypes and the development of transgenic lines that can perform better under Fe-deficient conditions and are efficient in Fe uptake from the recalcitrant pools seems to be the best and long-lasting solution to the problem.

The physiological effects of IDC in soybeans have been studied in detail, but its molecular mechanisms have not been resolved yet. Studies involving the molecular characterization of IDC in soybeans focused on genetically identical lines. Although the number of studies on this topic is high in the literature, the progress in understanding the molecular mechanisms of IDC tolerance in soybean is unsatisfactory since studies were generally focused on Fe uptake mechanisms. In this thesis study, molecular differences in IDC tolerance and sensitivity in different soybean genotypes were studied. Different from present studies in the literature, the incorporation of different soybean genotypes in this thesis has strengthened the identification of novel genes determining the sensitivity or tolerance to IDC.

Several studies have been done to study the physiological and biochemical effects of IDC in some soybean cultivars, but the molecular mechanisms behind IDC tolerance and sensitivity have not been understood well. Previous studies are related to the characterization of IDC-responsive genes in near-isogenic soybean lines (Clark (Fe-efficient line) and IsoClark (Fe-inefficient line) by microarray (O'Rourke et al., 2007) and recently by next-generation sequencing (NGS) techniques (Kohlhase et al., 2021: Atencio et al., 2021). In our previous study, the physiological and biochemical responses of 20 different soybean cultivars registered in Turkey were studied (Maqbool, 2018). Among them, two sensitive and two tolerant soybean cultivars in the 3rd maturation group (medium-late) were selected to be studied further in this thesis due to their differential responses under IDC.

The current study involves the transcriptomic analyses of the two tolerant soybean cultivars (Arısoy and Sa-88) against iron deficiency and the identification of molecular insights responsible for the tolerance mechanisms. Therefore, the main objective of this thesis is to characterize the molecular mechanisms responsible for the IDC tolerance of tolerant soybean genotypes, respectively. This characterization study led to the identification of novel transporters and/or transcription factors in soybeans. Previous

studies resembling this had been done on NIL (near-isogenic lines) while the current study involves the transcriptomic analyses of two distinct related cultivars under different iron available conditions. The use of two different cultivars led to the identification of different and unique new mechanisms which may help in reducing IDC yield losses and iron biofortification of different crop species.

CHAPTER II

LITERATURE REVIEW

2.1. Iron Deficiency in Plants

Particularly for all living organisms iron is an essential micronutrient as it acts as a cofactor of necessary metalloproteins involved in a wide range of physiological processes such as in the case of plants in sulfur and nitrogen assimilation, respiration, photosynthesis, and the biosynthesis of several amino acids (Li et al., 2023). According to the World Health Organization (WHO), almost 1.6 billion people are affected by iron deficiency (McLean et al., 2009). Fe homeostasis impairments in humans are linked to several health problems, including neurological illnesses, higher cancer risk, and Fe-deficient anemia (Li et al., 2023). Iron is the fourth most abundant element in the earth's crust, despite its high occurrence the chemical properties in oxygenated environments limit its bioavailability to the plants resulting in poor yield and nutrient value of the crop species. In plants, Fe deficiency leads to hampered chlorophyll synthesis and leaf chlorosis (Zhang et al., 2018). One of the interesting features of Fe deficiency in plants is that older leaves can grow at a normal rate while young leaves show chlorosis more prominently (Terry et al., 1995). Reduced leaf biomass and short plant stature are also the other symptoms of Fe deficiency in plants (Jiménez et al., 2019). As plants are the primary source of food, ultimately restricted uptake of Fe leads to Fe deficiency anemia in humans and animals (Lopez-Millan et al., 2013). Correcting the Fe deficiency in plants involves the use of Fe fertilizers and soil management practices. Among these fertilizers, synthetic chelates like Fe-EDDHA (Ethylenediamine di-2-hydroxyphenyl acetate ferric) and Fe-EDTA (ethylenedinitrilo) tetraacetate ferrate) are commonly used in agricultural practices. In some cases, foliar spray of iron (II) sulfate ($FeSO_4$) is being practiced but needs repetitions at different plant growth stages. In addition to the direct application of iron fertilizers, soil amendments are also being practiced, involving the application of organic matter in the soil. Organic matter application improves the soil structure, increases microbial activity, and releases chelating agents that help the plant with Fe uptake and solubilization (Barton et al., 2007).

2.2. Iron Uptake Strategies in Plants

To cope with inadequate iron availability plants have adopted two different strategies known as Strategy I and Strategy II (Marschner and Romheld, 1986), however, a combined strategy has been found in Strategy II rice as it can uptake Fe^{2+} as well as Fe^{3+} (Ricachenevsky and Sperotto, 2014). The main difference between these two strategies is the oxidized form of the iron i.e. Strategy I plant can take iron in the Fe^{2+} form while Strategy II plants involve the uptake of Fe^{3+} (Lucena et al. 2007). Dicots and non-gramineous monocots mobilize iron from the soil by Strategy I while grasses opt for Strategy II (Aksoy et al.,2018).

2.1.1 Reduction Strategy

In Strategy I, also known as reduction strategy, Fe is uptaken by the plants in three steps i.e.,

i) Acidification of rhizosphere by proton extrusion which is mediated by AHA2
ii) Reduction of non-soluble Fe^{3+} into Fe^{2+} by the action of the ferric chelate reductase FRO
iii) Uptake of Fe^{2+} by a divalent metal transporter IRT1, additionally low-affinity iron transporter NRAMP1 cooperates with the IRT1 for iron uptake under replete iron conditions (Castings et al., 2016).

In addition to this coumarins also take part in iron uptake in the reduction-based strategy plants. Depending on the external pH, plants decide to secrete the type of coumarin, which is sideretin, in case of low pH, and a more stable complex fraxetin at high pH. These coumarins not only chelate with the iron but may also have a role in its reduction at the root surface. PDR9 is the main candidate that helps in the extrusion of coumarins from the roots (Rajniak et al., 2018: Liang et al., 2022). Interestingly, Strategy I plant peanut is also able to absorb the Fe^{3+}–PS complex (secreting by neighboring gramineous plants), a mechanism followed by Strategy II plants (Xiong et al.,2013).

2.1.2 Chelation Strategy

On the other hand, grasses like rice, barley, and maize utilize Strategy II (also known as chelation strategy) which includes the release of phytosiderophores (PS) by plant roots. These phytosiderophores make complexes with Fe^{3+} (phytosiderophores-Fe^{3+}) present in the soil, PS has a strong affinity to chelate Fe^{3+}. Finally, these complexes are directly uptaken by the plant roots with the help of a plasma membrane-localized oligopeptide transporter known as YSL1 (Li et al., 2017; Zhang et al., 2019).

2.2. Long-distance Transport of Iron

IRT1 is localized at the outer membrane of root epidermal cells indicating where it first enters in the symplast transport route (Barberon et al., 2014). Here, another metal transporter, NATURAL RESISTANCE-ASSOCIATED MACROPHAGE PROTEIN1 (NRAMP1), is reported to cooperate with the IRT1 in Fe uptake (Castaings et al., 2016). Once entering the plant, body iron needs to be transported to the upper parts of the plants where it is needed in the leaves for chlorophyll synthesis and electron transport, etc. Low iron transportation leads to hampered chlorophyll synthesis resulting in severe chlorosis prominent in the younger leaves especially, indicating the strong sink region. Because of the redox nature of Fe^{2+}, which is harmful to the cells, within the plant body iron must always be transported in the chelated form, while on the other hand oxidized form of iron (Fe^{3+}) cannot be efficiently mobilized because its low solubility (Kobayashi et al., 2019). Therefore, long-distance translocation of iron in the xylem and phloem both require its chelation with the low molecular weight chelators to avoid its precipitation as well (Chao et al., 2022).

As the xylem consists of dead cells here the Fe translocation is passive compared to the phloem (living cells) (Kobayashi et al., 2019). In the xylem transpiration stream and root pressure are one of the possible ways of iron translocation. In the xylem, one of the key transporters that take part in iron homeostasis is the FERRIC REDUCTASE DEFECTIVE3 (FRD3), which is responsible for the efflux of citrate into the xylem apoplast. This citrate chelates with Fe^{3+}, forming the Fe^{3+}-citrate complex necessary for iron transportation via xylem (Green & Rogers, 2004). The transporters involved in the citrate efflux in the xylem are from the MATE family and are conserved in grasses (rice)

and non-grasses (*A. thaliana*). One of them is recognized as FRD3 in non-grasses and FRDL1 in grasses, indicating the similar xylem iron transportation pathways in both plant groups. However, the transporters that are involved in the efflux of Fe directly into the xylem are still unknown.

Iron transportation via phloem plays an important role in supplying sufficient iron to the growing tissue such as seeds, which is important for humans as edible parts in the case of most of the crop species. In phloem, iron is predominantly found as Fe^{2+}, chelated with low molecular weight compounds such as nicotianamine (NA) or deoxymugineic acid (DMA), which prevents its precipitation. In addition, it minimizes Fe toxicity as the chelation prevents radical production via the Fenton reaction. To reach sink tissues symplastic pathway continuity in the phloem helps with iron movement between the cells (Schuler et al., 2012). Iron remobilization is an important process during the senescence (aging) of the different plant tissues, here iron moves from source to sink, particularly from older leaves to the younger and growing tissues like siliques and seeds via the phloem. A schematic diagram of iron uptake in reduction-based strategy plants is given in Figure 2.1.

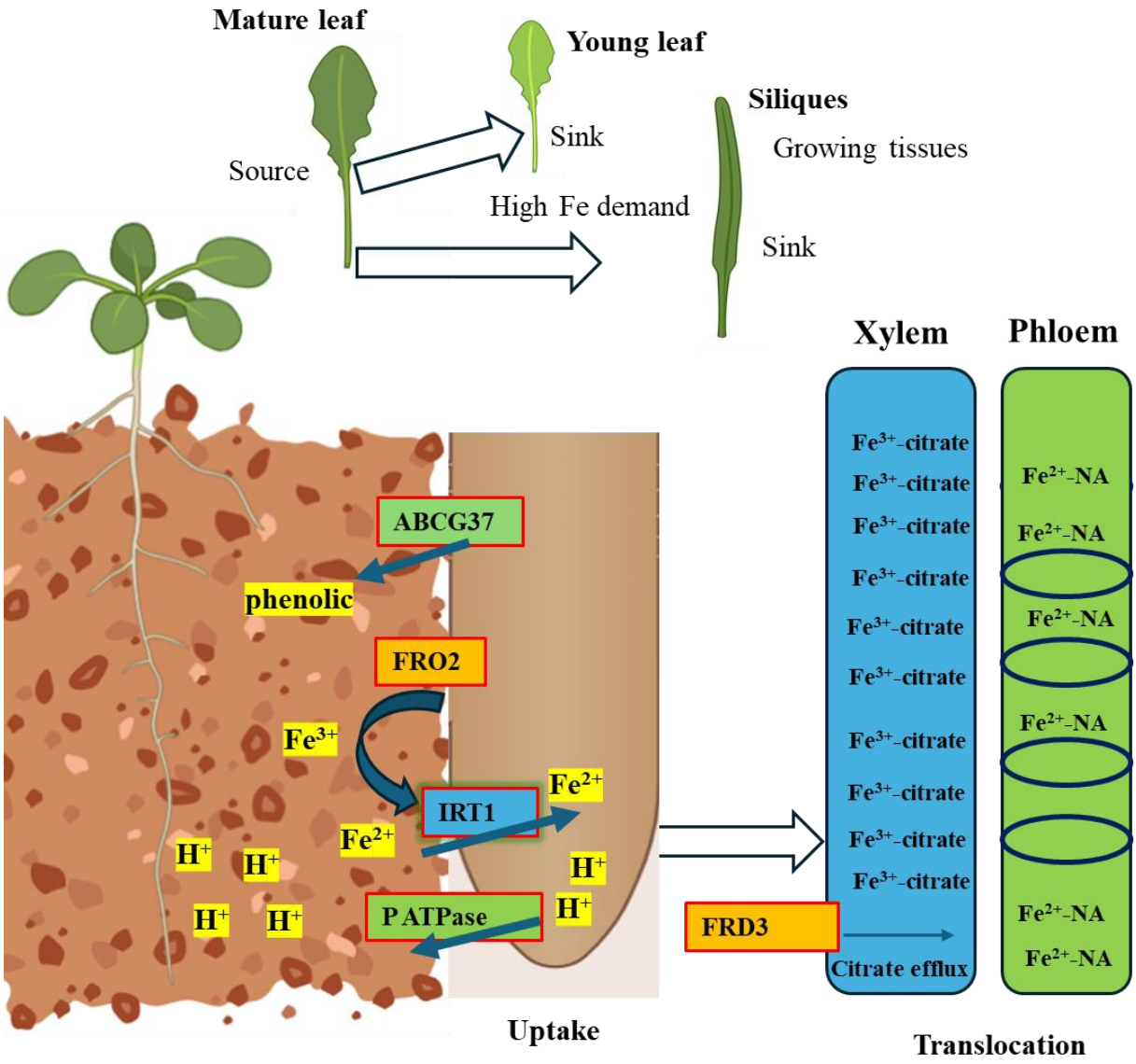

Figure 2.1. Schematic diagram of iron uptake in reduction-based strategy plants (dicots) and iron forms in xylem and phloem.

2.3. Iron Storage in Plants

Iron deficiency is a serious problem and maintaining adequate iron levels is crucial for plant cells while excess iron is toxic for the cells. To avoid toxicity and for re-utilization under iron deficiency, iron should be stored properly. Plants have adopted intricate pathways to store iron in their cells. Plants store intracellular iron primarily by exploiting the ferritin proteins located in the plastid (Zheng., 2010). The other hot spot for iron storage is vacuoles, which provide iron to plants under iron-deficient conditions and at

different growth stages (Liu et al., 2023). Iron storage in plants depends on the type and species of the plant. For example, in the case of *A. thaliana*, the vacuole is the major source of iron storage, which constitutes about 50 percent of the total iron while only 5% of iron storage is covered by the ferritins (Jeong et al., 2017; Ravet et al., 2009). However, in the case of pea, the amount of ferritin-iron is around 92% of the total seed iron in the embryo axis (Marentes et al., 1998). VACUOLAR IRON TRANSPORTER1 (VIT1) was first identified as the vacuolar iron transporter as an orthologue of the yeast iron transporter CCC1 (Kim et al., 2006; Connorton et al., 2017). Although no difference was found between the total iron content of *vit1* mutants and the wild type, iron accumulation was absent in the vacuoles of pro-vascular cells (Kim et al., 2006). Later, two other vacuolar iron transporters, AtNRAMP3 and AtNRAMP4, were identified for iron efflux into the cytosol at the seed germination stages under iron-deficient conditions (Thomine et al., 2003; Lanquar et al., 2005). As described above, only 5% of iron is stored as ferritins in Arabidopsis showing that ferritins are the minor source of iron storage in this plant. There are four ferritin genes known in Arabidopsis and they were named *FER1-4*. *AtFER1*, *AtFER3,* and *AtFER4* are known to be expressed in vegetative and green tissue of the plants while *AtFER2* is the only ferritin that is expressed in the seeds (Briat et al., 2010**)**. In plants, ferritins are predominantly located in the plastids, indicating the iron storage pool besides vacuoles in the cells (Connorton et al., 2017).

2.4. Transcriptional Control of Iron Homeostasis

To avoid both iron deficiency and toxicity, plants have adopted a sophisticated regulatory network to control its uptake and translocation. In *A. thaliana*, two main regulatory networks have been identified, which are reported to control different groups of genes to modulate the iron deficiency response for efficient iron uptake and translocation. The first one is the FER-LIKE IRON DEFICIENCY-INDUCED TRANSCRIPTION FACTOR (FIT) network and the second is the POPEYE (PYE) network. These regulatory networks also interact with each other (Maqbool et al., 2023). FIT and PYE transcription factors are the members of bHLH transcription factors (Zhang et al., 2015).

FER was the first regulatory gene reported from tomato and known to regulate the expression levels of *IRT1* and *FRO1* in tomato plants (Ling et al., 2002). Later, FER ortholog FER-LIKE IRON DEFICIENCY-INDUCED TRANSCRIPTION FACTOR

(FIT - AtbHLH29) was identified as the master regulator in the *A. thaliana,* which regulates the expression levels of iron homeostasis genes under low iron availability (Colangelo and Guerinot, 2004). Arabidopsis *fit* and tomato *fer* mutants show chlorosis even under normal conditions and require additional iron for their development. *fit* null mutant is lethal under normal conditions until additional iron is supplied (Colangelo and Guerinot, 2004). Under iron deficiency conditions, *FIT* is upregulated in general, while FIT protein levels are strongly controlled by the 26S proteasome-mediated degradation according to the plant's iron status (Lingam et al., 2011: Cui et al., 2018). Overexpression of FIT did not affect the regulation of *ITR1* and *FRO2*, because its regulatory control depends upon its dimerization with other Ib proteins including bHLH38, bHLH39, bHLH100, and bHLH101 (Maurer et al., 2014). These four proteins are expressed independently of the *FIT.* The regulation of these proteins depends on the low iron stress and their expressions are dramatically reduced when higher iron levels are supplied. The promoter activity of group Ib bHLH transcription factors has been detected mainly in the epidermis and lateral emergence zone of the roots (Gao et al., 2019), indicating their role in the iron uptake at the root surface. The FIT network together with other Ib proteins bHLH38, bHLH39, bHLH100, and bHLH101 showed the importance of the bHLH transcription factors family in iron homeostasis.

The other regulatory network includes the POPEYE (PYE – AtbHLH47), which is specifically induced in root pericycles under Fe-deficient conditions and plays an important role in iron homeostasis. *pye-1* mutants were sensitive to iron deficiency and PYE regulates the expression of *NICOTINAMINE SYNTHASE4* (*NAS4*), *FERRIC CHELATE REDUCTASE3* (*FRO3*), and *ZINC-INDUCED FACILITATOR10* (*ZIF10*). The expressions of *NAS4*, *FRO3,* and *ZIF10* are highly upregulated under Fe-deficient conditions in *pye-1* mutants (Long et al., 2010: Liu et al., 2015).

Interestingly, in rice, a PYE homolog protein *IRO3* transcript is induced 25–90 times higher in both roots and shoots under iron deficiency. Induction of *OsIRO3* was specific to iron deficiency and remained unchanged by other micronutrient deficiencies. The expression of *OsIRO3* is specifically induced by Fe deficiency, and not by other micronutrient deficiencies. While *IRO3* overexpression lines in rice were shown to be hypersensitive to low iron availability and suppress the expression patterns of iron homeostasis-responsive genes including *OsNAS1*, *OsNAS2, OsIRT1*, *OsIRO2*, *OsYSL15,*

and *OsNRAMP1*. Additionally, lower iron levels were observed in the shoots of *OsIRO3* overexpression lines than in the wild type. These results indicate that PYE homolog protein IRO3 is the negative regulator of iron homeostasis genes especially in rice (Zheng et al., 2010).

In addition to FIT and PYE regulatory networks, recent microarray analyses have identified many other bHLH transcription factors involved in iron homeostasis, including several members of the group I and IV bHLHs (Mai et al., 2016; Maurer et al., 2014; Sivitz et al., 2012). For example, in addition to bHLH group Ib members, it was recently found that the bHLH18, bHLH19, bHLH20, and bHLH25 transcription factors in subgroup IVa also physically interact with FIT and contribute to jasmonic acid-mediated FIT inhibition, thereby reducing the expression of *IRT1* and *FRO2* to prevent excess iron uptake (Cui et al., 2018). In another study, bHLH34 and bHLH104 were found to positively regulate the iron homeostasis gene networks, while the mutants of these had shown disrupted iron homeostasis and low iron levels in the plants while overexpression lines of *bHLH34* and *bHLH104* showed higher iron levels than the wild type (Li et al., 2016).

2.5. Roles of Other Transcription Factor Families in the Regulation of Iron Uptake and Distribution

In recent years, several other transcription factors from different families have been reported in addition to bHLH transcription factors to be involved in iron homeostasis, including MYBs, WRKYs, and NACs (Kobayashi et al., 2007, Yan et al., 2016). Du and Li et al. (2024) reported *ZmNAC78* as a crucial gene controlling iron loading into maize kernels, which can be used as a prominent candidate for iron biofortification and coping with iron deficiency in plants and humans. From the MYB family, *MYB10* and *MYB72* are known to be induced under iron deficiency and play an important role in coumarin production by regulating the *NAS4*. It was reported that MYB10 and MYB72 participate in Fe uptake and distribution by regulating the expression of *BGLU42* and *NAS4*, which are partially mediated by FIT (Palmer et al., 2013; Stringlis et al., 2018). Recently, Gao et al. (2024) reported the involvement of MYB8 in iron homeostasis. Mutants of *myb8* showed severe sensitivity against iron deficiency as shorter root lengths and chlorosis was observed in the leaves. Furthermore, lower iron levels were observed in both roots and

shoots while the overexpression lines of *MYB8* showed tolerance to iron deficiency and higher iron levels in both roots and shoots under low iron availability compared to the wild type and *myb8* mutants (Gong et al., 2024).

Other families include the WRKY transcription factors which have a role in iron homeostasis. Interestingly W-boxes are present in the promoter region of some iron homeostasis genes including *IRT1* and *NAS4,* which indicates that WRKY transcription factors can regulate their expression. Recently, WRKY46 was reported to be involved in the root-to-shoot iron translocation. *wrky46-1* showed disrupted root-to-shoot iron translocation, followed by severe chlorosis in the leaves. WRKY46 is capable of binding to the specific W-boxes present in the VITL1 (a vacuole iron transporter) promoter. WRK46 plays a critical role in Fe translocation from root to shoot by directly suppressing the expression of *VITL1*/*VTL1* (Yan et al., 2016). Another study revealed the role of WRKY12 in iron homeostasis and results showed that WRKY12 negatively regulates the iron entry into Arabidopsis seeds. WRKY12 can directly bind to the promoter regions of *YSL1* and *YSL3* and can inhibit their expression during seed development and maturation. *wrky12* showed tolerance to low iron conditions while *WRKY12* overexpression lines showed high sensitivity to iron deficiency, which is related to the downregulation of *YSL1* and *YSL3* transporters (Wu et al., 2023).

In studies conducted to reveal the role of ethylene signaling in the regulation of iron deficiency, it has been shown that ethylene response factors ERF4 and ERF72, which are members of the AP2/ERF transcription factor family, play a role in Fe homeostasis. Under Fe deficiency, ERF4 and ERF72 negatively regulate the iron uptake genes by inhibiting the expression of *IRT1* or *AHA2* (Liu et al., 2017a; Liu et al., 2017b). Recently Yang et al. (2022) also revealed the role of ERF109 in iron homeostasis. Transcriptome analyses revealed that *erf109* leaves under iron-sufficient conditions had shown 70% overlap with the wild-type leaf transcriptome profile under iron-deficient conditions. Interestingly compared to wild-type plants, homozygous *erf109* lines showed higher iron levels in leaves both under iron-sufficient and deficient conditions (Yang et al., 2022). *NAS4*, *bHLH101*, *bHlH38*, *bHLH39,* and *FER1* were upregulated in *erf109* mutants both under iron sufficient and deficient conditions compared to the wild type, mimicking the iron deficiency response activation in *erf109*. Additionally, the expression levels of *FER1* were downregulated in Col-0 under iron-deficient conditions compared to the iron-

sufficient conditions while *FER1* transcript levels were elevated in *erf109,* which can be related to the higher iron amount in the leaves of *erf109* (Yang et al., 2022).

In addition to these studies, it has been determined that the transcription factors ETHYLENE INSENSITIVE3 (EIN3) and ETHYLENE INSENSITIVE3 LIKE1 (EIL1), which are responsible for ethylene signaling, and the C2H2-type plant-specific zinc finger transcription factor ZAT12 play a role in iron uptake and distribution by modulating FIT protein stability (Lingam et al., 2011; Le et al., 2016).

2.6. The Role of GATA Transcription Factors in Plants

GATA transcription factors named after their binding preference to consequence sequence W-GATA-R [W, thymidine (T) or an adenosine (A); R, guanidine (G) or adenosine (Reyes et al., 2004). First, the characterization of the GATA transcription factor AreA from the fungus *Aspergillus nidulans* showed its crucial role in nitrogen signaling, and this led to the way of GATA transcription factor family characterization in plant nitrogen homeostasis (Daniel-Vedele and Caboche, 1993). 29 and 30 GATA transcription factors have been identified in the rice and Arabidopsis genomes, respectively, and they are divided into four conserved subgroups (Behringer and Schwechheimer, 2015: Liang et al., 2024). From soybean, *GmGATA58* is reported to be involved in chlorophyll synthesis. Overexpression of *GmGATA58* in wild-type *A. thaliana* plants resulted in increased chlorophyll levels whereas overexpression of *GmGATA58* in *AtGATA21* mutant (*gnc*), which is defective in chlorophyll synthesis, complemented the greening of leaves by regulating the expression of chlorophyll biosynthesis genes (Zhang et al., 2020). It has been found that GATA transcription factors are controlled by different hormones and thus play important roles in plant development and stress responses (Behringer and Schwechheimer, 2015).

In addition, it has been reported that the expression levels of *GATA21* and *GATA22* change depending on the amount of nitrogen and that they are differentially regulated by cytokinin, light, auxin, and gibberellic acid, and thus play important roles in greening, gibberellic acid biosynthesis, hypocotyl elongation, seed size, cotyledon development, flowering time, stamen length, senescence, and abscission (Behringer and Schwechheimer, 2015). Under short-term cold stress, GATA21 and GATA22 positively

regulate essential genes such as *CBF* and *COR*, and this regulation is dependent on the activity of the gibberellic acid-mediated DELLA transcription factor (Richter et al., 2013).

These studies showed the role of GATA transcription factors in nutrient and other abiotic stress responses but whether GATA transcription factors are involved in iron deficiency signaling remains unclear. A study has shown that DELLA proteins, which are possible regulators of GATA transcription factors, post-translationally control the major iron deficiency response regulator FIT in roots (Wild et al., 2016). DELLA repressor proteins of the gibberellic acid signaling can interact with the *FIT* and repress its expression. But during iron-deficient conditions, the DELLA protein is degraded in the root epidermis and FIT remains active to regulate iron homeostasis (Wild et al., 2016). These results indicate that DELLA degradation led to the FIT activation for iron uptake under replete iron conditions.

2.7. Known Roles of Peptide Transporters in Transporting Iron between Different Organs

YELLOW STRIPE-LIKE (YSL) proteins are members of the oligopeptide transporter (OPT) family. OPT proteins represent one of the classes of integral transmembrane proteins involved in the transport of a wide variety of substrates in the cell (Lubkowitz, 2011). OPTs are divided into two subgroups known as peptide transporters (PT) and YSL. Regardless of their overall classification, most OPT proteins are involved in metal transport and detoxification, depending on plant nutrient status and site of action (Stacey et al., 2006). Members of the YSL subfamily have important roles in metal (Fe, Zn, Cu, Mn, Ni) homeostasis as they are involved in the transport of metal chelates between plant organs (Curie et al., 2001; Schaaf et al., 2004; Ishimaru et al., 2010).

The OPT family has been bioinformatically well-defined in many plant species (Gross et al., 2003; Koike et al., 2004; Cao et al., 2011; Liu et al., 2012; Xiang et al., 2017; Pu et al., 2018; Kumar et al., 2019; Su et al., 2018). Studies have shown that OPTs are responsible for Fe transportation in different tissues and organs (Lubkowitz, 2011; Conte and Walker, 2012; Banakar et al., 2017). In-silico studies have shown that OPTs interact with many key proteins involved in Fe homeostasis (Dinesh et al., 2020).

YELLOW STRIPE1 (YS1), the first member of the YSL family encoding for a Fe^{3+}-DMA transporter, was first reported in maize (Curie et al., 2001). The *ZmYS1* and its rice ortholog *YS1-LIKE* (*OsYSL*) were induced in roots and shoots under Fe deficiency (Curie et al., 2001: Inoue et al., 2009). Arabidopsis has 8 orthologs of *ZmYS1* (*AtYSL1-8*) while there are 18 present in rice (*OsYSL1-18*) (Curie et al., 2001; Koike et al., 2004). YS1 can transport a few DMA-bound metal ions including Fe^{3+}, Zn^{2+}, Cu^{2+}, and Ni^{2+} as well as NA-chelated Ni^{2+}, Fe^{2+}, and Fe^{3+} complexes (Schaaf et al., 2004). OsYSL15 and OsYSL18 transport Fe^{3+}-DMA (Inoue et al., 2009; Aoyama et al., 2009) while OsYSL2 participates in the transport of Fe^{2+}-NA and Mn^{2+}-NA (Koike et al., 2004). *OsYSL16* carries Fe^{3+}-DMA and Cu^{2+}-NA (Kakei et al., 2012; Zheng et al., 2012). In short, YSL family transporters play important roles in metal homeostasis by transporting metal-DMA and metal-NA complexes. Arabidopsis *ysl1* single and *ysl1ysl3* double mutants and rice *ysl2* single mutant showed lower iron levels in seeds in comparison to the wild-type plants (Koike et al., 2004; Jean et al., 2005; Waters et al., 2006). It can be concluded that *YSL1*, *YSL2*, and *YSL3* are involved in the transport of Fe to the seeds. In addition, YSL4 and YSL6 are localized to the chloroplast (Divol et al., 2013), or tonoplast/ER membrane (Conte et al., 2013) in the developing embryo and may have important roles in iron transport to the embryo. Genome-wide identification studies of *YSL* genes in wheat revealed that they have pivotal roles in grain development and different abiotic/biotic stress tolerance (Kumar et al., 2019).

One of the first studies on the transport of Fe between organs and its accumulation in the seed reported that *OPT3* played a role in the accumulation of iron in the seed and the *opt3-1* mutant showed embryo lethality (Stacey et al., 2002). Later, it was determined that the *opt3-2* mutant, which did not show embryo lethality, accumulated high levels of Fe in roots and leaves, but showed Fe deficiency symptoms (increased *IRT1* and *FRO2* expressions) in the roots even when grown in a Fe-sufficient medium (Stacey et al., 2008). In addition, 30% less Fe accumulation was observed in the seeds of the *opt3-2* mutant compared to the wild-type (Mendoza-Cózatl et al., 2014). Although it has been suggested that OPT3 can transport Fe by chelating it with a peptide (Stacey et al., 2008), a later study indicated that it can transport Fe in the form of Fe^{2+} (Zhai et al., 2014). Interestingly, in a yeast complementation assay of *Δfet3fet4*, *OPT3* could not transport Fe^{2+} even when NA was added to the medium when the yeast overexpressed *OPT3* (Wintz et al., 2003). Another study in yeast reported that *OPT3* was not localized to the cell membrane;

therefore, it has been concluded that Fe cannot be transported in the form of Fe^{2+} and therefore no information can be reached about the substrate it carries (Mendoza-Cózatl et al., 2014). Although the expression level of *OPT2* is altered under Fe deficiency (Wintz et al., 2003), its roles in Fe or peptide transport have not been investigated to date. On the other hand, another transporter in the same family OPT8 is localized to the chloroplast membrane and is responsible for Fe transport (Aksoy, 2014). In addition to these studies, yeast complementation studies of OPTs in rice have shown that some OsOPTs can carry different forms of iron chelated with NA (Vasconcelos et al., 2008). Accordingly, *Δfet3fet4* yeast cells complemented with *OsOPT1* and *OsOPT4* grew well in a medium containing Fe^{2+}–NA and Fe^{3+}–NA while complementation with *OsOPT5* and *OsOPT7* showed slow growth in a medium containing Fe^{3+}–NA and did not grow on medium containing Fe^{2+}–NA. Interestingly, it was reported in another study that *OsOPT7* cannot transport Fe^{3+}-DMA and Fe^{2+}-NA, and therefore unable to complement the *Δfet3fet4* mutants (Bashir et al., 2015). Considering that the closest Arabidopsis ortholog of *OsOPT7* is *AtOPT3*, it is understood that Arabidopsis OPT proteins may play an important role in the transport of NA-chelated Fe forms. On the other hand, the contradictory findings regarding the chelated transport of Fe with peptides need to be re-evaluated. Since *AtOPT6* has been shown to transport peptides of different lengths (Pike et al., 2009), the roles of OPT transporters in the transport of Fe chelated by peptides need to be examined in detail.

2.8. DMT Amino Acid Transporters and Their Possible Roles in Metal Transport

According to the sequence similarity and transport properties, amino acid transporters are divided into two main families: Drug/Metabolite Transporter (DMT) or amino acid/auxin permease (amino acid/auxin permease - AAAP) family and amino acid transporter (ATF) or amino acid-polyamine-organocation (Acid-Polyamine-Organocation - APC) family (Ortiz-Lopez et al., 2000). The AAAP family includes amino acid permease (AAP) transporters, lysine and histidine transporters (LHTs), gamma-aminobutyric acid transporters (GATs), proline transporters (ProTs), indole-3-acetic acid transporters (AUXs), aromatic and neutral amino acid transporters (ANT), amino acid transporter-like (ATL) and vesicular aminergic-associated transporters (VAAT). The APC family is subdivided into cationic amino acid transporters (CATs), amino acid/choline transporters, and polyamine H^+ symporters (PHSs) (Yao et al., 2020). In addition to these groups, a

new transporter family named "usually multiple acids move in and out transporters (UMAMIT)" was discovered in the nodulin-like gene family (Dinkeloo et al., 2018).

The presence of DMT proteins in both prokaryotes and eukaryotes reveals their vital role in the transport of amino acids and associated metals. Studies conducted in bacteria have shown that DMT transporters can transport different amino acids (Tsuchiya et al., 2016). According to different studies, there are >60 amino acid transporters in *Arabidopsis thaliana* (Tegeder et al., 2012), 100 in potato (Ma et al., 2016), 189 in rice (Zhao et al., 2012), 72 in soybean (Cheng et al., 2016), 85 in wheat (Wan et al., 2017), 23 in poplar (Wu et al., 2015), 62 in *Selaginalla moellendorffii* (Wipf et al., 2012), 283 in *Ricinus communis* (Xie et al., 2016). It can be concluded that the amino acid transporter family consists of many proteins in plants due to their pivotal roles. Most of the transporters that have been characterized are localized to the plasma membrane and found to be involved in uptake while a small number of transporters are found in the vacuole, mitochondrial, and chloroplast membranes and play roles in intracellular compartmentalization (Yang et al., 2020). Studies related to heterologous expression systems such as *Saccharomyces cerevisiae* have shown differences in substrate selectivity and affinity of amino acid transporters (Yang et al., 2020; Kim et al., 2021). Homologous amino acid transporters have also been shown to exhibit tissue-specific expression profiles in different plant species (Liu and Bush, 2006). Therefore, there are significant gaps in our knowledge of amino acid transporters. Most of the studies in plants have focused specifically on the AAP family. Since it will not be possible to include all the studies carried out in this literature summary due to the large family of amino acid transporters, only the studies carried out in the UMAMIT family, which is the subject of the thesis, are mentioned below. Additional information and published reviews of other amino acid transporters can be found somewhere else (Yang et al., 2020; Yao et al., 2020; Kim et al., 2021).

2.9. UMAMIT Amino Acid Transporters in Plants

Although the existence of transporters involved in the transport of molecules out of the cytosol was experimentally proven in the 1980s, the first amino acid transporter with outward transport properties was characterized only in 2012 (Ladwig et al., 2012). The protein is known as SILIQUES ARE RED1 (SiAR1/AtUMAMIT18). SIAR1 is an amino acid transporter localized to the cell membrane, expressed in the excretory and pericycle

regions of roots. SIAR1 can transport amino acids in and out of the cell (as a bidirectional transporter) and takes part in amino acid transport to the developing siliques (Ladwig et al., 2012). The second UMAMIT protein studied in Arabidopsis is WALLS ARE THIN1 (WAT1/UMAMIT05), an auxin transporter localized to the tonoplast (Ranocha et al., 2013).

The name given to UMAMIT proteins comes from the term "umami". Umami is associated with the sense of taste, which is predominantly influenced by glutamate, one of the amino acids found in higher amounts only in phloem and xylem sap. AtUMAMIT11, 14, 24, 25, 28, 29 and SiAR1/AtUMAMIT18 have been shown to play roles in the transport of amino acids to the seed, loading, and unloading of the phloem (Ladwig et al., 2012; Müller et al., 2015; Besnard et al., 2016; Besnard et al., 2018). Experiments in yeast showed that UMAMIT14 can transport a wide range of amino acids (Besnard et al., 2016). In the same study, Arabidopsis *umamit14* mutants showed a decrease in the remobilization of amino acids in the leaves which was further decreased in *umamit14umamit18* double mutants. As a result of the study, it was found that UMAMIT14 is necessary for amino acid release from phloem to roots and from roots to soil. In another study in yeast, UMAMIT11, 14, 28, and 29 were found to be bidirectional amino acid transporters usually localized to the plasma membrane (Müller et al., 2015). Additionally, after fertilization, it is reported that *UMAMIT11* and *UMAMIT14* were localized in the unloading domain at the end of the vasculature of the funiculus.

Other studies on UMAMITs have shown that *UMAMIT18* is expressed in the chalazal seed coat in Arabidopsis at early embryogenesis and loss-of-function of *UMAMIT18* showed decreased amino acids in the siliques (Ladwig et al., 2012). *UMAMIT24* is mainly expressed in the tonoplast in the chalazal, and *UMAMIT25*, which is localized to the plasma membrane, is expressed in endosperm cells (Besnard et al., 2018). Interestingly, the seed amino acid contents of Arabidopsis *umamit24* and *umamit25* mutants were transiently lower during embryogenesis compared to the wild type and then recovered in mature seeds without any negative effects on yield (Besnard et al., 2018). There are limited studies in the literature to understand the roles of UMAMITs. According to Zhao et al. (2021), Arabidopsis UMAMIT family members are localized to the plasma membrane or tonoplast, and most of them can transport amino acids bidirectionally.

UMAMIT28 is expressed at the embryo torpedo stage in the innermost layer of the three-layered inner integument, the endothelium, while *UMAMIT29* is expressed from the early stages of embryo development until the late torpedo stage in the middle layer of the three-layered internal integuments. Hence, *UMAMIT28* and *UMAMIT29* play an important role in the transport of amino acids from the seed to the embryo in embryo development. In Arabidopsis *umamit28* and *umamit29* mutants, an increase in the small and non-polar amino acids (such as proline, tryptophan, methionine, and alanine) was observed in siliques while a significant decrease in seed size was observed compared to the wild type. However, the root lengths of these mutants are also shorter than the wild type (Müller et al., 2015). In the same study, it was shown that UMAMIT28 and UMAMIT 29 are localized to vascular tissue in roots and leaves. In addition to amino acid transport to the seed, UMAMIT28 and UMAMIT 29 may have roles in amino acid remobilization. This needs to be further examined. Although phenylalanine has been used as a substrate in amino acid transport studies with UMAMIT14, 24, and 25 to date (Besnard et al., 2016, 2018), different UMAMIT transporters were shown to transport different proteinogenic amino acids (Kim et al., 2021), indole-3-acetic acid (IAA) (Ranocha et al., 2013), Y-aminobutyric acid (Besnard et al., 2018) and citrulline (Ladwig et al., 2012). Therefore, UMAMITs have the potential to transport small molecules like amino acids. A recent study on UMAMIT transporters showed their involvement in glucosinolates transportation. UMAMIT29, UMAMIT30, and UMAMIT31 were reported as glucosinolate exporters with a uniport mechanism. Mutants of *umamit29*, *umamit30,* and *umamit31* showed lower concentrations of glucosinolates in the seeds compared to the wild type. This study showed the role of the UMAMIT family in glucosinolate transportation in *Arabidopsis thaliana* seeds (Xu et al., 2023).

In addition to citrate and NA, other carboxylic compounds (malate) and amino acids (histidine and glutamate) can act as chelators in the uptake or transport of Fe (Kerkeb and Krämer, 2003; Cui et al., 2020). In a recent study in Arabidopsis, it was reported that glutamate can chelate Fe (Cui et al., 2020). Chemical studies have shown that some amino acids can bind to Fe^{3+} (eg alanine, valine, leucine) and structurally resemble the Fe-ferritin protein complex (Holt et al., 1974; Tucker et al., 1975; Thundathil et al., 1977; Reddy and Mahoney, 1995). Fe^{3+}-amino acid complexes may also play important roles in the mitigation of Fe deficiency and the accumulation of Fe in the seed. Therefore, it is

important to investigate the roles of amino acid transporters such as UMAMIT28 in the distribution of amino acid-chelated Fe in the plant and its transport to the seed.

2.10. Copper Homeostasis in Plants

Cu is an imperative transition metal required by all life forms for proper growth and development. It participates in numerous fundamental cellular activities such as lignin biosynthesis, cell wall remodeling, hormone signaling, oxidative stress defense, and many other essential biological processes. It is the main constituent of many enzymes that take part in ROS detoxification, i.e., Cu/Zn superoxide dismutase (Yruela, 2005; Broadly et al., 2012). Cu excess and deficiency in plants results in oxidative stress (ROS production) which damages the DNA, proteins, and lipids. Thus, Cu homeostasis is tightly controlled by the plants for their proper growth (Sanz et al., 2019). Under Cu-deficient conditions, the transcriptional orchestration of Cu-responsive genes is mediated by the transcription factor SQUAMOSA PROMOTER BINDING PROTEIN-LIKE7 (SPL7) as it can bind GTAC motifs in the promoter domains of the Cu-responsive genes (mainly COPT family transporter genes). SPL7 reduces the plant's sensitivity to Cu deficiency by regulating the expression of Cu transporters (Garcia-Molina et al., 2014). Furthermore, SPL7 is reported to participate in the orchestration of Cu reductases (FRO4 and FRO5) (Printz et al., 2016). Under Cu-deficient conditions, plants uptake Cu through a high-affinity Cu transporter family known as COPPER TRANSPORTER (COPT). This family consists of 6 members (COPT1-6) in *A. thaliana*.

Localization of COPT family members suggests two pathways of Cu transport to the cytoplasm which is based on the type of COPT activated under Cu deficient conditions i.e direct uptake of copper from the rhizosphere or the release of stored copper from the internal cellular membranes i.e., COPT1, COPT2, and COPT6 are plasma membrane located transporters while COPT3 and COPT5 are localized at internal membranes (Sanz et al., 2019). COPT1 is the main transporter directly up taking Cu from the soil. Studies showed that *COPT1* expression increases under Cu deficiency and *COPT1* defective plants showed stunted root elongation and vegetative growth (Yamasaki et al. 2009). Furthermore, *COPT1* overexpression plants showed elevated Cu^{2+} levels and increased sensitivity to excess Cu in plants (Andres-Colas et al. 2010), which proposes that COPT1 plays a fundamental role in Cu acquisitions from the soil under Cu deficient conditions.

In Arabidopsis, COPT2 is reported to express under Fe and Cu deficiency, and it is considered redundant to *COPT1* in above-ground parts of the plants as both genes exhibit similar expression profiles under Cu deficiency (Perea-García et al., 2013). In the roots, *COPT2* is also known to be expressed at root hairs and lateral roots epidermis but interestingly its expression is absent in the meristematic regions (Perea-García et al., 2013). COPT3 is localized at the secretory pathway compartments and is reported to be expressed in vascular bundles and pollen grains (Colas et al., 2018). *COPT1* is expressed at the late pollen development stage while *COPT3* is expressed in the early stages of pollen grain development, which indicates its specific role in Cu transport to the pollens (Bock et al., 2006). Since Cu is an indispensable trace element mandatory for pollen growth and development (Bock et al., 2006), transcription factor *SPL7* and a Cu^{2+} deficiency-induced transcription factor *CITF1* are reported to participate in Cu transport to the anthers (Yan et al., 2017). Further investigation of Cu functions in pollen and anther development is necessary. Besides these transcription factors, *TCP16* is another transcription factor known to bind with *COPT3* and control Cu homeostasis by regulating *COPT3* expression. Overexpression of *TCP16* results in increased sensitivity of plants to Cu deficiency whereas the *tcp16* mutant plants are sensitive under excess Cu availability (Andrés-Colás et al., 2018).

Interestingly, COPT4 is not considered to show any known function in Cu uptake or translocation mechanisms in plants (Festa et al., 2011) whereas COPT5 is located at the tonoplast and is involved in the export of Cu from vacuoles to the cytoplasm in severe Cu deficiency. *COPT5* is mainly expressed in root vasculature and siliques and *copt5* mutants show severe sensitivity to Cu deficiency due to loss of vacuolar Cu^{2+} transport to the cells. Furthermore, the loss-of-function of *COPT5* results in more Cu^{2+} accumulation in roots and low Cu^{2+} levels in seeds and siliques, which indicates the function of COPT5 in the reallocation of Cu from roots to the other reproductive parts of the plants (Garcia-Molina et al., 2011: Klaumann et al., 2011). Finally, COPT6 functions in the redistribution of Cu^{2+} in the shoots as loss-of-function of *COPT6* led to disturbed Cu transport where increased Cu^{2+} levels were observed in leaves and low Cu^{2+} levels were observed in the seeds (Garcia-Molina et al., 2013), which indicates the possible role of COPT6 in Cu^{2+} translocation from leaves to the seeds.

Other than COPT family transporters, a P-type adenosine triphosphate (ATP) subfamily of pumps was also involved in Cu^{2+} transport from cytosol to other organelles in humans and plants (Williams et al., 2000: Williams and Mills., 2005). This specific family of transporters is known as the HEAVY METAL TRANSPORTER (HMA) family, and they participate in the Cu^{2+} homeostasis in plants. For instance, HMA7 mediates the translocation of Cu from the cytoplasm to the endomembrane compartment while HMA5 prevents Cu overload in cells (Aguirre and Pilon., 2016). Additionally, two members of the YSL metal transporter family i.e., YSL1 and YSL2 (which are involved in Fe homeostasis) are also involved in the Cu^{2+} transportation from leaves to the seeds (Waters et al., 2006).

2.11. Crosstalk between Iron and Copper

Both Fe and Cu are essential metals for plants required to complete their life cycle, but they can reach toxic levels when the plants are exposed to them in high concentrations. Therefore, there is a need for the tight regulation of both these trans metals at the cellular level. The interaction between Fe and Cu can be emphasized by the fact that under Fe-deficient conditions plants over-accumulate Cu while they accumulate higher Fe concentrations under Cu deficiency. Thus, there exists an antagonistic relationship between these two metals in the plant body (Chia et al., 2023). Alkaline soils can lead to both Fe and Cu deficiency. Interaction between the two trans metals has been reported in many living organisms, but the work on the transporters involved in the transport of both metals is limited. The interaction between these trans metals is interesting since soil alkalinity leads to the deficiency of both metals while 50 percent of the soil in the world is acidic, which leads to Fe toxicity. Moreover, Cu is one of the main additives in many pesticides and insecticides, which leads to the accumulation of toxic forms and levels of Cu in the soils (Chia et al., 2023). Additionally, like Fe, Cu can also take part in redox reactions and needs to be transported in the chelated form as a transition metal.

While *FRO2* has been identified as the primary locus responsible for the reduction of ferric iron chelates within the rhizosphere, it is noteworthy that the genome of Arabidopsis contains a total of eight distinct FRO family members. These additional seven FRO proteins are believed to function predominantly as metalloreductases, primarily participating in the reduction of Fe and potentially Cu ions. Studies on FRO2 indicate that

in addition to its function in Fe reduction, it may also reduce Cu^{2+} to Cu^{+} at the root surface (Yi and Guerinot, 1996; Robinson et al., 1999). Under Fe-deficient conditions, root copper reductase activity is elevated in Arabidopsis wild-type plants, but not in *frd1* mutants, mutants of *the FRO2* locus (Robinson et al., 1999). Despite this, *frd1* mutants do not exhibit decreased Cu levels, suggesting that other FROs may be able to reduce Cu at the root surface and that *FRO2* contribution to Cu reduction may not be essential. This phenotype can be explained alternatively by Cu uptake via a ZIP-type transporter without Cu^{2+} reduction. Notably, the expression of *ZIP2* and *ZIP4* is upregulated under Cu deficiency (Wintz et al., 2003), which shows their possible roles in direct uptake of Cu^{2+}. Nonetheless, research on stable isotopes supports a Cu uptake pathway based on reduction (Jouvin et al., 2012).

Indeed, some studies showed that some members of the FRO family are involved in Cu homeostasis in plants. *FRO4* and *FRO5* expressions are regulated by CITF1 and SPL7 under Cu deficiency. Bernal et al. (2012) showed the roles of FRO4 and FRO5 in Cu reduction at the root surface. A graphical description of the role of FRO family members in Cu and Fe reduction at the root surface is given in Figure 2.2.

Besides this research, several genes involved in Fe homeostasis also take part in Cu homeostasis. In a recent study, a phloem-specific Fe transporter OPT3 was also shown to be involved in Cu transport (Chia et al., 2023). *opt3* mutants showed a lower Cu concentration in the phloem than the wild type. It was also reported that the major transcription factor of Fe homeostasis FIT can also regulate the expression of the Cu uptake genes *COPT2*, *FRO4*, and *FRO5* under Fe-deficient conditions (Cai et al., 2021). Although the molecular mechanisms underlying Cu and Fe homeostasis individually are becoming clear, little is known about the genetic interaction of Cu and Fe transporters under Fe and Cu deficient conditions. Strong evidence exists demonstrating the relationship between Fe and Cu homeostasis. One example is the substitution of metalloproteins. One such interaction is the substitution of metalloproteins replacement of Arabidopsis Cu/Zn superoxide dismutase (Cu/ZnSOD) with the Fe (FeSOD) counterpart under Cu deficient conditions probably to save Cu for essential cuproproteins like plastocyanin (Carrió-Seguí et al., 2019). The transcription factor SPL7 and miR398 facilitate this mechanism, which regulates the Cu/ZnSOD1 (*CSD1*) and *CSD2* genes that encode chloroplastic and cytosolic Cu/ZnSODs. In contrast, Fe deficiency causes

Cu/ZnSOD to take the place of FeSOD since Fe availability downregulates the expression of *miR398*.

Studies in Arabidopsis, cucumber, and pumpkin suggest that Fe status modulates Cu uptake and accumulation in the leaves (Waters and Armbrust, 2013; Waters et al., 2012; Waters et al., 2014). Below optimal Cu concentrations inhibit FCR activity, suggesting that Cu is required for the synthesis or activity of FCR. Conversely, when Cu is increased above optimal concentrations, a decrease in FCR activity is observed (Waters and Armbrust, 2013). Elevated Cu levels lead to more efficient or rapid synthesis of Cu proteins, which replace Fe proteins, thus reducing Fe demand and generating a feedback inhibition of FCR activity. However, toxic Cu concentrations suppress FCR activity, indicating that Cu blocks expression rather than the function of FCR-encoding genes (Waters and Armbrust, 2013).

Additionally, the Fe chelator NA demonstrates the ability to bind both Fe and Cu (von Wirén et al., 1999). Fe-deficient plants, including both grasses and dicots, have been shown to accumulate additional Cu in leaf tissues (Waters et al., 2012; Rai et al., 2021). YSL16 is a Cu-NA transporter that is required for delivering Cu to the developing young tissues and seeds through phloem transport (Zheng et al., 2012). *YSL16* is expressed in the phloem of nodes and vascular stature in the leaves. At the vegetative stage, the knock-out mutant of *YSL16* in rice showed lower Cu concentrations in the young leaves and higher concentrations in the older leaves. At the reproductive stage, mutants showed higher Cu concentrations in flag leaf and husk while lower in the rice seeds. Furthermore, isotope studies showed that *ysl16* mutants in rice had failed to translocate the Cu from older leaves to the younger leaves and from flag leaf to panicle (Zheng et al., 2012).Kakei et al. (2012) reported the role of YSL16 in Fe^{3+}-DMA transportation. *YSL16* fully complemented the yeast mutant *Δfet3fet4* when grown on a medium enriched with Fe^{3+}-DMA but not when the mutant yeast expressing *YSL16* was grown on a medium containing Fe^{2+}-NA. While the rice mutants were more chlorotic, no differences were found in the Fe concentrations of the shoots between the wild type and the mutants. Interestingly, more Fe was found to be stuck in the vascular bundle of the leaves in the mutants than in the wild type. These studies indicate the role and choice of Fe and Cu chelates transport by YSL16 between two different metals.

2.12. Aim of the Thesis

This thesis aims to understand the molecular mechanisms of IDC-tolerance in soybean grown under calcareous-alkaline soil conditions via QTL and RNA sequencing analyses and characterize a transcription factor and an amino acid transporter playing important roles in Fe homeostasis in plants.

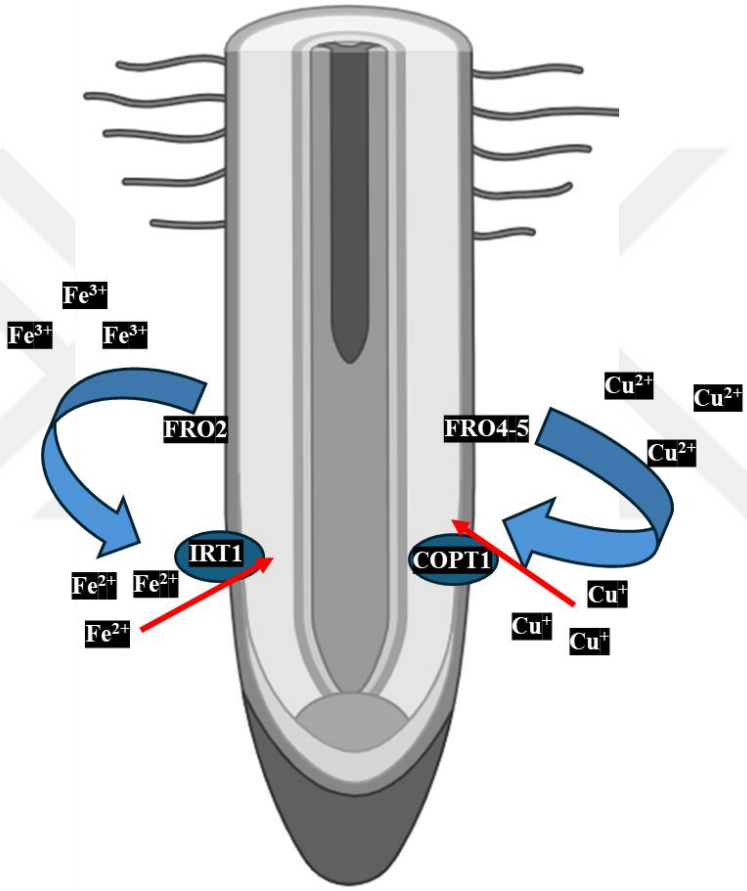

Figure 2.2. Graphical description of the roles of the FRO family members in iron and copper reduction at the root surface in dicots.

CHAPTER III

MATERIALS AND METHODS

The thesis is divided into four sub-studies interconnected to each other.

Part1: Effect of iron fertilization on soybean cultivars differing in IDC tolerance

In the first part, IDC-sensitive and tolerant soybean cultivars were exposed to different dosages of Fe fertilization to understand the genetics and agronomic biofortification.

Part 2: Genome-wide Identification of QTLs Associated with Iron Deficiency Tolerance in Soybean

In the second part, QTLs associated with Fe deficiency tolerance in soybean were investigated to identify a novel transcription factor.

Part3: Transcriptomics of IDC-tolerant Soybean Cultivars in Calcareous-alkaline Soil

This part of the thesis aimed to identify the novel genetic players involved in conferring tolerance to Fe deficiency in IDC-tolerant soybean cultivars in calcareous-alkaline soil.

Part 4: Characterization of *AtUMAMIT28* in Arabidopsis thaliana under transmetal deficiencies

In the last part of this study, transcriptomic analyses of differentially expressed transporters were conducted, leading to the identification of a novel family amino acid transporter family, UMAMIT. The in-silico analyses of this amino acid transporter family suggested the potential involvement of one of the members, *AtUMAMIT28* in metal homeostasis. Accordingly, this section of the thesis focuses on the characterization of *AtUMAMIT28* in Arabidopsis thaliana under transmetal deficiencies.

3.1. Part 1: Iron Fertilization of Soybean Genotypes Differing in Iron Use Efficiency

Soybean falls into the group of crops highly sensitive to Fe deficiency. However, the sensitivity to Fe deficiency varies among soybean cultivars, spanning a wide spectrum from highly sensitive to more tolerant varieties. Several studies have shown that Fe supplementation alleviated IDC, but how sensitive and tolerant cultivars respond to different dosages of Fe in the recalcitrant pools (calcareous-alkaline conditions) is poorly understood. Therefore, this part of the thesis aims to assess the effectiveness of Fe-EDDHA fertilization at different dosages on IDC-tolerant and sensitive soybean cultivars, focusing on Fe uptake, seed micronutrients, total protein, and phytate contents under calcareous-alkaline soil conditions. This part of the thesis is under review.

3.1.1. Plant growth conditions

The seeds of two IDC-tolerant (Arısoy and Sa-88) and two IDC-sensitive (Nova and Atakişi) Turkish soybean cultivars (Maqbool, 2018) were germinated on Petri plates for five days in the dark. Then, the roots of the germinated seedlings of similar size were covered with *Rhizobium japonicum* (USDA 110 strain) and transferred to 20-L pots containing a potting mixture of peat and perlite at a 2:1 ratio (defined as soil from now on). In one set of the pots (normal soil pH), the soil pH was measured as 5.7 according to Baker et al. (1983). In the second set, iron deficiency was applied by increasing the soil pH to 8.7 by mixing thoroughly 9 g of calcium oxide (CaO, Sigma) / kg soil. 6% Fe-EDDHA (4.8% o-o) was used as a fertilizer source since it is the most frequently used Fe fertilizer around the world with dosage variation in different crops (Schenkeveld et al., 2008). In total, 8 treatments were used in the study (Table 3.1). The experiment was set up according to a completely randomized design, where each pot represented one biological replicate, and a total of six replications were used for each treatment. Plants were grown in a greenhouse at 25 ± 1 °C (day) and 20 ± 1 °C (night) and 50% humidity under a regional light cycle (14/10 h of day/night) under 580 ± 75 µmol PAR m^{-2} s^{-1} in Niğde, Türkiye during the summer of 2020. All physiological, biochemical, and molecular measurements were taken after 35 days of growth when the plants reached vegetative 3 (V_3) growth stage. Measurements related to seeds were taken at the crop maturity stage after harvesting of seeds.

Table 3.1. Treatments used in the study

Treatments	Explanation of the treatment
T1	0 mg Fe-EDDHA / kg soil with pH 5.7
T2	0 mg Fe-EDDHA / kg soil with pH 8.7
T3	12.5 mg Fe-EDDHA / kg soil with pH 8.7
T4	18.75 mg Fe-EDDHA / kg soil with pH 8.7
T5	24.9 mg Fe-EDDHA / kg soil with pH 8.7
T6	30.6 mg Fe-EDDHA / kg soil with pH 8.7
T7	37.25 mg Fe-EDDHA / kg soil with pH 8.7
T8	43.25 mg Fe-EDDHA /kg soil with pH 8.7

3.1.2. Physiological measurements

At noontime, the photosynthesis rates were measured by LICOR-6400, and the chlorophyll index was measured by a SPAD meter (Minolta SPAD-502) from the top third trifoliate leaves. Each data was collected from at least six independent measurements from each plant grown under different conditions (T1-T8). Then, root lengths were measured by using measuring tape. The top third trifoliate leaves and roots were collected and dried at 65°C for two days, and dry weights were recorded. Seed sizes were measured by vernier caliper, and 100-seed weight was recorded. Total chlorophyll contents were determined from the top third trifoliate leaves according to Lichtenthaler (1987) while the ferric reductase (FCR) activity was determined from the entire roots according to Aksoy and Koiwa (2013).

3.1.3. Metal content analysis

Roots, the top third trifoliate leaves, and seeds were collected and pooled together from three biological replicates for each organ. Samples were incubated in 2 mM $CaSO_4$ and 10 mM EDTA for 10 minutes followed by washing thrice with distilled water to eliminate any metal particles attached to the sample surface. The samples were divided into 3 technical repeats of 100 mg and dried in acid-resistant borosilicate test tubes for 48 hours at 65 °C (Aksoy et al., 2013). Then, the samples were digested in 4 mL of 98.8% HNO_3 (Sigma) and 1 mL of concentrated HCl (Sigma) at 100 °C for 1 hour, 150 °C for 1 hour, 180 °C for 1.5 hours, and lastly at 210 °C until no liquid is left in the test tubes

(Vasconcelos et al., 2006). Finally, the samples were re-dissolved with 10 mL of 2% HNO_3, and the Fe, Zn, and Mn levels were determined in Inductively Coupled Plasma Mass Spectrometry (ICP-MS) (Bruker Aurora M90). Each sample was read five times in the pulse detector mode.

3.1.4. Protein and oil content analyses

After careful analysis of all the above-mentioned parameters treatments, T1, T2, T3, and T4 were selected for total protein and oil content analyses to check how the lowest and maximum dosages of Fe-EDDHA are affecting the total protein and oil contents at high pH-induced iron deficiency in sensitive and tolerant cultivars. Total protein content was determined by the Kjeldahl apparatus (Çalışkan et al., 2018). Oil content was measured from well-ground seeds according to the method described by Am, A.A.P., 2005 by using the ANKOM extractor (Çalışkan et al., 2018).

3.1.5. Phytic acid and phosphorus content analyses

Accurately weighed 1 gram of finely crushed seed powder of each sample was continuously stirred in 20 mL of hydrochloric acid (0.66 M) for 3 h at room temperature. Then, the aliquot of each sample extract (1 mL) was neutralized with 0.5 mL of 0.75 M NaOH (Sigma-Aldrich) followed by 10 min. of centrifugation. Phytic acid and phosphorus content analyses were done by using a kit (Megazyme K-PHYT 05/19).

3.1.6. Gene expression analysis

Total RNA was extracted from the top third trifoliate leaves and roots of the treatments T1, T2, T3, and T4 using TRIzol reagent (Sigma) (Chomczynski and Sacchi, 1987). Following the removal of genomic DNA by DNase I treatment, 1 µg total RNA was converted to first strand cDNA using SuperScript® VILO ™ cDNA synthesis kit (Invitrogen). Reverse transcribed products were analyzed by Real-Time qPCR (Qiagene) in a reaction of 20 ng of cDNA mixed with 12.5 µl of RealQ Plus 2x Master Mix (Ampliqon) and 0.8 µM of the specific primers in a final volume of 25 µl. The expressions of *GmIRT1-like*, *GmFRO2*, *GmFRD3,* and *GmFIT* were determined in the roots, and *GmOPT3*, and *GmFER* in the leaves (Santos et al., 2015) (**Table 3.2**). *GmELONGATION FACTOR 1-BETA* (*EFL1B*) was used as an internal control to normalize the data (Jian et

al., 2008). Each reaction was run in three technical replicates and data was analyzed according to the $2^{-\Delta\Delta Ct}$ method as described by Salzman et al. (2005). Results represent three biological replicates (n = 3).

Table 3.2. RT-qPCR primers used in gene expression analyses

Primer Name	**Gene**	**Sequences (5' – 3')**
*GmELF1B*_QPCR _F	*ELFB1*	GTTGAAAAGCCAGGGGACA
*GmELF1B*_QPCR _R	*ELFB1*	TCTTACCCCTTGAGCGTGG
GmFRO2 _QPCR_F	*FRO2*	AGGTGCTTATCTTCTGTTGTACACTTTCCCA
GmFRO2 _QPCR_R	*FRO2*	GCATTGCAGCTCTCTGTGTTGGA
Gmferritin _QPCR_F	*FER*	CCCCTTATGCCTCTTTCCTC
Gmferritin _QPCR_R	*FER*	GCTTTTCAGCGTGCTCTCTT
*GmIRT1-like*_ QPCR _F	*IRT1*	CAGCAAAGGCCTTAACCATA
*GmIRT1-like*_ QPCR _R	*IRT1*	TGCTTGGACTCACACCAGAG
*GmOPT3*_QPCR_F	*OPT3*	TTACGGCAACCCTCACTCAT
GmOPT3_QPCR_R	*OPT3*	CGCCATGCTCCCAAACAATA
*GmFRD3*_QPCR_F	*FRD3*	CCTCATTGGCAGCAAGGTTT
*GmFRD3*_QPCR_R	*FRD3*	TCTGGAGAGTTCGTGTTGCT
*GmFIT*_QPCR_F	*FIT*	CTGCTCTTCTGAACCAAGGC
*GmFIT*_QPCR_F	*FIT*	AAAACGAAGGTAGCAACGGG

3.1.7. Statistical analyses

The data were analyzed in Statistix software via variation analysis according to the completely randomized design (n = 6 or n = 3, depending on the analyses). Then, Fisher's LSD test was performed following one-way ANOVA (analysis of variance) at the significance level of 5%.

3.2. Part 2: Genome-wide Identification of QTLs Associated with Iron Deficiency Tolerance in Soybean

In silico studies of already available QTL data and prediction of genes and their functional characterization in response to Fe deficiency can help in broadening our ability to understand the mechanisms behind Fe deficiency tolerance in soybean. Therefore, this part of the thesis aimed to identify the IDC-related genes present in the previously reported IDC-responsive QTLs in soybeans and determine their expression levels under limited Fe conditions. This section of the thesis was published in an SCI journal (Maqbool et al., 2023).

3.2.1. Identification of QTL linked with Fe deficiency tolerance in soybean

QTL regions linked with Fe deficiency symptoms, especially with the IDC score and SPAD measurement, were previously generated from six different experiments, representing a divergence in genetic background, experimental setup, field, and environmental conditions (Diers et al., 1992; Lin et al., 1997; Lin et al., 2000a; Lin et al., 2000b; Charlson et al., 2005; Peiffer et al., 2012) (**Appendix 1 and Appendix 2**). The QTL data were obtained from SoyBase (https://www.soybase.org/) and are summarized in **Table 3.3**. Among a total of 40 QTL regions generated from the 6 experiments, only 19 represented unique regions. Chromosomal distribution of the 19 QTL regions was generated using Geneious software (Kearse et al., 2012) according to the soybean chromosome sizes and distribution of the QTL regions compared to the size of the chromosomes (Nepal et al., 2015). The centromere position was determined by identifying 91–92 nucleotide tandem repeats within the centromeric region. A total of 6593 genes were found in the 19 QTL regions by screening through the SoyBase Genome Browser (Nepal et al., 2015). For proper annotation of the identified genes, their

Arabidopsis thaliana orthologs were obtained from a BLASTp search of each gene against the A. thaliana genome in The Arabidopsis Information Resource (TAIR) (Lamesch et al., 2012) with preset parameters, and the top query hit was selected as the ortholog, where the percent similarity was >75% and E < 10–5.

Table 3.3 QTL data used in the study.

QTL number	QTL name	Parent1	Parent 2	Nearest sequence-based genetic marker				Reference
				5' end	position	3' end	position	
7	Fe effic 1-1	A81356022	PI468916	BARC-011635-00314	Gm08:6809647	BARC-028361-05840	Gm08:7723315	1
1	Fe effic 1-2	A81356022	PI468916	Satt129	Gm01:55166202	BARC-018211-03157	Gm01:56113247	1
2	Fe effic 1-3	A81356022	PI468916	Satt407	Gm01:53174848	Sat_160	Gm01:54121486	1
3	Fe effic 1-4	A81356022	PI468916	BARC-020113-04470	Gm01:52286178	BARC-039805-07589	Gm01:53429616	1
12	Fe effic 1-5	A81356022	PI468916	Satt217	Gm18:4713017	Sat_315	Gm18:5348175	1
-	Fe effic 2-1	A81356022	PI468916	-	-	-	-	1
9	Fe effic 3-1	Pride B216 Fe inefficient	A15 Fe efficient	Satt122	Gm14:17619136	Sat_424	Gm14:46281808	2
-	Fe effic 3-2	Pride B216 Fe inefficient	A15 Fe efficient	Satt063	Gm14:45993714	BARC-039667-07534	Gm14:47205629	2
13	Fe effic 3-3	Pride B216 Fe inefficient	A15 Fe efficient	BARC-017185-02246	Gm18:50785143	BARC-018441-03188	Gm18:52157617	2
4	Fe effic 3-4	Pride B216 Fe inefficient	A15 Fe efficient	Satt159	Gm03:3197845	BARC-016199-02307	Gm03:5664735	2
-	Fe effic 4-1	Pride B216 Fe inefficient	A15 Fe efficient	BARC-013927-01275	Gm14:16752071	BARC-056587-14511	Gm14:16256888	2
-	Fe effic 4-2	Pride B216 Fe inefficient	A15 Fe efficient	BARC-029827-06444	Gm20:24177772	Sat_104	Gm20:37789703	2
-	Fe effic 4-3	Pride B216 Fe inefficient	A15 Fe efficient	Sat_334	Gm12:9131428	BARC-049209-10821	Gm12:35692712	2
5	Fe effic 5-1	Anoka Fe inefficient	A7 Fe efficient	BARC-020479-04634	Gm05:32322642	BARC-014463-01558	Gm05:34473339	2
-	Fe effic 5-2	Anoka Fe inefficient	A7 Fe efficient	Sat_033	Gm03:32837825	Satt237	Gm03:38104512	2
-	Fe effic 6-1	Anoka Fe inefficient	A7 Fe efficient	BARC-029827-06444	Gm20:24177772	Sat_104	Gm20:37789703	2
-	Fe effic 6-2	Anoka Fe inefficient	A7 Fe efficient	Sat_033	Gm03:32837825	Satt237	Gm03:38104512	2
-	Fe effic 7-1	Pride B216 Fe inefficient	A15 Fe efficient	Satt012	Gm18:49174114	BARC-018441-03188	Gm18:52157617	2
-	Fe effic 7-2	Pride B216 Fe inefficient	A15 Fe efficient	BARC-044085-08610	Gm03:7805399	BARC-013561-01160	Gm03:33280183	2
10	Fe effic 8-1	Pride B216 Fe inefficient	A15 Fe efficient	Satt020	Gm14:41294144	Sat_424	Gm14:46281808	2
-	Fe effic 8-2	Pride B216 Fe inefficient	A15 Fe efficient	Satt012	Gm18:49174114	BARC-018441-03188	Gm18:52157617	2
-	Fe effic 8-3	Pride B216 Fe inefficient	A15 Fe efficient	Sat_334	Gm12:9131428	BARC-049209-10821	Gm12:35692712	2
-	Fe effic 8-4	Pride B216 Fe inefficient	A15 Fe efficient	BARC-044085-08610	Gm03:7805399	BARC-013561-01160	Gm03:33280183	2

Table 3.3 QTL data used in the study. (**Continue**)

QTL number	QTL name	Parent1	Parent 2	Nearest sequence-based genetic marker				Reference
				5' end	position	3' end	position	
8	Fe effic 9-1	Pride B216 Fe inefficient	A15 Fe efficient	Sat_270	Gm11:4234139	BARC-059851-16137	Gm11:24571364	3
-	Fe effic 9-2	Pride B216 Fe inefficient	A15 Fe efficient	Satt063	Gm14:45993714	BARC-039667-07534	Gm14:47205629	3
14	Fe effic 9-3	Pride B216 Fe inefficient	A15 Fe efficient	Satt012	Gm18:49174114	BARC-018441-03188	Gm18:52157617	3
15	Fe effic 9-4	Pride B216 Fe inefficient	A15 Fe efficient	BARC-044913-08839	Gm19:43329322	BARC-013505-00505	Gm19:45014383	3
-	Fe effic 9-5	Pride B216 Fe inefficient	A15 Fe efficient	BARC-044085-08610	Gm03:7805399	BARC-013561-01160	Gm03:33280183	3
-	Fe effic 10-1	Anoka Fe inefficient	A7 Fe efficient	BARC-029827-06444	Gm20:24177772	Sat_104	Gm20:37789703	3
-	Fe effic 10-2	Anoka Fe inefficient	A7 Fe efficient	Sat_033	Gm03:32837825	Satt237	Gm03:38104512	3
11	Fe effic 10-3	Anoka Fe inefficient	A7 Fe efficient	Sat_189	Gm14:16352945	BARC-039667-07534	Gm14:47205629	3
-	Fe effic 11-1	Pride B216 Fe inefficient	A15 Fe efficient	BARC-013927-01275	Gm14:16752071	BARC-056587-14511	Gm14:16256888	4
-	Fe effic 11-2	Pride B216 Fe inefficient	A15 Fe efficient	BARC-029827-06444	Gm20:24177772	Sat_104	Gm20:37789703	4
-	Fe effic 11-3	Pride B216 Fe inefficient	A15 Fe efficient	Sat_334	Gm12:9131428	BARC-049209-10821	Gm12:35692712	4
-	Fe effic 12-1	Anoka Fe inefficient	A7 Fe efficient	BARC-029827-06444	Gm20:24177772	Sat_104	Gm20:37789703	4
-	Fe effic 12-2	Anoka Fe inefficient	A7 Fe efficient	Sat_033	Gm03:32837825	Satt237	Gm03:38104512	4
6	Fe effic 13-1	P9254 Low Fe chlorosis resistance	A97-770012 High Fe chlorosis resistance	BARC-060051-16321	Gm05:41877400	BARC-018681-02991	Gm05:41347323	5
16	Fe effic 13-2	P9254 Low Fe chlorosis resistance	A97-770012 High Fe chlorosis resistance	BARC-059657-15973	Gm19:40154846	Satt156	Gm19:40637071	5
17	Fe effic 13-3	P9254 Low Fe chlorosis resistance	A97-770012 High Fe chlorosis resistance	BARC-038869-07359	Gm20:37596189	BARC-030259-06840	Gm20:38262192	5
-	Fe effic 14-1	Anoka Fe inefficient	A7 Fe efficient	Sat_033	Gm03:32837825	BARC-040277-07706	Gm03:36368900	6

[a] All data was obtained from the SoyBase QTL database (https://soybase.org/search/qtllist_by_symbol.php#I).References: 1: Diers et al., 1992; 2: Lin et al., 1997; 3: Lin et al., 2000b; 4: Lin et al., 2000a; 5: Charlson et al., 2005; 6: Peiffer et al., 2012.

3.2.2. *In silico* expression and gene set enrichment analysis (GSEA) of the IDC-related genes

The expression levels of single-copy Arabidopsis orthologs were determined using Genvestigator (Zimmermann et al., 2004) in five microarray experiments generated from the whole roots of wild-type Col-0 exposed to Fe deficiency. The Gene Expression Omnibus (GEO) datasets used in the *in-silico* analyses included GSE40076 (Sivitz et al., 2012), GSE24348 (Schuler et al., 2011), GSE21582 (Long et al., 2010), GSE15189 (Buckhout et al., 2009), and GSE10576 (Dinneny et al., 2008). Differentially expressed genes (DEGs) were identified via gene search analysis of perturbations with a minimum target log ratio of 0.5, maximum target p-value of 0.05, and tolerance percent of 0. Expression patterns of the Fe deficiency-related Arabidopsis orthologous genes were determined in the bhlh100 bhlh101 (GSE40076 - (Sivitz et al., 2012)) and pye1-1 (GSE21582 - (Long et al., 2010)) mutants using Genevestigator (Zimmermann et al., 2004). The heat map construction and/or hierarchical clustering of the genes was completed in Genevestigator according to the Manhattan correlation distance and the average linkage rule (Eisen et al., 1998). The gene ontology (GO) enrichment was performed using PANTHER 14.0 according to Fisher's exact test and corrected by Bonferroni correction for multiple testing, where $p < 0.05$ (Mi et al., 2019). To prove the relation of the core group genes with Fe deficiency, GSEA was done using GeneTrail (Schuler et al., 2011) as explained previously (Eroglu and Aksoy, 2017). GSEA was performed against datasets obtained from the GEO accessions of GSE40076 (Sivitz et al., 2012), GSE24348 (Schuler et al., 2011), GSE21582 (Long et al., 2010), GSE15189 (Buckhout et al., 2009), GSE10576 (Dinneny et al., 2008), E-MEXP2378 (Mizoguchi et al., 2010), and E-MEXP475 (Nishimura et al., 2007), and NASCArray accessions 176 (Goda Backes et al., 2008), 139 (Kilian et al., 2007), and 140 (Nakashima et al., 2006). The gene set consisting of constitutively expressed genes in Arabidopsis was used as a negative control in the analysis (Czechowski et al., 2005). The false discovery rate was set at $p < 0.05$. The genes that coexpressed together with the core group genes were identified using ATTED-II Network Drawer (Obayashi et al., 2007), where the coexpression option was set to 'add a few genes and the PPI was set to 'Draw PPIs'.

3.2.3. Plant material

A Turkish soybean (*Glycine max* (L.) Merr.) variety known to be IDC-sensitive (Atakişi) was used in the study (Maqbool, 2018) and the seeds were generously provided by Prof. Sevgi Çalışkan from Niğde Ömer Halisdemir University, Niğde, Türkiye.

3.2.4. Plant growth and stress application

In the experiment, a custom-made hydroponics culture system was used with some modifications (Kurtz, 2017). A cheesecloth was stretched over the mouth of 0.5-L polypropylene cups and the seeds placed on this setup were covered with polypropylene transparent cups with a 25-mm opening on the top for 10 days while they were germinating. The soybean seeds were surface sterilized by washing with 70% ethanol for 5 min, followed by washing with 0.25% sodium hypochlorite for 2 min. Then, they were rinsed 5 times with sterile distilled water. For the stratification of the seeds, they were kept at 4 °C in the dark for 2 days in sterile distilled water. Subsequently, the seeds were transferred to the hydroponics 1 h before the lights were turned on and germinated on ½ × Hoagland's solution at the following mineral element concentrations: 7.5 mM N, 3.0 mM K, 0.5 mM P, 2.5 mM Ca, 1.0 mM Mg, 1, 0 mM S, 50 µM Fe, 7.4 µM Mn, 0.96 µM Zn, 1.04 µM Cu, 7.13 µM B, and 0.01 µM Mo (Hoagland et al., n.d.). Fe was applied as sodium Fe-EDTA (Carl Zeiss Str., Roedermark, Germany). Three plants were transferred to each cup (as technical replicates) and 4 cups were used for each application as biological replicates. The cups were wrapped with aluminum foil to prevent algal growth. Under these conditions, the plants were grown for 2 weeks under Fe deficiency (0 µM Fe-EDTA, pH: 5.7), high pH (50 µM Fe-EDTA, pH: 9.0), or the control conditions (50 µM Fe-EDTA, pH: 5.7) in a controlled growth chamber at 25/20 °C (day/night) under a long day cycle (16:8 h light/ dark photoperiod), 70% – 80% relative humidity, and 200 µmol PAR m^{-2} s^{-1} light provided by high-pressure sodium lamps placed over the plant canopy to prevent excessive light, and thus reduce the photoinhibition on the photosystem. The plants were sampled at the V2 stage since the IDC symptoms are best observed at this developmental stage in soybean. During the study, growth media were replaced with new ones every 48 h, thus eliminating the diminishing element and oxygen deficiencies in the environment. The experiment was performed in 5 replicates according

to the randomized block design, where the location of the cups was randomly changed every 2 days.

3.2.5. Physiological and biochemical measurements

All the aboveground measurements were taken from the top second trifoliate leaves that completed their full development. Chlorophyll index measurements were taken at noon using the SPAD-502 chlorophyll meter (Konica Minolta, Tokyo, Japan) from at least 3 independent measurements from each leaf and evaluated by calculating the mean and standard deviation. After the measurements, the second trifoliate leaves were used for total chlorophyll determination following extraction in 80% acetone (Aksoy et al., 2013). The absorbance readings of the extracts were determined at 470, 646.8, and 663.2 nm and compared to 80% acetone. Plant roots and shoots were photographed with a digital camera at the end of the stress application. Root and shoot lengths were determined by ImageJ software (http:// rsbweb.nih.gov/ij/) (Aksoy et al., 2013). After imaging, the fresh weights (FWs) of roots and shoots were recorded. FCR activity was analyzed from the roots following the method in (Aksoy and Koiwa, 2013). Briefly, after the physiological measurements were completed, the plant roots were washed 3 times in distilled water, dried with tissue paper, and weighed. Then, the root samples were placed in the FCR activity solution (0.1 mM of Fe (III)- ethylenediaminetetraacetic acid (EDTA) and 0.3 mM of ferrozine in distilled water). The samples were kept in the solution for 12 h in the dark at room temperature. Then, the absorbance of the solution was read at 562 nm against a blank without the roots. The enzyme activity was calculated with a molar extinction coefficient of 28.6 mM^{-1} cm^{-1} and presented as normalized to root FW. Purple-colored Fe (II)-ferrozine complex formation is quantified using a molar extinction coefficient of 28.6/mM/cm as in the equation:

$$\text{Root Ferric Chelate Reductase Activity} = \frac{(A/28.6)*V}{Root\ FW*12}$$

3.2.6. Total RNA extraction and gene expression analyses

Total RNA was isolated from 200 mg of root sample in a 1-step method using TRIzol reagent (Thermo Fisher Scientific Inc., Waltham, MA, USA) (Chomczynski and Sacchi,

1987). After elimination of the genomic DNA contamination using a RapidOut DNA removal kit (Thermo Fisher Scientific) according to the manufacturer's instructions, RNA integrity and quantity were determined using 1% agarose gel electrophoresis and a microspectrophotometer, respectively. Complementary DNA was produced by the RevertAid First Strand cDNA synthesis kit (Thermo Fisher Scientific) by using random hexamers according to the manufacturer's instructions. Finally, the expression levels of the genes (*DIN1*, *MTPA2*, *AIP1*, *IREG2*, *ST2A*, and *GATA12*) were determined by real-time quantitative polymerase chain reaction (RT qPCR) (Qiagen, USA) using the SYBR Green PCR kit (Roche Diagnostics, Basel, Basel-Stadt, Switzerland) and the primers given in Table 3.4 following our previous study (Aksoy et al., 2013). Relative gene expression was calculated according to the $2^{-\Delta\Delta Ct}$ method (Livak and Schmittgen, 2001) after data normalization with *ELF1B* (Glyma.02g44460) reference gene (Jian et al., 2008). RT qPCR experiments were designed in 2 biological and 3 technical replicates.

Table 3.4. RT-qPCR primers used in gene expression analyses

AGI number	SoyBase Number	Gene Code	Forward primer (5' – 3')	Reverse primer (5' – 3')
AT3G47340	Glyma.11g170300	*ASN1 / DIN6*	CATACTTGCTGTGCTTGGTTG	GCCCACTCCAGTCAGGACCA
AT3G58810	Glyma.11g135500	*MTP3 / MTPA2*	GGAAAGGACACCAAGTGAGA	CCTGCACTCCCTTGATATTTCTG
AT4G27450	Glyma.12g150500	*AIP1*	CCCTGCATCTAACAGTGGCT	GGAAGGTGGATCAGGACGAG
AT5G03570	Glyma.03g042400	*IREG2 / FPN2*	AGAGCCTCTTCTTGCCCAAC	AATTCCCACATCCTGGCACC
AT5G07010	Glyma.11g158900	*ST2A*	GGTCACTACCCACATTGGCA	AATGGGCCAAAACCAACCAC
AT5G25830	Glyma.14g145700	*GATA12*	GGCATGAATGCGCGAAACTA	CTCATAGTGGAGCCCGCC
AT5G12110	Glyma.02g44460	*ELF1B*	GTTGAAAAGCCAGGGGACA	TCTTACCCCTTGAGCGTGG

3.2.7. Statistical analysis

The data were analyzed in Statistix software via variation analysis according to the completely randomized design (n = 6 or n = 3, depending on the analyses). Then, Fisher's LSD test was performed following two-way ANOVA (analysis of variance) at the significance level of 5%. Principal component analysis (PCA) for seed parameters was done by using XLSTAT.

3.3. Part 3: Transcriptomics of IDC-tolerant Soybean Cultivars in Calcareous-alkaline Soil

Iron deficiency tolerance is a complex trait involving several genetic networks. Although several studies have been done until now to identify the genes behind Fe tolerance, many of the genes and transcription factors are still unknown. Therefore, this part of the thesis aimed to identify the novel genetic players involved in conferring tolerance to Fe deficiency in IDC-tolerant soybean cultivars in calcareous-alkaline soil.

3.3.1. Plant material and the growth conditions

Four Turkish soybean cultivars with opposing phenotypes under high soil pH were used in the study. Nova and Atakişi were reported as IDC-sensitive while Arısoy and Sa-88 were tolerant (Maqbool, 2018). After surface sterilization by washing the seeds in 0.25% sodium hypochlorite for 5 mins, followed by 3 times washing with distilled water, the seeds were germinated *in vitro* on Petri plates for five days in between wet tissue papers in a growth chamber at 25 ± 1 °C and 60% relative humidity. After five days, germinated seedlings with similar root lengths (at similar growth stages) were transferred to the potting mixture (peat and perlite mixture at a ratio of 2:1). Before transferring the seedlings into the potting mixture, the roots were dipped into *Rhizobium japonicum* (USDA 110 strain) containing solution, which was prepared by overnight growth of 2 g of *R. japonicum* in 200 mL of Luria-Bertani (LB) liquid medium (Mullen et al., 1988). Plants were grown in a growth chamber in pots of 28 cm diameter at 25 ± 1 °C and 60% relative humidity. A total of 6 pots were prepared for each cultivar. Half of the pots were designated as Fe-sufficient (control) and half of them were designated as alkalinity-triggered Fe deficient (or in short Fe-deficient) by the addition of the CaO (9 g/kg potting

mixture). While the pH of the control pots was 6, the pH of iron-deficient pots was maintained at 8.7. The pH of the prepared mixes was measured by the glass electrode method before sowing.

3.3.2. Sample Collection and Physiological Measurements

When the soybean plants grown under Fe-sufficient and Fe-deficient conditions reached at V_2-V_3 developmental stage (25-30 days after the germinated plants were transferred to the soil) photosynthesis rate, and stomatal conductance were measured from the top third trifoliate leaf that was fully developed at noontime by using LICOR-6400 portable photosynthesis measurement system. The chlorophyll index was measured by a Minolta SPAD-502 Speedometer. Each data was collected from at least three independent measurements from each plant, and a total of 27 measurements (9 plants x 3 measurements) were taken separately from plants grown under Fe-sufficient and Fe-deficient conditions. Leaf biomass was measured by a digital balance in three replications. Then, leaf samples were dried in the oven at 65 °C for two days, and then the dry weights were measured by a balance.

After the completion of all the physiological measurements, some of the trifoliate leaves of the plants were collected and frozen with liquid nitrogen and stored at -80 °C for total RNA isolation while some were used for the measurement of total chlorophyll contents. For root sample collection, plants were carefully removed from the soil, and roots were washed 3 times with distilled water for 5 minutes each. Root lengths were measured immediately by measuring tape and samples were collected for total RNA isolation and stored at -80 °C. The rest of the root samples were subjected to the following processes for FCR enzyme activity measurements.

3.3.3. FCR enzyme activity and total chlorophyll contents

Samples for spectrophotometric chlorophyll and FCR enzyme activity analyses were collected from 3 plants in each pot, where each plant in the pot was designed as a technical repeat and each pot as a biological replicate. A total of 3 biological repeats and 3 technical repeats were done for each measurement. Chlorophyll and FCR enzyme activities were measured according to the method described in the above parts of the thesis.

3.3.4. Determination of the xylem sap L-glutamine levels and pH

Sensitive (Nova and Atakişi) and tolerant (Arısoy and Sa-88) cultivars were grown under three different treatments: 1) Control (pH 6.0), 2) High soil pH-induced Fe deficiency (pH 8.7), and 3) High soil pH-induced Fe deficiency (pH 8.7) + 43.25 mg Fe-EDDHA /kg soil. For the analysis of L-glutamine concentration in the xylem sap, 30-day-old plants at the V_3 developmental stage were decapitated 3 cm above the soil surface using a sharp blade. The initial 30 µL of xylem sap was discarded. Subsequently, xylem sap was collected for 25 minutes, with up to 1000 µL obtained from each treatment across eight different replicates by a sterile pipet tip. The samples were stored at -86°C for subsequent analysis. The L-glutamine concentration in the soybean xylem sap was determined using the L-glutamine assay kit from Megazyme (Reference code: K-GLNAM, SKU: 700004295) following the manufacturer's protocol. For the xylem sap pH analysis, at least 1 mL of xylem sap was collected in a 1.5 mL Eppendorf tube from each cultivar and treatment. The xylem sap pH was determined using a pHmeter with a mini probe (Lazar Micro Instruments). pH measurement was done from 3 biological replicates in 12 technical repeats.

3.3.5. Total RNA isolation for next-generation sequencing

From the four cultivars used in the trial two IDC-tolerant cultivars (Arısoy and SA-88) were selected for the transcriptomic analyses. For RNA sequencing, the total RNA was extracted from the top third trifoliate leaves and roots by Qiagen RNeasy Mini Kit according to the manufacturer's protocol in three biological replicates. Then, total RNA samples were treated with DNase I (Thermo Scientific) to remove genomic DNA contamination according to the manufacturer’s manual. The RNA concentrations were determined with a microspectrophotometer (nanodrop) (Table 4.3), and its quality and integrity were monitored with a 1% agarose gel containing 0.5X TBE buffer. In the integrity analysis of the isolated total RNAs, attention was paid to clear 28S and 18S rRNA bands (Figure 4.19).

Following RNA isolation, samples with high concentration and integrity were combined in an equal concentration in a separate tube and at the end divided into two equal parts in

two separate tubes (which were considered as two replicates for each treatment and each cultivar), and then these samples were shipped to the center where the next-generation sequencing (NGS) was carried out to form sequencing libraries. RNAStable kit and special packaging envelopes ("Sample Pouch") were used to avoid RNA degradation during the sample shipment. Before sending the samples to the company, as a trial 1 tube from the RNAStable kit was checked by putting the RNA sample in it, and that RNA sample was placed at room temperature for four days (estimated time to reach the sequencing center), then at the fifth day, its quality and integrity was monitored with a 1% agarose gel containing 0.5X TBE buffer (Figure 4.20).

3.3.6. Determination of the transcriptome changes with NGS and bioinformatic analyses of sequencing data

Pair-end transcriptome sequencing of the total RNA samples was done using the Illumina HiSeq 4000 next-generation sequencing system (Varshney et al., 2009). Accordingly, mRNA isolation and enrichment were carried out from the total RNA samples, whereby the sequencing of rRNA and tRNAs, which constitute nearly 90% of the transcript, was prevented. After sequencing, low-quality readings were filtered from the RNA sequences, and the adapter sequences were removed (low-quality score cut-off value 20 and 1% error margin; sliding window size 5 bp; length score cut-off value 36 bp). Then, the contigs were assembled and aligned against the soybean genome sequence completed in 2010 (Shultz et al., 2006, Schmutz et al., 2010). Using the soybean genome as a reference (Brown et al., 2021), firstly, the mapping of transcriptomes was completed and the transcriptome joining was done using matching sequences. The bioinformatics analysis program (Cufflinks version 2.2.1) used during transcriptome joining also creates data on the number of repetitions of RNA sequences in the transcriptome, i.e. the amount of gene expression (Trapnell et al., 2012). At this stage, the expression levels of gene transcripts were also obtained in addition to the transcriptome joining.

As the last part of the bioinformatics analysis, the original gene sequences obtained from the transcriptome joining were annotated. For this purpose, annotations were made in 7 functional citation databases in the form of BLAST alignments using the unigene sequences. These are NR, NT, GO, COG, KEGG, Swissprot, and InterproScan databases. Contigs with an E-value of 1e-5, showing more than 80% homology, were referred to as

protein-coding gene sequences and were selected. These sequences were scanned against the sequences in the UniProtKB knowledge base with Blast2GO and Ontologizer 2.0 (UniProt Consortium, 2015), and the functional groupings of each were done according to the Gene Ontology (GO) in the TAIR database (Hernandez et al., 2002).

With the Kyoto Encyclopedia of Genes and Genomes (KEGG) analysis, the pathways where these transcripts take part were determined (Kanehisa et al., 2000). Based on these analyzes, key genes were divided into broad functional groups according to the following priorities:

1) Examining gene expression patterns with Gene Cluster analysis,
2) Identification of differentially expressed transcripts, to understand the tolerance mechanisms of Arısoy and Sa-88 cultivars against iron deficiency and to identify the pathways in which these genes are involved.
3) Identification of transcription factors whose expression varies under iron deficiency in Arısoy and Sa-88 roots and leaves.
4) Determination of transmetal transporters whose expression varies under iron deficiency in Arısoy and Sa-88 roots and leaves.
5) Hierarchical grouping of genes with varying expression between two cultivars and tissues by using the Manhattan approach.
6) The gene ontology (GO) enrichment was performed using PANTHER 14.0 according to Fisher's exact test and corrected by Bonferroni correction for multiple testing, where $p < 0.05$ (Mi et al., 2019).
7) Examining the expression patterns of differentially expressed transporters of *Glycine max* orthologs in *Arabidopsis thaliana* under 14 different iron deficiency studies by using Genevestigator (Zimmermann et al., 2004).
8) Co-expression analysis of UMAMIT family was done by using the ATTED (II) (http://atted.jp/), Network Drawer (Obayashi et al., 2007), where the co-expression option was set to 'add a few genes and the PPI was set to 'Draw PPIs'. While the genevestigator (Zimmermann et al., 2004) was used to analyze the expression patterns of selected UMAMIT (*AtUMAMIT28*) under iron deficient studies.

3.3.7. Statistical analyses

The data were analyzed in Statistix software via variation analysis according to the completely randomized design (n = 6 or n = 3, depending on the analyses). Then, Fisher's LSD test was performed following two-way ANOVA (analysis of variance) at the significance level of 5%. Student's t-test was used to compare two groups at the significance level of 5% if needed.

3.4. Part 4: Characterization of UMAMIT28 in Arabidopsis thaliana under transmetal deficiencies

Since many members of the UMAMIT family of transporters were differentially expressed in IDC-tolerant soybean cultivars under alkaline conditions, we hypothesized that UMAMITs might be involved in Fe homeostasis and IDC-tolerance in plants. To prove this hypothesis, this part of the thesis aimed to identify the most promising candidate UMAMIT in the family and characterize it in the model plant *Arabidopsis thaliana* under transmetal deficiencies.

3.4.1. Confirmation of homozygous lines of *umamit28-1* and *umamit29-1*

umamit 28-1 (SALK_099741C) and *umamit 29-1* (SALK_133129C) mutant seeds were obtained from Nottingham Arabidopsis Stock Center (NASC). Sterilization *of umamit28-1 (*SALK_099741C), *umamit29-1* (SALK_133129C) lines, and wild-type Col-0 seeds was done by washing in 70% ethanol for 1 minute and then washing 3 times with sterile distilled water (Aksoy et al., 2013; Aksoy, 2014). For general growth, mutants and wild-type Col-0 seeds were plated on the ¼ strength MS media, 1% Sucrose, and 1% agar. After stratification for 2 d at 4°C, the plates were kept in a growth incubator under a long-day photoperiod (16 h of light, 8 h of darkness) at 22°C for 10 d. Afterward, the plants were transferred to peat and perlite growing media 2:1 (Peat: Perlite) and allowed to grow under control conditions in the growth chamber at (16 h of light, and 8 h of darkness) at 22°C for the next 10 days. Later on, leaf samples were collected for the Wild type and T-DNA PCR analysis. Primers used for the PCR are given in Table 3.5. Confirmation of *umamit 28-1* (SALK_099741C) and *umamit 29-1* (SALK_133129C) was done by using the gene specific and T-DNA salk primer (LB6301R) (Table 3.5).

Table 3.5. Primers used in T-DNA and wild-type PCR confirmation of *umamit 28-1* (SALK_099741C) and *umamit 29-1* (SALK_133129C).

Primer Name	Sequences (5' – 3')
SALK_099741C _F	GCAATCACCTTCGCTTTGGC
SALK_099741C _R	CGTCGTCATTGCTTGTCCTA
SALK_133129C_F	GATGAAGGAAGAACAATGGG
SALK_133129C_R	GTTGCTGACGTGTACGAAAGC
Salk_LB6313R	TCAAACAGGATTTTCGCCTGCT

3.4.2. Cloning of *AtUMAMIT28* CDS region in *pDONR207*

The coding sequence of *AtUMAMIT28* (1097 bp) was cloned from the cDNA of the whole plant using the Gateway cloning system (ThermoScientific). This amplification process was carried out using gene-specific forward and reverse primers with partial sequences of universal primers U3 and U5 (Table 3.6). The PCR product was loaded on a 1% agarose gel to determine whether the amplification had taken place. The PCR product was purified from the gel with the help of the QIquick Gel Extraction Kit (Qiagen) following the manufacturer's protocol and then used for the BP reaction (Invitrogen) following the manufacturer's protocol (Invitrogen Gateway™ BP Clonase™ II Enzyme mix, Catalog number: 11789100). A reaction without BP Colonase enzyme was used as a negative control to check whether the BP reaction was taking place properly. In the BP reaction, *pDONR207* (Figure 3.1) was used as an entry clone. In short, *Escherichia coli DH5α* competent cells were transformed with the BP reaction product prepared above according to a previous study. For this, 1 µl of BP reaction was transferred to 100 µL of *DH5α* competent cells. Cells were incubated on ice for 30 minutes and heat shock was delivered at 42 °C for 1 minute. Tubes were then kept on ice for 1-2 minutes. After this 200 µL of pre-warmed 2YT medium (at 37 °C) was added in the tubes and incubated for 1 hour at 37 °C, at 225 rpm. Then, 200 µL of the bacterial solution was spread on the plates (LB agar) containing 50 µg / ml of gentamycin.

Then, the plates were kept at 37 °C overnight. The next day, 15 colonies were selected for the colony PCR, which was done by using gene specific forward and reverse primers (Table 3.6). Then, PCR products were loaded and analyzed on 1% agarose gel. The colonies containing the gene were removed from petri and cultured overnight in liquid LB at 37 °C, 225 rpm in a shaking incubator.

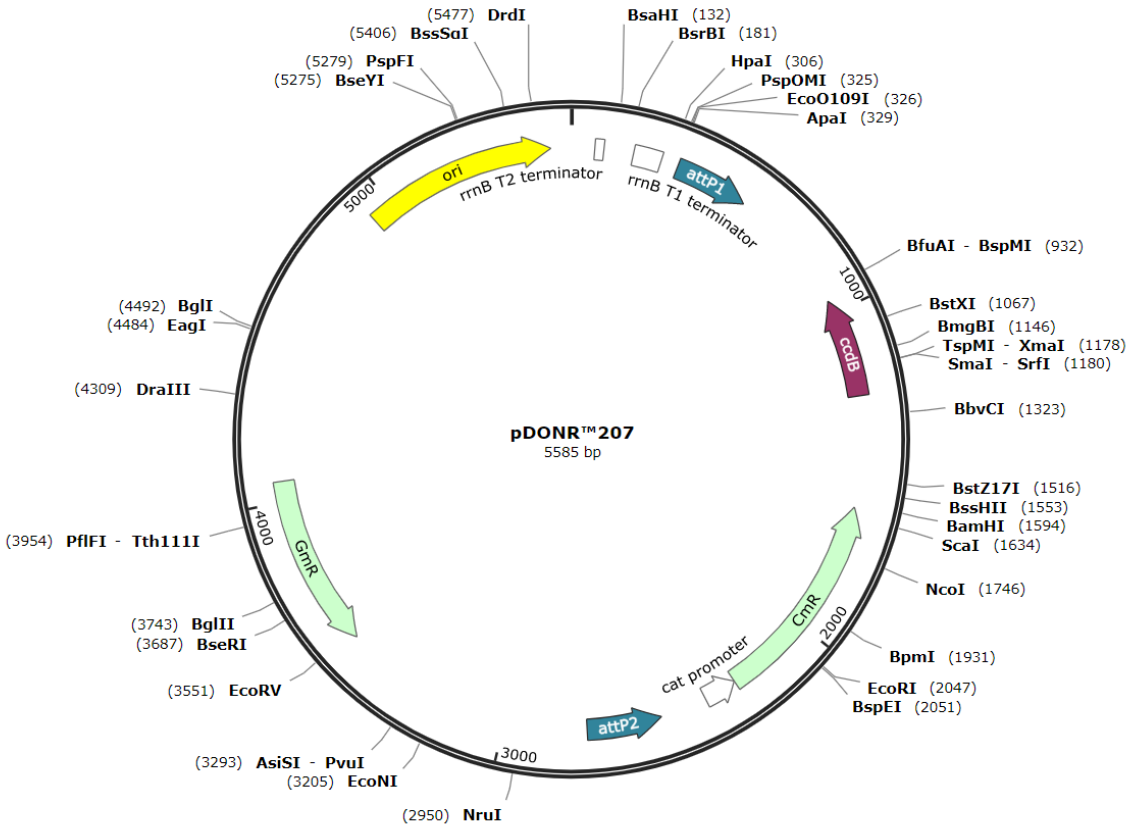

Figure 3.1. *pDNOR207* is used as an entry clone for the AtUMAMIT28 coding region.

The next day, plasmid isolation was performed using the High Pure Plasmid Isolation kit (Roche) according to the manufacturer's protocol. The plasmid DNA was stored at -20 °C. Plasmids isolated from the three positive colonies were sent for sequencing to Eurofins (https://eurofinsgenomics.eu/). Three independent clones were sequenced by forward and reverse primers for bilateral service to verify the insertion of the gene in the correct sequence into the vector. Chromatogram analysis of the series was obtained through Geneious software. The colony with the correct sequence was used for further reactions.

3.4.3. Cloning of *AtUMAMIT28* CDS region in plant and yeast expression vectors

In the next step, the *AtUMAMIT28* gene (without stop codon) was transferred to the plasmid *pMDC83* (Curtis and Grossniklaus, 2003) (Figure 3.2) to generate the expression clone via LR reaction. For the transfer of the *AtUMAMIT28* gene to a yeast-specific expression clone, a stop codon was added by site-directed mutagenesis using the QuikChange II kit (Agilent) according to the manufacturer's protocol. Then, the LR reaction was done to insert the *AtUMAMIT28* CDS region in the *pDR195* (Figure 3.3) vector. For the LR reactions, the manufacturer's protocol was followed (Invitrogen Gateway™ LR Clonase™ II Enzyme mix, Catalog number: 11791020).

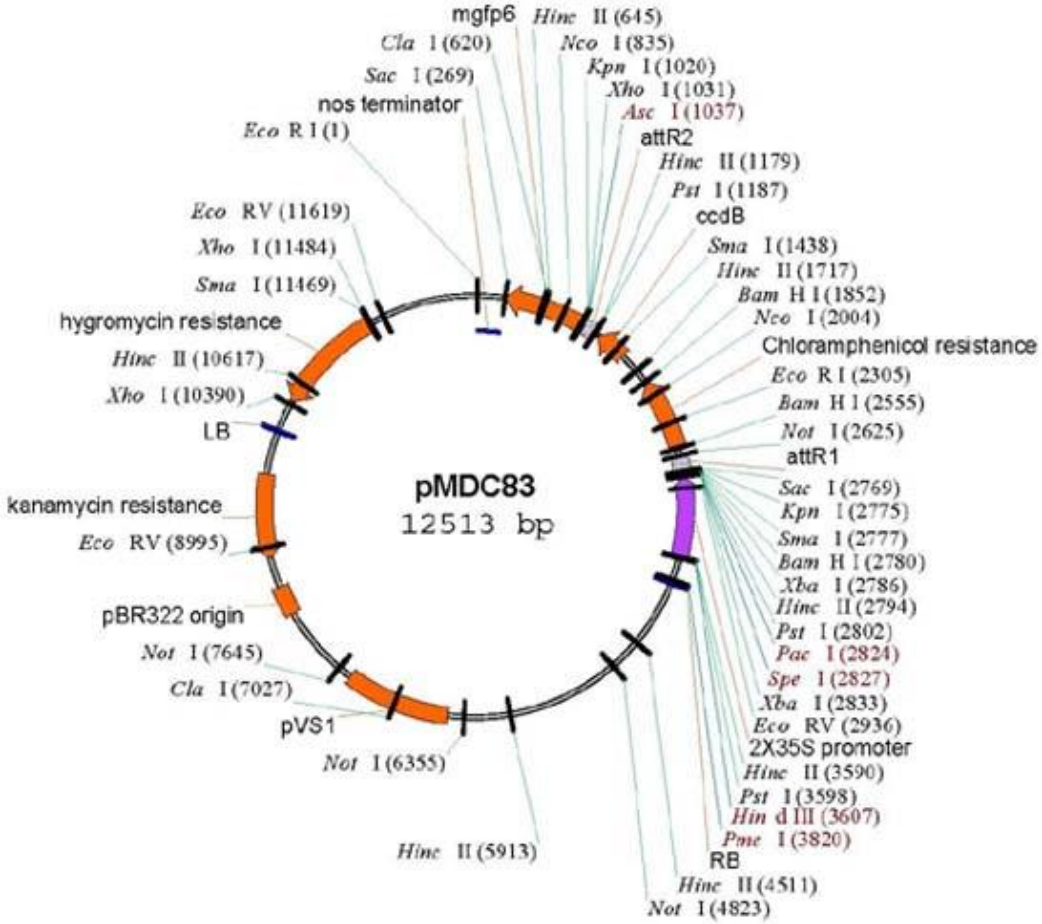

Figure 3.2. *pMDC83* is used as a destination vector to generate plant expression clones. (Curtis and Grossniklaus, 2003)

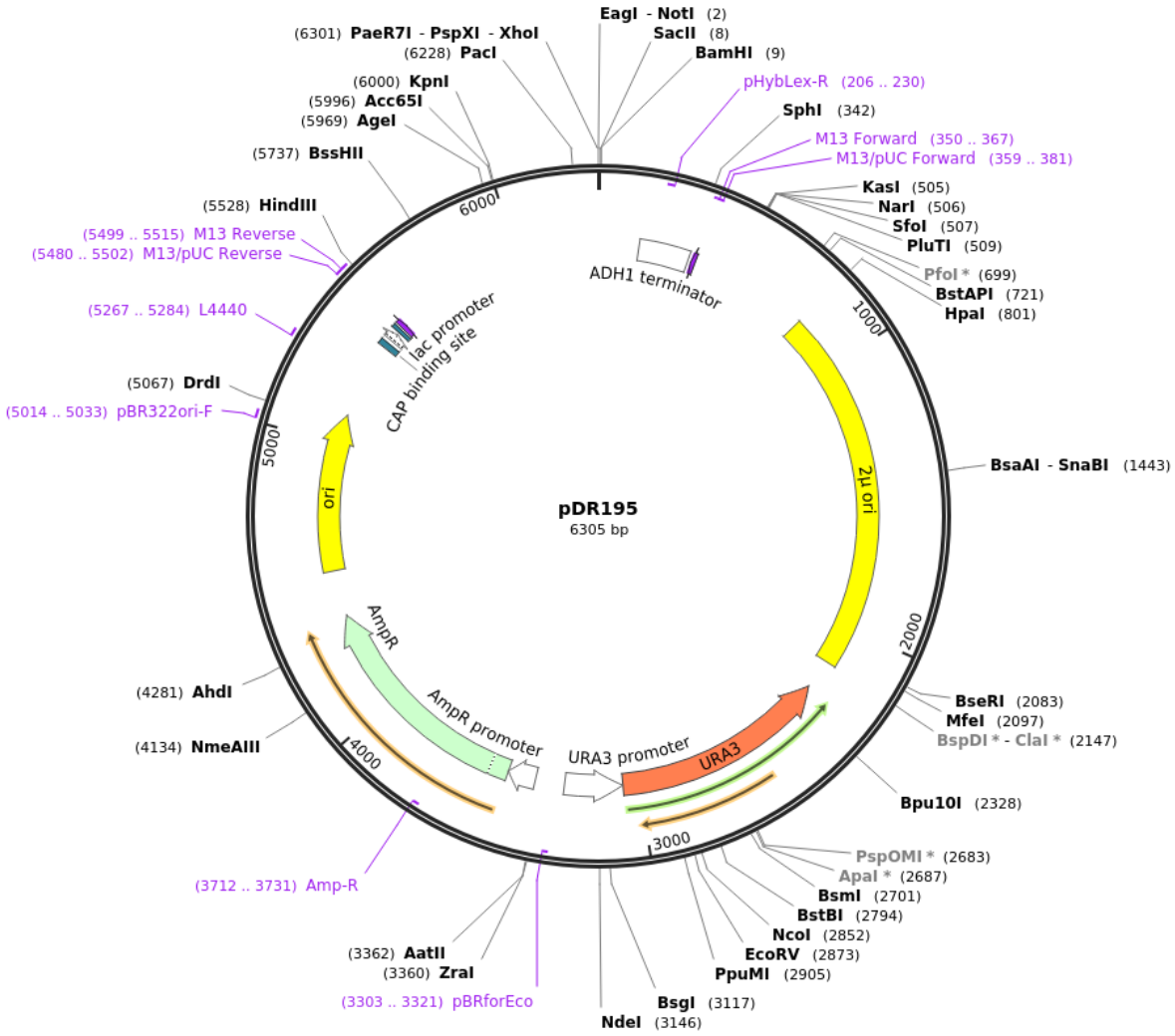

Figure 3.3. *pDR195* is used as a destination vector to generate yeast expression clones.

3.4.4. Transformation of *pMDC83-AtUMAMIT28* in E. coli and A. tumefaciens

Transformation into *E. coli* cells were done by using the same procedure as done after the BP reaction and explained above. Then, the colony PCR was performed to identify the correct colonies. The colonies containing the gene were grown in liquid LB with appropriate antibiotics overnight. To verify the insertion of genes into the target vector in the correct sequence, at least 3 independent clones were sequenced with forward and reverse primers specific to the gene.

For the transformation of clones into *Agrobacterium tumefaciens Agl-0* strain, 1 µg of the target vector was added to 100 µL of competent cells and the tube was incubated for half an hour with the target vector on ice. Then, the cells were transformed by electroporation (BioRad) via the electric pulse at 2.5 Kv + 25 uf. After electroporation, 200 µL of 2YT medium was immediately added to the cuvettes. Then, the solution was recovered and transferred to a 1.5 mL Eppendorf tube and incubated at 28 °C at 200 rpm for 2 hours. Next, the transformed colonies were selected on LB agar plates containing rifamycin (50 µg/mL) and kanamycin (50 µg/mL) at 28 °C. Colonies were obtained after 2 days. Then, the colonies were confirmed by a colony PCR. Ten colonies were removed with toothpicks and drawn on a kanamycin + rifamycin petri dish and incubated at 28 °C.

3.4.5. Transformation of *Arabidopsis thaliana* plants

Agrobacterium cells transformed with target vectors were cultured for 5 hours at 250 rpm in 5 mL LB (Kanamycin 100 µg / mL, Carbenicillin 200 µg / mL). Then, 5 mL of culture was added to 200 mL of LB in a 1 L-flask and the culture was shaken at 250 rpm at 28 °C until the OD600 measurement reached 0.6. Following 13000 rpm of 15 minutes of centrifugation at 20 °C, the cells were collected in 50 mL falcon tubes. After the supernatant was discarded, the cells were resuspended with a solution containing 300 mL of 5% sucrose and Silwet L-77 to a concentration of 0.05%.

The 6-week-old Arabidopsis (flowers started to open but before the formation of silicates) Col-0 ecotype and *umamit28-1* (for complementation) flowers were soaked for 45 seconds with the resuspended cell solution. The plants were laid on the side for 10 minutes and placed in a plastic box, covered with a plastic cap, and the boxes were placed in the growth chamber. Subsequently, the plants were grown at 24 ± 1 ºC under a long-day photoperiod (16 hours light, 8 hours dark), in extremely high humidity (70%). All the primers used for cloning, colony PCR, and site-directed mutagenesis are given in Table 3.6.

3.4.6. Development of *AtUMAMIT28* overexpression and complementation lines of *A. thaliana*

After seed sterilization with 70 percent ethanol for 1 minute followed by three times washing with distilled water, T_1 transformed seeds with *pMDC83: UMAMIT28* CDS region was spread on ½ MS media containing 1% sucrose, 0.8 % agar and 20 μM/ml of hygromycin. Seed stratification was done at 4 ^{0}C for two days. Later plates were kept under light for three hours and afterwards covered with aluminum foil in the dark for three days. Next, the plates were kept under light for 3 days. Plants with longer hypocotyls length were transferred to the rescue media ½ MS media containing 1% sucrose, and 0.8 % agar for further 5 days. Then the plants were transferred to soil in an automatic growth chamber at 24 ± 1 C of constant temperature with relative humidity of 40 - 60% in a long day photoperiod for confirmation of transgenic lines by PCR analysis and to collect the seeds for the next generation. T_2 seeds were sterilized with 70 percent ethanol for 1 minute followed by three times washing with distilled water, seeds were spread on ½ MS media containing 1% sucrose, 0.8 % agar, and 20 μM/ml of hygromycin. Seed stratification was done at 4 ^{0}C for two days. Later, the plates were kept under light for three hours and then covered with aluminum foil in the dark for three days. Next, the plates were kept under light for 3 days. Transgenic plant lines that were showing 3:1 long hypocotyl: short hypocotyl on hygromycin media were selected for PCR confirmation to collect the T_3 Seeds. On the other hand, lines showing 15:1 were discarded to avoid the multiple insertion lines for further analysis. For the PCR confirmation of transgenic lines primer 35S Promoter F and *UMAMIT28* R were used as given in Table 3.6. Then, the lines that highly expressed the *UMAMAIT28* were selected for further analysis (primers are given in Table 3.6).

Table 3.6. Primer sequences used for cloning, colony PCR, and site-directed mutagenesis analyzes.

Primer Name	**Sequences (5' – 3')**
U3	CAAGAAAGCTGGGTCAACGGGCGACTTAGAGTCGTTATCC
U5	GGGACAAGTTTGTACAAAAAAGCAGGCTTCGAAGGAGATAGAACCATG
UMAMIT28 F	GAGATAGAACCATGGCTGGAGATATGCAAGGAGTAGTGAG
UMAMIT28 R without stop codon	CAAGAAAGCTGGGTCAACGGGCGACTTAGAGTCGTTATCC
UMAMIT28 R with stop codon	GGATAACGACTCTAAGTCGCCCGTTTAAGACCCAGCTTTCTTG
35S Promoter F	AGGGTCTTGCGAAGGATAGTG
UMAMIT28 R	CCAATCACCTTCAACATTCCTGCT
*UMAMIT28*_QPCR_F	CGTCATCATATACGCTGGAGTGG
*UMAMIT28*_QPCR_R	TTAAACGGGCGACTTAGAGTCG

3.4.7. Iron deficiency treatment

AtUMAMIT28 homozygous overexpression lines, namely *AtUMAMIT28* OE1 and *AtUMAMIT28* OE2, and *umamit28-1* mutants used in Fe deficiency experiments together with wild type Colombia-0 (Col-0) ecotype. The seeds were washed 3 times with sterile distilled water after surface sterilization for 1 minute in 70% ethanol. ABIS media was used as a plant growth media containing 1% sucrose, 2.5 mM $H3PO_4$, 5 mM KNO_3, 2 mM $MgSO_4$, 1 mM $Ca(NO_3)_2$, Murashige&Skoog microelements, 1% agar, 1 mM 2-(N-morpholino) ethanesulfonic acid (MES) adjusted with KOH to pH 6 and 50 µM Fe - EDTA (for control treatment), for the iron-deficient media no iron was added to the media and as a further additional treatment to overcome the iron contamination from agar and sucrose 200µM of FZN (ferrozine 200µM, [3-(2-pyridyl)-5,6-diphenyl-1,2,4-triazine sulfonate) was added to the media (Molins et al.,2013). Sterile plastic petri plates having a size of 90 x 15 mm (diameter x height) were used in the study. Cellophane membranes (Sigma), which were cut to the size of the Petri dishes, were placed on the control medium after being sterilized in an autoclave for easy stress applications. Cellophane membranes have nano-sized holes in them and the membranes allow for the passage of nutrients. Therefore, they are often used in plant nutrient stress applications (Koiwa et al., 2006; Aksoy et al., 2013).

Synchronized germination and development were achieved by placing 8 overexpression, or mutant seeds in half of the petri dishes and 8 Col-0 seeds in the other half. The seeds were placed along an imaginary line above the cellophane membrane, at least with 4 mm between them, so that they do not touch each other, or the petri walls. After placing the sterilized seeds on the Petri dishes in a sterile laminar cabinet, they were closed with surgical tape which allows air passage. Then, the Petri dishes were kept in the dark for 2 days at 4 ºC for seed stratification. Next, the plates were placed in a growth chamber and the plants were grown vertically at 23 ± 1 ºC of constant temperature in a long-day photoperiod for five days. The light intensity was adjusted to 150 µmol PAR m^{-2} s^{-1} light provided by white LED light (Lamptime cool-light 6500K) over the plant canopy.

After 4 days of growth on the control medium, plants were transferred to either control, Fe deficient, or FZN (no iron + 200µM Ferrozine) media in a sterile laminar cabinet. Then, the plants were allowed to grow in a controlled growth chamber on control and FZN medium for the next five days. Each petri dish was considered as one biological replicate and was replicated 10 times.

3.4.8. Physiological and biochemical measurements

Plants exposed to Fe deficiency for 5 days on FZN medium were photographed and the root lengths were analyzed using ImageJ (http://rsbweb.nih.gov/ij/) software (Cookson & Granier, 2005). Then, the root and shoot fresh weights were measured by a digital balance. Next, the samples were dried in a 65 °C oven for 24 hours and their dry weights were weighed. A total of 5 biological replicates were used in fresh and dry weight analyses.
FCR enzyme activity and total chlorophyll contents were measured according to the methods described in Part 1. The roots and shoots of 8 plants in each petri dish were separated and their dry weights were recorded. For the seed metal content analysis plants were grown in the growth chamber at 22 ± 1 °C and 60% relative humidity. Peat moss was used as a soil medium. Samples were collected when the plants were matured. After keeping the seeds at 60°C for 2 days dry weights of the seeds were recorded, and metal content analysis was done according to the methods defined in the previous parts of the thesis.

3.4.9. Gene expression analysis

After five days of stress application, total RNA was isolated from the root and shoots according to the method described in Part 1. After the quality and quantity determinations, DNase I application and cDNA synthesis were performed. Then, the expression levels of Fe uptake and signaling genes (*IRT1, FRO2, FER, FIT*) were determined by qRT-PCR as described in Part 1. The primer sequences are given in Table 3.7.

Table 3.7. Primer used for iron homeostasis gene expression analyses.

Oligo name	Gene	Sequences (5' – 3')
*FIT*_QPCR_F	*FIT*	ACCTCTTCGACGAATTGCCTGACT
*FIT*_QPCR_R	*FIT*	TTCATCTTCTTCACCACCGGCTCT
*IRT1*_QPCR_F	*IRT1*	ACCCGTGCGTCAACAAAGCTAAAG
*IRT1*_QPCR_R	*IRT1*	TCCCGGAGGCGAAACACTTAATGA
*FRO2*_QPCR_F	*FRO2*	TGTGGCTCTTCTTCTCTGGTGCTT
*FRO2*_QPCR_R	*FRO2*	TGCCACAAAGATTCGTCATGTGCG
*FER1*_QPCR_F	*FER1*	CGTTGCTATGAAGGGACTAG
*FER1*_QPCR_R	*FER1*	CTGAGATAGGTGAGACGATAGG
18S _QPCR_F	*18S rRNA*	CATAAACGATGCCGACCAG
18S _QPCR_R	*18S rRNA*	AGGCTTGCGACCATACTTC

3.4.10. Subcellular localization of *AtUMAMIT28*

After five days of stress application, root tips, meristematic zone, elongation zone, and differentiation zone of at least three *UMAMIT28 OE* lines were wet-mounted, and confocal images were obtained on a Leica SP8 microscope to acquire GFP (λex= 490 nm, λem= 500–550 nm) using a Photometrics EMCCD Evolve camera.

3.4.11. Yeast transformation and complementation assay

Yeast strains used in the current metal homeostasis study were *S. cerevisiae* BY4741 and mutants with the BY4741 background including *Δzrt1zrt2* (defective in zinc uptake), *Δctr1* (defective in copper uptake), *Δfet3fet4* (defective in iron uptake), *Δsmf1* (defective in manganese uptake) and *Δycf1* (sensitive to cadmium). Yeast strains were transformed with either *pDR195:UMAMIT28* or *pDR195:GUS* according to the lithium acetate method described by Gietzet al. (1995).

Yeast containing the desired expression vectors was grown on liquid synthetic dropout (SD)-uracil media (Yeast Nitrogen Base, 1% glucose, dropout medium lacking uracil). All strains are grown as pre-cultures exponential to the beginning of the stationary phase. For all solid media experiments, when the OD_{600} of strains was reached at 1, the dilution was made to OD_{600} 1, 0.1, 0.01, and 0.001 and was spotted onto SD-uracil medium

containing 6.7 grams/L of yeast nitrogen base (Sigma), 1.92/L of yeast synthetic drop-out media without uracil (Sigma) and 2% glucose (Sigma) either with or without additional metal salts ($CdCl_2$, $FeCl_3$, $MnSO_4$, $ZnSO_4$, $CuSO_4$) and chelators for testing yeast growth. Growth details of each strain are given below.

3.4.11.1. Complementation of *Δsmf1*

Wild-type yeast (*S. cerevisiae* BY4741) and *Δsmf1* mutant, either transformed with *pDR195:AtUMAMIT28 CDS* or *pDR195:GUS*, were used in the study. For testing on the solid media (Yeast Nitrogen Base, 1% glucose, dropout medium lacking uracil, 20 g/L Bacto agar, buffered to pH 6 with 50 mM MES), the growth media was supplemented with 5-10 mM EGTA and 100 µM $MnSO_4$ or 0 µM $MnSO_4$. For the growth assay analysis in liquid culture, yeast strains were grown in control liquid media (Yeast Nitrogen Base, 1% glucose, dropout medium lacking uracil + 100 µM $MnSO_4$) and Mn deficient media (Yeast Nitrogen Base, 1% glucose, dropout medium lacking uracil + 0 µM $MnSO_4$ + 10mM EGTA).

3.4.11.2. Complementation of *Δfet3fet4*

In this study, we investigated the growth of *S. cerevisiae* BY4741 wild-type and the *Δfet3fet4* mutant strains, each transformed with either the *pDR195:AtUMAMIT28,* or *pDR195:GUS*, under varying iron conditions. Growth was assessed on solid media composed of Yeast Nitrogen Base (YNB) w/o amino acids with 1% glucose, dropout medium lacking uracil, and 20 g/L Bacto agar, buffered to pH 6 using 50 mM MES. The media were supplemented with either 200 µM $FeCl_3$ and 100 µM BPDS as a control or with 30 µM $FeCl_3$ and 10 µM $FeCl_3$, both in combination with 100 µM BPDS, to create iron-deficient conditions.

For liquid culture assays, yeast strains were grown in control media (YNB with 1% glucose, dropout medium - uracil, 200 µM $FeCl_3$, and 100 µM BPDS) and in iron-deficient media (YNB with 1% glucose, dropout medium - uracil, 30 µM $FeCl_3$, and 100 µM BPDS).

3.4.11.3. Complementation of *Δzrt1zrt2*

S. cerevisiae BY4741 wild-type and the *Δzrt1zrt2* mutant strains, each transformed with either the *pDR195:AtUMAMIT28,* or *pDR195:GUS*, were used to investigate their growth under varying zinc conditions. Growth assays were performed on solid media consisting of Yeast Nitrogen Base (YNB) with 1% glucose, dropout medium lacking uracil, and 20 g/L Bacto agar, buffered to pH 6 with 50 mM MES. The media was supplemented with either 100 µM $MnSO_4$ as a control or with 0 µM $ZnSO_4$ + 5 mM EDTA and 0 µM $ZnSO_4$ +10 mM EDTA to create zinc-deficient conditions. For liquid culture assays, yeast strains were grown in control media (YNB with 1% glucose, dropout medium - uracil, 100 µM $MnSO_4$) and in zinc-deficient media (YNB with 1% glucose, dropout medium - uracil, 0 µM $ZnSO_4$ + 5 mM EDTA and 0 µM $ZnSO_4$ + 10 mM EDTA).

3.4.11.4. Complementation *Δctr1*

S. cerevisiae BY4741 wild-type and the *Δctr1* mutant strains, each transformed with either the *pDR195:AtUMAMIT28,* or *pDR195:GUS*, were used to investigate their growth under varying copper conditions. Growth assays were performed on solid media consisting of Yeast Nitrogen Base (YNB) with 1% glucose, dropout medium lacking uracil, and 20 g/L Bacto agar, buffered to pH 6 with 50 mM MES. The media was supplemented with a gradient of copper concentrations, specifically 0, 10, 20, 50, and 100 µM $CuSO_4$, to assess the impact of copper availability on yeast growth.

3.4.11.5. Complementation *Δycf1*

S. cerevisiae BY4741 wild-type and the *Δycf1* mutant strains, each transformed with either the *pDR195:AtUMAMIT28,* or *pDR195:GUS*, were used to investigate their growth under varying cadmium conditions. Growth assays were performed on solid media consisting of Yeast Nitrogen Base (YNB) with 1% glucose, dropout medium lacking uracil, and 20 g/L Bacto agar, buffered to pH 6 with 50 mM MES. The media was supplemented with 0 or 20 µM $Cdcl_2$.

3.4.11.6 Growing conditions and measurements

For all yeast experiments on the solid media, yeast strains were spotted on plates at OD_{600} dilutions of 1, 0.1, 0.01, and 0.001. These plates were then incubated overnight at 30°C. Following incubation, growth patterns were observed and documented through photography. For the liquid culture assays, the cultures were incubated at 30°C for 72 hours at 180 rpm, with OD_{600} measurements taken every 24 hours to monitor growth progression.

3.4.12. Determination of trace metal levels in yeast

For the metal content analysis of the copper experiment, wild-type yeast and *Δctr1* mutants, either transformed with *AtUMAMIT28* CDS or with the empty vector *GUS*, were grown in yeast synthetic media without uracil, supplemented with 10 µM $CuSO_4$, for 24 hours. For iron studies, wild-type yeast and *Δfet3fet4* mutants, similarly transformed with *AtUMAMIT28* CDS or the empty vector GUS, were grown in yeast synthetic media without uracil, supplemented with 100 µM $FeCl_3$, for 24 hours. For $CdCl_2$ content analysis, wild-type yeast and *Δycf1* mutants, either transformed with *AtUMAMIT28* CDS or with the empty vector GUS, were grown in yeast synthetic media without uracil, supplemented with 20 µM $CdCl_2$ or 0 µM $CdCl_2$, for 48 hours. In all the experiments mentioned above, yeast cultures were incubated with shaking at 180 rpm at 30°C to facilitate growth. After incubation, the yeast samples were placed on ice. Yeast cells were recovered by centrifugation (1,300 g, 5 min, 4°C), washed first in 50 ml of ice-cold 10 mM EDTA and 50 mM Tris-HCl (pH 6.5), pelleted, and then washed in ice-cold ultrapure water. The dry weight (DW) of the yeast samples was measured after drying at 60°C for 3 days. The samples in the test tubes were stored overnight at room temperature in 2 mL of 98.8% nitric acid (HNO_3) (re-distilled) (Sigma) and 1 mL of concentrated hydrochloric acid (HCl) (trace metal grade) (Sigma). The next day, the samples were kept at 100°C for 1 hour, 150°C for 1 hour, 180°C for 1.5 hours, and lastly at 210°C until no liquid was left in the test tubes (Vasconcelos et al., 2006). A Muffle furnace was used for acid digestion of samples. The dried specimens were re-dissolved with up to 20 ml of 2% HNO_3, and filtered and the metal levels were determined by ICP-OES (Agilent Technologies).

3.4.13. L-Glutamine Experiment:

For the glutamine experiment, homozygous *irt1*, *frd3-1,* and *fro2* lines together with the wild-type Colombia-0 (Col-0) ecotype were grown on ABIS media with similar nutrient concentrations used as described above. In addition to the control and iron-deficient media, two additional treatments were considered, where 10 mM of L-glutamine was added to the control (50 µM Fe-HBED) and Fe-deficient media (0 µM Fe-HBED). In short, seeds were stratified for 2 days at 4°C and later grown vertically on the control media for five days, and then they were transferred to either control, iron-deficient media with or without 10 mM L-glutamine. Total chlorophyll content, root lengths, and FRO/FCR enzyme activities of plants were measured according to the methods described above.

3.4.14. Copper experiment

AtUMAMIT28 homozygous overexpression lines, namely OE1 and OE2, and *umamit28-1* mutants used in Fe deficiency experiments together with wild-type Colombia-0 (Col-0) ecotype. The seeds were washed 3 times with sterile distilled water after surface sterilization for 1 minute in 70% ethanol. As described above plates containing ABIS media were used as a growth medium for the experiment. In short, seeds were plated on ABIS media and stratified for 2 days at 4 ºC in the dark. Next, the plates were placed in a growth chamber and the plants were grown vertically at 23 ± 1 ºC of constant temperature in a long-day photoperiod for five days. The light intensity was adjusted to 150 µmol PAR m^{-2} s^{-1} light provided by white LED light (Lamp time cool-light 6500K) over the plant canopy. After four days plants were either transferred to control or Cu deficient media (0 µm $CuSO_4$ + 50 µm BCPS) for the next 6 days. Then, measurements were taken. Root lengths, total chlorophyll contents, and gene expression analyses were done as described above. Primers used for the gene expression analyses are given in Table 3.8.

Table3.8. Primer sequences used for Cu homeostasis gene expression analysis.

Oligo name	Gene	Sequences (5' – 3')
qAT Actin-F	*Actin*	GACCTTTAACTCTCCCGCTA
qAT Actin-R	*Actin*	GGAAGAGAGAAACCCTCGTA
qAT CITF1-F	*CITF1*	ACGAGGTCCTTCTATTCGAGCA
qAT CITF1-R	*CITF1*	ACCCTTTGCTCTCGGCAAACTT
qAT COPT1-F	*COPT1*	CATGTCGTTTAACGCCGGTGTGTT
qAT COPT1-R	*COPT1*	CCGGAAAGTTTGGCTTCCGAACAA
qAT COPT2-F	*COPT2*	TGGTGATGCTCGCTGTTATGTCCT
qAT COPT2-R	*COPT2*	TCTGGTCATCGGAGGGTTTCTTGA
qAT FRO5-F	*FRO5*	TACCCAAAAGCAACCCTCCC
qAT FRO5-R	*FRO5*	ATCATCACCCTCCCCATTCT

3.4.15. Statistical analyses

The data were analyzed in Statistix software via variation analysis according to the completely randomized design (n = 6 or n = 3, depending on the analyses). Then, Fisher's LSD test was performed following two-way ANOVA (analysis of variance) at the significance level of 5%. Student's t-test was used to compare two groups at the significance level of 5% if needed.

CHAPTER IV

RESULTS

Part 1: Effect of iron fertilization on soybean cultivars differing in IDC tolerance

4.1.1 Sensitive cultivars require higher Fe-EDDHA application to overcome IDC symptoms

Low iron availability leads to hampered chlorophyll biosynthesis, which results in low photosynthetic rates (Kim and Guerinot, 2007), ultimately reducing plant growth and yield. Therefore, we determined the total chlorophyll contents and photosynthetic rates of soybean cultivars after Fe-EDDHA application under high soil pH. Total chlorophyll contents and the chlorophyll index values were low in all cultivars under high soil pH (Figure. 4.1). However, this reduction was much more drastic in IDC-sensitive cultivars (Atakişi and Nova) than in the tolerant ones (Arısoy and Sa-88) (Figure. 4.1 a, b). This observation was similar to our previous study (Maqbool, 2018). IDC-tolerant cultivars showed the maximum chlorophyll levels at 24.9 mg/kg Fe-EDDHA supplementation followed by a slight decrease at higher dosages, while the sensitive cultivars required higher dosages of additional iron to reach the maximum chlorophyll content. Parallel to these results, the photosynthesis rates of tolerant cultivars were higher or remained unchanged under high pH while the sensitive cultivars showed significant decreases in their photosynthesis rates (Figure. 4.1 c). Further, the photosynthesis rates of IDC-tolerant cultivars were significantly increased depending on the Fe application doses while sensitive cultivars only responded by a slight non-significant change in their photosynthesis rates.

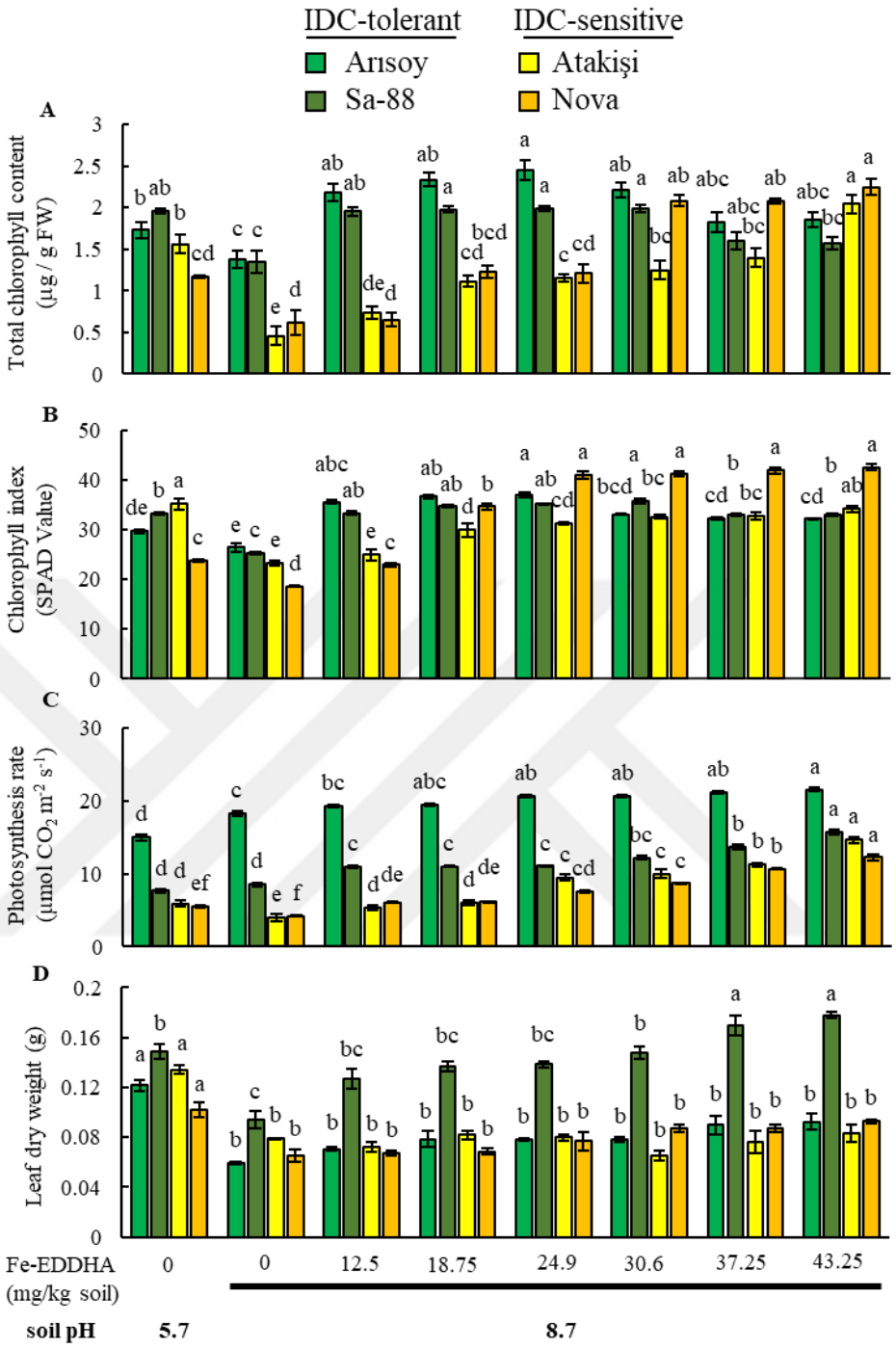

Figure 4.1. Leaf responses of IDC-tolerant (Arısoy, Sa-88) and IDC-sensitive (Atakişi and Nova) soybean cultivars to increasing Fe fertilization under high soil pH. A. Total chlorophyll content. B. Chlorophyll index. C. Photosynthesis rate. D. Leaf dry weight of different soybean cultivars at the V3 stage. FW: fresh weight. The values present the means of six biological replicates ± SE (n = 6). Statistical analysis was done for each cultivar individually. Different letters on the bars indicate statistical differences from each other ($p < 0.05$).

Leaf dry weight is the direct indication of the number of minerals and nutrients in the leaves. Under alkaline conditions, a significantly lower dry weight was observed in all cultivars which did not increase with the addition of different Fe doses in Atakişi, Arısoy, and Nova (Figure. 4. 1 d). However, the leaf dry weight of SA-88 was significantly increased upon Fe supplementation. This can be related to the interaction of iron with other nutrients as these cultivars may accumulate lower levels of other nutrients because of high iron uptake (Elkhouni et al., 2018). Taken together, these results indicate that tolerant cultivars responded more efficiently to the Fe fertilization under high soil pH than did sensitive cultivars, which required higher Fe-EDDHA application to overcome the IDC symptoms.

4.1.2. Effect of Fe-EDDHA on FCR activity and root morphology

Plants modify their roots under different nutrient deficiencies. Low Fe availability (Fe-EDDHA 0 mg/kg soil, pH 8.7) significantly increased the root lengths in all cultivars except for Sa-88 (Figure. 4.2 a). The root lengths of Arısoy, Sa-88, Atakişi, and Nova increased by 46%, 10%, 250%, and 78%, respectively, under high soil pH. Higher Fe-EDDHA dosages significantly increased Sa-88 and Atakişi root lengths while decreasing the Arısoy and Nova root lengths under high soil pH.

An increase in FCR activities was observed in all cultivars under high soil pH, which was decreased with Fe supplementation (Figure. 4.2 b). FCR activities increased by 0.33, 2.6, 5.3, and 1.8 times under high soil pH in the roots of Arısoy, Sa-88, Atakişi, and Nova, respectively. The decrease in the FCR activities after Fe-EDDHA supplementation was more drastic in the tolerant cultivars since even the lowest dosage of Fe-EDDHA application was enough to bring the FCR activity back to the control condition. Overall, FCR activities of sensitive cultivars were recorded significantly higher in all high pH (8.7) treatments than in the tolerant ones.

A linear increase was observed in the root dry weights of IDC-tolerant cultivars with Fe supplementation compared to the control treatment (Figure. 4.2 c). However, the sensitive cultivars did not show any significant changes in the root dry weight under increasing Fe

doses. These results suggest that IDC-tolerant and sensitive cultivars responded similarly to the high soil pH; however, their recovery rates were different after Fe fertilization.

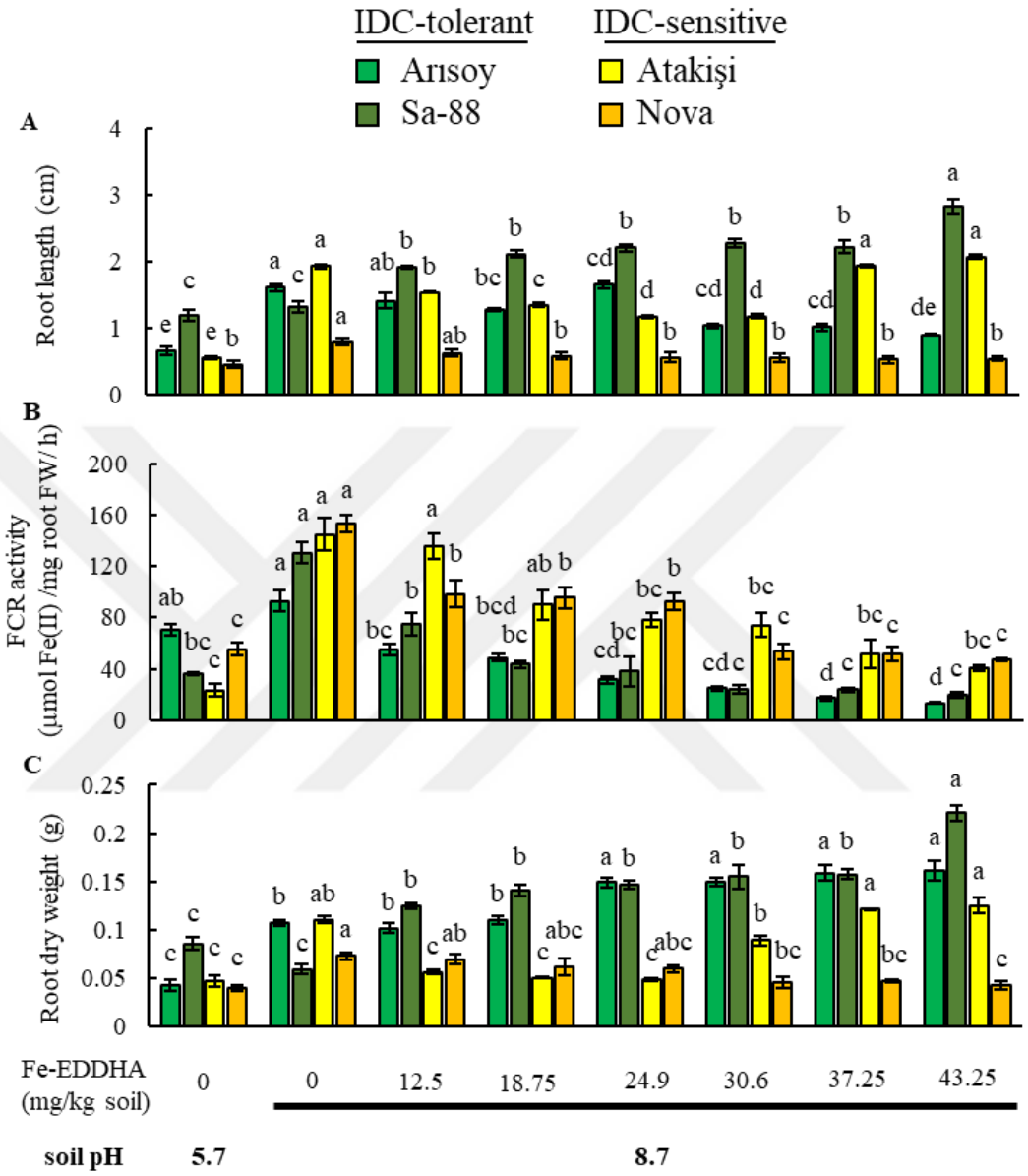

Figure 4.2. Root responses of IDC-tolerant (Arısoy, Sa-88) and IDC-sensitive (Atakişi and Nova) soybean cultivars to increasing Fe fertilization under high soil pH. A. Root length. B. FCR activity. C. Root dry weight of different soybean cultivars at V3 stage. FW: fresh weight. The values present the means of six biological replicates ± SE (n = 6). Statistical analysis was done for each cultivar individually. Different letters on the bars indicate statistical differences from each other ($p < 0.05$).

4.1.3. Fe fertilization rescues Fe uptake and root-to-shoot translocation more effectively in IDC-tolerant cultivars under high soil pH

High pH is known to restrict the iron uptake and translocation in the edible parts of the plant partly due to the limited FCR activity. Compared to pH 5.7, Arısoy, Sa-88, and Nova accumulated higher Fe in their roots under pH 8.7 with 0 mg/kg Fe-EDDHA addition, while Atakişi showed lower Fe levels (Figure. 4.3 a). Root Fe contents of all cultivars increased in parallel to an increase in the Fe fertilizer application, reaching the maximum levels at lower fertilizer dosages in IDC-tolerant cultivars than in IDC-sensitive ones.

Even though all cultivars experienced a decrease in leaf Fe contents under pH 8.7 without 0 mg/kg Fe-EDDHA addition, the reduction was more significant in IDC-sensitive Atakişi and Nova, which showed a decline of 61% and 33%, respectively (Figure 4.4 a). The larger decrease in leaf Fe contents of IDC-sensitive cultivars could be the reason behind their observed higher reduction in chlorophyll contents (Figure. 4.1 a, b) since several chlorophyll biosynthesis enzymes utilize Fe as a cofactor (Miller et al., 1995). Similar to the increase in the root Fe levels, Fe fertilization enhanced the leaf Fe content in all cultivars (Figure. 4.4 a). The highest dose of 43.25 mg/kg Fe-EDDHA addition was enough to recover the leaf Fe content of IDC-tolerant Arısoy and Sa-88. However, it was not enough for the recovery of sensitive genotypes. Taken together, these results indicate that the IDC-sensitive soybean cultivars have a less efficient root-to-shoot translocation of Fe than the tolerant cultivars.

4.1.4 Fe fertilization alters the divalent metal contents according to genotypic differences regardless of tolerance level

Plants uptake more Mn and Zn under Fe deficiency since these divalent metals are taken in the root epidermis by the same family of transporters (Spielmann et al., 2022). According to our results, in general, all cultivars accumulated higher levels of Mn and Zn in their roots and leaves under pH 8.7 without 0 mg/kg Fe-EDDHA addition (Figure. 4.3 b, c and Figure. 4.4 b, c), representing an expected phenomenon under Fe deficiency. Interestingly, IDC-sensitive and tolerant cultivars responded differently to the Fe-EDDHA supplementation under high soil pH in terms of Mn and Zn accumulation in roots and leaves. Tolerant cultivars exhibited higher levels of Mn and Zn in both roots and leaves, even with moderate Fe-EDDHA supplementation under high soil pH.

However, sensitive cultivars experienced reduced Mn and Zn levels following the lowest Fe-EDDHA dosage. Notably, in the tolerant Arısoy, root Mn and Zn levels significantly decreased after 24.9 mg/kg Fe-EDDHA supplementation. In the tolerant Sa-88, leaf Mn and Zn levels decreased significantly after 18.75 mg/kg and 30.6 mg/kg Fe-EDDHA supplementation, revealing genotypic differences in dose-response, regardless of tolerance level. Similar results were observed in a rice study performed on alkaline soil, where Zn content was affected by the genotypes irrespective of Fe fertilizer application (Butsai et al., 2019).

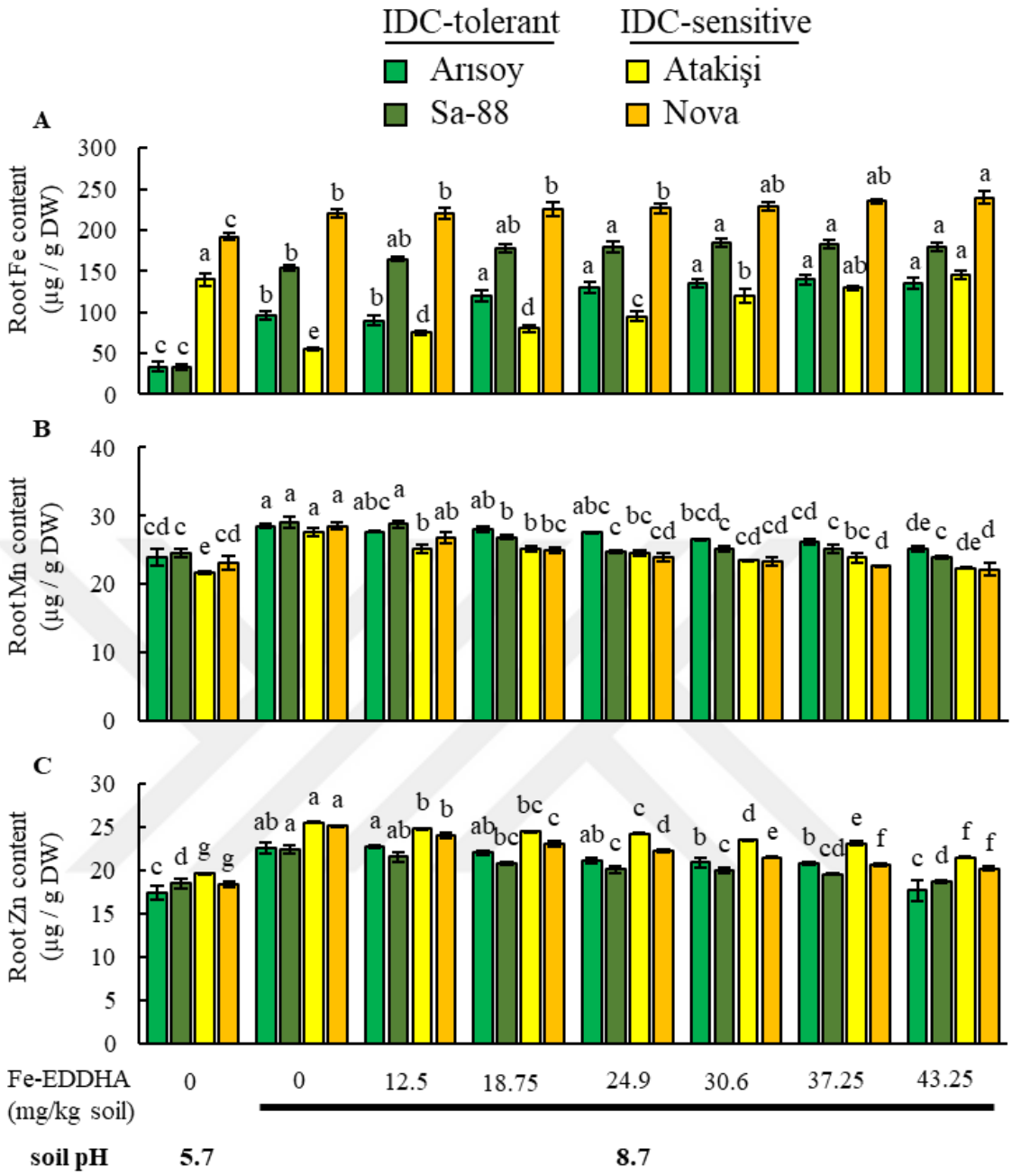

Figure 4.3. Root Fe, Mn, and Zn contents of IDC-tolerant (Arısoy, Sa-88) and IDC-sensitive (Atakişi and Nova) soybean cultivars in response to increasing Fe fertilization under high soil pH. A. Root Fe content. B. Root Mn content. C. Root Zn content of different soybean cultivars. Mineral contents were measured at V3 stage. DW: dry weight. The values present the means of three biological replicates ± SE (n = 3). Statistical analysis was done for each cultivar individually. Different letters on the bars indicate statistical differences from each other ($p < 0.05$).

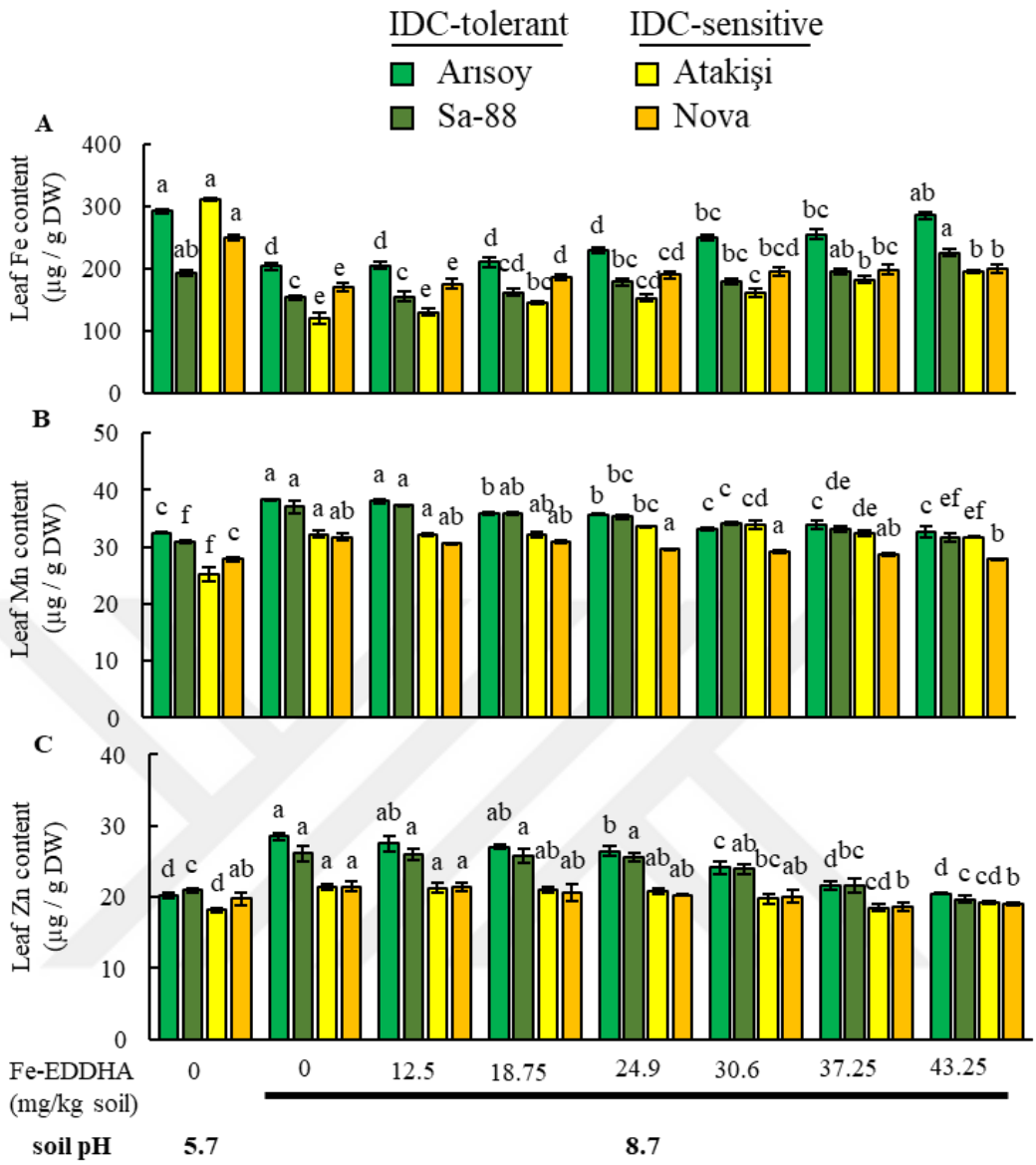

Figure 4.4. Leaf Fe, Mn, and Zn contents of IDC-tolerant (Arısoy, Sa-88) and IDC-sensitive (Atakişi and Nova) soybean cultivars in response to increasing Fe fertilization under high soil pH. A. Leaf Fe content. B. Leaf Mn content. C. Leaf Zn content of different soybean cultivars. Mineral contents were measured at V3 stage. DW: dry weight. The values present the means of three biological replicates ± SE (n = 3). Statistical analysis was done for each cultivar individually. Different letters on the bars indicate statistical differences from each other ($p < 0.05$).

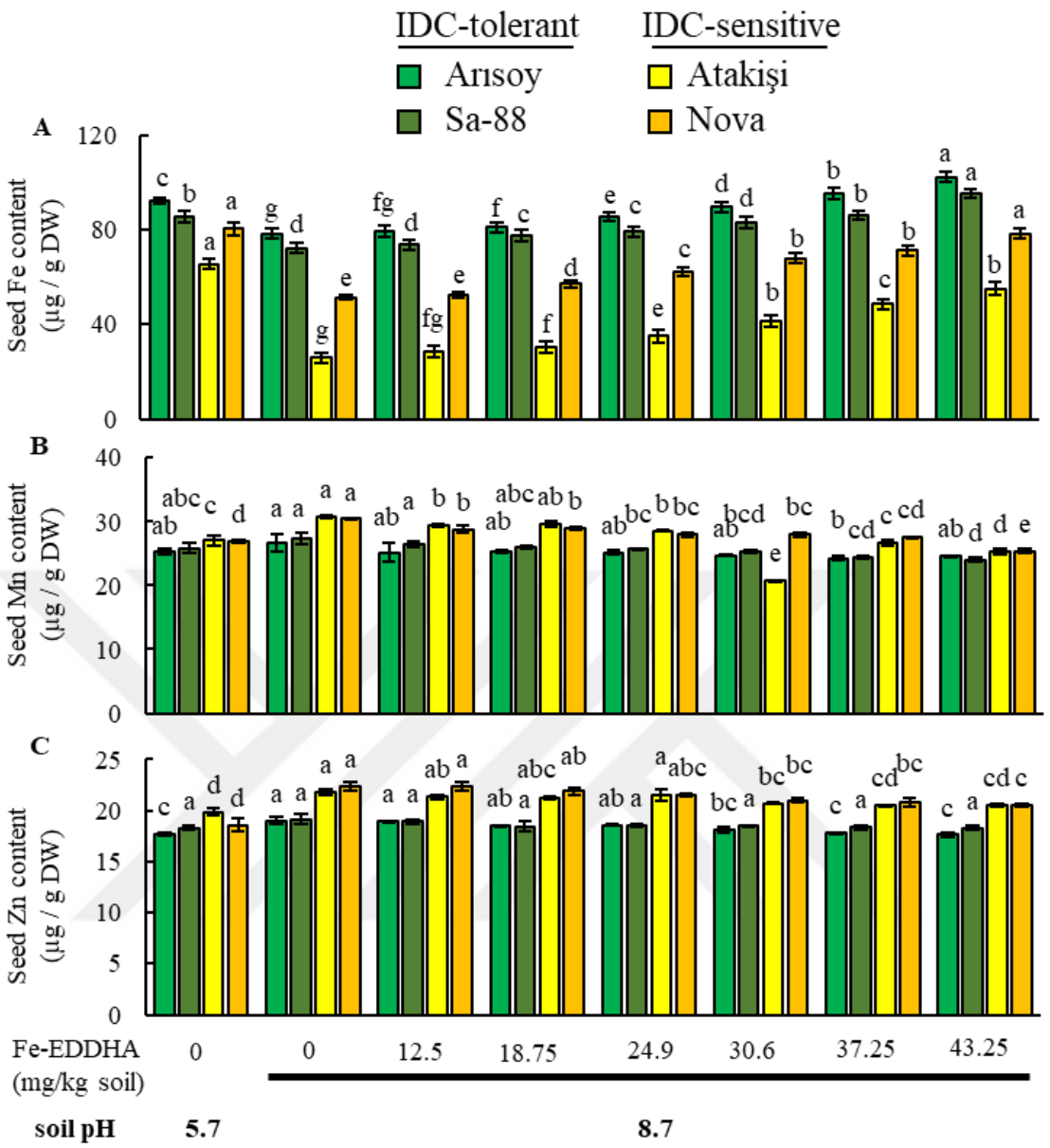

Figure 4.5. Seed Fe, Mn, and Zn contents of IDC-tolerant (Arısoy, Sa-88) and IDC-sensitive (Atakişi and Nova) soybean cultivars in response to increasing Fe fertilization under high soil pH. A. Seed Fe content. B. Seed Mn content. C. Seed Zn content of different soybean cultivars. Mineral contents were measured at maturity. DW: dry weight. The values present the means of three biological replicates ± SE (n = 3). Statistical analysis was done for each cultivar individually. Different letters on the bars indicate statistical differences from each other ($p < 0.05$).

4.1.5. Fe-EDDHA application represses the Fe utilization genes but induces seed Fe storage genes under high soil pH

The expression levels of known genes involved in Fe uptake (*GmFIT, GmFRO2, GmIRT1-like*), root-to-shoot Fe translocation (*GmFRD3*), phloem loading of Fe (*GmOPT3*), and Fe storage in the seeds (*GmFER*) were determined by using RT-qPCR after Fe fertilization under high soil pH in soybean. Overall, an increase in the expression levels of these genes except for *GmFER* was observed in all cultivars under high pH with no Fe supplementation (Figure. 4.6). The expression levels of *GmFIT, GmFRO2, GmIRT1-like,* and *GmFRD3* drastically decreased upon Fe fertilizer application. On the other hand, the *GmOPT3* levels remained higher in the leaves upon iron fertilization. Furthermore, the expression levels of *GmOPT3* were higher in tolerant cultivars than in the sensitive ones under control conditions (Fe-EDDHA 0 mg/kg soil, pH 5.7), which indicates the natural variation among sensitive and tolerant cultivars as the tolerant cultivars may translocate iron to the seeds more efficiently. Finally, *GmFER* expression was lower in all cultivars under high soil pH and its expression level increased after Fe supplementation.

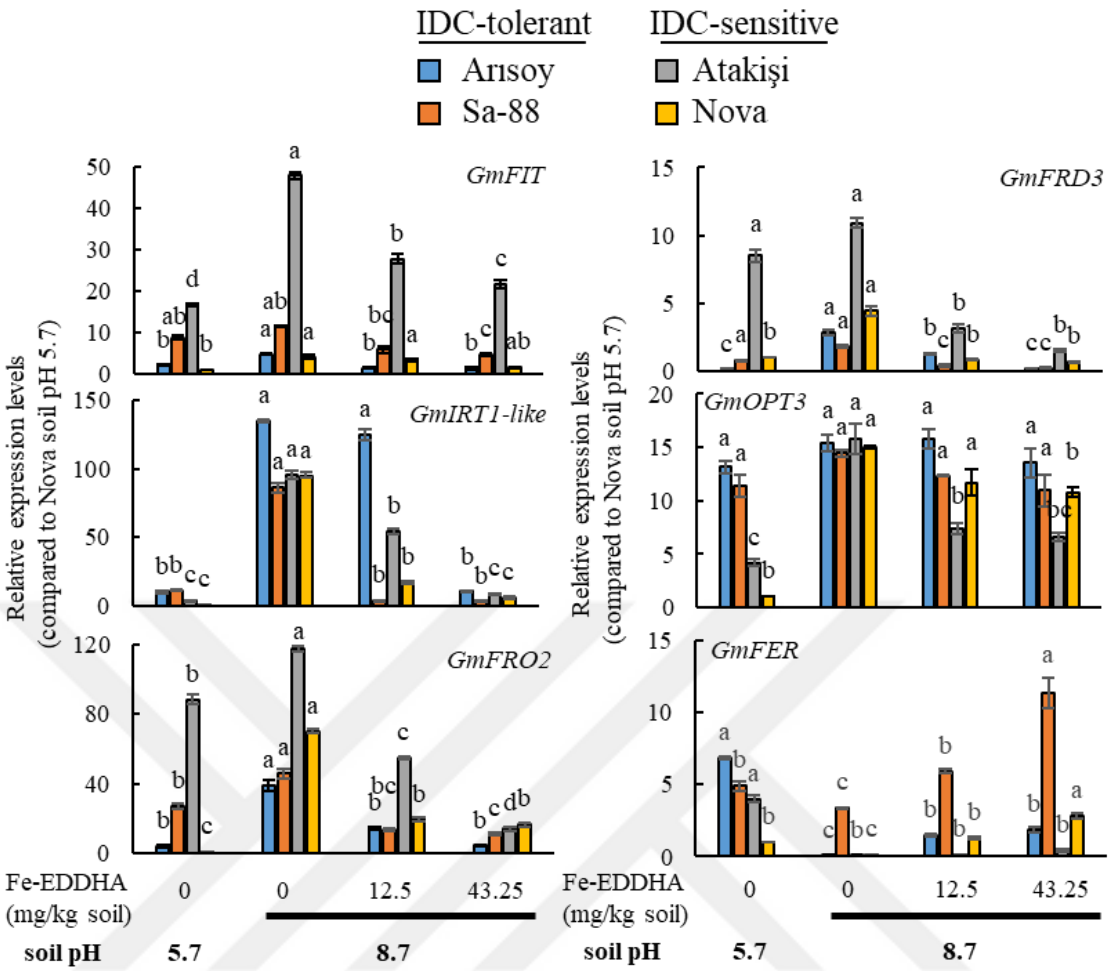

Figure 4.6. Expression levels of Fe utilization genes in IDC-tolerant (Arısoy, Sa-88) and IDC-sensitive (Atakişi and Nova) soybean cultivars in response to increasing Fe fertilization under high soil pH. RT-qPCR analyses of GmIRT1-like, GmFIT, GmFRD3, and GmFRO2 transcript levels were measured in the roots while GmOPT3 and GmFER transcript levels were measured in the leaves of soybean cultivars under different treatments against roots or leaves of Nova (0 FeEDDHA, pH 5.7). The values present the means of three biological replicates ± SE (n = 3). Statistical analysis was done for each cultivar individually. Different letters on the bars indicate statistical differences from each other ($p < 0.05$).

4.1.6. Fe-EDDHA application increases seed iron and protein content and iron bioavailability under high soil pH

Seed is the ultimate storage organ for micronutrients. Seed Fe levels were lower under pH 8.7 in all cultivars as compared to pH 5.7 (0 Fe-EDDHA) irrespective of IDC tolerance (Figure. 4.5 a). Indeed, it decreased by an average of 15% in tolerant cultivars and 48% in sensitive cultivars, with the most substantial decrease (up to 60%) observed in Atakişi. Under high pH, the highest Fe-EDDHA dosages elevated the iron levels in the seeds of tolerant cultivars more than the control condition (0 Fe-EDDHA mg/kg soil, pH 5.7) while seed iron levels in sensitive cultivars did not exceed the control levels.

Increasing pH decreased the total protein contents of both tolerant and sensitive cultivars included in the study (Figure. 4.7 a). The highest protein contents in all cultivars were recorded under low pH where Fe is available. The unavailability of Fe under high pH with no Fe supplementation significantly reduced the total protein contents of all cultivars and this decrease was higher for sensitive cultivars (on average 31.5%) compared to tolerant ones (on average 16.5%). The Fe supplementation improved the total protein contents in all cultivars; however, they remained lower than the protein contests recorded under pH 5.7 conditions.

The oil contents were slightly affected by different Fe availability regimes under high pH. The sensitive cultivars recorded higher oil contents in all treatments at pH 8.7 compared to the treatment at pH 5.7. The tolerant cultivars did not show any change in oil contents both under low and high pH and with all Fe supplementation doses (Figure. 4.7 b).

Phytic acid is a natural anti-nutrient that can bind with essential metal micronutrients such as iron and zinc, reducing their absorption by humans and animals. It can also interfere with proteins, making them nutritionally less available (Punjabi et al., 2018; Goßner et al., 2018). Consequently, diets high in phytic acid are believed to exacerbate micronutrient and protein deficiencies. In high pH conditions, all cultivars exhibited a significant increase in seed phytic acid content (Figure. 4.7c). This increase was particularly pronounced in IDC-sensitive cultivars, showing a significant rise of approximately 133.5% on average. This suggests that sensitive cultivars tend to accumulate higher levels of phytic acid when grown in alkaline soils. Interestingly, seed

phytic acid content significantly decreased in all cultivars except for Nova following Fe-EDDHA fertilization in alkaline soil. This indicates that high pH-induced iron deficiency in plants not only impacts iron uptake but also results in reduced dietary bioavailability of nutrients and proteins for humans and animals. Fe-EDDHA supplementation not only raises iron levels in the seeds but also has the potential to enhance its bioavailability to humans and animals by reducing the seed phytic acid content.

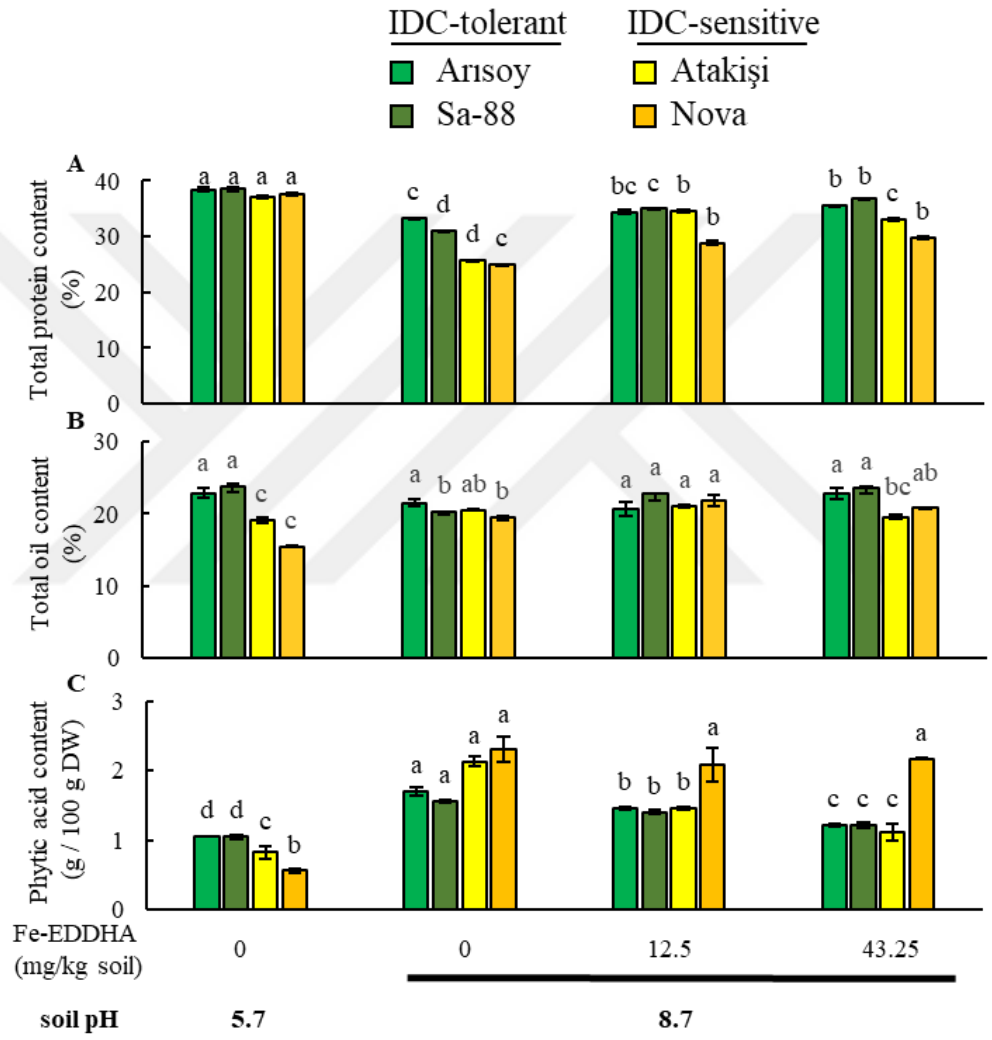

Figure 4.7. Seed quality parameters of IDC-tolerant (Arısoy, Sa-88) and IDC-sensitive (Atakişi and Nova) soybean cultivars in response to increasing Fe fertilization under high soil pH. A. Seed phytic acid content. B. Total protein content. C. Total oil contents of soybean cultivars. The values present the means of three biological replicates ± SE (n = 3). Statistical analysis was done for each cultivar individually. Different letters on the bars indicate statistical differences from each other ($p < 0.05$).

4.1.7. Fe-EDDHA application decreases seed manganese and zinc contents under high soil pH

Seed Mn levels significantly increased in IDC-sensitive cultivars whereas seed Zn levels increased in all cultivars except Sa-88 under alkalinity (Figure. 4.5 b, c). Seed Mn and Zn content decreased by increasing rates of Fe-EDDHA, especially in sensitive cultivars, indicating the importance of genotypic differences in divalent metal utilization when applying fertilizers. Since Fe and Zn transporters can also uptake and translocate other divalent metals, such as in the case of *IRT1* (Vert et al., 2002) and *OPT3* (Mendoza-Cózatl et al., 2014), a balanced divalent inorganic metal nutrition is critical for future studies considering the genetic and agronomic biofortification of soybean.

4.1.8. Fe-EDDHA application increases seed size and weight under high soil pH

The high pH levels had a discernible impact on the 100-seed weight and seed size of both tolerant and sensitive cultivars (Figure. 4.8). Notably, the reduction in parameters such as 100-seed weight and seed size are particularly pronounced in the sensitive cultivars in comparison to the tolerant ones (Figure. 4.8 b). Iron supplementation increased the 100-seed weight across all cultivars while it's notable that the 100-seed weight remained lower than that achieved under the conditions of low pH treatment (pH 5.7) even with higher iron supplementation dosage (Figure. 4.8 a). This observation suggests that even the utilization of the highest available dose of Fe-EDDHA was insufficient to completely reverse the deleterious impacts of elevated pH levels on all cultivars. However, tolerant cultivars showed similar seed sizes to the low pH treatment at the highest dosage of iron while the sensitive ones still had smaller sizes (Figure. 4.8 b). This observation may indicate a positive correlation between seed Fe content and seed size since tolerant cultivars have more efficient mechanisms to transfer applied iron in comparison to sensitive ones.

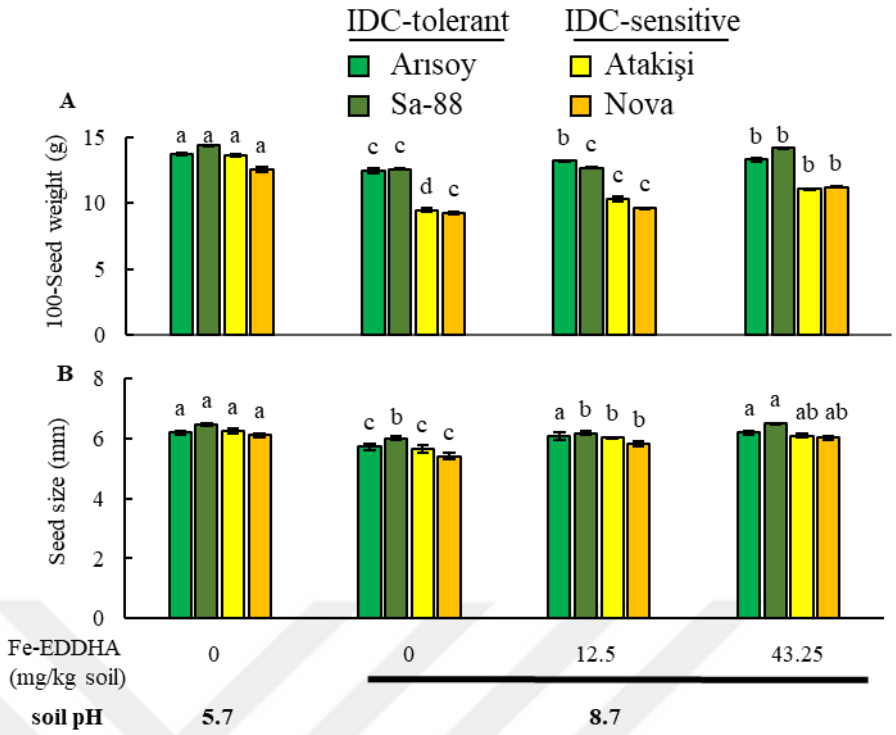

Figure 4.8 Yield and yield-components of IDC-tolerant (Arısoy, Sa-88) and IDC-sensitive (Atakişi and Nova) soybean cultivars in response to increasing Fe fertilization under high soil pH. **A**. 100-seed weight. **B**. Seed size of different soybean cultivars. The values present the means of three biological replicates ± SE (n = 3). Statistical analysis was done for each cultivar individually. Different letters on the bars indicate statistical differences from each other ($p < 0.05$).

Part 2: Genome-wide Identification of QTLs Associated with Iron Deficiency Tolerance in Soybean

4.2.1. QTLs related to Fe deficiency tolerance in soybean

The analysis of 40 QTL regions linked with Fe deficiency tolerance found that only 19 represented unique regions in the soybean genome, demonstrating a conserved high-level genetic effect of IDC tolerance in soybean (Figure 4.9). Distributed on 10 soybean chromosomes, these regions encompass a total size of 101.763 megabases, representing 0.88% of the entire soybean genome (1.15 Gb) (Shultz et al., 2006). All the genes in each QTL region were identified and this list was named the master gene list (Appendix 3). Accordingly, a total of 6593 genes were found in the master gene list and 347 genes on average occupied each QTL region. Genes with multiple copies in the soybean were

eliminated from future analyses since Glycine species contain paleopolyploid genomes that were established by an ancient genome duplication event that occurred 50,000 years ago (Shoemaker et al., 2006). As the soybean genome has not been well-annotated yet, a BLASTp search was performed of the proteins encoded by each gene against the A. thaliana genome to find its Arabidopsis ortholog and as a result, 3822 unique genes were found.

4.2.2 Identification of loci linked with Fe deficiency tolerance in soybean

To understand if the selected Arabidopsis orthologs were related to the Fe deficiency, their in silico expression levels under Fe deficiency were checked. Out of the 3822 unique genes, 607 were selected because their expression levels were differentially altered by more than 1.5 times (where $p < 0.05$) by one or more of the Fe deficiency treatments on the Arabidopsis (Figure 4.10).

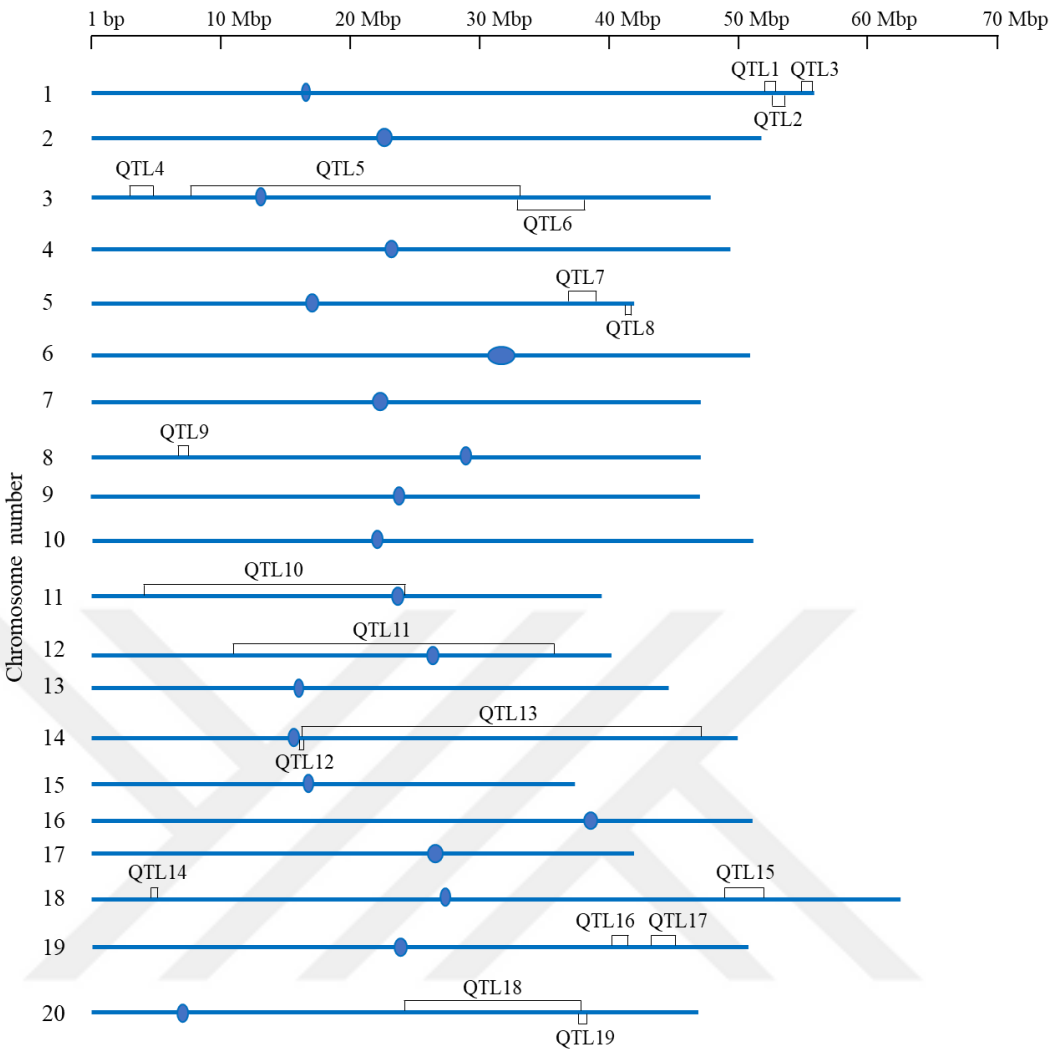

Figure 4.9. 18 QTL regions are distributed on ten soybean chromosomes. The figure is generated in Geneious software (Kearse et al., 2012) according to the soybean chromosome sizes and distribution of QTL regions compared to the size of the chromosomes (Grant et al., 2010; Nepal and Benson, 2015). Centromere position was determined by identifying 91–92 nucleotide tandem repeats within the centromeric region.

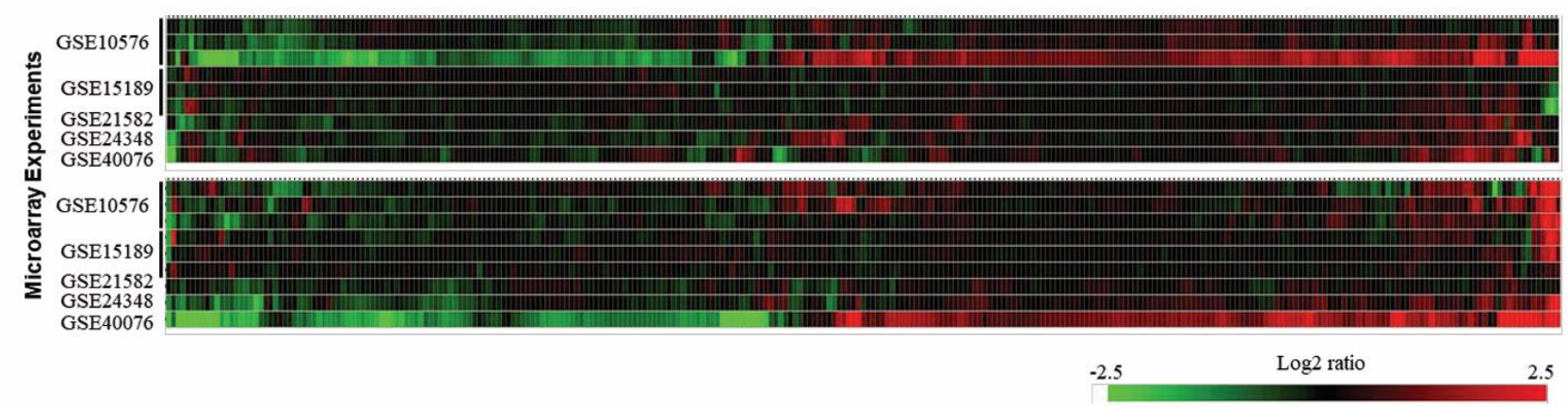

Figure 4.10. Expression levels of Arabidopsis orthologs under Fe deficiency. The heat map of 607 unique genes was generated from microarray experiments, including the Fe deficiency treatment to the whole roots by Genevestigator (Zimmermann et al., 2004). GEO datasets used in the heat map construction included GSE40076 (Sivitz et al., 2012), GSE24348 (Schuler et al., 2011), GSE21582 (Long et al., 2010), GSE15189 (Buckhout et al., 2009), and GSE10576 (Dinneny et al., 2008).

As the list of DEGs was long, how many of these genes were also affected by Fe deficiency signaling was further investigated. To this end, the expression levels of 607 genes were further evaluated in microarray experiments of Fe deficiency signaling mutants, i.e., *bhlh100bhlh101* and *pye1-1* (also known as *pye*). Thus, 68 genes were found to be differentially altered specifically in the *bhlh100bhlh101* mutant, while 13 DEGs were exclusively identified in the *pye1-1* mutant (Figure 4.11 a, Table S4). It is interesting to note that DEGs identified in both *bhlh100bhlh101,* or *pye1-1* suggested that they are unique genes that might be under the control of these transcription factors. Ten DEGs were found to be affected by both *bHLH100-bHLH1001* and *PYE*, suggesting their importance in Fe uptake and/or translocation in plants. These core set of 10 genes include DNA J PROTEINC77 (*DJC77*), GLUTAMINE-DEPENDENT ASPARAGINE SYNTHASE1/DARK INDUCIBLE6 (*ASN1*/*DIN6*), UDP-GLUCOSYL TRANSFERASE72E1 (*UGT21E1*), METAL TOLERANCE PROTEIN3 (MTP3), IRON REGULATED PROTEIN2/FERROPORTIN2 (*IREG2*/ *FPN2*), SULFOTRANSFERASE2A (*ST2A*), GATA TRANSCRIPTION FACTOR12 (*GATA12*), CONSERVED IN THE GREEN LINEAGE AND DIATOMS27 (*CGLD27*), an adenine nucleotide alpha hydrolases domain containing protein kinase (AT1G77280) and ALUMINUM-INDUCED PROTEIN1 (AT4G27450) (Table 4.1). Their gene expression levels were upregulated under Fe deficiency in at least one of the microarray experiments performed from the roots, and all of them showed a high level of similar expression patterns under Fe deficiency in a hierarchical clustering analysis (Figure 4.11 b), suggesting their close evolutionary relationship with each other. As the core group genes were not linked with Fe deficiency before, we performed a GSEA of 10 genes under available Fe deficiency microarray experiments (Appendix 5). As expected, the core group genes were explicitly enriched as a group in Fe deficiency, while they were not enriched in salinity, abscisic acid, or drought stresses. Overall, these analyses revealed that the core set of 10 genes was upregulated under Fe deficiency and might be under the control of bHLH transcription factors in plant roots for providing tolerance to Fe deficiency in soybean.

Table 4.1 Ten core genes commonly expressed in *bhlh100bhlh101* and *pye1-1* mutants.

AGI number	SoyBase Number	Gene Name	Gene Code	Relative Expression								
				GSE40076	GSE24348	GSE21582	GSE15189			GSE10576		
				10 days	1 week	24 h	1 h	6 h	24 h	3-6 h	12-24 h	48-72 h
AT1G77280	Glyma.11g108000	adenine nucleotide alpha hydrolases-domain containing protein kinase	-	**2.80**	**1.57**	**2.99**	-1.01	1.40	**1.53**	1.06	**1.93**	**5.21**
AT2G42750	Glyma.12g130000	*DNA J PROTEINC77*	*DJC77*	**2.34**	**1.93**	**1.87**	-1.06	**1.65**	**1.83**	1.39	**1.64**	**6.29**
AT3G47340	Glyma.11g170300	*GLUTAMINE-DEPENDENT ASPARAGINE SYNTHASE1 / DARK INDUCIBLE6*	*ASN1 / DIN6*	-1.12	**2.11**	**-2.06**	**1.84**	1.04	**2.53**	-1.21	**-1.65**	1.23
AT3G50740	Glyma.03g032600	*UDP-GLUCOSYL TRANSFERASE 72E1*	*UGT72E1*	**2.61**	**3.06**	**2.51**	1.12	**1.81**	**1.68**	-1.19	**2.02**	**5.52**
AT3G58810	Glyma.11g135500	*METAL TOLERANCE PROTEIN3 / METAL TOLERANCE PROTEINA2*	*ATMTP3 / MTPA2*	**4.95**	**3.63**	**8.78**	1.35	**3.53**	**2.57**	1.02	**1.82**	**1.91**
AT4G27450	Glyma.12g150500	Aluminum induced protein YGL and LRDR motifs	*AIP1*	**2.41**	1.13	-1.42	-1.09	**-2.57**	**-2.18**	1.09	1.49	**13.86**
AT5G03570	Glyma.03g042400	IRON-REGULATED PROTEIN2 / FERROPORTIN2	*IREG2 / FPN2*	**5.33**	**1.54**	**3.11**	1.14	**1.53**	**1.94**	-1.09	**2.54**	**6.72**
AT5G07010	Glyma.11g158900	*SULFOTRANSFERASE2A*	*ST2A*	1.27	**3.78**	-1.37	**2.67**	1.38	-1.09	1.27	**2.91**	**11.28**
AT5G25830	Glyma.14g145700	*GATA TRANSCRIPTION FACTOR12*	*GATA12*	**1.96**	-1.00	1.24	1.25	-1.07	1.03	1.15	**2.23**	**3.20**
AT5G67370	Glyma.01g191600	*CONSERVED IN THE GREEN LINEAGE AND DIATOMS27*	*CGLD27*	**5.74**	**8.30**	**4.20**	1.46	**7.22**	**6.60**	1.19	**7.07**	**4.67**

Relative expression levels in bold indicate a statistically significant differential expression (cut-off value of 1.5 times) compared to the control condition (P<0.05). GSE40076: Sivitz et al., 2012; GSE24348: Schuler et al., 2011; GSE21582: Long et al., 2010; GSE15189: Buckhout et al., 2009 and GSE10576: Dinneny et al., 2008.

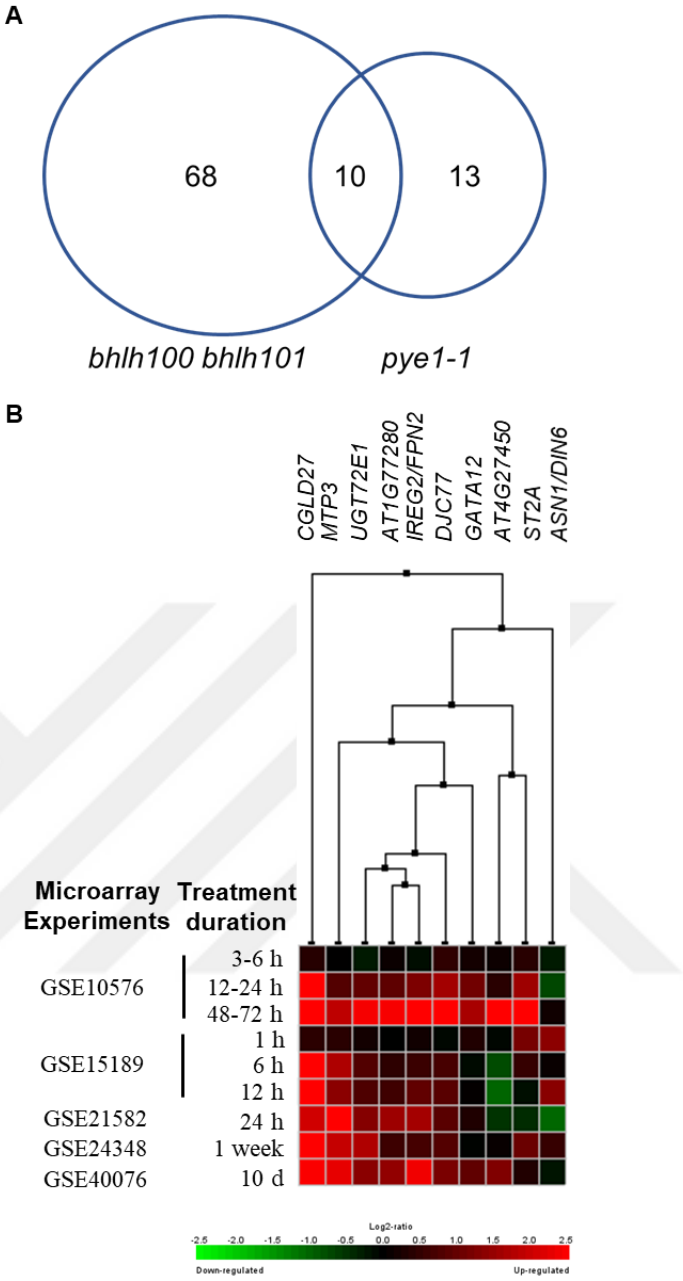

Figure 4.11. Genes linked with Fe signaling in Arabidopsis roots. Expression patterns of Fe deficiency-related Arabidopsis orthologous genes are determined in *bhlh100 bhlh101* (GSE40076 - Sivitz et al., 2012) and pye1-1 (GSE21582 - Long et al., 2010) mutants by using Genevestigator (Zimmermann et al., 2004). A) Venn diagram of DEGs in *bhlh100bhlh1011* and pye1-1 mutants. B) Hierarchical clustering of 10 DEGs common in *bhlh100bhlh1011* and *pye1-1* under Fe deficiency microarrays. GEO datasets used in the hierarchical clustering construction include GSE40076 (Sivitz et al., 2012), GSE24348 (Schuler et al., 2011), GSE21582 (Long et al., 2010), GSE15189 (Buckhout et al., 2009) and GSE10576 (Dinneny et al., 2008).

4.2.3. Core group gene association with metal ion transport and Fe deficiency signaling

For the functional characterization of the core group genes, GO enrichment was utilized (Table 4.2). Accordingly, the top 10 most enriched GOs include metal ion transport, specifically Fe and zinc, in the biological processes, whereas Fe and zinc ion transmembrane transporter activity was enriched in the molecular functions. Some additionally enriched GOs include asparagine metabolic process ($p = 1.82 \times 10–03$), (glutamine-hydrolyzing) asparagine synthase activity ($p = 1.82 \times 10–03$), and sulfotransferase activity ($p = 6.91 \times 10–03$), providing a clue for the involvement of sugar and sulfur metabolisms in Fe deficiency response and/or tolerance in plants. To infer the potential functions of the core group genes, genes that coexpressed together with them were determined (Figure 4.4). The coexpression gene network identified both Fe-signaling components (i.e., *PYE* and *FIT*/*FRU*) as linked with the core group genes. The network also included several transcription factors and metal transporters with known functions in metal translocation and Fe homeostasis. Interestingly, there were some genes involved in sugar and amino acid metabolism in the network. As the network analysis presented coexpressing genes with known functions in Fe uptake, translocation, and signaling as well as the ones involved in other metabolic pathways, the network was divided into 6 clusters according to the network topology (Figure 4.12 and Appendix 6) and a GO enrichment was performed for the genes included in each of the 6 clusters (Appendix 7). As known from previous bioinformatics studies (Schwarz and Bauer, 2020), clusters 1 and 2 included the genes involved in the Fe-signaling networks regulated by *PYE* and *FIT* in the root stele and epidermis, respectively. Surprisingly, cluster 3 which was centered around *GATA12*, represented a knob between the 2 Fe-signaling networks, indicating the potential missing link between the 2 most important Fe-signaling components of Fe homeostasis in plant roots. Cluster 4 contained the genes with GO enrichment in amino acid metabolism, while clusters 5 and 6 contained the genes with GO enrichment in ethylene response and gibberellic acid-mediated signaling, respectively. Taken together, these data indicated that the core group genes are associated with metal ion transport and Fe deficiency signaling in plants (Table 4.2).

Table 4.2 Gene ontology enrichment of ten core genes.

GO term	Fold Enrichment	raw P value
Biological process		
detoxification of zinc ion	> 100	3.65E-04
stress response to zinc ion	> 100	7.29E-04
asparagine metabolic process	> 100	1.82E-03
cellular response to iron ion starvation	> 100	2.91E-03
iron ion transmembrane transport	> 100	3.28E-03
response to iron ion starvation	> 100	4.37E-03
stress response to metal ion	> 100	6.18E-03
zinc ion transport	> 100	9.80E-03
iron ion transport	88.44	1.12E-02
cellular iron ion homeostasis	70.30	1.41E-02
Molecular function		
asparagine synthase (glutamine-hydrolyzing) activity	> 100	1.82E-03
sulfotransferase activity	> 100	6.91E-03
iron ion transmembrane transporter activity	> 100	8.72E-03
zinc ion transmembrane transporter activity	> 100	9.80E-03
transferase activity	80.64	1.27E-02
transition metal ion transmembrane transporter activity	74.10	3.36E-04
divalent inorganic cation transmembrane transporter activity	68.54	1.49E-02
ligase activity	38.08	2.63E-02
metal ion transmembrane transporter activity	23.33	3.20E-03
inorganic anion transmembrane transporter activity	21.93	4.50E-02

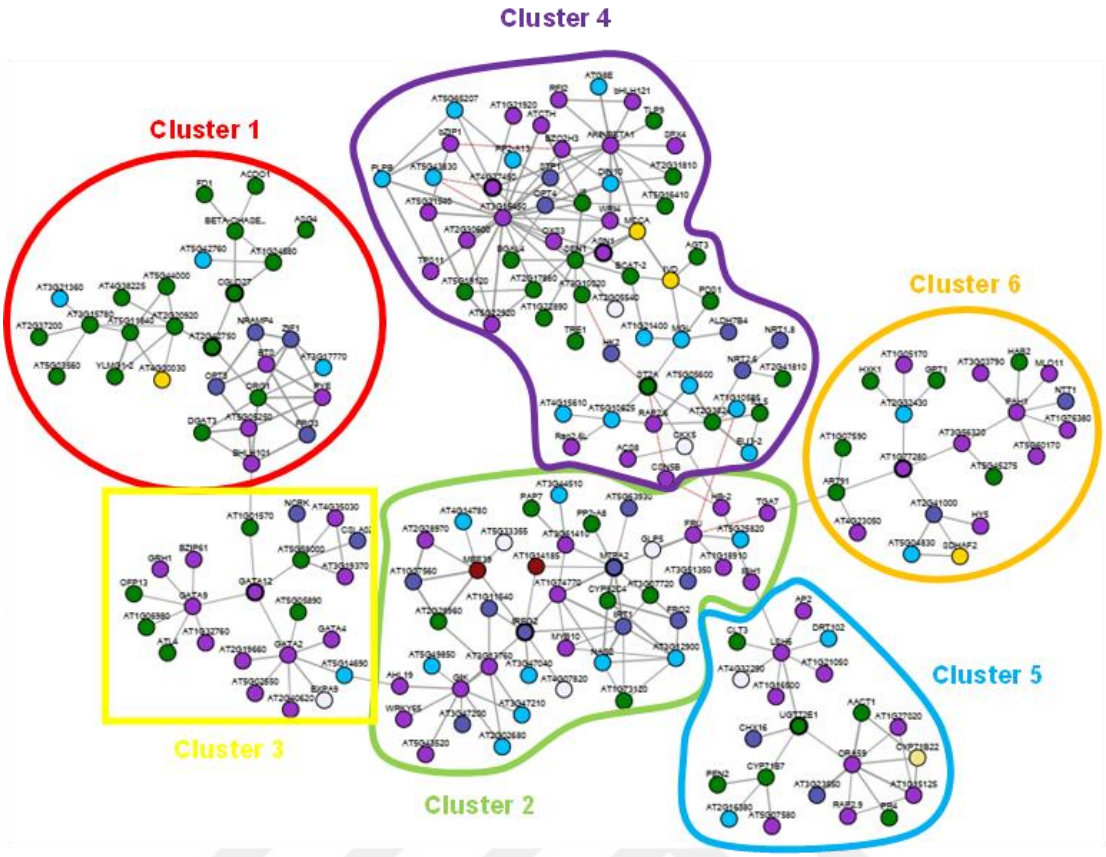

Figure 4.12. Co-expression network analysis of the core group genes. The co-expression network drawer of Atted II (Obayashi et al., 2007) was used to generate the network map. Dark circles present 10 core group genes. Colors indicate the predicted subcellular localizations according to WoLF PSORT (Horton et al., 2007). Green: Chloroplast, Yellow: Mitochondria, Purple: Nucleus, Pale Blue: Cytosol, Red: Vacuole, Dark Blue: Plasma Membrane, Pale Grey: Extracellular, Beige: Peroxisome.

4.2.4. Core group genes induced by Fe deficiency and high pH in soybean roots

Finally, to prove that the core group genes identified in the bioinformatic analyses were induced by Fe deficiency in the soybean roots, Fe deficiency-sensitive soybean plants (Atakişi variety) were exposed to Fe deficiency for 2 weeks. Except for the FCR activity, the root and shoot lengths, root, and shoot FWs, soil plant analysis development (SPAD) value, and chlorophyll content were significantly decreased in the plants exposed to Fe deficiency, whereas the FCR activity increased by 2 times under Fe deficiency (Figure 4.13). As plants cannot uptake divalent elements such as Fe2+ efficiently in alkaline soils (Olsen and Brown, 1980), also investigated was the effect of a high pH (9.0) on the growth and development of the Atakişi variety. Except for the shoot length and FCR activity, the

other parameters increased significantly with a high pH, as expected. On the other hand, the high pH did not affect the shoot length and FCR activity, suggesting that the induction of the FCR enzyme is unique to the Fe deficiency treatment. The expression levels of some genes in the core group were determined in the plant roots exposed to Fe deficiency or high pH (Figure 4.14). The expressions of *DIN1*, *MTPA2*, *AIP1*, *IREG2*, *ST2A*, and *GATA12* increased significantly under Fe deficiency and a high pH compared to the control group. Under a high pH, the induction of *ST2A* and *GATA12* reached 10 and 20 times, respectively. Overall, this indicated that the core group genes were induced by Fe deficiency and high pH in soybean roots and therefore their functions in Fe uptake and/or translocation in plants should be investigated in future studies.

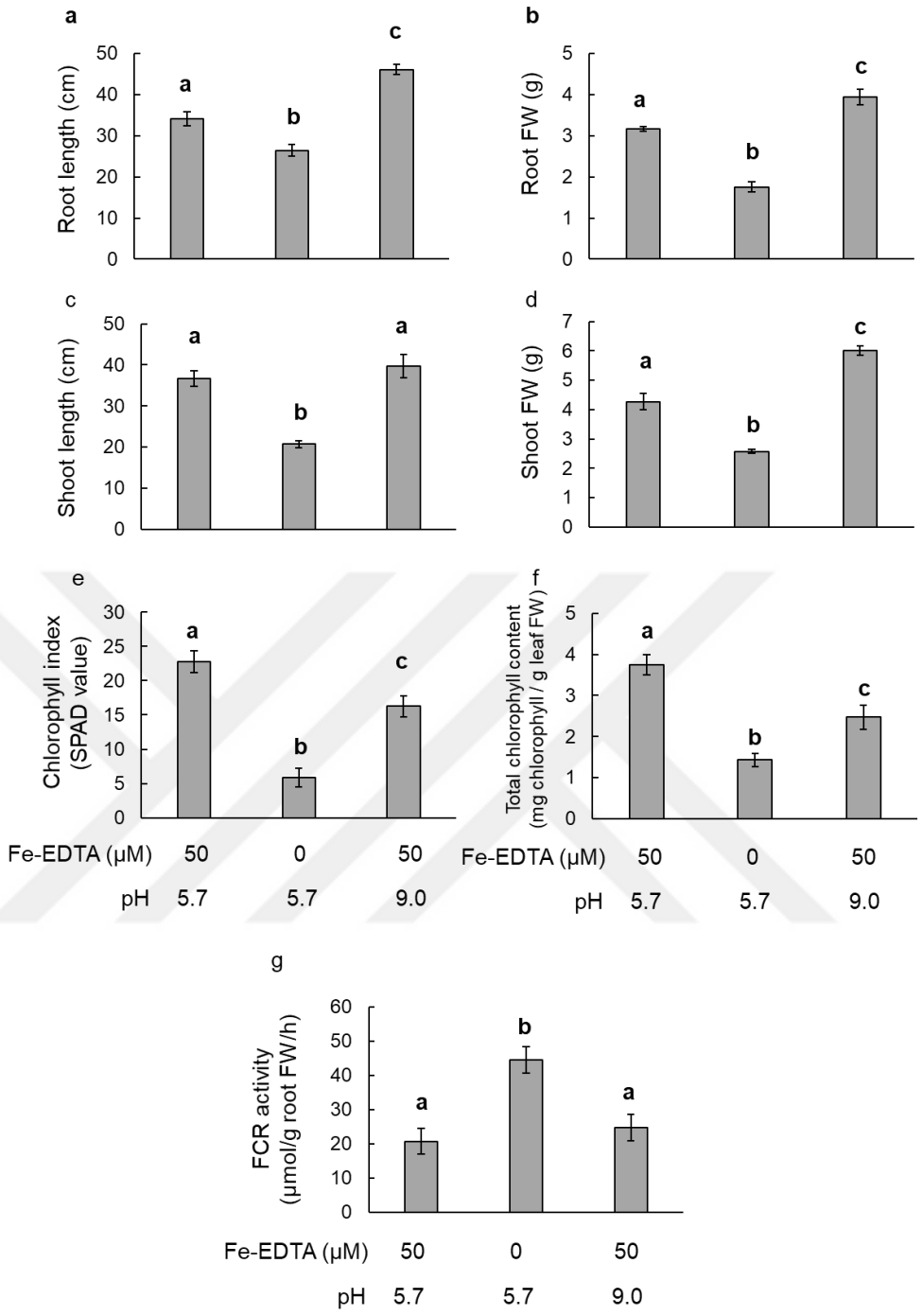

Figure 4.13. Physiological and biochemical responses of soybean under Fe deficiency and high pH. Soybean plants were grown on Fe deficiency (0 μM Fe-EDTA, pH: 5.7) and high pH (50 μM Fe-EDTA, pH: 9.0) compared to the control conditions (50 μM Fe-EDTA, pH: 5.7) for 2 weeks. **a**) Root length. **b**) Root FW. **c**) Shoot length. **d**) Shoot FW. **e**) SPAD value. **f)** Chlorophyll content. **g**) FCR enzyme activity. Values indicate the means ± SEM (n≥3). Different letters indicate significant changes among treatments ($p<0.05$).

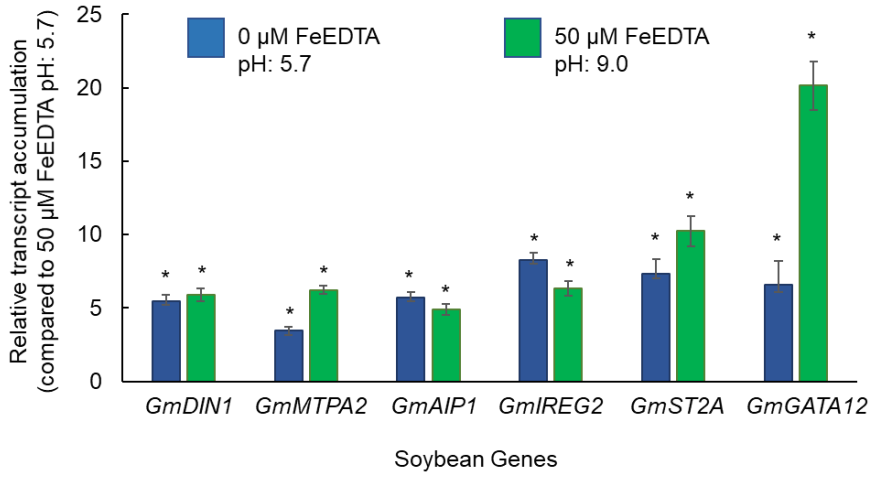

Figure 4.14. Expression levels of *DIN1*, *MTPA2*, *AIP1*, *IREG2*, *ST2A* and *GATA12* in soybean roots under Fe deficiency and high pH. Gene expression levels were determined in the roots of soybean plants grown on Fe deficiency (0 µM Fe-EDTA, pH: 5.7) and high pH (50 µM Fe-EDTA, pH: 9.0) compared to the control conditions (50 µM Fe-EDTA, pH: 5.7) for 2 weeks. Values indicate the means of relative gene expression ± SEM (n=3). * Indicates significant change compared to the control ($p<0.05$).

Part3: Transcriptomics of IDC-tolerant Soybean Cultivars in Calcareous-alkaline Soil

4.3.1. Iron deficiency significantly affected the leaf biomass

Plants raised under low iron available conditions show poor growth and lower biomass (Dunisijevic et al. 2012: Khobra et al.,2014). Leaf fresh weight of four soybean cultivars under two different iron treatments (Fe+ and Fe-) was depicted in Figure 4.15. a. The interaction between varieties and Fe treatments was found to be significant ($P<0.05$). Maximum leaf fresh weight was recorded in SA-88 with Fe+ conditions while minimum was observed in Nova under Fe- conditions. A significant decrease was noted in leaf fresh weight with Fe- treatment as compared to Fe+ in all cultivars. Maximum reduction was found in Nova contrarily a minimum reduction was documented in SA-88. It might be due to the tolerant behavior of the latter. The same behavior of minimum decrease with two contrasting Fe treatments was found in Arısoy. However, Arısoy showed lower leaf fresh weight in both iron treatments as compared to SA-88. Atakişi also showed a similar response as observed in Nova, with a significant reduction of leaf fresh weight in Fe-

treatment. The leaf dry weight of four soybean cultivars under two different iron treatments (Fe+ and Fe-) was depicted in Figure 4.15. b. The interaction between varieties and Fe treatments was found to be significant (P<0.05). The trend of leaf dry weight was found to be in accordance with leaf fresh weight. Maximum leaf dry weight was recorded in SA88 with Fe+ conditions while minimum was observed in Nova and Atakişi under Fe- conditions. A significant decrease was noted in leaf dry weight with Fe- treatment as compared to Fe+ in all cultivars. Maximum reduction was found in Nova contrarily a minimum reduction was documented in SA-88. It might be due to the tolerant behavior of the latter. The same behavior of minimum decrease with two contrasting Fe treatments was found in Arısoy. However, Arısoy showed lower leaf dry weight in both iron treatments as compared to SA-88. Atakişi also showed a similar response as observed in Nova, with a significant reduction of leaf dry in Fe- treatment. Similar results were reported by Khobra et al. (2014) where tolerant wheat cultivars had shown higher biomass under iron-deficient conditions.

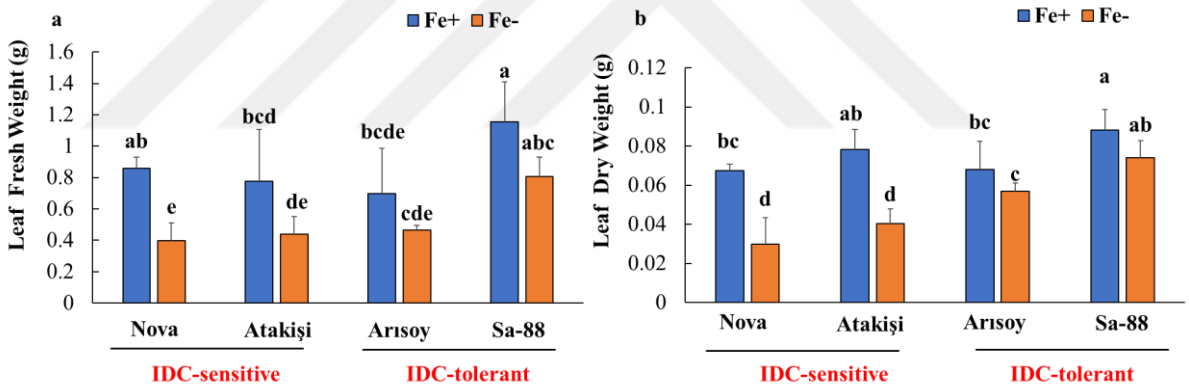

Figure 4.15. Leaf fresh and dry weights of IDC-sensitive and tolerant cultivars under iron-deficiency. a) Mean leaf fresh and b) Dry weights of cultivars grown under control (pH 5.7) and iron-deficient conditions (pH 8.7). Different letters on the bars indicate statistical differences from each other ($p < 0.05$).

4.3.2. Sensitive cultivars had shown severe hampered chlorophyll synthesis

SPAD measurement is an indicator of chlorophyll content in plants. Highly significant differences (P<0.01) were observed for the interaction effects between cultivars and iron treatments. Soybean cultivars Atakişi and Sa-88 gave maximum SPAD readings with Fe+

treatment, while the minimum was found in Nova with Fe- treatment. Fe- treatment caused a significant reduction ($p<0.05$) in the SPAD value as compared to Fe+, though a similar trend was observed in Sa-88 but the percentage of reduction was less (17% in comparison to 39.6% in Atakişi). A significant reduction of 27% SPAD value was found in Nova. Arısoy observed the lowest decrease in SPAD value in Fe- treatment (10%). Thus, the data suggested that Atakişi showed the maximum SPAD index in Fe+ treatment while the lowest SPAD value was recorded from Atakişi under Fe- conditions. Contrarily, Sa-88 behavior was tolerant and was reluctant to decrease the SPAD index in Fe- treatment. The same was observed in Arısoy (Figure 4.16 a.).

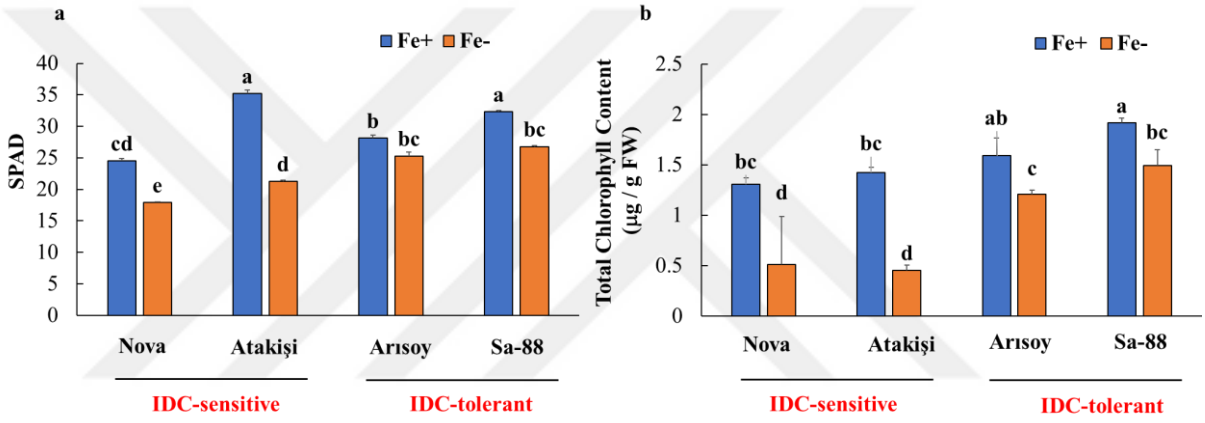

Figure 4.16. SPAD and total chlorophyll contents of IDC-sensitive and tolerant cultivars under iron-deficiency. a) Mean SPAD value and b) Total chlorophyll contents of cultivars grown under control (pH 5.7) and iron-deficient conditions (pH 8.7). Different letters on the bars indicate statistical differences from each other ($p < 0.05$).

Total chlorophyll contents showed a similar response as observed in the SPAD index. Interaction between cultivars and Fe treatments was found to be significant ($p < 0.05$). All Fe- treatments recorded a decrease in total chlorophyll contents in comparison to Fe+. A maximum decline of 68% and 60% was observed in Atakişi and Nova, respectively. Tolerant behavior was observed in Sa-88 and Arısoy with a minimum reduction of 22% and 23.8% total chlorophyll contents in Fe- treatment (Figure 4.16 b.).

4.3.3. High pH-induced Iron deficiency significantly increased the root FRO activities and root length

Root length was found to be significantly different ($p < 0.05$) for the interaction effects of cultivars and Fe treatments. Fe- treatments recorded maximum root length in all cultivars as compared to Fe+ treatments. Maximum root length was found in Atakişi under Fe- conditions, while the minimum was observed in Nova, Atakişi, and Arısoy with Fe+ treatments. Fe+ conditions recorded a significantly higher root length in Sa-88 as compared to the rest of the cultivars. This might be due to the high responsiveness of Sa-88 to the Fe+ environment (Figure 4.17 b). The interaction between cultivars and Fe treatments was found to be highly significant ($P<0.01$) for the FRO enzyme activity. Maximum FRO enzyme activity was found in Nova with Fe- conditions, while the minimum was observed in Atakişi with Fe+ treatment. All Fe- treatments recorded significantly maximum FRO enzyme activity as compared to Fe+ conditions. A higher FRO enzyme activity of 69% and 67.5% was observed in cultivar Nova and Sa-88, respectively, under Fe- conditions as compared to Fe+ treatments. A maximum increase (84%) of FRO enzyme activity was observed in Atakişi as compared to other cultivars under Fe-deficient conditions. The sensitive response of Atakişi was attributed to the minimum FRO enzyme activity under Fe+ conditions (Figure 4.17 a).

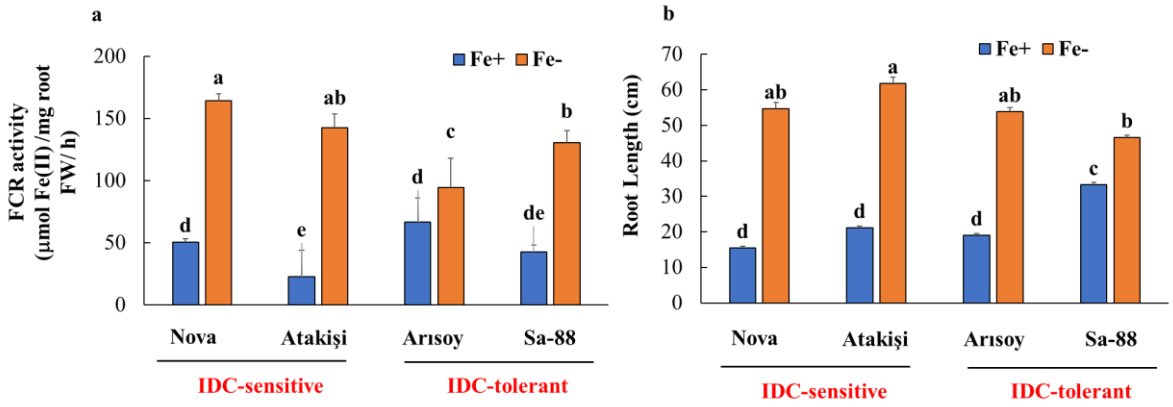

Figure 4.17. FCR activity and root lengths of IDC-sensitive and tolerant cultivars under iron-deficiency. a) FCR activities and b) Root length of cultivars grown under control (pH 5.7) and iron-deficient conditions (pH 8.7). Different letters on the bars indicate statistical differences from each other ($p < 0.05$).

4.3.4. Photosynthesis and stomatal conductance

The interaction effects of cultivars and Fe treatments were significant ($p < 0.05$) for the variable photosynthesis. Maximum photosynthesis was observed in Nova and Atakişi under Fe+ conditions, while the minimum was recorded in Nova under Fe-deficient conditions. Fe-sufficient conditions improve the photosynthesis in soybean cultivars as evidenced by the results which depicted that Fe+ conditions significantly increase photosynthesis in all cultivars. SA-88 showed less damage to the photosynthetic apparatus by maintaining photosynthesis under Fe-deficient conditions (Figure 4.18 a).

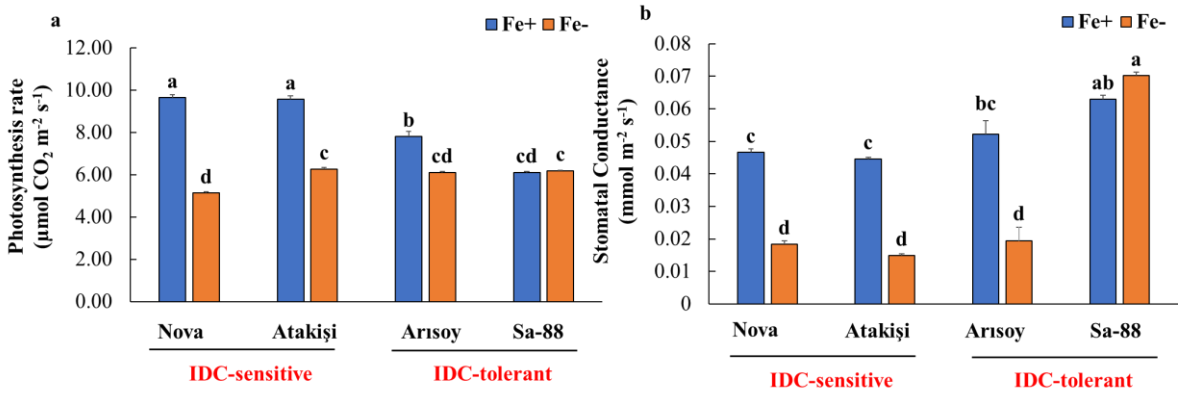

Figure 4.18. Photosynthetic and stomatal conductance rates of of IDC-sensitive and tolerant cultivars under iron-deficiency. a) Mean photosynthetic rates and b) Stomatal conductance of cultivars grown under control (pH 5.7) and iron-deficient conditions (pH 8.7). Different letters on the bars indicate statistical differences from each other ($p < 0.05$).

The interaction effects of cultivars and Fe treatments were significant ($p<0.05$) for the variable stomatal conductance. All cultivars showed a significant decrease in stomatal conductance under Fe-deficient conditions as compared to the Fe+ environment except Sa-88, which showed higher stomatal conductance under Fe- conditions. Maximum stomatal conductance was reported in Sa-88 under Fe- conditions, while the minimum was recorded in Nova, Atakişi, and Arısoy under the same conditions (Figure 4.18 b).

4.3.5. Transcriptome analyses of two tolerant soybean cultivars against iron deficiency

Iron deficiency tolerance is a complex mechanism, and a network of genes takes part in the mechanism. To understand the tolerance mechanisms against high pH-induced iron deficiency of two tolerant cultivars. For this reason, two tolerant cultivars were grown under control and high pH conditions and after 30 days of growth when the plants reached at V_3 stage leaf and root samples were collected for transcriptomic studies. Keeping in view the reason that iron deficiency symptoms are most prominent at the V_3 stage, this stage was selected. RNA Samples were collected by using the Qiagen RNeasy Mini Kit according to the manufacturer's protocol. To check the integrity of the RNA, samples were run on 1% agarose gel and the clear RNA bands can be seen in Figure 4.19.

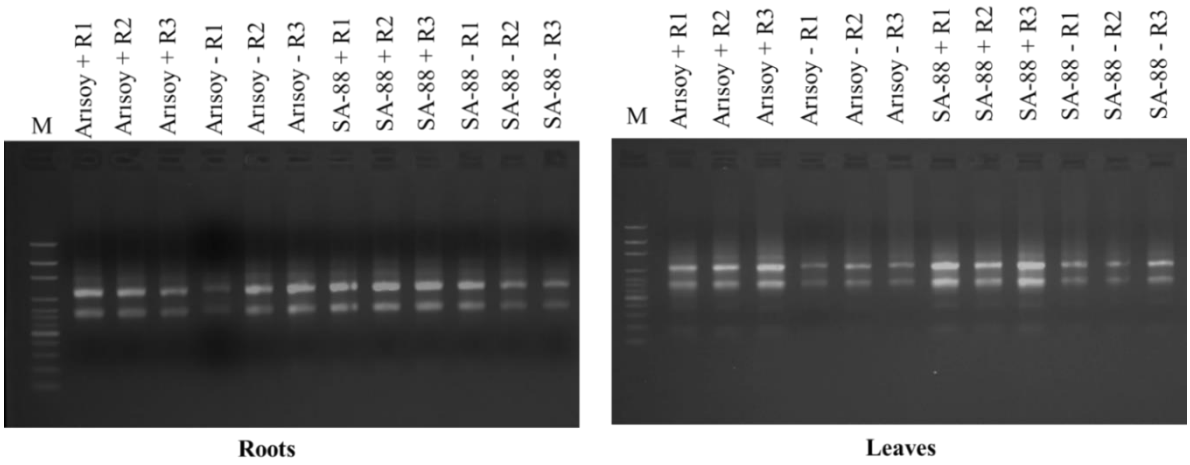

Figure 4.19. Quality of Roots total RNAs isolated from soybean genotypes. Two microliters of RNA samples were separated on 0.5X TBE buffer for 1 hour. M represents 1 kb DNA ladder (Thermo Scientific).

RNAStable kit and special packaging envelopes ("Sample Pouch") were used to avoid RNA degradation during the sending of samples to the sequencing company. The advantage of the RNAStable Kit is that while transferring RNA samples for next-generation sequencing to the sequencing center, there is no risk of degradation at room temperature. To check the reliability of the KIT RNA samples were kept at room temperature for four days and afterward samples were run on 1% agarose gel. Distinct RNA bands can be observed in Figure 4.20.

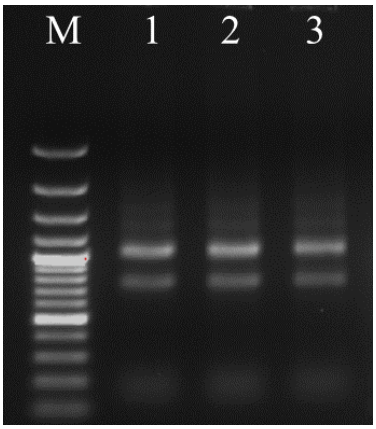

Figure 4.20. Quality of RNAs isolated from soybean genotypes. Two microliters of RNA samples were separated on 0.5X TBE buffer for 1 hour. M represents 1 kb DNA ladder (Thermo Scientific).

Table 4.3. RNA sample concentrations and amount sent to the Nova Gene for Sequencing.

Sample Name	Tissue	Conc. (ng/ µl)	Vol (µl)	Total Amount (ng)
Aricoy C R1	Roots	260.09	22.5	5852.02
Arısoy C R2	Roots	260.09	22.5	5852.02
Arısoy Fe- R1	Roots	246	22.5	5535.07
Arısoy Fe- 2	Roots	246	22.5	5535.07
Sa-88 C R1	Roots	298.43	22.5	6714.67
Sa-88 C R2	Roots	298.43	22.5	6714.67
Sa-88 Fe- R1	Roots	187.23	22.5	4212.67
Sa-88 Fe- R2	Roots	187.23	22.5	4212.67
Aricoy C R1	Leaves	494.48	22.5	11125.87
Arısoy C R2	Leaves	494.48	22.5	11125.87
Arısoy Fe- R1	Leaves	172.84	22.5	3888.9
Arısoy Fe- 2	Leaves	172.84	22.5	3888.9
Sa-88 C R1	Leaves	417.94	22.5	9403.8
Sa-88 C R2	Leaves	417.94	22.5	9403.8
Sa-88 Fe- R1	Leaves	198.42	22.5	4464.6
Sa-88 Fe- R2	Leaves	198.42	22.5	4464.6

The concentrations of RNA that were subjected to the sequencing are given in Table 4.3. Q20 indicates a base call accuracy of 98%, while Q30 indicates an accuracy of 99.9%. Typically, Q20 values should exceed 85%, and Q30 values should be over 80%. In our RNA quality analysis, high-quality score values were obtained in the quality control as Q20 and Q30 showed a minimum score of 97% and 92 %, which indicates that 97% of the bases have a quality score of 20 and 92 % of the bases have a quality score of 92 %. Furthermore, the quality of RNA was found to be robust, as can be seen in the table all samples exhibited high read counts, low error rates, high-quality scores, and consistent GC content (Table 4.4.). The number of raw reads and clear reads are high among all the samples indicating good quality RNA. Furthermore, GC content was found to be constant among all the samples ranging from 43.54% to 45.18% (Table 4.4.). GC content varies by species and genomic regions, and a significant deviation (>10%) from the expected value may indicate any type of contamination.

Sequences that passed quality control were aligned to the reference soybean genome using TOPHAT2 (Trapnell et al., 2012) software (Table 4.5). The analysis was conducted to evaluate the mapping efficiency of RNA samples extracted from two tolerant cultivars Arısoy and SA-88 grown under two different soil pH conditions 5.7 and 8.7. A total of 16 samples were subjected to the analysis. Results showed that the total mapped reads were consistently high across all samples, with percentages ranging from 96.21% to 97.52%, indicating excellent alignment quality. The percentage of multiple mapped reads was low, between 1.82% and 3.24%, suggesting a minimal presence of ambiguous reads, which may align with the multiple locations in the genome making it unclear from which gene it comes. Half of the aligned reads matched to a DNA strand and the other half to the complement DNA strand. While at least 56.62% of the readings corresponded to non-splice reads, 36.99% of them corresponded to most splice reads. The results of the analyses are summarized in Table 4.5.

Table 4.4. Quality analysis of RNA sequencing data.

Sample	Raw_reads	Clean_reads	Raw_data(G)	Clean_data(G)	Error_rate(%)	Q20(%)	Q30(%)	GC_content(%)
Arısoy pH: 5,7 Roots 1	48453626	47559772	13,05	12,84	0,03	97,43	92,83	43,54
Arısoy pH: 5,7 Roots 2	43239182	42459139	12,93	12,78	0,03	97,60	93,23	43,56
Arısoy pH: 8,7 Roots 1	50125106	49333036	13,00	12,77	0,03	97,60	93,25	43,67
Arısoy pH: 8,7 Roots 2	42317829	41565752	14,57	14,30	0,02	98,05	94,26	43,67
Sa-88 pH: 5,7 Roots 1	41997538	41435664	13,45	13,21	0,03	97,64	93,26	43,55
Sa-88 pH: 5,7 Roots 2	43734986	43187087	14,66	14,48	0,03	97,65	93,34	43,71
Sa-88 pH: 8,7 Roots 1	44712549	43918487	12,89	12,74	0,03	97,42	92,89	43,60
Sa-88 pH: 8,7 Roots 2	52028060	51156565	15,65	15,38	0,03	97,59	93,27	43,57
Arısoy pH: 5,7 Leaves 1	52153137	51525099	15,68	15,49	0,03	97,71	93,44	45,18
Arısoy pH: 5,7 Leaves 2	49847297	49122091	14,99	14,77	0,03	97,69	93,40	45,14
Arısoy pH: 8,7 Leaves 1	43396975	42714989	12,73	12,50	0,03	97,20	92,35	44,95
Arısoy pH: 8,7 Leaves 2	43007644	42487353	15,07	14,84	0,03	97,46	92,89	44,98
Sa-88 pH: 5,7 Leaves 1	42871359	42358222	12,63	12,46	0,02	98,29	94,79	45,13
Sa-88 pH: 5,7 Leaves 2	48754270	48158988	12,96	12,74	0,02	98,06	94,24	44,95
Sa-88 pH: 8,7 Leaves 1	47966868	47258656	14,42	14,21	0,02	98,01	94,18	44,82
Sa-88 pH: 8,7 Leaves 2	43085463	42353569	13,15	12,99	0,03	97,97	94,09	44,85

pH 5.7: Control; pH 8.7: Iron deficiency

Table 4.5 Quality analysis of RNA readings aligned to the reference genome

Sample	Total reads	Total mapped	Multiple mapped	Uniquely mapped	Reads map to '+'	Reads map to '-'	Non-splice reads	Splice reads
Arısoy pH: 5,7 Roots 1	95119544	91733805 (96.44%)	1773135 (1.86%)	89960670 (94.58%)	44931870 (47.24%)	45028800 (47.34%)	56354413 (59.25%)	33606257 (35.33%)
Arısoy pH: 5,7 Roots 2	84918278	82019277 (96.59%)	1546927 (1.82%)	80472350 (94.76%)	40196273 (47.34%)	40276077 (47.43%)	50472799 (59.44%)	29999551 (35.33%)
Arısoy pH: 8,7 Roots 1	98666072	95174985 (96.46%)	1826321 (1.85%)	93348664 (94.61%)	46639167 (47.27%)	46709497 (47.34%)	57827061 (58.61%)	35521603 (36.00%)
Arısoy pH: 8,7 Roots 2	83131504	80268032 (96.56%)	1535280 (1.85%)	78732752 (94.71%)	39335971 (47.32%)	39396781 (47.39%)	48703482 (58.59%)	30029270 (36.12%)
Sa-88 pH: 5,7 Roots 1	82871328	80285588 (96.88%)	1525049 (1.84%)	78760539 (95.04%)	39346137 (47.48%)	39414402 (47.56%)	48980644 (59.10%)	29779895 (35.94%)
Sa-88 pH: 5,7 Roots 2	86374174	83593118 (96.78%)	1593090 (1.84%)	82000028 (94.94%)	40964579 (47.43%)	41035449 (47.51%)	51038629 (59.09%)	30961399 (35.85%)
Sa-88 pH: 8,7 Roots 1	87836974	84509992 (96.21%)	1726860 (1.97%)	82783132 (94.25%)	41355535 (47.08%)	41427597 (47.16%)	51863405 (59.05%)	30919727 (35.20%)
Sa-88 pH: 8,7 Roots 2	102313130	98549937 (96.32%)	2042251 (2.00%)	96507686 (94.33%)	48213495 (47.12%)	48294191 (47.20%)	60454897 (59.09%)	36052789 (35.24%)
Arısoy pH: 5,7 Leaves1	103050198	100341813 (97.37%)	3342505 (3.24%)	96999308 (94.13%)	48449051 (47.02%)	48550257 (47.11%)	59832425 (58.06%)	37166883 (36.07%)
Arısoy pH: 5,7 Leaves 2	98244182	95621709 (97.33%)	3008672 (3.06%)	92613037 (94.27%)	46257427 (47.08%)	46355610 (47.18%)	56997550 (58.02%)	35615487 (36.25%)
Arısoy pH: 8,7 Leaves 1	85429978	82481518 (96.55%)	2573408 (3.01%)	79908110 (93.54%)	39907092 (46.71%)	40001018 (46.82%)	48387558 (56.64%)	31520552 (36.90%)
Arısoy pH: 8,7 Leaves 2	84974706	82150988 (96.68%)	2606591 (3.07%)	79544397 (93.61%)	39730261 (46.76%)	39814136 (46.85%)	48113106 (56.62%)	31431291 (36.99%)
Sa-88 pH: 5,7 Leaves 1	84716444	82511419 (97.40%)	2267732 (2.68%)	80243687 (94.72%)	40082010 (47.31%)	40161677 (47.41%)	49421535 (58.34%)	30822152 (36.38%)
Sa-88 pH: 5,7 Leaves 2	96317976	93930463 (97.52%)	2585203 (2.68%)	91345260 (94.84%)	45626654 (47.37%)	45718606 (47.47%)	56162303 (58.31%)	35182957 (36.53%)
Sa-88 pH: 8,7 Leaves 1	94517312	91324955 (96.62%)	2642042 (2.80%)	88682913 (93.83%)	44308740 (46.88%)	44374173 (46.95%)	54154700 (57.30%)	34528213 (36.53%)
Sa-88 pH: 8,7 Leaves 2	84707138	81929271 (96.72%)	2297396 (2.71%)	79631875 (94.01%)	39785851 (46.97%)	39846024 (47.04%)	48672790 (57.46%)	30959085 (36.55%)

pH 5.7: Control; pH 8.7: Iron deficiency

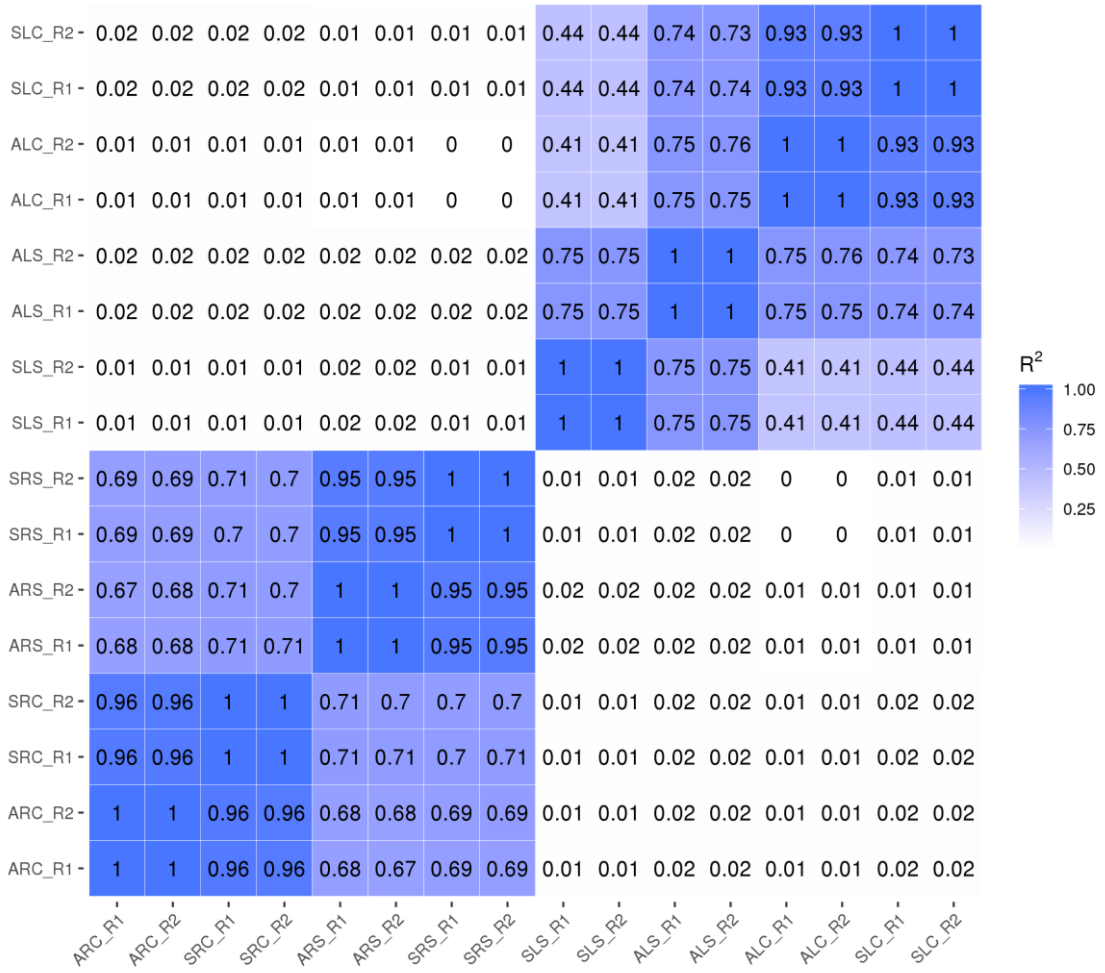

Figure 4.21. Correlation between samples according to gene expression levels. Pearson's correlation was used in the calculation. Sample definitions: ARC: Arısoy root control; SRC: Sa-88 root control; ARS: Arısoy root stress; SRS: Sa-88 root stress; ALC: Arısoy leaf control; SLC: Sa-88 leaf control; ALS: Arısoy leaf stress; SLS: Sa-88 leaf stress. R1 and R2 show the technical repeat numbers.

4.3.6. Determination of unigenes and FPKM values

Subsequently, the transcriptomes were combined, and the read data were transformed into FPKM values. As a result, a total of 57147 unique genes (unigene) were determined, and the correlation between samples was calculated according to the gene expression levels obtained (Figure 4.21). Accordingly, while a high correlation was determined between similar tissues and similar applications (R2≥0.93), the correlation between varieties was between 0.67 and 0.76 depending on the tissue or application. As there is a strong correlation between applications and varieties according to this, it can be understood that

the responses of varieties against iron deficiency can be explained by the gene expression levels. Given the strong correlation between conditions and cultivars, it can be assumed that the cultivars' responses to iron deficiency are likely explained by differences in gene expression levels (Figure 4.21).

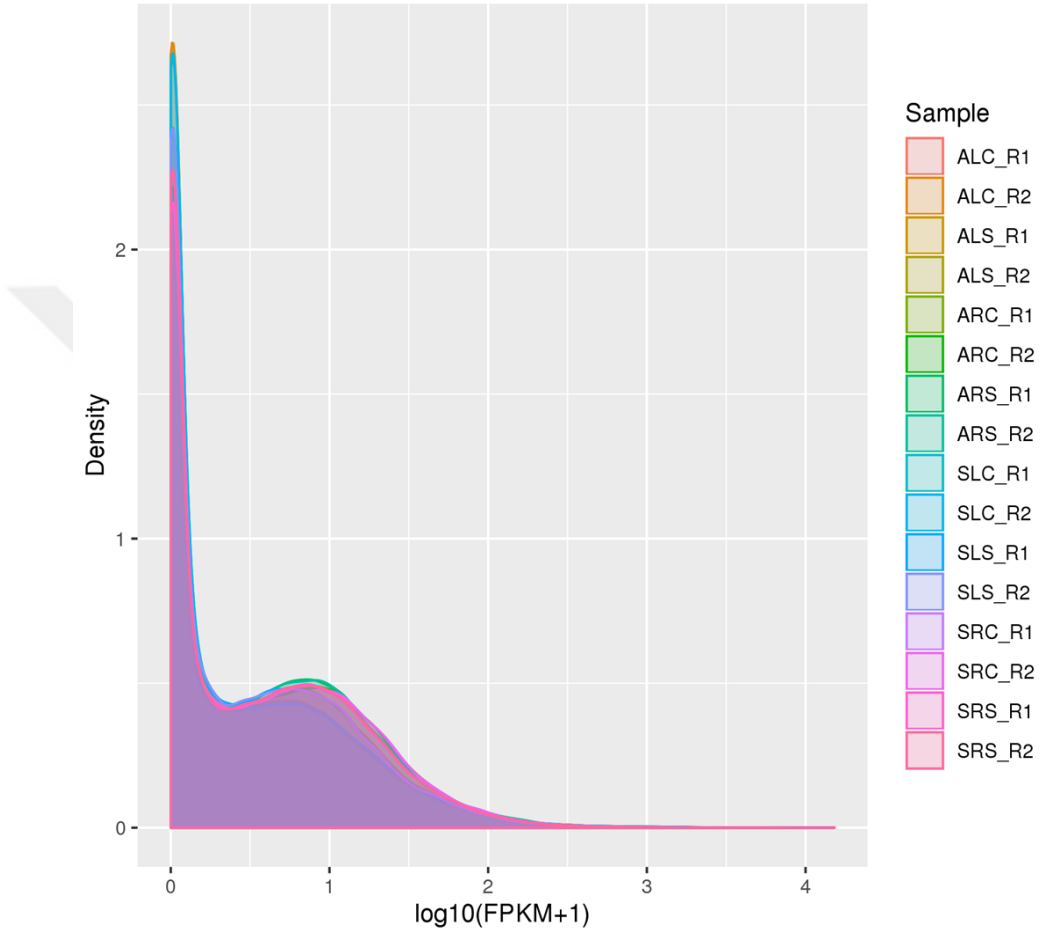

Figure 4.22. General distribution of the gene expression levels. Sample definitions: ARC: Arısoy root control; SRC: Sa-88 root control; ARS: Arısoy root stress; SRS: Sa-88 root stress; ALC: Arısoy leaf control; SLC: Sa-88 leaf control; ALS: Arısoy leaf stress; SLS: Sa-88 leaf stress.R1 and R2 show the technical repeat numbers.

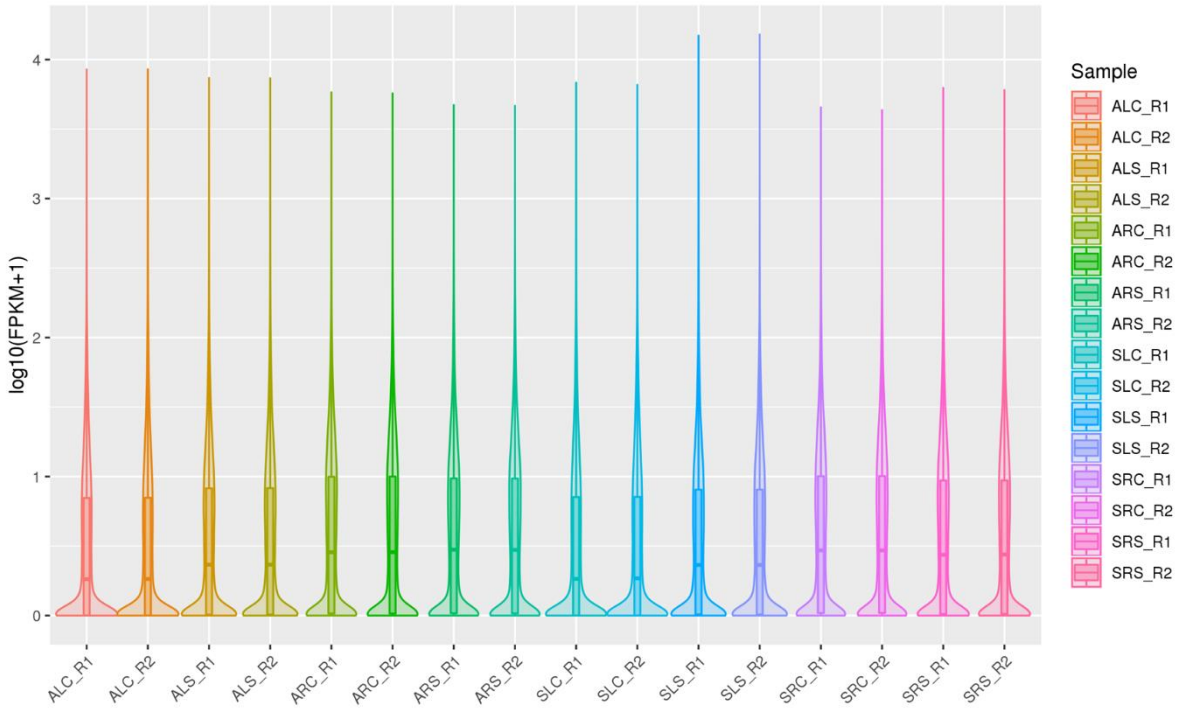

Figure 4.23. Distribution of gene expression levels in samples. Sample definitions: ARC: Arısoy, root, control; SRC: Sa-88, root, control; ARS: Arısoy, root, stress; SRS: Sa-88, root, stress; ALC: Arısoy, leaf, control; SLC: Sa-88, leaf, control; ALS: Arısoy, leaf, stress; SLS: Sa-88, leaf, stress. R1 and R2 show the technical repeat numbers.

While the detected transcripts generally contain a large percentage of genes expressed at low levels, it was found that a very low percentage of genes were expressed at high levels (Figure 4.22). Considering the expression level distributions in the different samples, it was observed that the expression level distributions follow the pattern of each other in general. Interestingly, FPKM values exceed 4 in leaf samples of the SA-88 variety, grown under high pH soil conditions (pH 8.7) (Figure 4.23). Next the sequences of the genes obtained were taken, and the references were made by scanning in NR, NT, GO, COG, KEGG, Swissprot, and InterproScan databases as BLAST alignments. Accordingly, the citations in NR - NCBI, NT - NCBI, GO Resource, COG, KEGG, Swissprot, InterproScan, Trembl, PlantCyc, refPlant, Phytozome and SoyBase databases are 85.62, 86.45, 83.85, 63.56, 58.90, 60.20, 65.75, 85.96, 89.56, 91.25, 90.65, 92.52 (Table 4.6) and the average citation rate was determined as 79.52%.

Subsequently, the obtained gene sequences were compared against several databases, including NR, NT, GO, COG, KEGG, Swissprot, and InterproScan, using BLAST

alignments. The citation rates for these databases were as follows: NR - NCBI (85.62%), NT - NCBI (86.45%), GO Resource (83.85%), COG (63.56%), KEGG (58.90%), Swissprot (60.20%), InterproScan (65.75%), Trembl (85.96%), PlantCyc (89.56%), refPlant (91.25%), Phytozome (90.65%), and SoyBase (92.52%) (Table 4.6). The average citation rate across these databases was calculated as 79.52%.

Table 4.6. Citation percentages of specific genes in different data banks.

Data Bases	**Percentage (%) of attributed genes**
NR – NCBI	85,62
NT – NCBI	86,45
GO Resource	83,85
COG	63,56
KEGG	58,90
Swissprot	60,20
InterproScan	65,75
Trembl	85,96
PlantCyc	89,56
refPlant	91,25
Phytozome	90,65
SoyBase	92,52
Average	79,52

Later on, the obtained FPKM data was normalized, and the gene lists were compared to identify differently expressed genes, and the genes that were statistically expressed differently ($p < 0.05$ and fold change> 2) were determined. Accordingly, the volcano graphics of the compared samples are shown in Figure 4.24. 9749 genes were upregulated

in Arısoy roots under iron stress and 9408 were downregulated. While 11778 genes were upregulated in Arısoy leaves and 9867 were downregulated. In the case of SA-88, 8368 genes were upregulated and 7853 were downregulated in roots. For the leaves, 13509 genes had shown upregulation and 9235 had shown downregulation under iron deficiency stress conditions (pH 8.7) compared to the control (pH 5.7) as shown in Figure 4.24.

4.3.7. GO and KEGG analyses

Gene ontology (GO) analyses were performed for functional attribution of the genes in the lists obtained, and as GO terms the biological process (Figure 4.13) and molecular function (Figure 4.14) categories were considered for the analysis. In GO results subsequently, it was determined statistically which of the GO terms were enriched. According to this analysis, the terms "generation of precursor metabolites", "small molecule metabolic process" and "biosynthetic process" were enriched, respectively, in Arısoy roots, under iron deficiency conditions (Figure 4.13 a); Specific to molecular functions, the terms "structural constituent of ribosome", "oxidoreductase activity" and "structural molecule activity" have been enriched, respectively (Figure 4.14 a). On the leaves of the same variety, the terms "small molecule metabolic process", "generation of precursor metabolites" and "cofactor metabolic process" were enriched, respectively, specific to biological processes (Figure 4.13 b); Specific to molecular functions, the terms "oxidoreductase activity", "phosphatase" and "isomerase" are enriched respectively (Figure 16 b). On the other hand, the terms "transmembrane transport", "generation of precursor metabolites" and "cofactor metabolic process" were enriched in the roots of Sa-88, respectively, specific to biological processes (Figure 4.13 c); Specific to molecular functions, the terms "transmembrane transporter activity", "DNA binding transcription factor activity" and "transferase activity" have been enriched respectively (Figure 4.14 c). On the leaves of the same variety, the terms "photosynthesis", "generation of precursor metabolites" and "translation" were enriched respectively, specific to biological processes (Figure 4.13 d); Specific to molecular functions, the terms "structural molecule activity", "structural constituent of ribosome" and "oxidoreductase activity" have been enriched, respectively (Figure 4.14 d).

Gene ontology (GO) analyses were performed for functional attribution of the genes in the lists obtained, and as GO terms the biological process and molecular function categories were considered for the analysis of two tolerant cultivars. In the case of Arısoy roots, the terms “generation of precursor metabolites”, “small molecule metabolic process” and “biosynthetic process” were significantly enriched in the biological process category (Figure 4.25a). For molecular functions, the enriched terms were “structural constituent of ribosome”, “oxidoreductase activity” and “structural molecule activity” (Figure 4.26a). While the leaves showed the enrichment of the terms “small molecule metabolic process”, “generation of precursor metabolites” and “cofactor metabolic process” respectively, specific to biological processes (Figure 4.25b). While for the molecular function terms enriched were “oxidoreductase activity”, “phosphatase activity” and “isomerase activity” (Figure 4.26b).

In SA-88 roots, the biological process terms “transmembrane transport”, “generation of precursor metabolites” and “cofactor metabolic process” were enriched (Figure 4.27a). The molecular functions that were enriched included “transmembrane transporter activity”, “DNA binding transcription factor activity” and “transferase activity” (Figure 4.28a). For the leaves, the biological process terms “photosynthesis”, “generation of precursor metabolites” and “translation” were enriched (Figure 4.27a). The enriched molecular functions were “structural molecule activity”, “structural constituent of ribosome” and “oxidoreductase activity” (Figure 4.28. b)

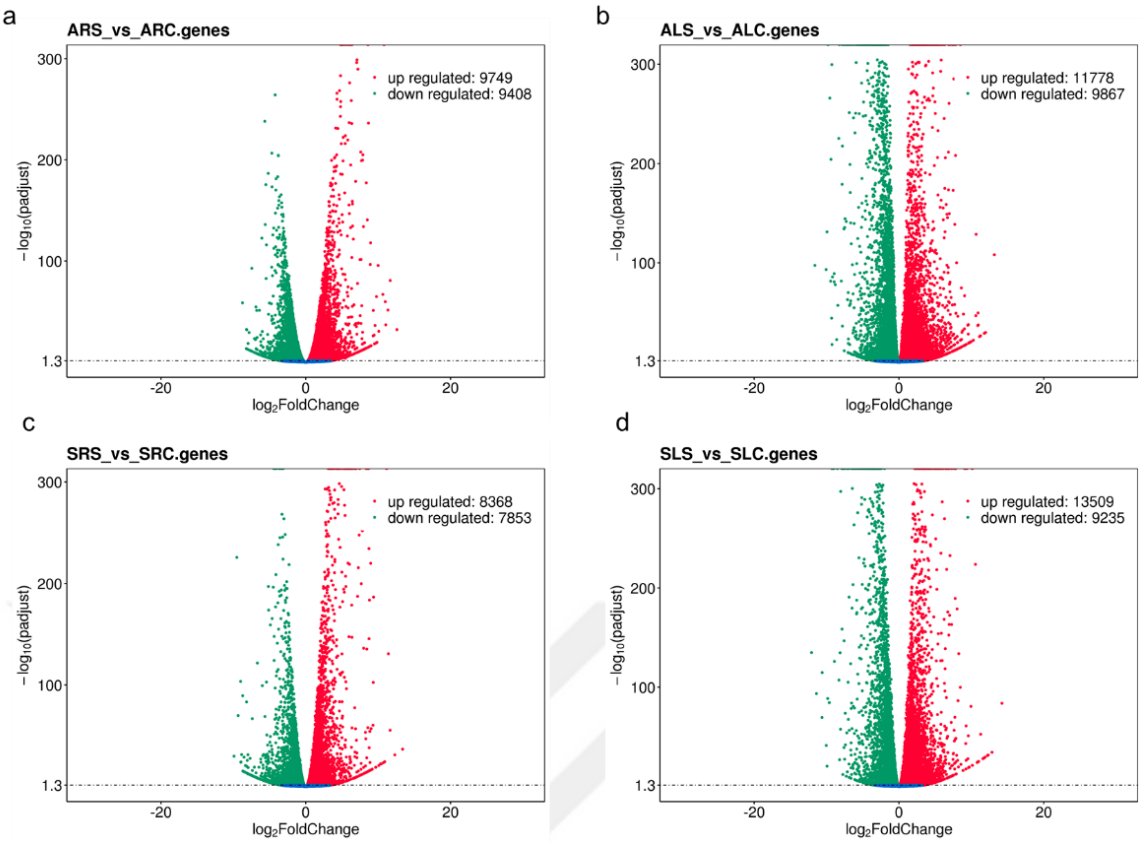

Figure 4.24. Volcano plots of compared samples. a) A comparison of pH 8.7 and pH 5.7 of Arısoy roots. b) Comparison of pH 8.7 and pH 5.7 of Arısoy leaves. c) Comparison of pH 8.7 and pH 5.7 of Sa-88 roots. d) Comparison of Sa-88 leaves with pH 8.7 and pH 5.7. Sample definitions: ARC: Arısoy root control; SRC: Sa-88 root control; ARS: Arısoy root stress; SRS: Sa-88 root stress; ALC: Arısoy leaf control; SLC: Sa-88 leaf control; ALS: Arısoy leaf stress; SLS: Sa-88 leaf stress.

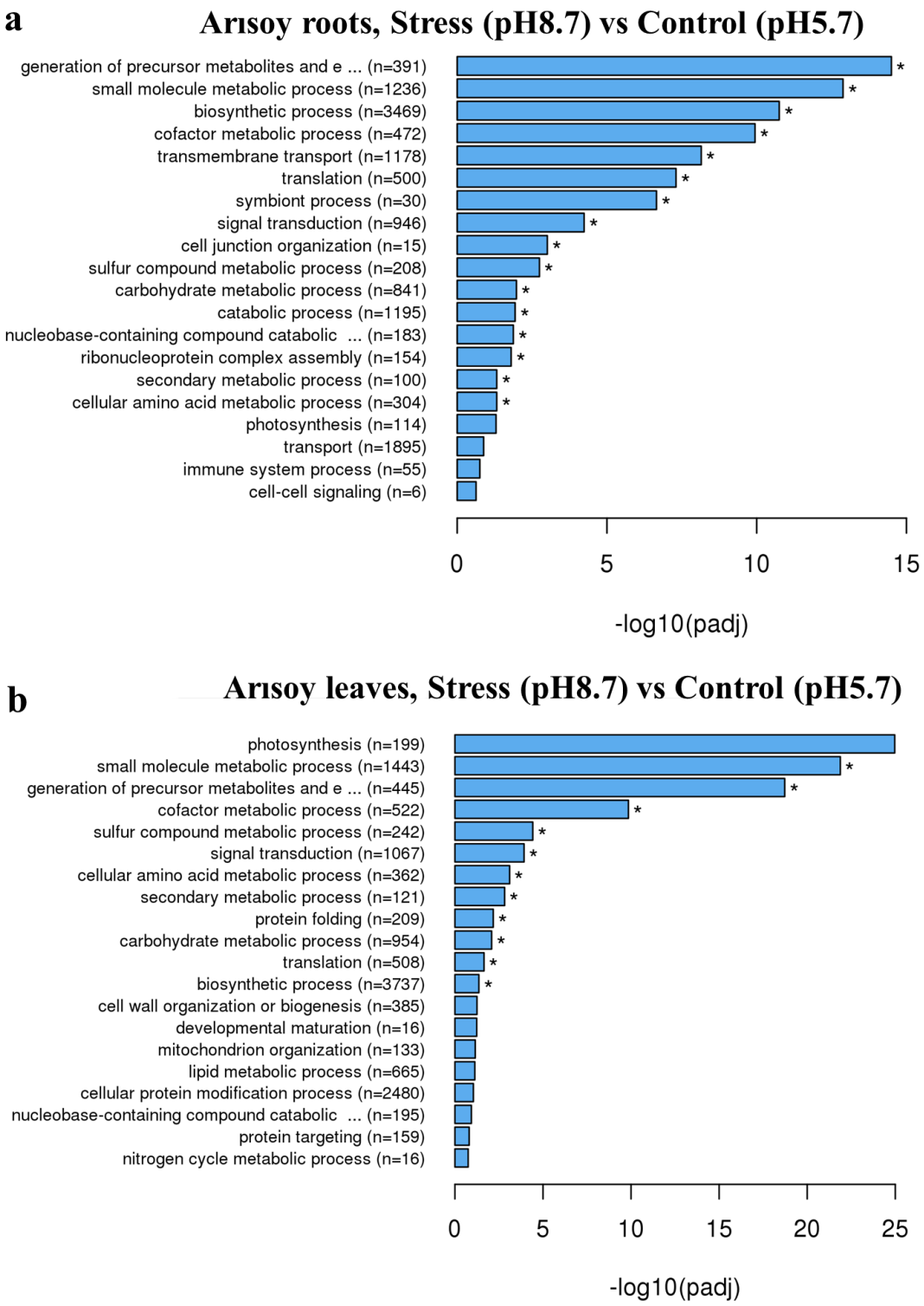

Figure 4.25. Gene ontology enrichment analysis related to the biological process of genes with different expression levels. * Indicates statistically enriched gene ontologies ($p < 0.05$).

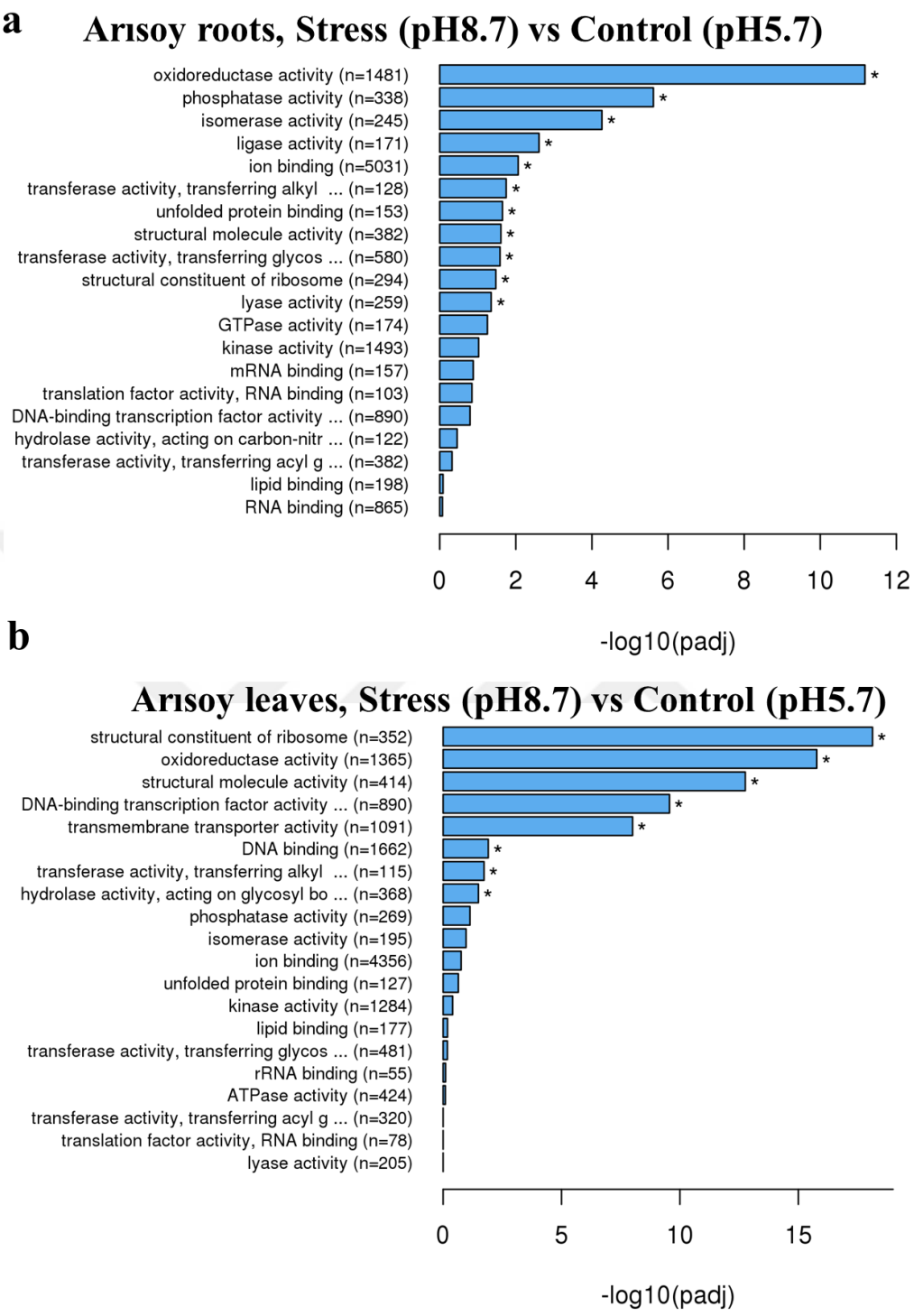

Figure 4.26. Gene ontology enrichment analysis related to the molecular function of genes with different expression levels in Arısoy. * Indicates statistically enriched gene ontologies ($p < 0.05$).

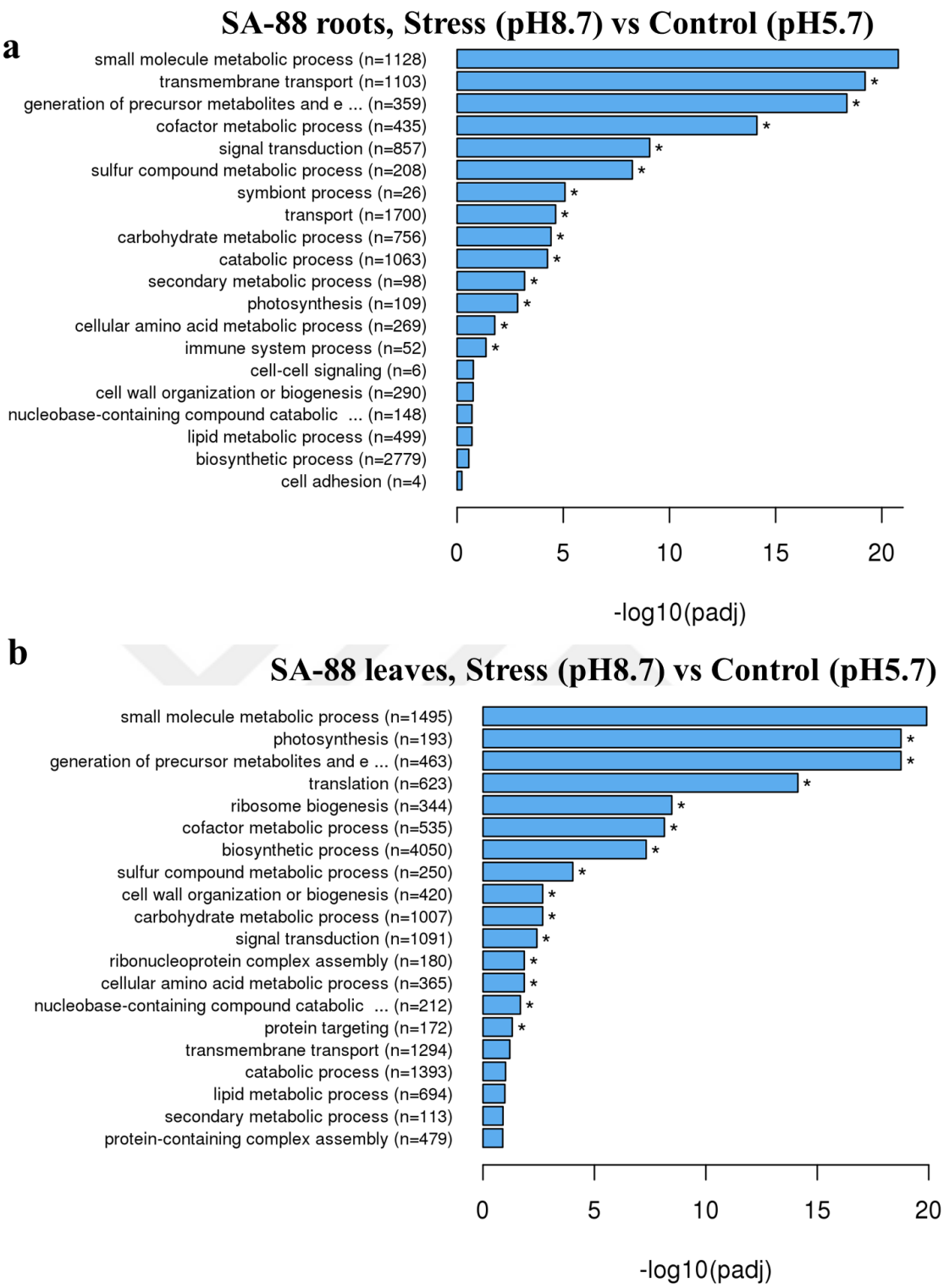

Figure 4.27. Gene ontology enrichment analysis related to the biological process of genes with different expression levels in Sa-88. * Indicates statistically enriched gene ontologies ($p < 0.05$).

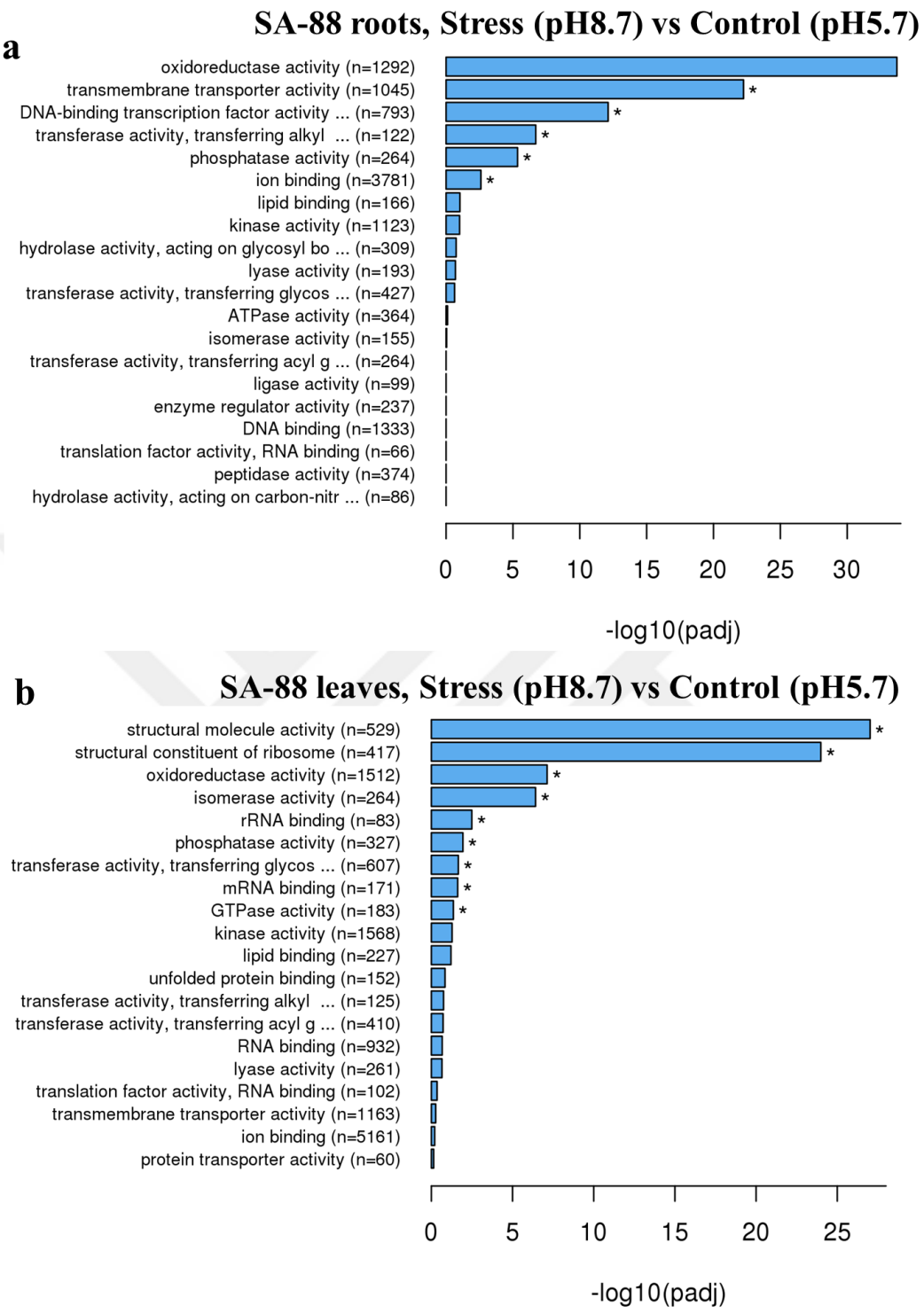

Figure 4.28. Gene ontology enrichment analysis related to the molecular function of genes with different expression levels in Arısoy. * Indicates statistically enriched gene ontologies ($p < 0.05$).

Then KEGG pathway analysis was done to determine the pathways in which genes are enriched. According to analysis, the pathways of "biosynthesis of secondary metabolites", "carbon metabolism" and "biosynthetic of amino acids", "biosynthesis of secondary metabolites", "carbon metabolism" and the pathways of "plant-pathogen interaction" were enriched, respectively, in Arısoy roots and leaves (Figure 4.29 a and b).

On the other hand, in SA-88 roots the pathways “biosynthesis of secondary metabolites”, “carbon metabolism” and “biosynthetic of amino acids” were enriched, respectively, in the leaves “biosynthesis of secondary metabolites”, “carbon metabolism” and “plant” - pathogen interaction” pathways have been enriched (Figure 4.30 a and b). In Arısoy roots and leaves genes associated with circadian rhythm, and pathways associated with oxidative stress were affected (Figures 4.29 a and b). On the other hand, sugar and amino acid metabolism were affected especially in SA-88 roots, while lipid metabolism was affected in the leaves (Figure 4.30 a and b). These results indicate that the mechanisms activated in response to iron deficiency are different in the two tested cultivars.

Under iron deficiency stress the common pathways affected in both cultivars and tissue were found to be glycolysis/gluconeogenesis, TCA cycle, galactose and starch metabolism, and pyruvate metabolism (Figure 4.31). Interestingly, unlike SA-88, inositol phosphate metabolism, linoleic acid metabolism, RNA degradation, spliceosome pathways, and nicotinamide metabolism were affected in the cultivars Arısoy (Figure 4.31). On the other hand, specific to SA-88, oxidative phosphorylation, terpenoid metabolism, unsaturated fatty acid biosynthesis metabolism, autophagy regulation pathway, and protein regulation pathway in the endoplasmic reticulum were affected (Figure 4.31).

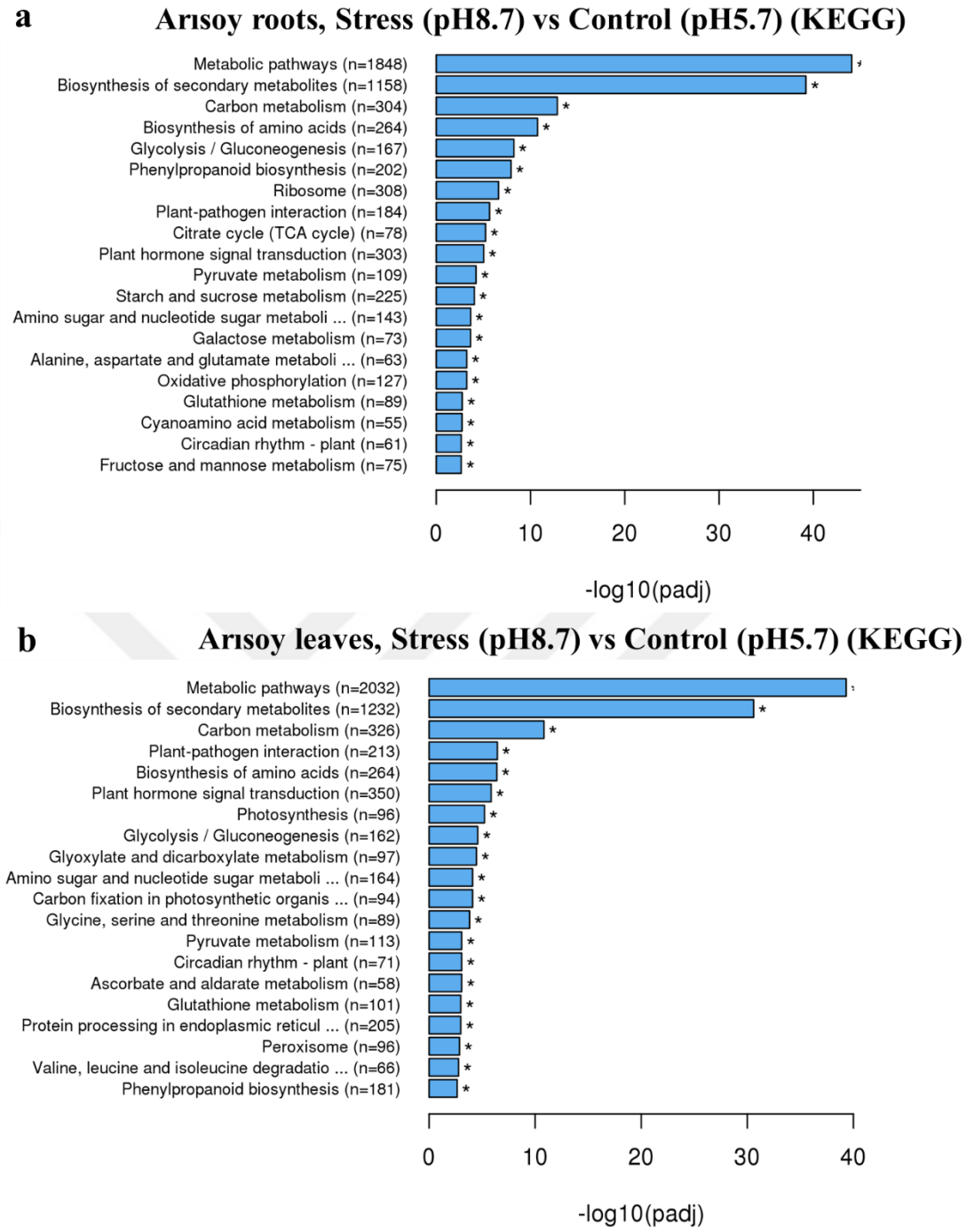

Figure 4.29. Enrichment analysis in KEGG pathways of genes with different expression levels in the roots and leaves of Arısoy. * Indicates statistically significant enriched pathways ($p < 0.05$).

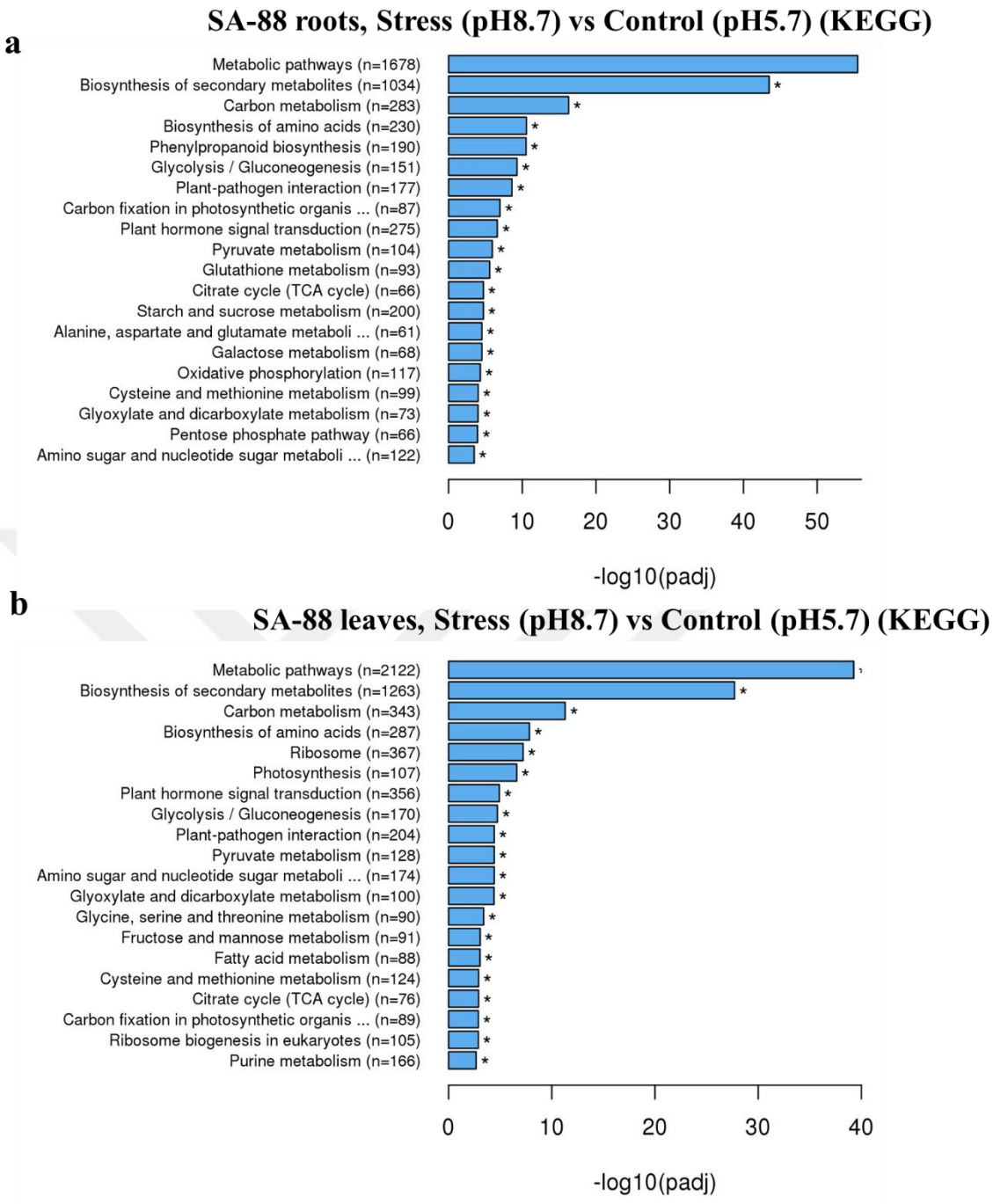

Figure 4.30. Enrichment analysis in KEGG pathways of genes with different expression levels in the roots and leaves of SA-88. * Indicates statistically significant enriched pathways ($p < 0.05$)

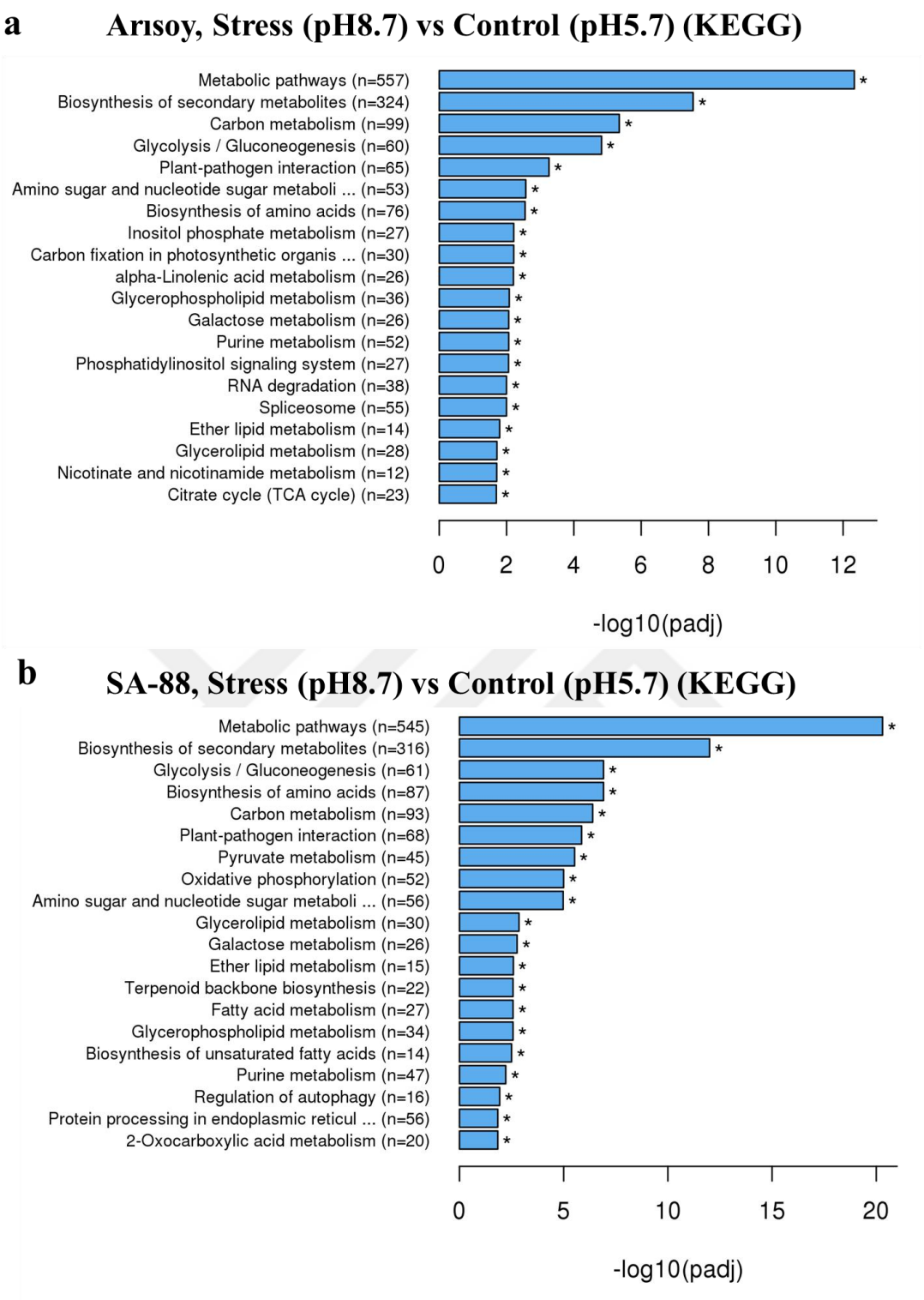

Figure 4.31. Enrichment analysis of all differentially expressed genes in KEGG pathways in both cultivars. * Indicates statistically enriched pathways ($p < 0.05$).

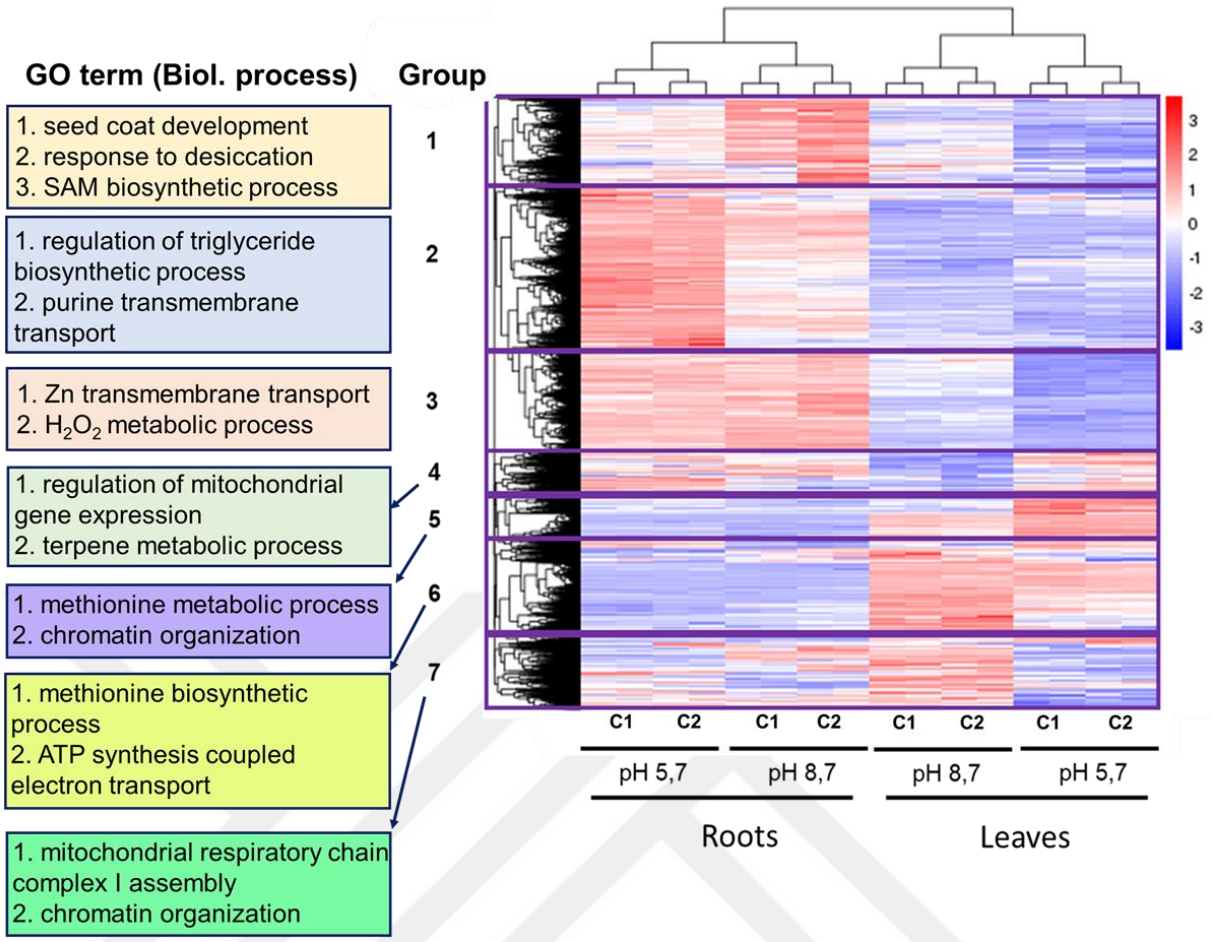

Figure 4.32. Hierarchical grouping of genes with varying expression between groups.

A Heat map was created with the Manhattan approach for hierarchical grouping in different samples according to the expression levels of the genes that show statistically significant changes (Figure 4.32). Accordingly, in the first group, some genes were expressed at high levels in the roots of both varieties under pH 8.7, but the expression level of these genes in the leaves of both cultivars was lower even than the control. The genes expressed in the first group were associated with seed coat development, response to desiccation, and SAM biosynthesis process.

In the second and third groups, there were genes whose expression levels were high in the roots and lower in the leaves. Interestingly the expression level of genes in the second group had shown higher levels at pH 5.7 than the pH 8.7. Genes expressed in the second group were found to be associated with the regulation of triglyceride and purine

transmembrane transport. The expression levels of genes in the fourth group were found to be lower in the leaves of the plants grown at pH 8.7 and higher in other conditions. In the fifth group, the expression level of genes was found higher in the leaves of both cultivars under pH 5.7 compared to the stress conditions (pH 8.7). The expression level profiles of genes in the sixth group show an opposite profile to those in the second and third groups. While the expression levels of the genes in this group were lower in the roots, but more in the leaves, higher expression was more in the leaves of the plants grown at pH 8.7. Interestingly, the methionine metabolic process was found to be associated with the genes fifth and sixth groups. Although the expression levels of the genes in the seventh group show a mixed profile, showed higher expression, especially in the leaves of the plants grown at pH 8.7 (Figure 4.32).

Table 4.7. Ontology enrichment of the genes in hierarchical groups.

GO Description	Enrichment Score	P-value
Group 1		
Biological process		
seed coat development	> 100	3.54E-03
response to desiccation	> 100	9.40E-03
S-adenosylmethionine biosynthetic process	70.54	1.52E-02
Molecular function		
folic acid binding	> 100	7.06E-03
tyrosyl-DNA phosphodiesterase activity	> 100	8.23E-03
hydroxymethylglutaryl-CoA reductase activity	> 100	1.06E-02
Group 2		
Biological proses		
regulation of triglyceride biosynthetic process	> 100	4.60E-03
positive gravitropism	> 100	6.13E-03
purine nucleobase transmembrane transport	> 100	1.07E-02
Molecular function		
telomerase activity	> 100	4.60E-03
purine nucleobase transmembrane transporter activity	> 100	1.07E-02
RNA-directed DNA polymerase activity	92.80	1.22E-02
Group 3		
Biological proses		
zinc ion transmembrane transport	9.56	4.01E-05
hydrogen peroxide metabolic process	5.12	8.09E-06
cellular oxidant detoxification	3.72	4.49E-05
Molecular function		
zinc ion transmembrane transporter activity	9.56	4.01E-05
peroxidase activity	4.80	3.36E-05
metal ion transmembrane transporter activity	3.50	8.37E-05
Group 4		
Biological proses		
regulation of mitochondrial gene expression	49.35	5.51E-05
terpene metabolic process	32.90	9.01E-07
respiratory electron transport chain	10.80	1.84E-04
Molecular function		
carotenoid dioxygenase activity	65.80	4.58E-08
mitochondrial ribosome binding	39.48	1.62E-03
receptor ligand activity	10.40	3.85E-03

* The top three ontologies in the ranking according to the enrichment coefficient were taken.

Table 4.7. (continue) Ontology enrichment of the genes in hierarchical groups.

GO Description	Enrichment Score	P value
Group 5		
Biological proses		
methionine metabolic process	15.90	2.07E-04
chromatin organization involved in regulation of transcription	10.89	4.83E-04
aspartate family amino acid biosynthetic process	8.57	2.44E-04
Molecular function		
3-hydroxyisobutyryl-CoA hydrolase activity	46.55	7.48E-05
protein heterodimerization activity	7.55	1.77E-05
structural constituent of ribosome	5.87	2.57E-13
Group 6		
Biological proses		
methionine biosynthetic process	13.76	2.95E-04
ATP synthesis coupled electron transport	8.65	5.72E-05
oxidative phosphorylation	9.60	7.94E-05
Molecular function		
3-hydroxyisobutyryl-CoA hydrolase activity	41.29	1.06E-04
protein heterodimerization activity	6.70	4.10E-05
structural constituent of ribosome	5.21	4.50E-12
Group 7		
Biological proses		
mitochondrial respiratory chain complex I assembly	14.94	2.51E-04
chromatin organization	9.83	2.89E-04
Peptide biosynthetic process	9.59	2.12E-06
Molecular function		
steroid dehydrogenase activity	13.69	1.96E-03
Translation elongation factor activity	6.32	4.64E-03
oxidoreductase activity	5.32	5.04E-04

* The top three ontologies in the ranking according to the enrichment coefficient were taken.

Due to the large number of genes in these lists, the lists are not presented in the thesis, and since the genes were grouped in sets, GO enrichment was performed in each group to understand the ontologies statistically enriched in each hierarchical group (Table 4.7). According to this analysis, the genes in the first group were enriched in GO terminologies related to drought stress and S-adenosyl methionine (SAM) metabolism, while the genes in the second group were enriched in GO terminologies related to telomerase activity, RNA-based DNA polymerase activity and positive gravitropism. The third group of genes were particularly related to Zn transport and oxidative stress while those in the fourth group were enriched in terpene and carotenoid metabolisms and ontologies related to the electron transfer system. The fifth group of genes were associated with methionine metabolism and chromatin regulation. Genes in the sixth group were associated with both methionine metabolism and oxidative phosphorylation. Indeed, the expression level change trends of the genes in these two groups (5 and 6) were similar (Figure 4.32). Genes in the seventh group were found to be related to chromatin organization, oxidoreductase activity and electron transfer system (Table 4.7).

As can be seen, while iron deficiency affected different metabolisms, it induced genes related to mineral transport and oxidative stress. In addition, there were changes in the expression levels of genes responsible for the changes associated with genetic regulation (particularly transcriptional control). Oxidative stress may be caused by the problems observed in electron transport especially in the chloroplast and mitochondria due to less available iron. In addition, it can be said that iron deficiency results in inducing reactions like drought stress, which results in the enrichment of SAM-related pathways in the roots. Furthermore, methionine biosynthesis, oxidative phosphorylation, and electron transport are induced in the leaf (Figure 4.32).

4.3.8. Clustering of differentially expressed genes

In the next step, the genes having fold change more than two (either upregulated or downregulated) were filtered for further analysis. As a result of comparing the genes in the gene lists with each other, the common genes affected in the roots and leaves of the varieties and the genes affected in the same organs of the varieties were determined (Figure 4.33). Accordingly, the number of common genes affected by iron deficiency in both organs of Arısoy and SA-88 was determined as 731 and 710, respectively (Figure

4.33a). On the other hand, the number of common genes affected by iron deficiency in the roots and leaves of both varieties was found to be 1648 and 2818 respectively (Figure 4.33b).

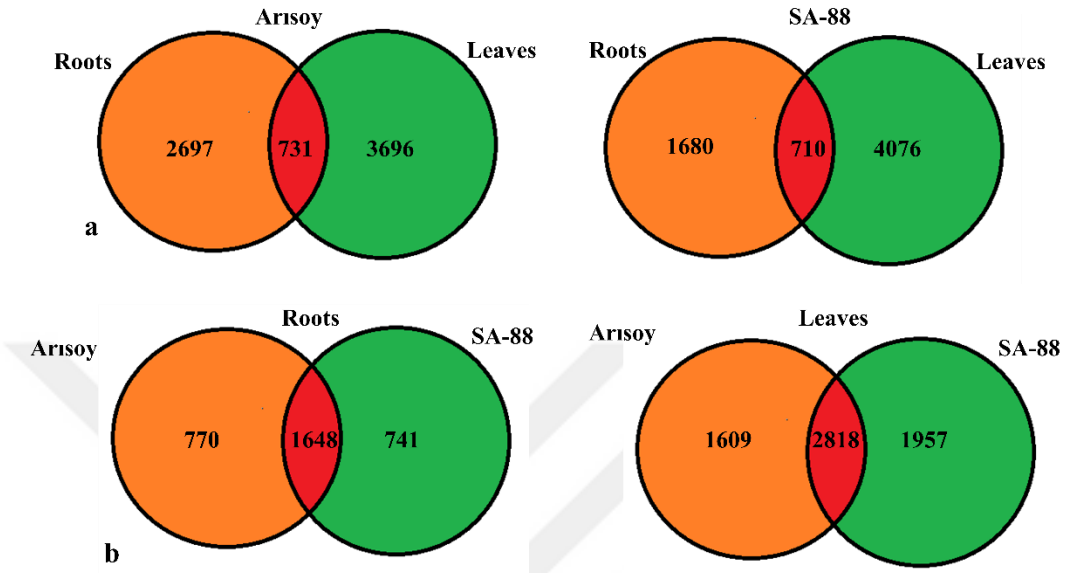

Figure 4.33. Clustering of gene lists. a) Comparison of the genes determined in the roots and leaves of the two cultivars. b) Comparison of the genes determined in the roots and leaves in each cultivar.

Subsequently, genes exhibiting a fold change greater than two, whether upregulated or downregulated, were selected for further analysis. This analysis was conducted using three distinct approaches to ensure that genes of significant interest were not overlooked within the extensive dataset. Initially, genes common in both cultivars were identified, resulting in a total of 4,246 differentially expressed genes. Subsequently, Gene Ontology (GO) analysis was performed on these 4,246 genes, with a particular focus directed toward those involved in transporter activity. The GO analysis revealed a total of 277 genes associated with transporter activity (Appendix 8), and additionally, 267 genes were identified as transcription factors among the 4,246 targeted common genes (Appendix 9).

In the next step, the genes common in roots and leaves of Arısoy and SA-88 were identified and as a result, a total of 466 common genes were found. Following the same procedure as in step one, GO analysis was conducted, identifying 37 genes involved in

transporter activity. In RNA seq data studies the top up-regulated and top down-regulated genes are of great importance against specific stress. Luckily, all transporters and transcription factors found in step 2 were present in the step one list as well. Because of this the 100 top upregulated and 100 top downregulated genes in both tissues of two cultivars were further considered for the gene ontology analysis. As a result, 59 transporters and 43 transcription factors were found. Step three shared most of the transporters and transcription factors which were found in step 1 and 2 except the distinct 13 transporters and 6 transcription factors. The final list was prepared by combining all transporters and transcription factors from three analyses for further investigation (Appendix 8 and 9). For the transporters, the GO result of *Glycine max* genes orthologs in *Arabidopsis thaliana* showed the pathways affected in "localization", "cellular process" and "homeostatic response" in the term biological process (Figure 4.34 a). For the term molecular function, the term "Transporter activity", "ATP Binding Activity" and "binding" were enriched (Figure 4.34 b). GO result of *Glycine max* Transcription factors orthologs in *Arabidopsis thaliana* terms "biological regulation", "response to stimuli" and "cellular process" were enriched in biological process (Figure 4.35 a) while the terms "transcription regulator activity" and "binding" were enriched in molecular function (Figure 4.35 b).

As can be seen from the list, some of these genes have not been previously associated with iron deficiency. Since some of the genes determined in this gene ontology were not associated with iron deficiency in soy before, all genes included in this ontology were taken as a set and compared to transcriptomic studies performed in soybean, gene set enrichment was performed (Appendix 8) (Appendix 9).

CYP707A2, *FRUCT4*, *ALDH5F1*, and *CEP9* were oppositely expressed in the roots between the two cultivars while *ASP1*, *WIP4*, *MLP43*, *RPM1*, *UGT73B5*, *HRD*, *LT1,* and *ATNYE1* were oppositely expressed in the leaves of both cultivars (Appendix 10). CYP707A2 is responsible for the regulation of ABA levels during seed development and germination (Okamoto et al., 2006; Matakiadis et al., 2009), while abscisic acid is also known to alleviate the iron deficiency in apple plants by regulating the iron distribution and root development (Zhang et al., 2020). Genes like *CYP707A2, CEP9*, and *HRD* could be central to iron deficiency tolerance by affecting root architecture, stress response, and nutrient homeostasis. The differential expression of these genes between Arısoy and Sa-

88 highlights their potential roles in determining the cultivars' varying abilities to tolerate low iron conditions.

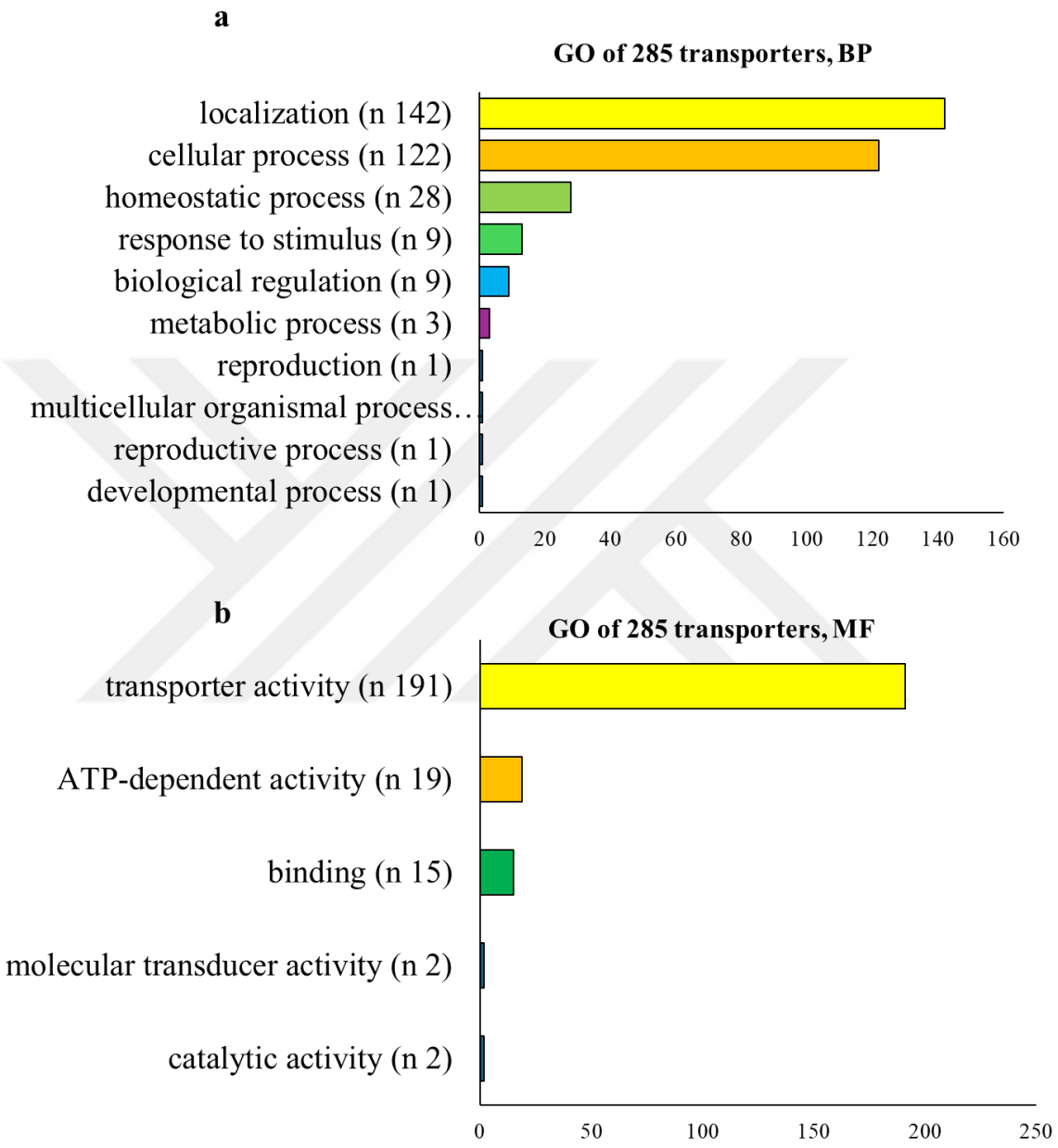

Figure 4.34. GO enrichment analyses of selected transporter genes. a) Enrichment analysis of 285 transporters genes in biological process pathways. b) Enrichment analysis of 285 transporters genes in Molecular function pathways. * Indicates statistically enriched pathways ($p < 0.05$).

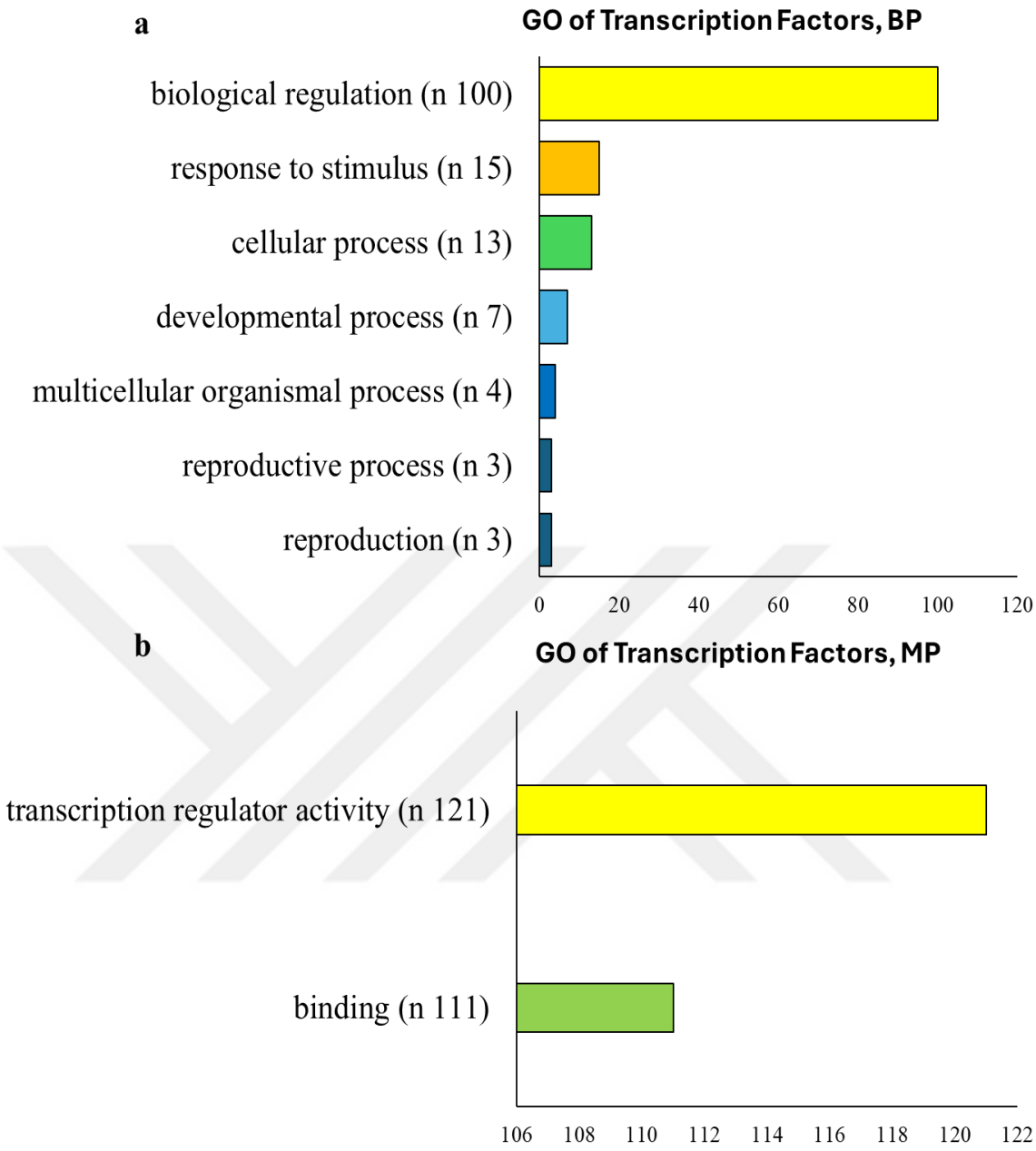

Figure 4.35. a) Enrichment analysis of transcription factors in biological process pathways. b) Enrichment analysis of 285 transcription factors in Molecular function pathways. * Indicates statistically enriched pathways ($p < 0.05$).

To better understand the relationship of these carrier genes with the iron deficiency signaling pathway, the expression levels of Arabidopsis orthologs of these transporters under iron deficiency were determined in 14 different transcriptome studies using Genevestigator, where a low percentage of genes and transcription factors had shown differential expression under iron deficiency conditions, which can be related to the early

and late iron deficiency response. These studies contain the data set in early iron deficiency response while soybean was subjected to an iron deficiency environment for a long term (plants were grown for 30 days) (Figure 4.36, Figure 4.37).

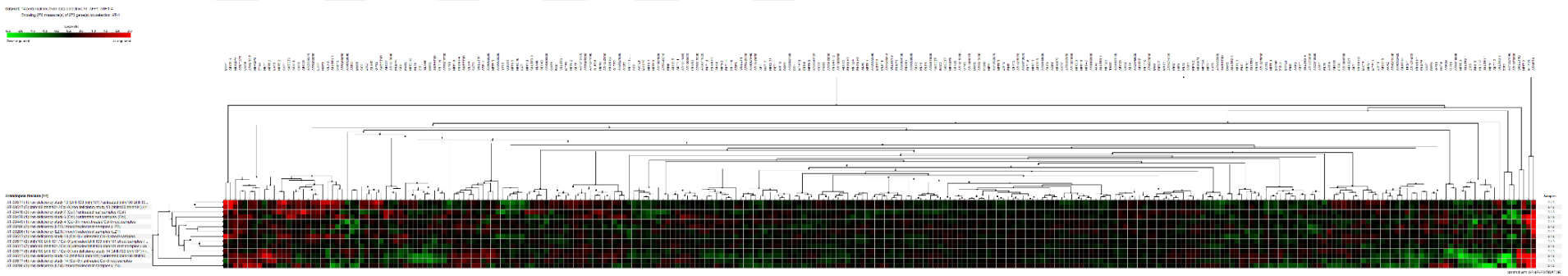

Figure 4.36. Expression levels of transporters in 14 different studies by Genevestigator.

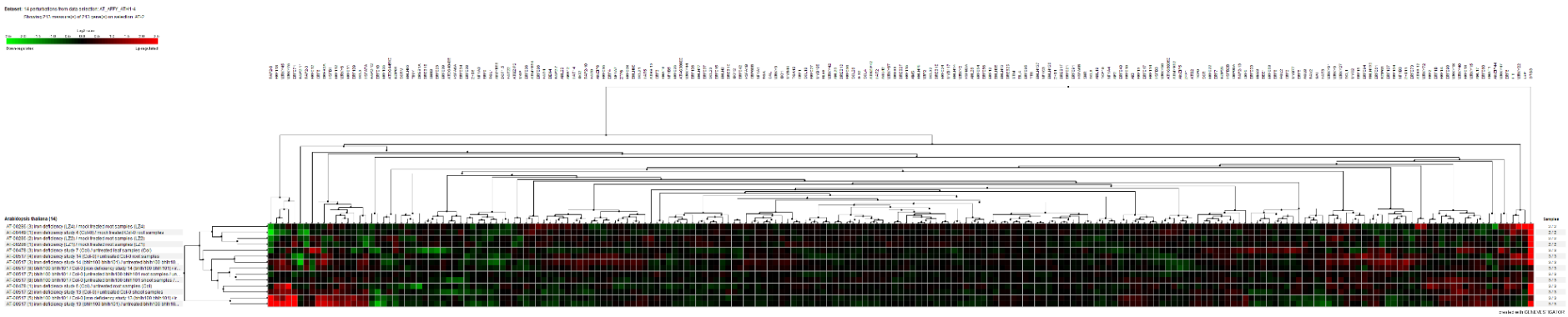

Figure 4.37. Expression levels of transcription factors in 14 different studies related to iron deficiency by Genevestigator.

4.3.9. Xylem sap pH and L-glutamine levels

The analysis of transporter genes revealed that 21 transporters from the UMAMIT family were differentially expressed in soybean roots and leaves, suggesting a potential role in iron homeostasis in plants. Members of the UMAMIT transporter family are found to be involved in the transport of L-glutamine (Muller et al., 2015), it was hypothesized that iron might bind with L-glutamine, and it may be one of its possible forms of translocation between different organs. To investigate this hypothesis, soybean plants were grown under varying iron availability conditions, and L-glutamine levels in the xylem sap were measured. Results indicated that under high pH conditions, where iron is less available, all cultivars exhibited a significant increase in L-glutamine levels (Figure 4.38). Conversely, in the high pH treatment where 43.25 mg/kg Fe-EDDHA was added as an iron source, lower L-glutamine levels were observed compared to the stress conditions. These findings suggest that high pH-induced iron deficiency leads to increased L-glutamine levels in the soybean xylem sap (Figure 4.38).

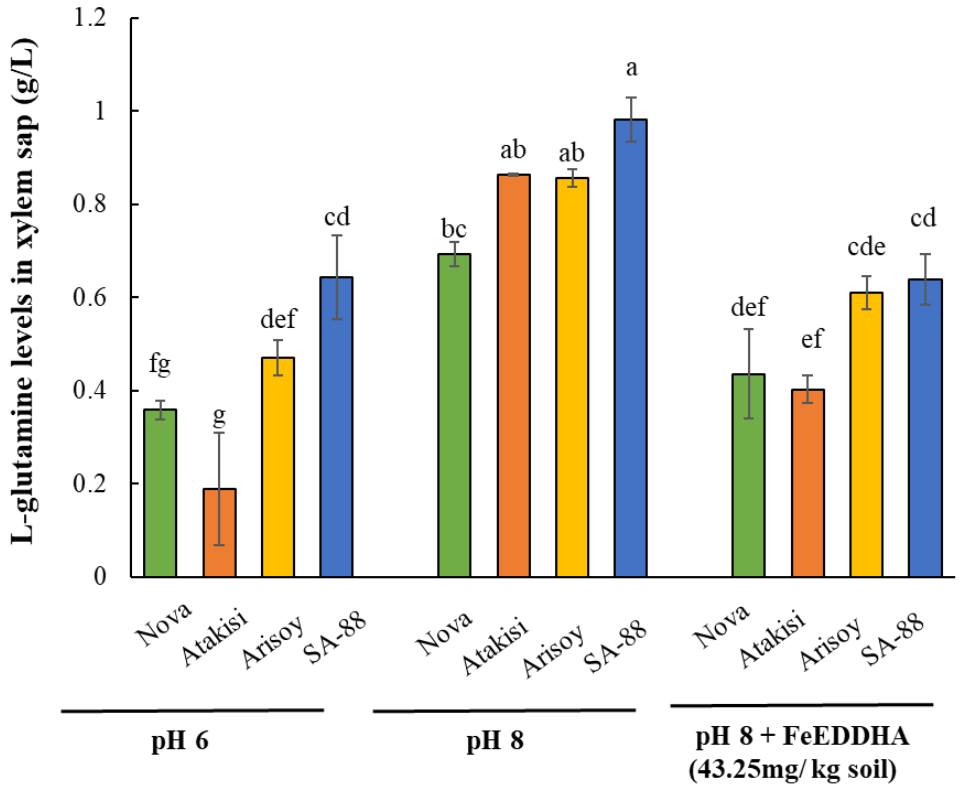

Figure 4.38. L-glutamine levels of soybean grown under different iron availability regimes. Different letters on the bars indicate statistical differences from each other ($p < 0.05$).

Plants exhibit tightened regulation of xylem sap pH under various stress conditions. Alkalinization of xylem sap due to high external pH may constrain iron translocation to the aerial parts under iron-limited conditions. To investigate whether soybean xylem sap pH increases or decreases under high pH conditions, the xylem sap pH of soybean cultivars grown under different iron availability regimes was measured. Surprisingly, a decrease in xylem sap pH was observed in sensitive cultivars at high pH, whereas tolerant cultivars showed no significant change compared to control conditions. In the high pH treatment with 43.25 mg/kg FeEDDHA as an iron source, the xylem sap pH was similar to that of the control conditions. These findings suggest that soybean decreases its xylem sap pH under iron deficiency to enhance iron translocation (Figure 4.39). Similar results were reported by Larbi et al. (2010), where the xylem sap pH of *Beta vulgaris* was approximately 6.2 in control leaves and 5.7 in markedly Fe-deficient leaves.

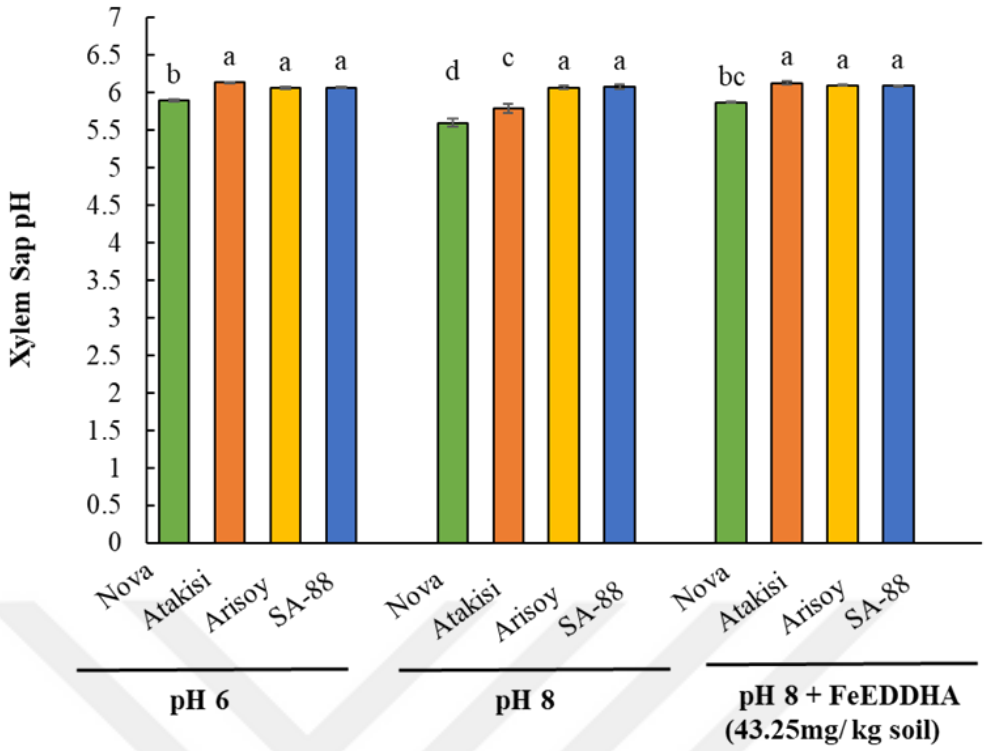

Figure 4.39. Xylem sap pH of soybean grown under different iron availability regimes. Different letters on the bars indicate statistical differences from each other ($p < 0.05$).

Part 4: Characterization of *AtUMAMIT28* in Arabidopsis thaliana under transmetal deficiencies

4.4.1. In Silico analyses of *AtUMAMIT28*

In silico analysis of *UMAMIT* family genes revealed that *AtUMAMIT28* can be the potential candidate that may be involved in iron homeostasis since the co-expression results showed that *AtUMAMIT28* is expressed together with many iron homeostasis genes as shown in Figure 4.40. These results indicate that AtUMAMIT28 may have a role in iron uptake (as it co-express with *YSL1*), vacuolar iron storage or efflux (as it co-express with *NRAMP3*, *NRAMP4, VIT1, and VIT2*) or translocation (as it co-express with *FRD3* and NAS family genes).

a

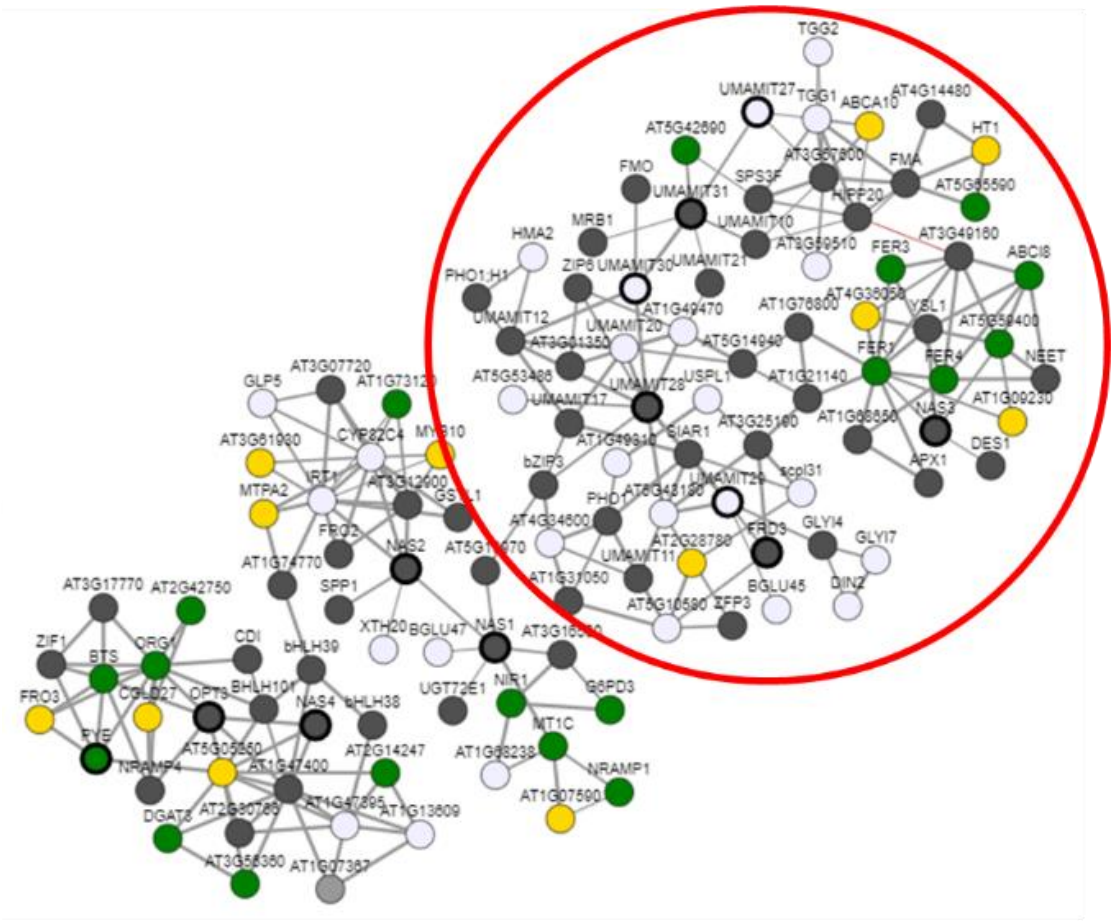

b

Number	Gene name	Number	Gene name	Number	Gene name
1	*FRD3*	**6**	*NRAMP6*	**11**	*YSL2*
2	*VIT1*	**7**	*FRO2*	**12**	*NAS1*
3	*VIT2*	**8**	*BHLH104*	**13**	*NAS2*
4	*NRAMP1*	**9**	*BHLH034*	**14**	*NAS3*
5	*NRAMP3*	**10**	*YSL1*	**15**	*NAS4*

Figure 4.40. Co-expression analysis of *AtUMAMIT28*. a) Co-expression analysis of some *UMAMIT* family genes revealed their interaction with several Fe deficiency-responsive genes. b) Known iron homeostasis genes interacting with *AtUMAMIT28*.

4.4.2. Development of *AtUMAMIT28* overexpression lines and mutants confirmation

To characterize the *AtUMAMIT28* in *Arabidopsis thaliana* under iron-deficient conditions, *umamit28-1* and *umamit29-1* homozygous lines were confirmed by gene-specific primers and T-DNA PCR primers as shown in Figure 4.41 and Figure 4.42.

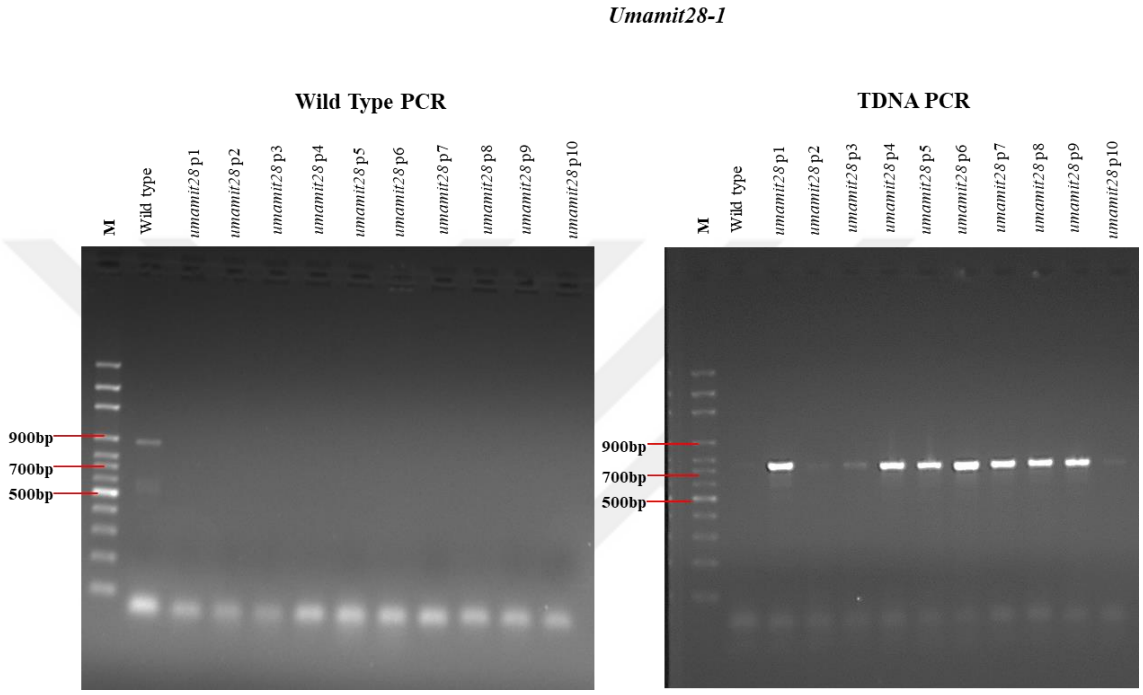

Figure 4.41. Confirmation of the homozygous *umamit28-1* lines. 10 µl of PCR products were separated on 1% agarose gel electrophoresis in 1 X TAE buffer for 40 minutes. M represents for 1 kb DNA ladder (Thermo Scientific). P1-P10 represents the number of screened plants.

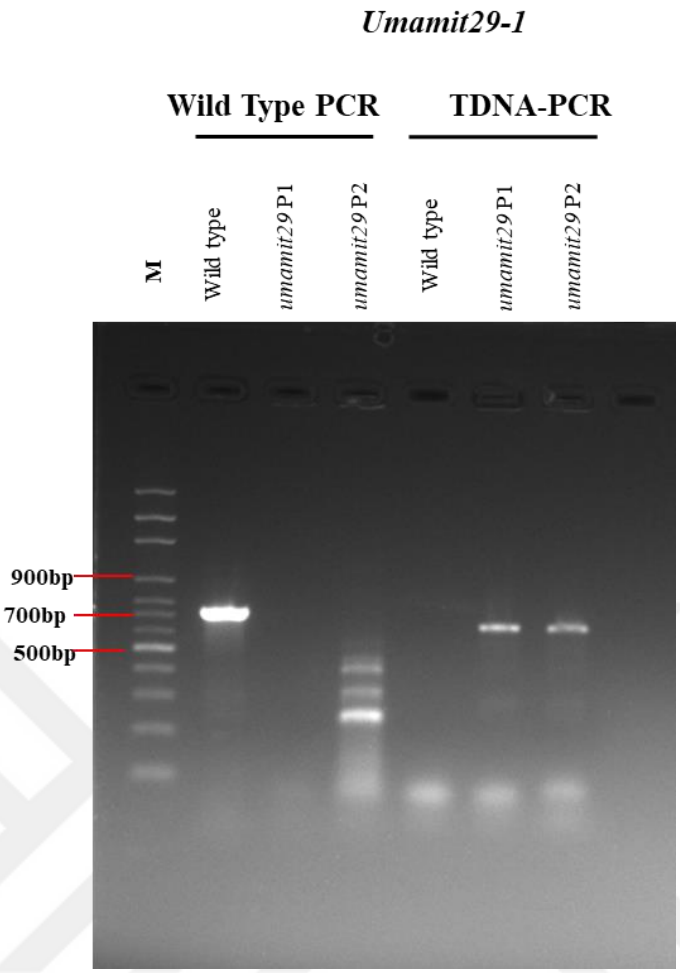

Figure 4.42. Confirmation of the homozygous *umamit29-1* lines. 10 µl of PCR products were separated on 1% agarose gel electrophoresis in 1 X TAE buffer for 40 minutes. M represents for 1 kb DNA ladder (Thermo Scientific). Here P1 and P2 represent the number of screened plants.

For the development of *AtUMAMIT28* overexpression lines, the CDS region of *AtUMAMIT28* was amplified as shown in Figure 4.43. A clear band can be observed of size 1098 bp (CDS region) after the gel purification in Figure 4.44.

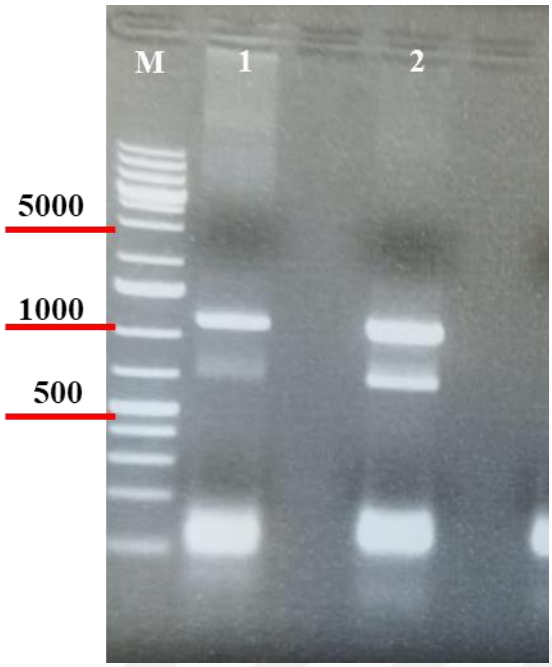

Figure 4.43. Amplification of the CDS region of *AtUMAMIT28* by Nested PCR. 20 µl of samples were separated on 0.8% agarose gel electrophoresis in 1 X TAE buffer for 40 minutes. M represents for 1 kb DNA ladder (Thermo Scientific).

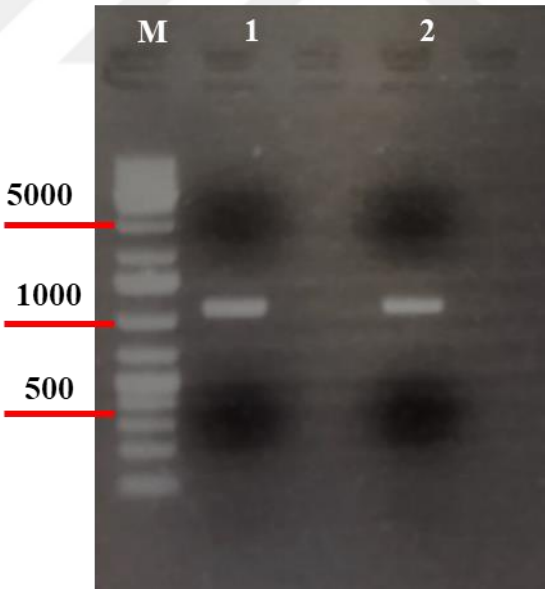

Figure 4.44. Gel image showing the extracted band of 1098 bp after gel purification (*AtUMAMIT28*). 20 µl of samples were separated on 0.8% agarose gel electrophoresis in 1 X TAE buffer for 40 minutes. M represents for 1 kb DNA ladder (Thermo Scientific).

After the BP reaction and transformation of the BP reaction product in the *E. coli* competent cells, three positive colonies (C4, C13, and C15) were selected on the selection medium (Figure 4.45). Next, plasmid extraction was done, and samples were sent for sequencing. Following the acquisition of sequencing results, the obtained sequences were aligned with the reference coding DNA sequence (CDS) of *AtUMAMIT28*. Notably, sequences from Colony 14 and Colony 15 exhibited both base deletions (highlighted in red) and base insertions (highlighted in light green). In contrast, the sequence from Colony 4 showed complete concordance with the reference gene sequence. Consequently, Colony 4 was selected for subsequent experimental reactions (Figure 4.46).

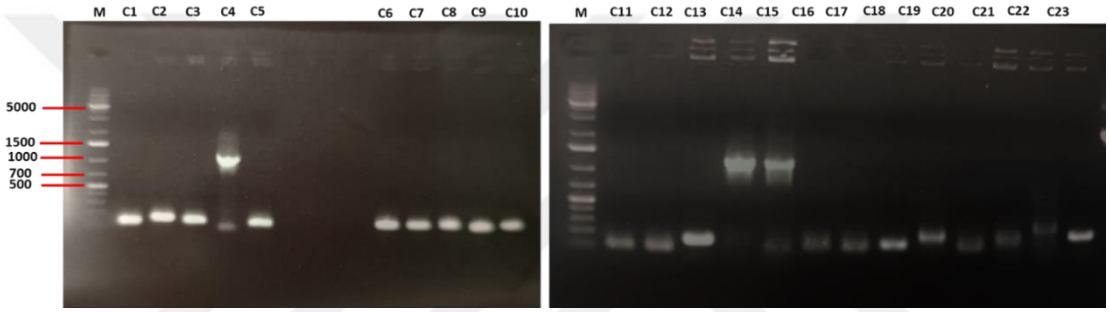

Figure 4.45. Gel image of colony PCR after BP reaction for the colonies containing *pDNOR207:AtUMAMIT28*. 10 µl of samples were separated on 1% agarose gel electrophoresis in 1 X TAE buffer for 40 minutes. M represents for 1 kb DNA ladder (Thermo Scientific). Numbers from C1-C23 show the colony numbers subjected to PCR.

Figure 4.46. Sequencing results of positive colonies**.** The base deletions were highlighted in red and base insertions were highlighted in light green. Colony 4 was selected for further use in the reactions.

Plasmid extracted (*pDNOR207*: *AtUMAMIT28*) from Colony 4 was used in the LR reaction where *pMDC83* was used as a destination vector. Afterwards, the product of the LR reaction was transformed into *E. coli* and subjected to colony PCR. The colony PCR showed that all the colonies were positive and had successful cloning of the gene of interest (Figure 4.47).

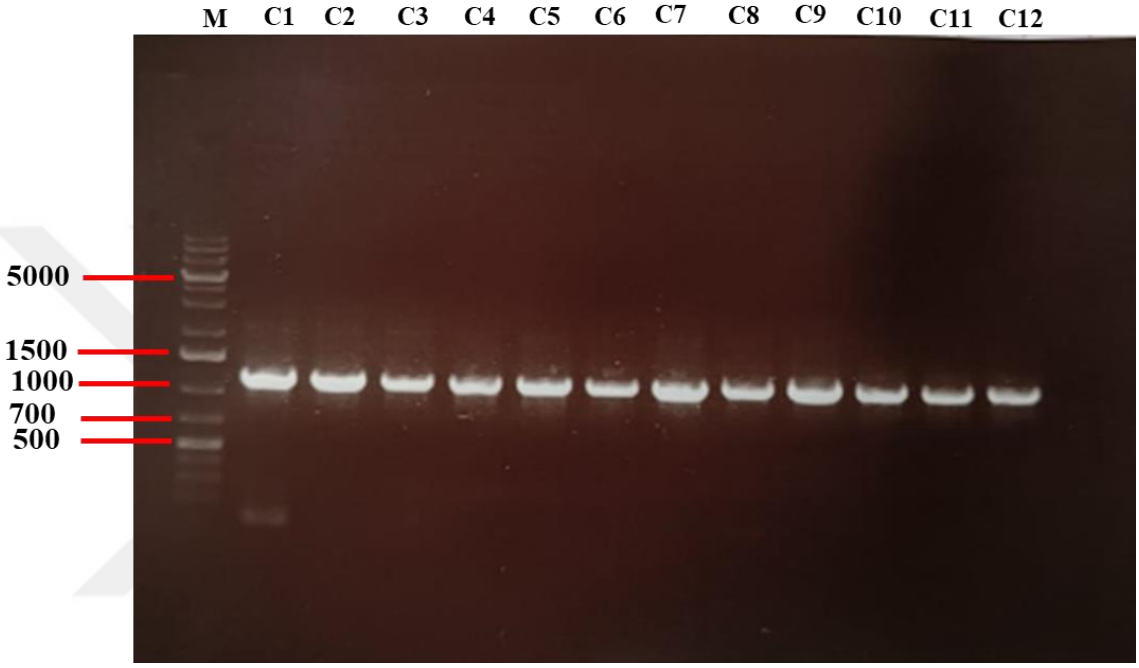

Figure 4.47. Colony PCR after transformation of LR product of *pMDC83:AtUMAMIT28* without stop codon in *E. coli* cells. 10 µl of samples were separated on 1% agarose gel electrophoresis in 1 X TAE buffer for 40 minutes. M represents for 1 kb DNA ladder (Thermo Scientific). Numbers C1-C12 show the colony numbers.

Later, plasmid extraction was done from the positive colonies, and the destination vector with the gene of interest was transformed into *Agrobacterium Agl-0* cells with electroporation. Then, confirmation was done by PCR, which showed that all the colonies were positive and had a successful transformation of the gene of interest (Figure 4.48).

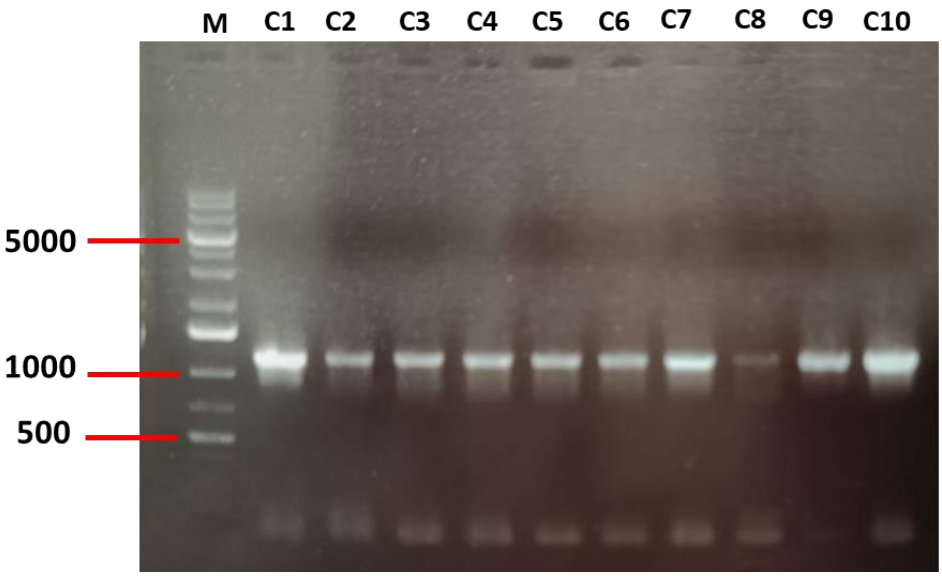

Figure 4.48. Colony PCR of *Agl-0* strain after transformation of *pMDC83*: *AtUMAMIT28* without stop codon. 10 µl of samples were separated on 1% agarose gel electrophoresis in 1 X TAE buffer for 40 minutes. M represents for 1 kb DNA ladder (Thermo Scientific). Numbers C1-C10 show the colony numbers.

4.4.3. Selection of *AtUMAMIT28* Overexpression lines

Plants expressing the *pMDC83*:*AtUMAMIT28* were grown on the selection media (supplemented with 20 µg/ml hygromycin). 39 T_1 plants with longer hypocotyls were selected as transgenics for further confirmation by PCR (Figure 4.49). Later, these selected T_1 plants were confirmed by the PCR (Figure 4.50). Out of 39 plants, 34 were found PCR positive and they were grown on soil in controlled conditions and their seeds were collected. Then, lines P4, P8, and P9 were selected for further progeny analyses. The T_2 plants were further subjected to selection on hygromycin media (20 µg/ml) to determine single insertion lines. The plants that were following 3:1 segregation were selected and the ones with 15:1 segregation or unusual growth patterns were discarded (Figure 4.51). Next, selected T_2 plants were also confirmed by PCR via vector and gene-specific primers (Figure 4.52-54).

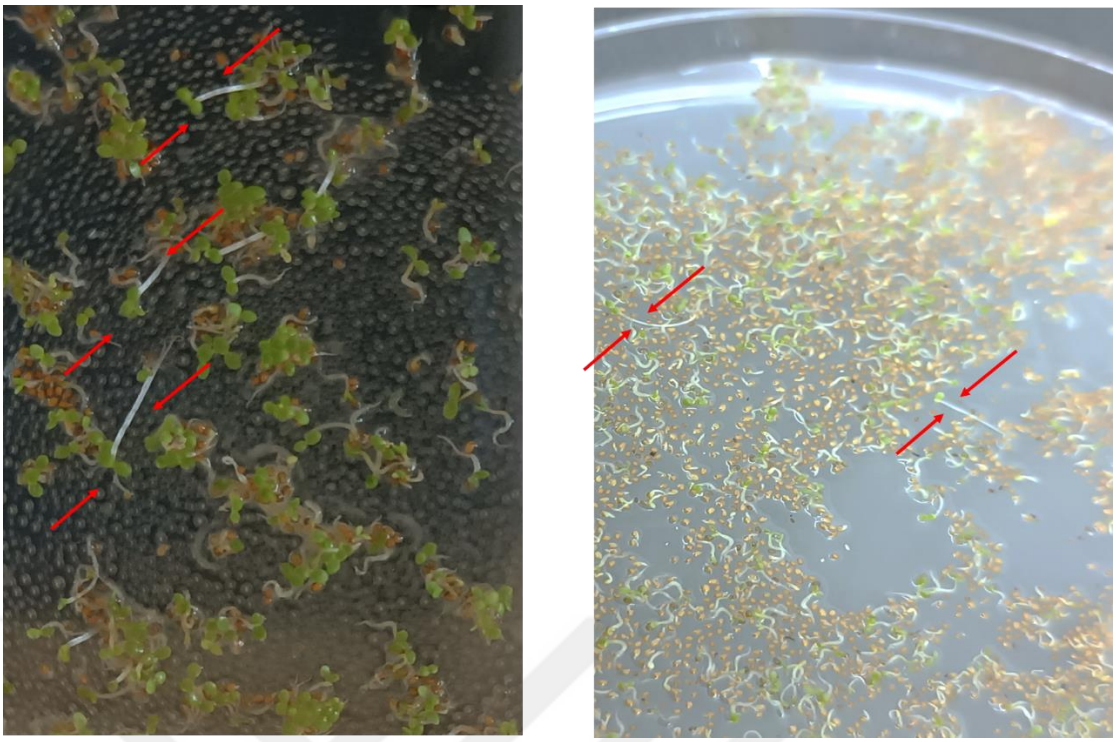

Figure 4.49. Selection of T_1 transgenic plants on 20 µg/ml hygromycin-containing media. Seed stratification was done at 4°C for two days. Later plates were kept under light conditions for three hours. Next, they were covered with aluminum foil in the dark for three days. Finally, the plates were kept under light for 3 days. Red arrows represent the selected transgenic T_1 plants with elongated hypocotyls.

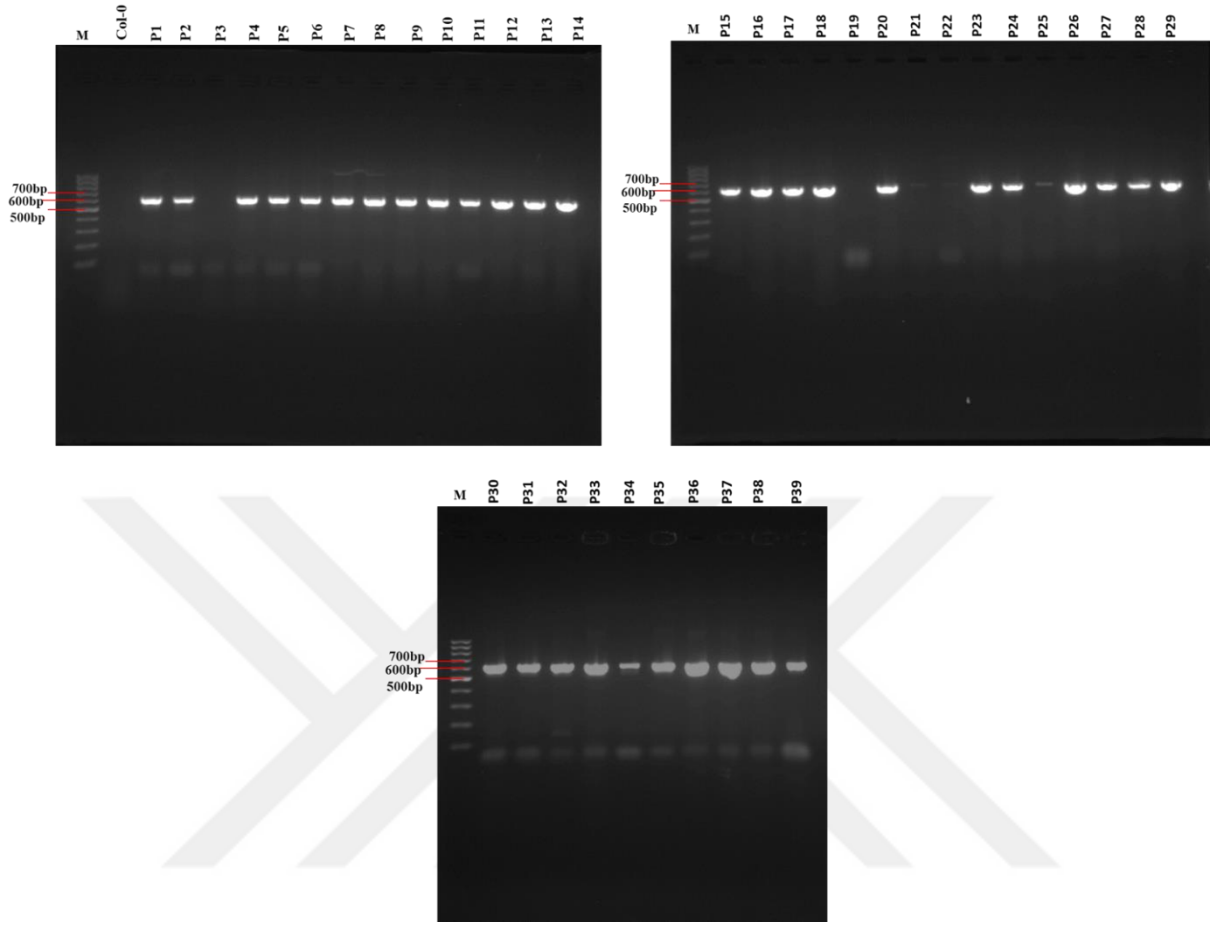

Figure 4.50. PCR confirmation of T_1 plants selected on hygromycin media. P shows the number of T_1 plants from 1 to 39. The PCR product was run for 75 minutes on 1% agarose gel containing 0.5% TBE. 100 bp plus ladder (Thermo Scientific) was used as a marker. Col-0 was used as a negative control.

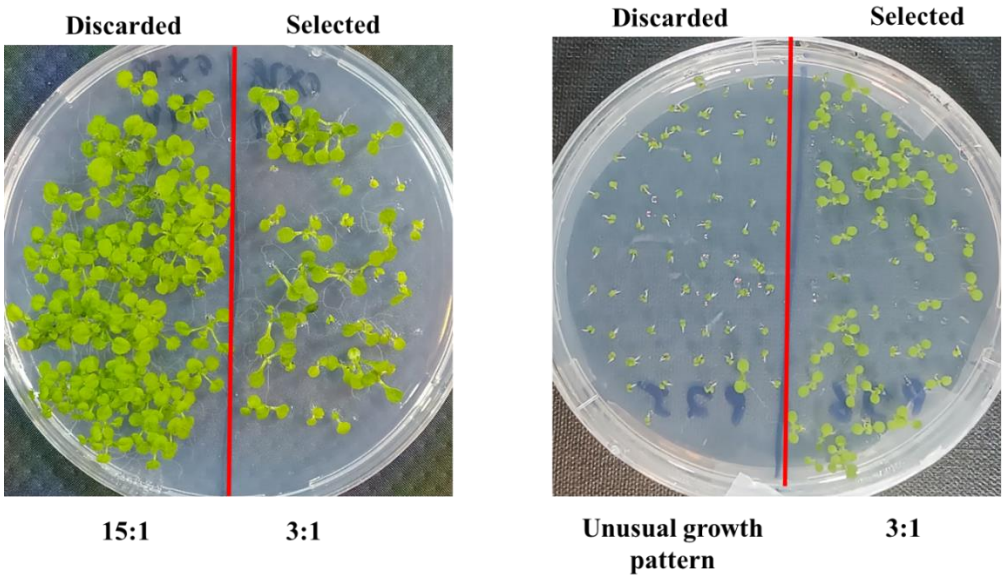

Figure 4.51. Screening of T_2 transgenic plants on 20 µg/ml hygromycin media. Seed stratification was done at 4°C for two days. Later, the plates were grown under a controlled growth room for 7-8 days.

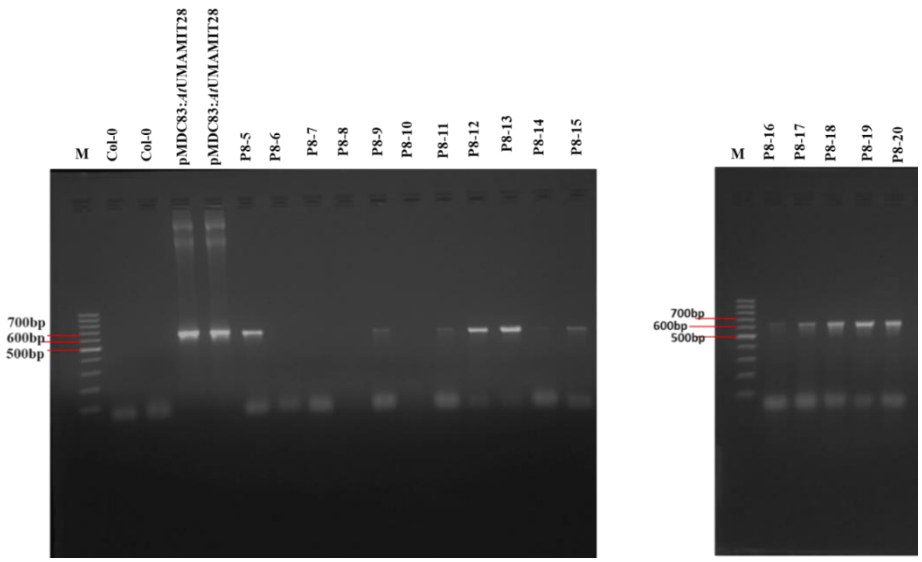

Figure 4.52. Confirmation of T_2 plants (progeny of P8) with a segregation ratio of 3:1. PCR products were run for 75 minutes on 1% agarose gel containing 0.5% TBE. 100 bp plus ladder (Thermo Scientific) was used as a marker. Numbers from P1- P20 show the number of plants subjected to PCR. Col-0 was used as a negative control while the plasmid of *pMDC83:UMAMIT28* was used as a positive control.

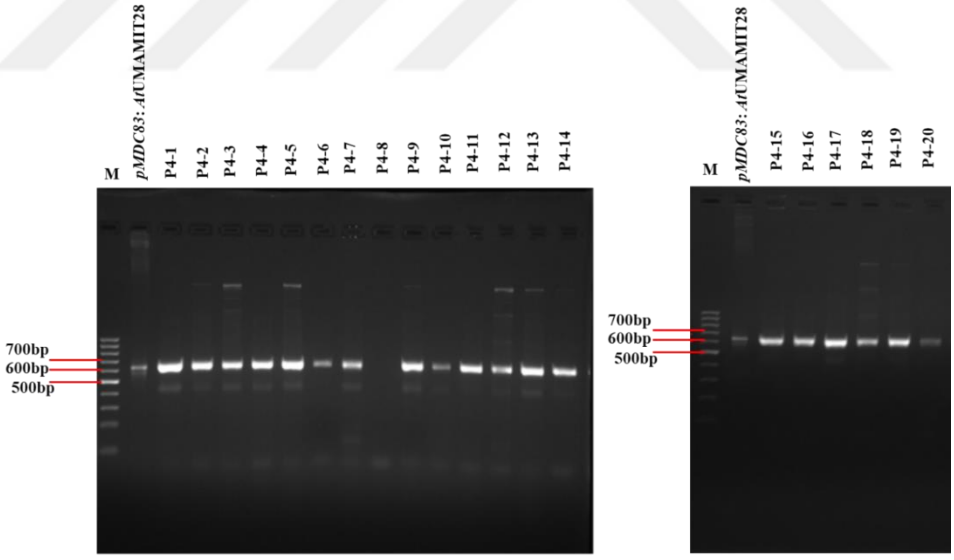

Figure 4.53. Confirmation of T_2 plants (progeny of P4) with a segregation ratio of 3:1. PCR products were run for 75 minutes on 1% agarose gel containing 0.5% TBE. 100 bp plus ladder (Thermo Scientific) was used as a marker. Numbers from P1- P20 show the number of plants subjected to PCR. Col-0 was used as a negative control while the plasmid of *pMDC83:AtUMAMIT28* was used as a positive control.

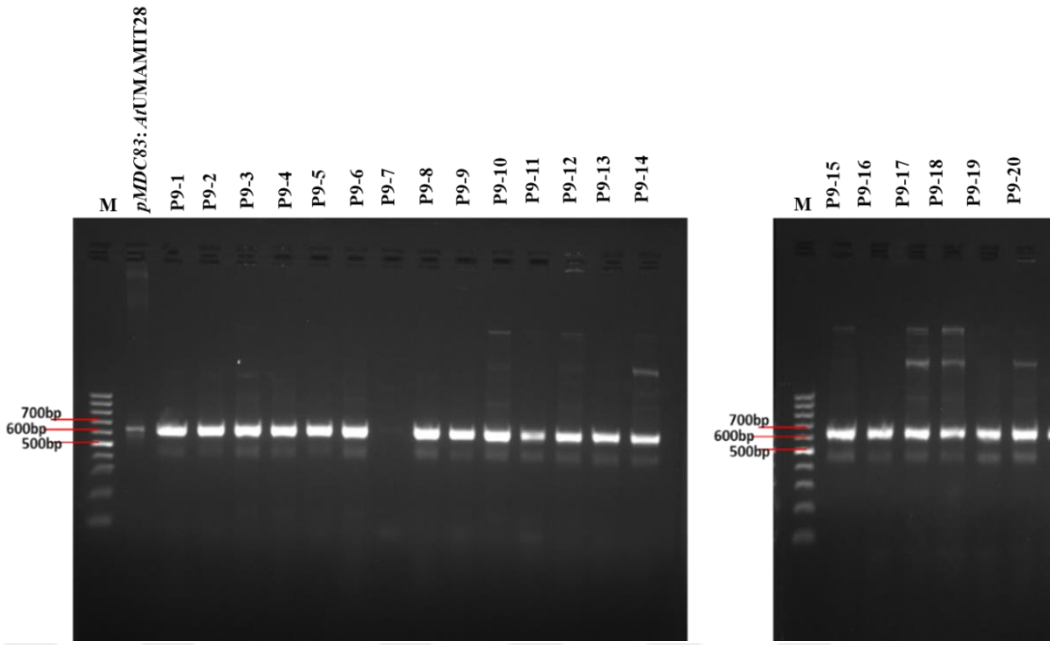

Figure 4.54. Confirmation of T_2 plants (progeny of P9) with a segregation ratio of 3:1. PCR products were run for 75 minutes on 1% agarose gel containing 0.5% TBE. 100 bp plus ladder (Thermo Scientific) was used as a marker. Numbers from P1- P20 show the number of plants subjected to PCR. Col-0 was used as a negative control while the plasmid of *pMDC83:UMAMIT28* was used as a positive control.

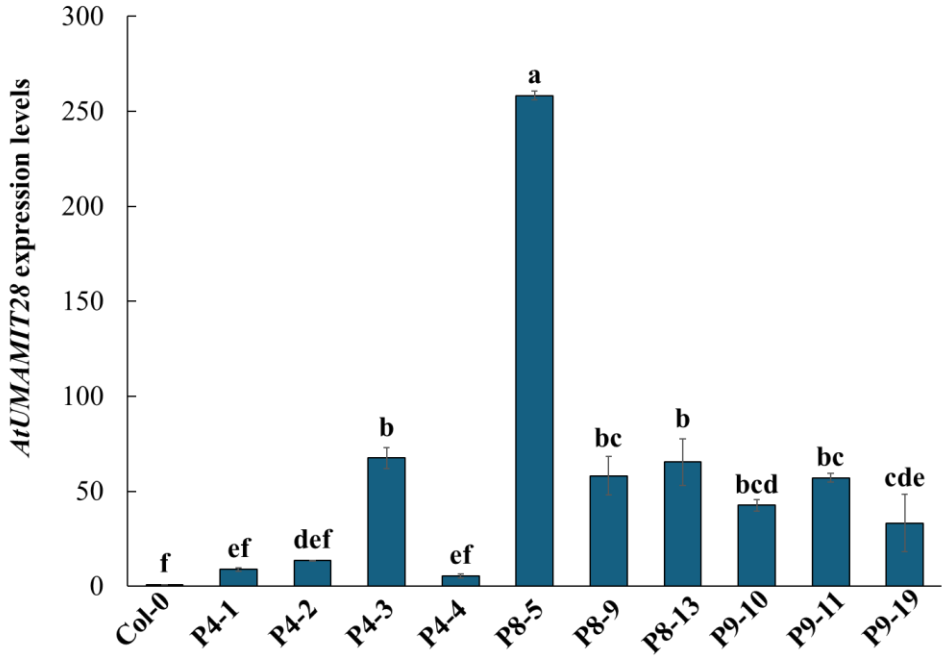

Figure 4.55. *AtUMAMIT28* expression levels in selected transgenic lines T_3 lines. Different letters indicate significant changes among treatments ($p<0.05$).

Subsequently, T_3 seeds were collected, and plants were grown in soil (peat:perlite, 2:1) under controlled conditions. After 30 days of growth, the confirmation of *AtUMAMIT28* overexpression lines was done by quantitative real-time PCR (qRT-PCR). Compared to Col-0, the transgenic lines overexpressing the *AtUMAMIT28* exhibited varied levels of *AtUMAMIT28* expression, ranging from a minimum increase of 4.45-fold (P4-4) to a maximum of 258.38-fold (P8-5). For further studies, lines P8-5 (258.38-fold change) and P9-11 (57.09-fold change) were selected as overexpression lines, hereafter referred to as OE1 and OE2 (Figure 4.55).

4.4.4. Characterization of *AtUMAMIT28* under iron deficiency

Among the plants grown on ABIS media with different concentrations of iron, higher FRO/FCR activities were observed for the *umamait28-1* mutants while overexpression lines showed no significant difference compared to the Col-0 under controlled conditions. Under iron deficiency, FRO/FCR enzyme activities of *umamit28-1* again remained higher than the Col-0 while lower FRO enzyme activities were observed for the overexpression lines 1 and 2 (Figure 4.56 b). Interestingly, mutants and overexpression lines showed longer root lengths than the wild-type Col-0 under mild iron-deficient conditions (0 µM Fe) while overexpression line 1 showed longer root lengths compared to the other genotypes in the treatment 0 µM Fe + 200 µM Ferrozine (Figure 4.56 c). Furthermore, *umamit28-1* and overexpression lines showed higher total chlorophyll contents under mild iron deficiency conditions (0 µM Fe) while mutants showed low levels of chlorophyll concentrations under extreme iron deficiency conditions (0 µM Fe + 200 µM Ferrozine). On the contrary, overexpression lines showed higher levels of chlorophyll concentrations in comparison with Col-0 (Figure 4.57).

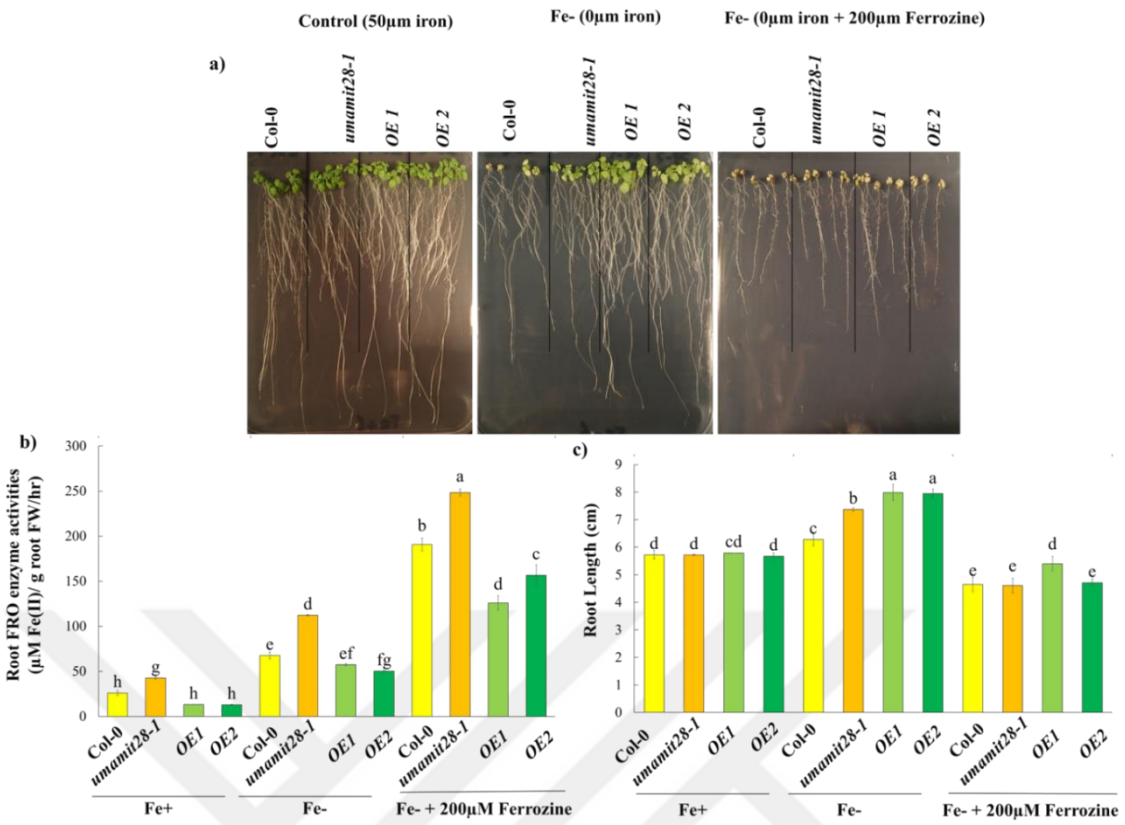

Figure 4.56. Physiological responses of *umamit28-1* and *AtUMAMIT28* overexpression lines under varied iron availability (a). The overall growth of genotypes. (b). Root ferric chelate reductase activities of genotypes. (c) Root lengths. Different letters indicate significant changes among treatments ($p<0.05$).

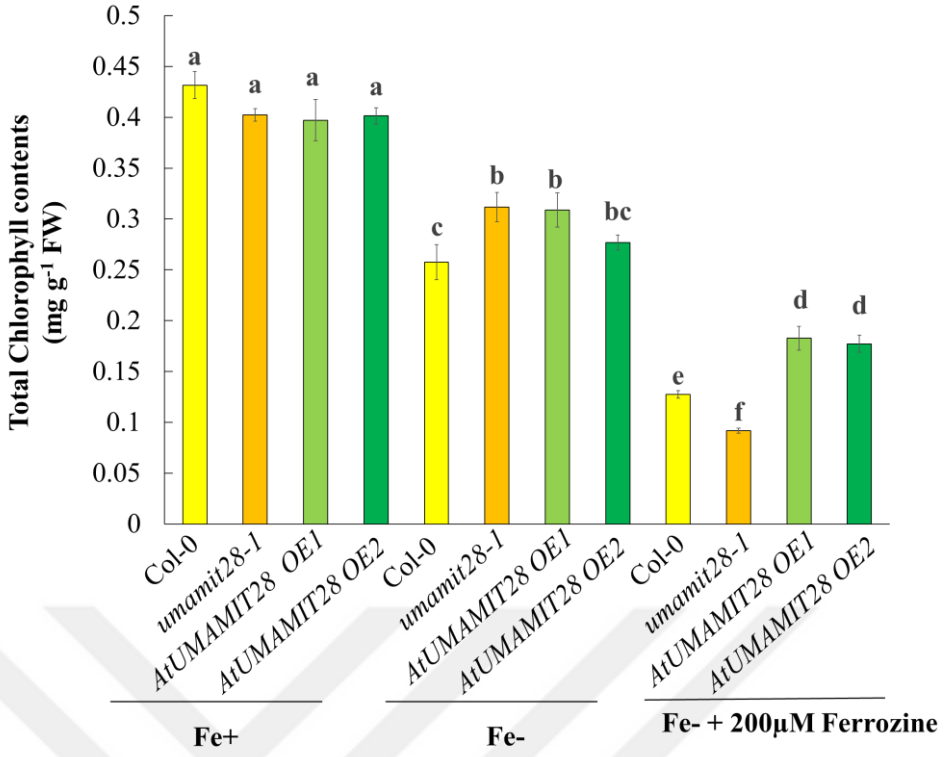

Figure 4.57. Total chlorophyll contents of *umamit28-1* and *AtUMAMIT28* overexpression lines under varied iron availability. Different letters indicate significant changes among treatments ($p<0.05$).

4.4.5. Metal content analyses

No significant difference was observed in the root metal content for all the genotypes under control conditions (50 µM Fe) where sufficient iron was present while lower iron concentrations were observed in *umamit28-1* compared to the wild type under low iron availability (0 µM Fe) and extreme iron deficiency conditions (0 µM Fe + 200 µM Ferrozine). Higher iron concentrations were observed in overexpression lines under extreme iron deficiency conditions (0 µM Fe + 200 µM Ferrozine) in comparison with wild type (Figure 4.58). Leaf iron contents revealed lower iron concentrations accumulated in the overexpression lines under control conditions while no significant difference was observed between the wild type and the mutant. On the other hand, lower iron concentrations were observed in *umamit28-1* compared to the wild type under low iron availability (0 µM Fe) and extreme iron deficiency conditions (0 µM Fe + 200 µM Ferrozine) while overexpression line 2 showed higher iron concentrations.

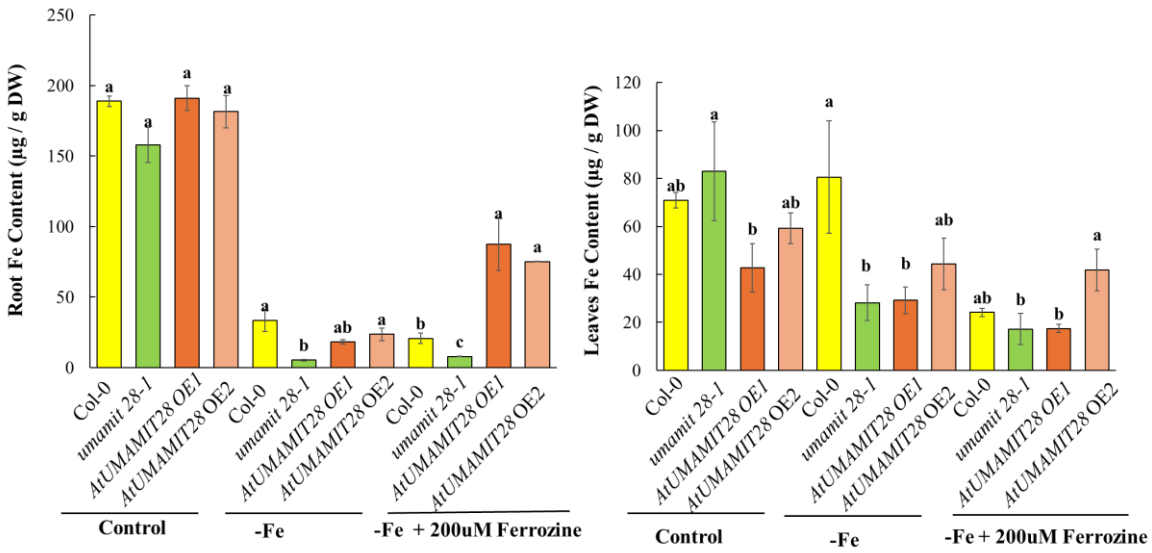

Figure 4.58. Leaf and root metal concentrations of *umamit28-1* and *AtUMAMIT28* overexpression lines under varied iron availability. Different letters indicate significant changes among treatments ($p<0.05$).

Metal content analyses of the plants grown under control conditions showed that *umamit28-1* and *umamit29-1* mutants accumulated higher levels of Fe, Mn, and Zn than the wild type in their seeds while no difference was observed for the overexpression lines. Interestingly lower Cu levels were observed in the seeds of *umamit28-1* and *umamit29-1* mutants and higher levels of Cu were observed for the *AtUMAMIT28* overexpression lines, indicating that AtUMAMIT28 may function in Cu deposition in the seeds (Figure 4.59).

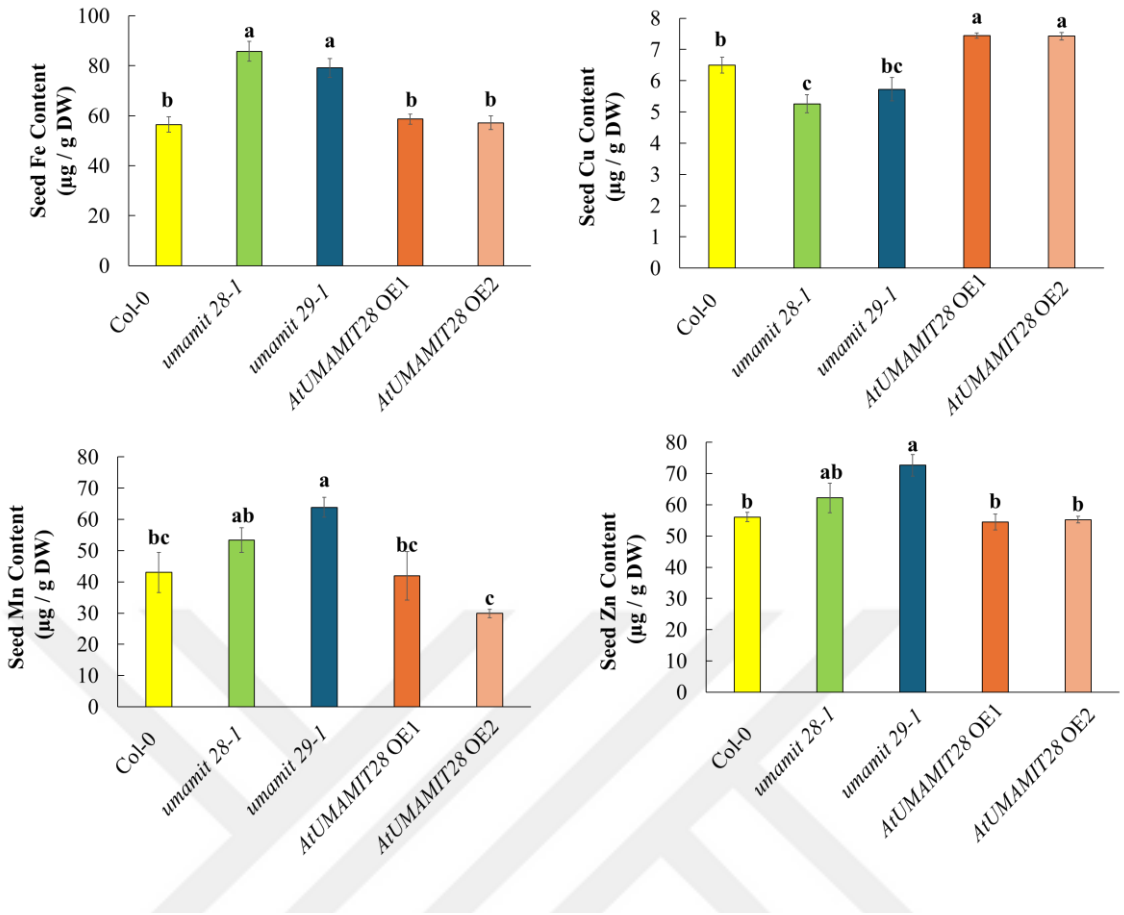

Figure 4.59. Seed metal concentrations of *umamit28-1* and *AtUMAMIT28* overexpression lines under varied iron availability. Different letters indicate significant changes among treatments ($p<0.05$).

4.4.6. Photosynthetic efficiency

The Fv/Fm ratio is a parameter commonly used in plant physiology, particularly in studies of photosynthesis. It represents the maximum quantum efficiency of Photosystem II (PSII) in dark-adapted conditions and is a useful indicator of the health and stress status of plants (Sommer et al., 2023). Prity et al. (2021) reported that the Fv/Fm ratio declined in sorghum when plants were treated with Fe deficiency. Therefore, to understand the direct effect of Fe deficiency on plant photosynthetic activity, the Fv/Fm ratio was measured from the plants treated with 4 days of Fe deficiency. *umamit28-1* mutants showed a significantly lower Fv/Fm ratio under control conditions (50 µM Fe) and iron-deficient conditions (0 µM Fe) compared to the wild type. Overexpression line 1 showed a similar Fv/Fm ratio to the wild type under control conditions while OE2 showed a slightly lower Fv/Fm ratio than the wild type. Under iron-deficient conditions, the Fv/Fm ratio of OE1 was similar to the wild-type and the mutant whereas OE2 showed a

significantly lower ratio than the other genotypes. Additionally, OE2 showed better photosynthetic efficiency in the FZN treatment (0 µM iron + 200 µM Ferrozine) than the rest of the genotypes (Figure 4.60).

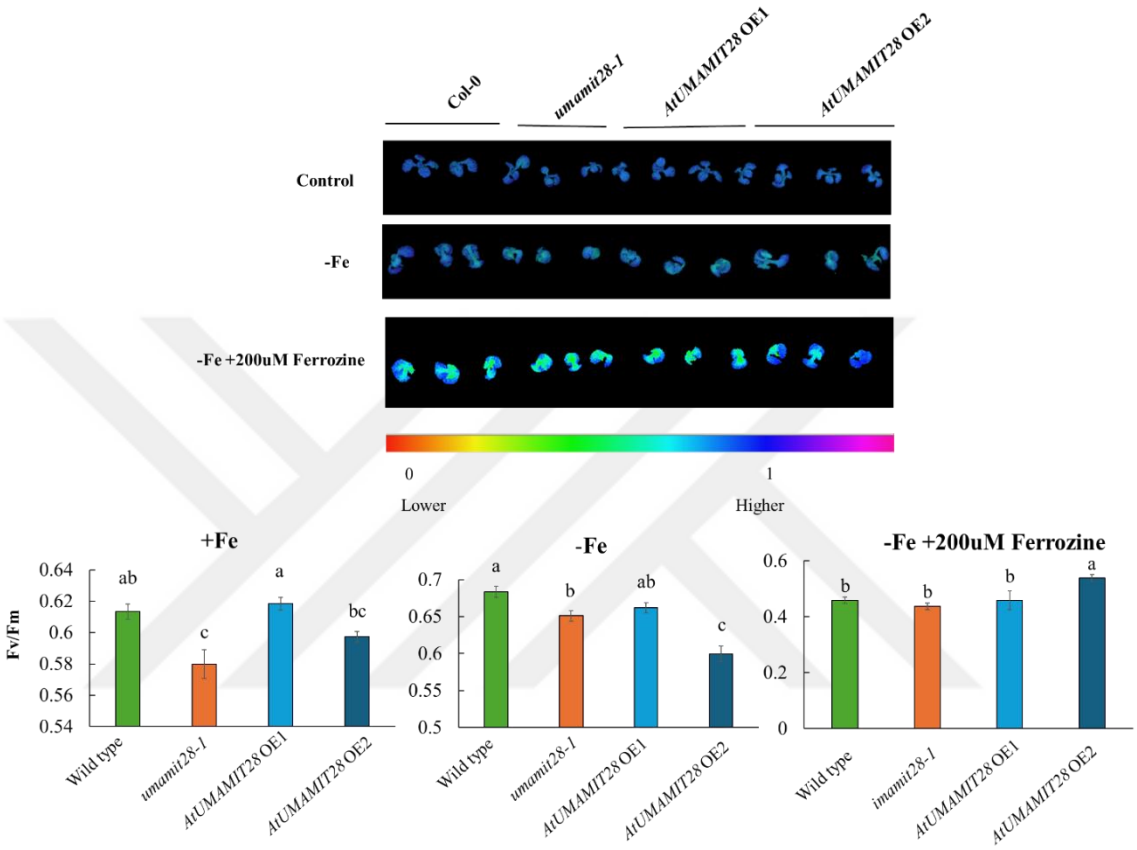

Figure 4.60. Photosynthetic efficiency by using PAM, fv/fm ratio after 4 days of stress. Different letters indicate significant changes among treatments ($p<0.05$).

4.7. Subcellular localization analyses of AtUMAMIT28

The subcellular localization analyses of AtUMAMIT28 by confocal microscopy showed that it is localized to the plasma membrane under iron-deficient conditions (Figure 4.61). Application of Fe deficiency did not affect the expression levels.

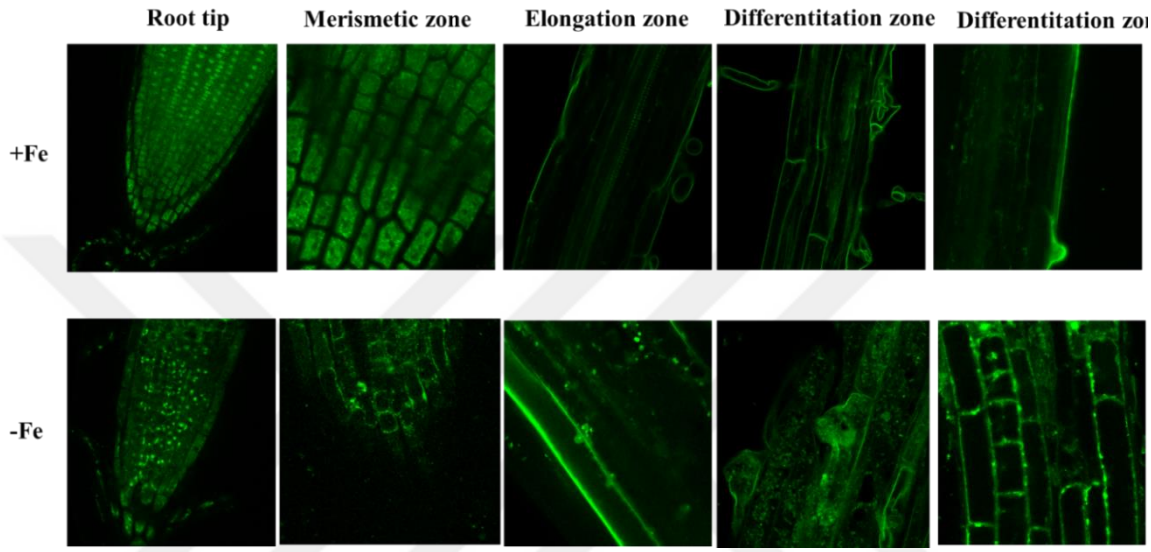

Figure 4.61. Subcellular localization of AtUMAMIT28 in *A. thaliana* roots under sufficient iron and deficient conditions.

4.4.8. Gene expression patterns of iron homeostasis genes

FIT is the major transcription factor which regulates the expression of many iron homeostasis genes (including *IRT1* and *FRO2*) under iron deficiency. *FIT* is upregulated by iron deficiency at the transcriptional level (Cui et al.,2018) . In the current study, gene expression analysis showed that *FIT* was upregulated in all lines including the Col-0, *umamit28-1*, *AtUMAMIT28* OE1 and *At*UMAMIT28 OE2 compared to the control condition under iron deficienct conditions. Compared to Col-0, the *umamit28-1* showed higher transcript levels of *FIT* while *AtUMAMIT28* OE1 and *AtUMAMIT28* OE2 lines showed lower expression levels of *FIT* under iron deficient conditions (Figure 4.62). IRT1 is divalent metal transporter known to involve in the direct uptake of Fe^{2+} at the root surface while FRO2 is involve in the iron reduction at the root surface (Connorton et al., 2017). Similar to *FIT* expression levels under iron deficient conditions, *FRO2* and *IRT1*

are upregulated in all tested lines. Compared to Col-0, the *umamit28-1* showed higher expression levels of *FRO2* and *IRT1* while *AtUMAMIT28* OE1 and *AtUMAMIT28* OE2 showed lower expression *FRO2* and *IRT1*. These results indicate that *AtUMAMIT28* may involve in iron homeostasis in plants.

4.4.9. Growth of mutants under high pH conditions

High pH-induced iron deficiency is one of the major problems for plants causing severe yield losses. Wild type and *umamait28-1* and *umamit29-1* mutants were grown under pH 6 and pH 8 on soil. Interestingly, mutants showed chlorosis and defective growth under alkaline soil conditions. Additionally, the FRO enzyme activities of the mutants were significantly higher in both growth conditions compared to the wild type, which indicates the involvement of UMAMIT28 and UMAMIT29 in iron homeostasis under alkaline conditions (Figure 4.63).

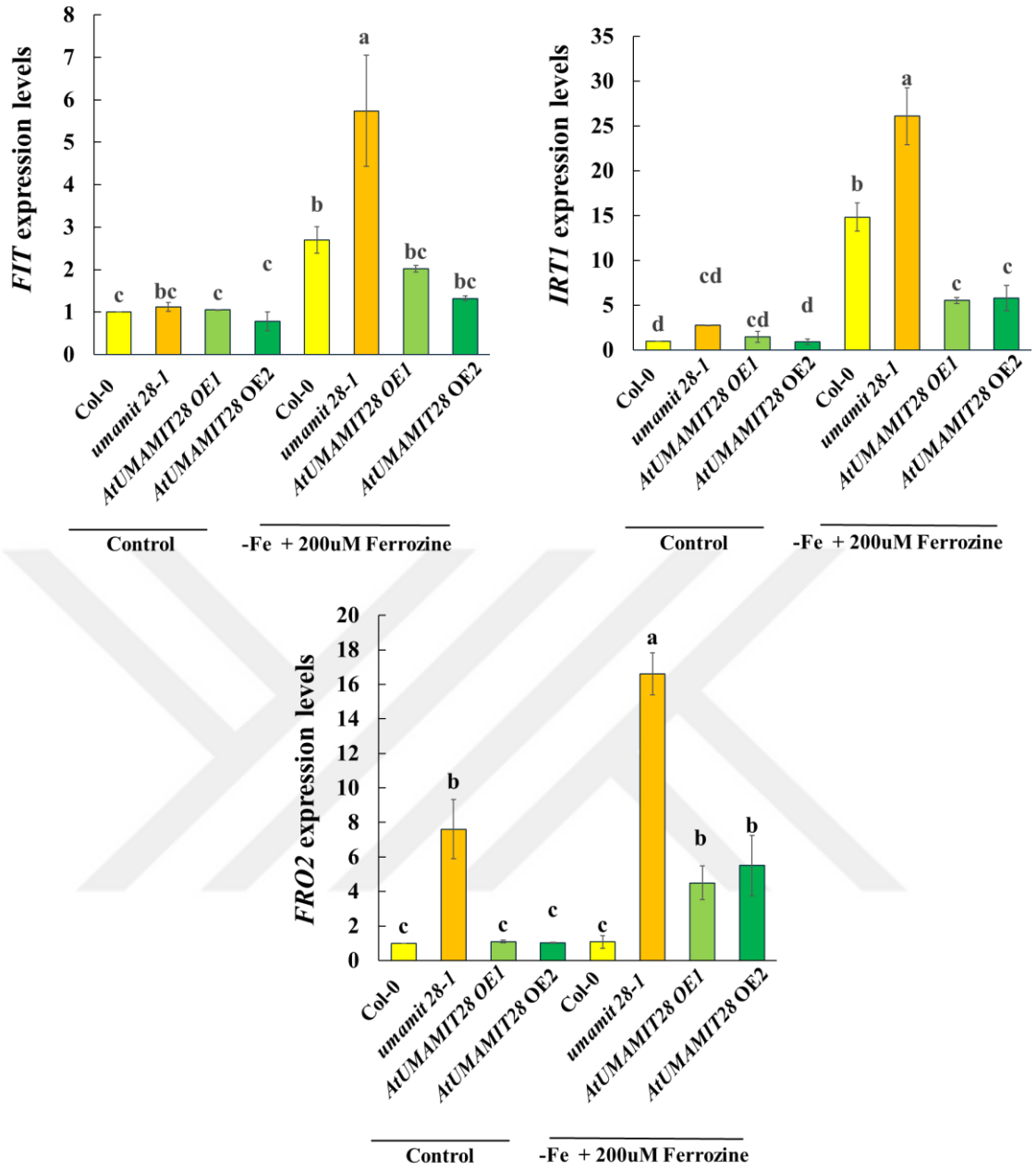

Figure 4.62. Gene expression levels of iron homeostasis genes in *umamit28-1* and *AtUMAMIT28* OE lines under control and iron-deficient conditions. Plants were grown on iron-sufficient media for 4 days and transferred and grown on either iron-sufficient or deficient media for the next 7 days. Different letters indicate significant changes among treatments ($p<0.05$).

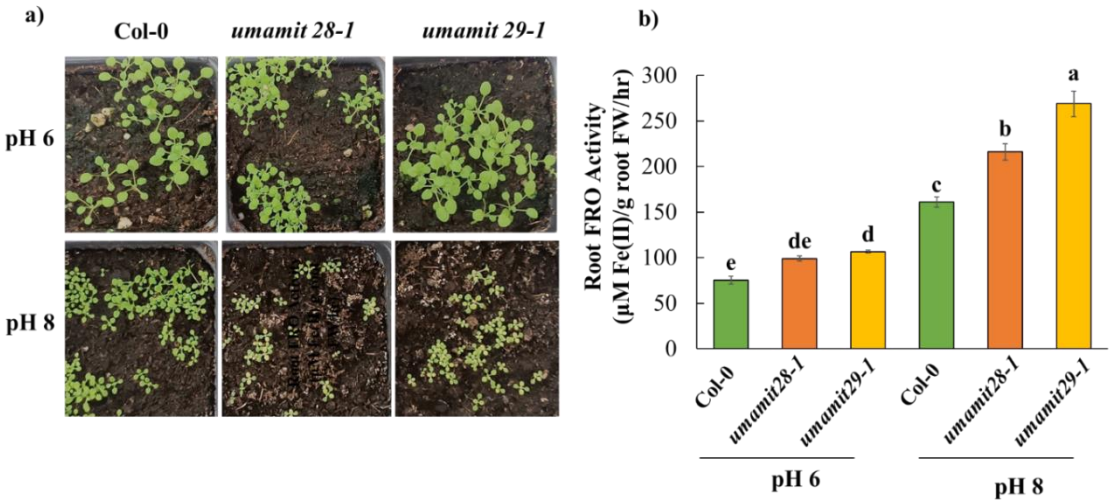

Figure 4.63. Physiological responses of *umamit28-1* and *umamit29-1* mutants to alkaline conditions. (**a**). Growth of *umamit28-1* and *umamit29-1* mutants under normal and alkaline soil conditions. (**b**). Root ferric chelate reductase activities of plants grown under normal and alkaline soil conditions. Different letters indicate significant changes among treatments ($p<0.05$).

4.4.10. Exogenously applied L-glutamine significantly affected the mutants defective in iron homeostasis

In plants, Fe must chelate with other compounds to facilitate its transport, as soluble Fe^{2+} is toxic to plant cells, while Fe^{3+} is immobile due to its poor solubility. Compounds such as citric acid, phenolics, nicotianamine (NA), and mugineic acids (MAs) play important roles in the translocation of Fe by chelating with iron within the plant (Kobayashi et al., 2019). Likewise these chelating compounds we hypothesized that L-glutamine can bind with iron, and it can be one of the possible forms of iron in the plant body. To test our hypothesis, we have exogenously applied L-glutamine in the media and grown the mutants defective in iron uptake (*irt1-2*), reduction (*fro2*), and translocation (*frd3-1*). Results showed that compared to the Col-0 wild type the growth of iron homeostasis defective mutants was singnificantly affected by the L-glutamine added treatments. Compared to the control treatments either iron sufficient or deficient in 10mM L-glutamine added treatments all mutants had shown shorter root lengths (Figure 4.64), higher FRO enzyme activities, and lower chlorophyll concentrations (Figure 4.65). These results indicate that iron may bind with L-glutamine *in vivo*, and plants are unable to

uptake the chelated iron when there is an excess amount of L-glutamine is available in the growth medium, thereby subjecting plants to iron deficiency stress.

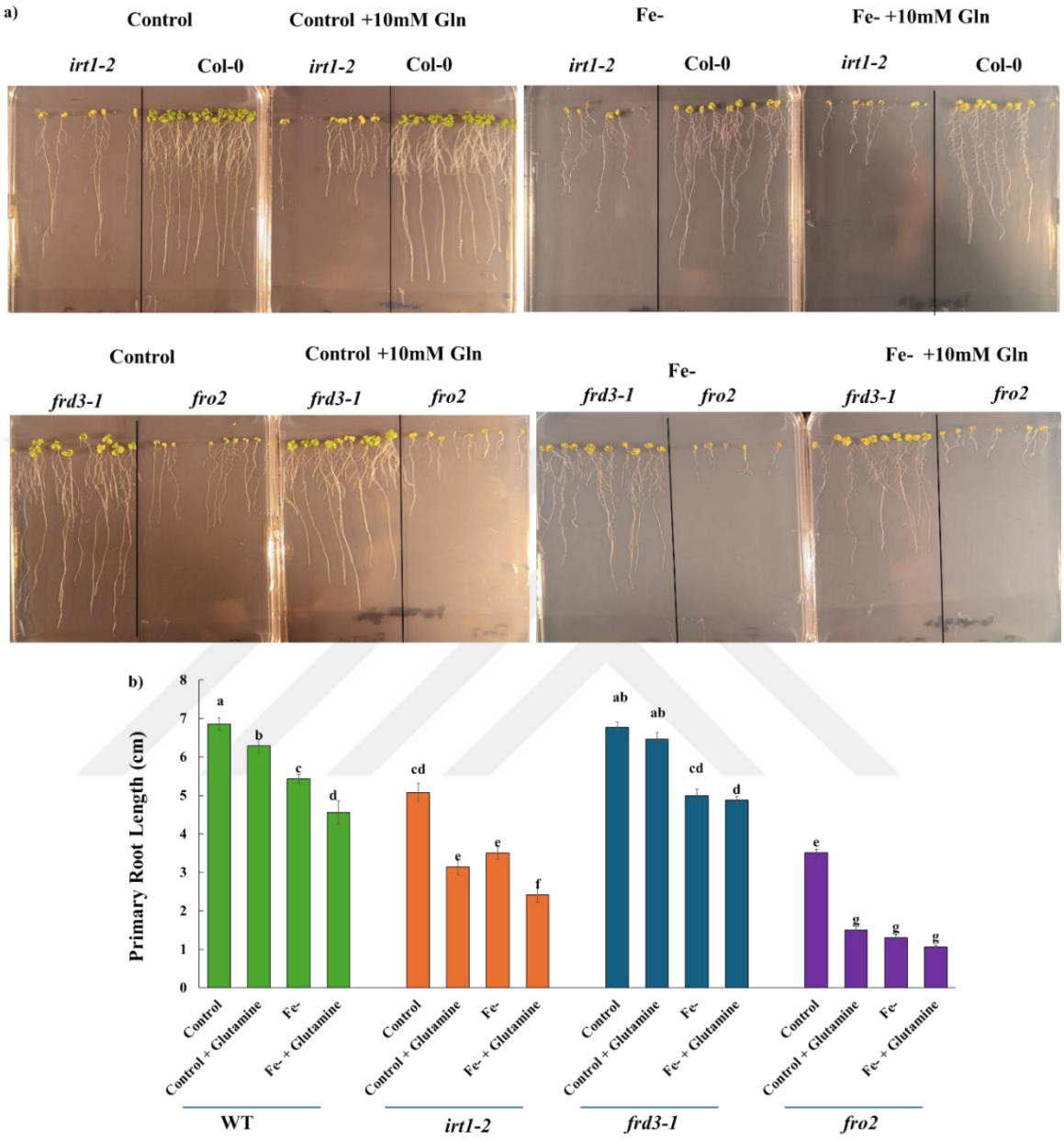

Figure 4.64. Physiological responses of the mutants defective in iron uptake and translocation in glutamine addition under iron deficiency. **a)** Phenotypic response of *frd3-1*, *fro*2, and *irt1-2* under different iron and glutamine (0 and 10 mM) concentrations. **b)** Root lengths of *frd3-1*, *fro2,* and *irt1-2* under different iron and glutamine (0 and 10 mM) concentrations. Different letters indicate significant changes among treatments ($p<0.05$).

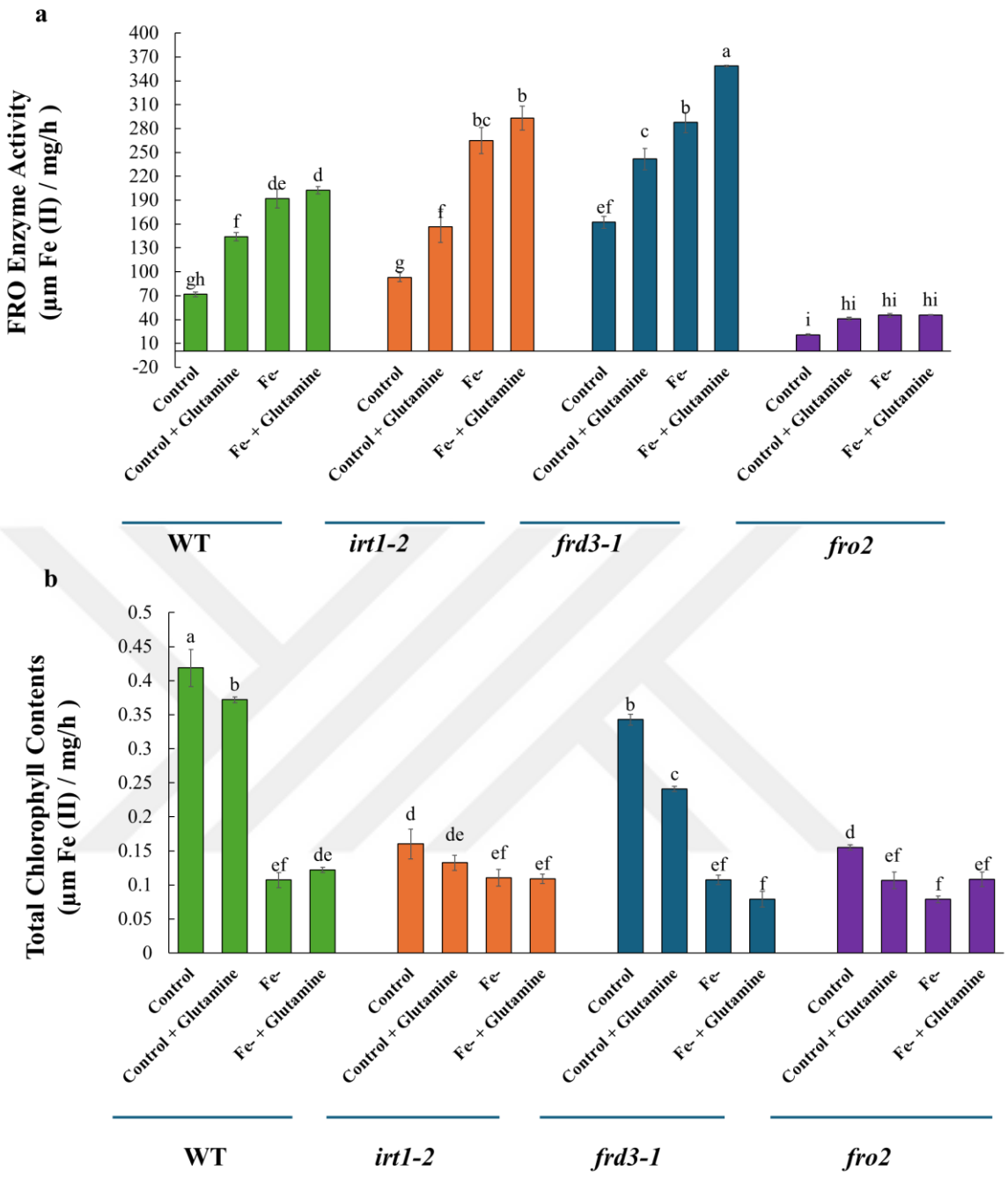

Figure 4.65. FRO activities and total chlorophyll contents of the mutants defective in iron uptake and translocation in glutamine addition under iron deficiency. **a)** Root FRO enzyme activities of *frd3-1*, *fro2,* and *irt1-2* under different iron and glutamine (0 and 10 mM) concentrations. **b)** Total chlorophyll contents of *frd3-1*, *fro2* and *irt1-2* under different iron and glutamine (0 and 10 mM) concentrations. Different letters indicate significant changes among treatments ($p<0.05$).

4.4.11. Yeast complementation assays

To express the *AtUMAMIT28* in the yeast-specific expression vector, site-directed mutagenesis was done to add the stop codon by the end of the *AtUMAMIT28* CDS region. After the site-directed mutagenesis reaction, Colony 4 was found as positive, and plasmid extraction was done from this colony. Next, the samples were sent for sequencing and results showed that the stop codon was successfully added to the CDS region of *AtUMAMIT28* in the *pDNOR207*:*AtUMAMIT28* plasmid (Figure 4.66).

Figure 4.66. Gel and sequencing results after site-directed mutagenesis to introduce stop codon for the yeast expression vectors. 10 µl of samples were separated on 1% agarose gel electrophoresis in 1 X TAE buffer for 40 minutes. M represents for 1 kb DNA ladder (Thermo Scientific). Numbers from C1-C5 show the colony numbers.

Then, *pDNOR207*:*AtUMAMIT28* with a stop codon was used in the LR reaction with *pDR195*. Gel results after colony PCR showed that all of the grown colonies contained the *AtUMAMIT28* CDS region (Figure 4.67).

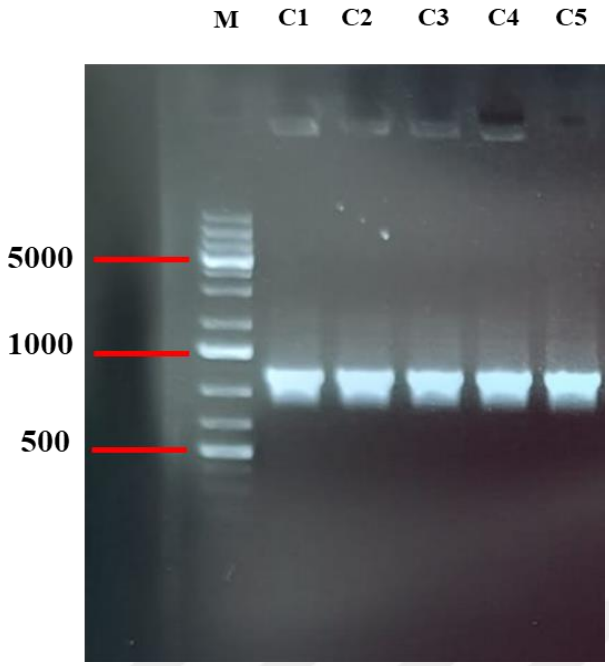

Figure 4.67. Colony PCR after transformation of the LR product of *pDNOR207:AtUMAMIT28* CDS region with a stop codon in *E. coli*. 10 µl of samples were separated on 1% agarose gel electrophoresis in 1 X TAE buffer for 40 minutes. M represents for 1 kb DNA ladder (Thermo Scientific). Numbers from C1-C5 show the colony numbers.

Yeast strains were transformed with *pDNOR207*:*AtUMAMIT28* by lithium acetate method as described in the methods part of the thesis. Yeast transformation was confirmed by auxotrophic selection and gel results of colony PCR of positive colonies are shown in Figure 4.68. Yeast growth assays of *Δfet3fet4*, *Δzrt1zrt2*, and *Δsmf1* showed that the presence of *AtUMAMIT28* either in the wild type or in the mutant yeast strains makes the yeast strains sensitive against respective metal deficiencies (Figure 4.69-4.71), which may be related to higher affinity of any other metals by *AtUMAMIT28,* or it is acting as an efflux transporter. When the yeast mutant *Δfet3fet4* (defective in iron uptake) and wild type (BY4741) cells were transformed with *pDR195*:*AtUMAMIT28*, they showed slower growth, which indicates either this gene is an efflux transporter, or it inhibits the iron uptake by taking up any other metals (Figure 4.69).

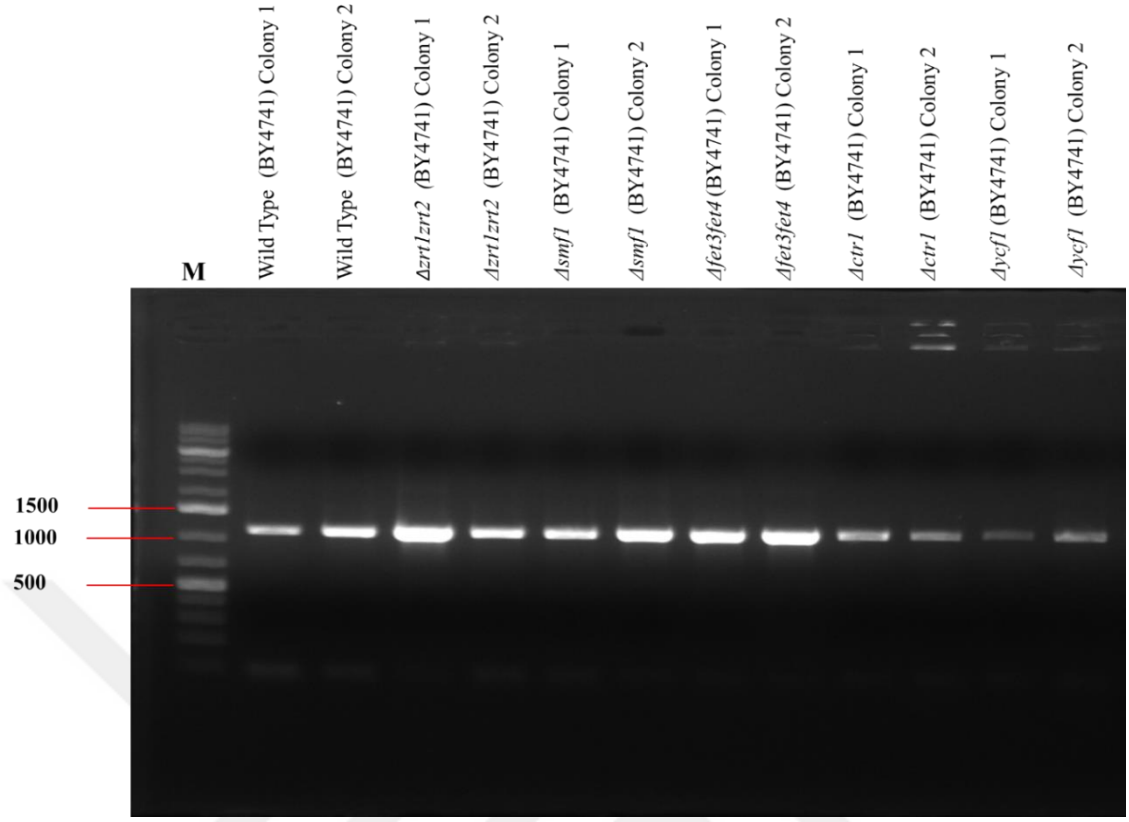

Figure 4.68. Colony PCR of different yeast strains transformed with *pDR195:AtUMAMIT28* plasmid.

Interestingly, *AtUMAMIT28* successfully complemented the *Δctr1* mutant which is defective in Cu uptake (Figure 4.72). Metal content analyses of wild-type yeast and *Δctr1* transformed with *AtUMAMIT28* showed higher Cu levels, which cleared the role of this transporter in Cu uptake. Additionally, higher iron levels were observed in wild-type yeast transformed with *AtUMAMIT28,* which indicates its role in iron homeostasis. Moreover, the highest iron content was observed in the *Δctr1* mutant, which explains the interplay between iron and copper in yeast. Furthermore, lower zinc and manganese concentrations were found in the *Δctr1* yeast cells (Figure 4.72). Liquid growth assays of *Δctr1* under varied Cu concentrations showed that *AtUMAMIT28* fully complemented the *Δctr1* growth under both Cu sufficient and deficient conditions (Figure 4.73). Similar results were observed in the case of yeast dry weights, where higher dry weights were observed for the *Δctr1* strain complemented with *AtUMAMIT28* under Cu-sufficient conditions (Figure 4.74).

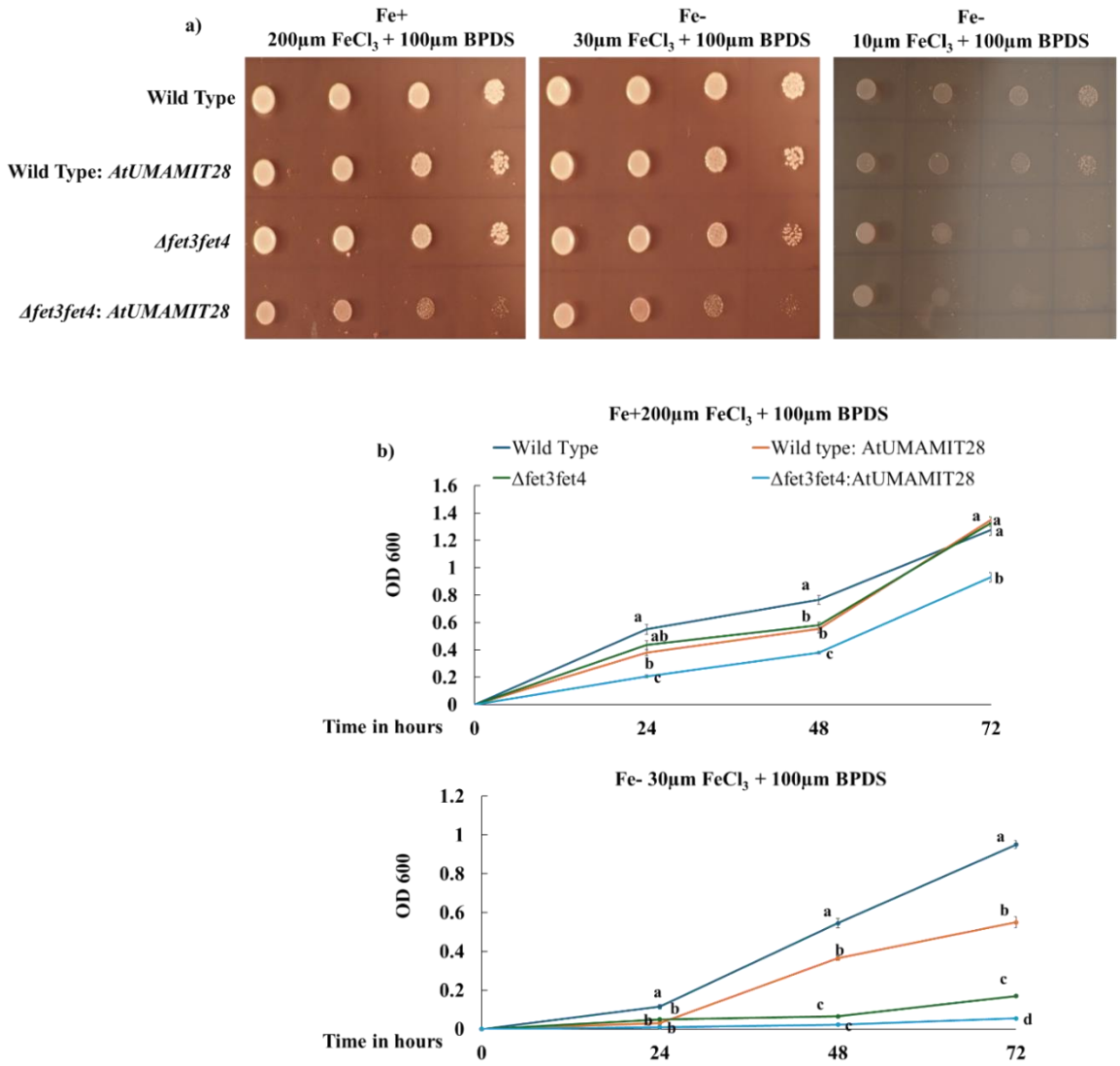

Figure 4.69. *Δfet3fet4* complementation assay. **a)** The growth assay of the wild type and *Δfet3fet4* yeast strains (transformed with or without *AtUMAMIT28*) in varied Fe concentrations with Fe chelator BPDS on solid media. **b)** The growth assay of the wild type and *Δfet3fet4* yeast strains (transformed with or without *AtUMAMIT28*) in varied Fe concentrations with Fe chelator BPDS on liquid media. Different letters indicate significant changes among treatments ($p<0.05$).

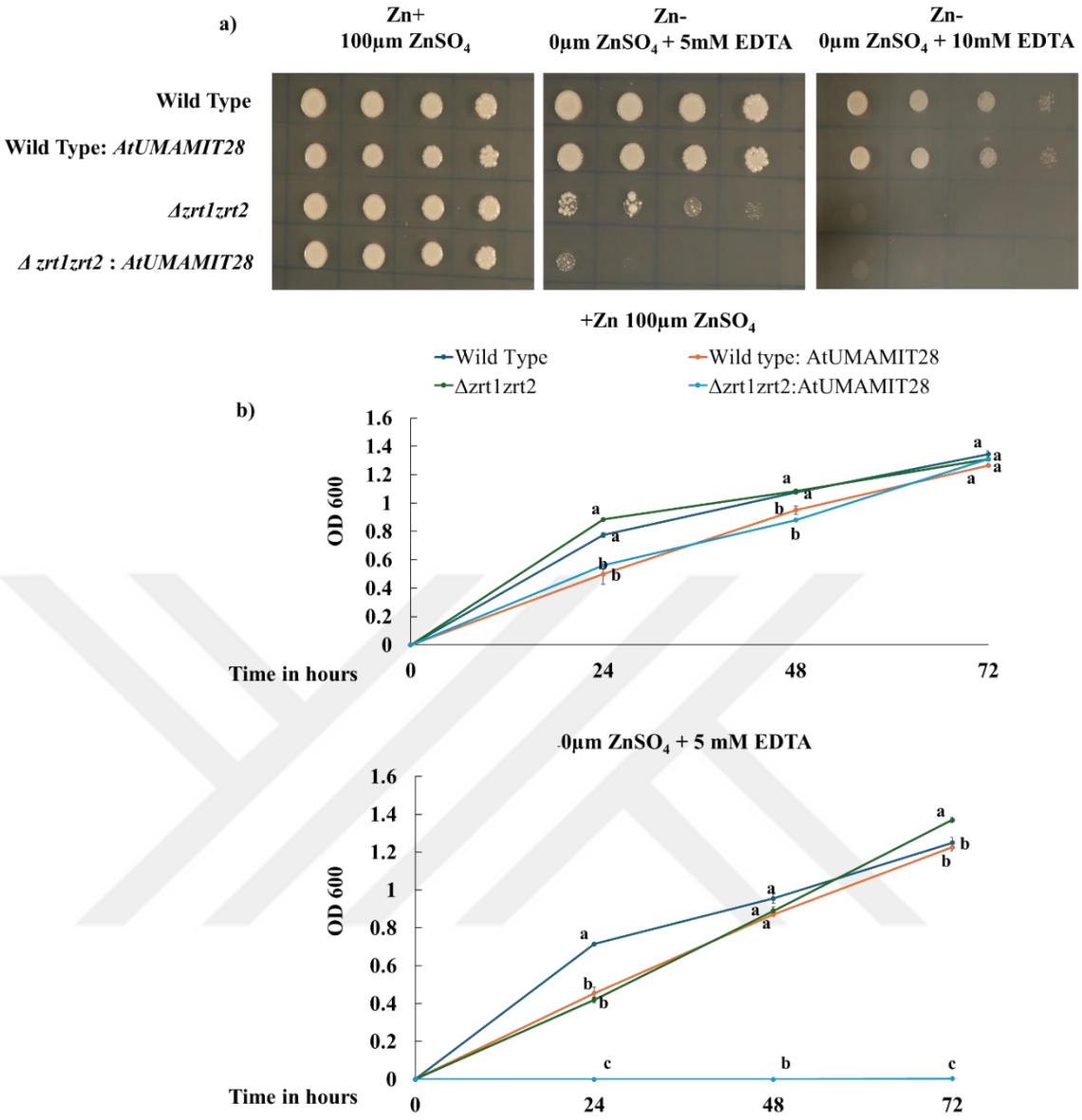

Figure 4.70. *Δzrt1zrt2* complementation assay. **a)** The growth assay of the wild type and *Δzrt1zrt2* yeast strains (transformed with or without *AtUMAMIT28*) in varied Zn concentrations with or without Zn chelator EDTA on solid media. **b)** The growth assay of the wild type and *Δzrt1zrt2* yeast strains (transformed with or without *AtUMAMIT28*) in varied Zn concentrations with Zn chelator EDTA on liquid media. Different letters indicate significant changes among treatments ($p<0.05$).

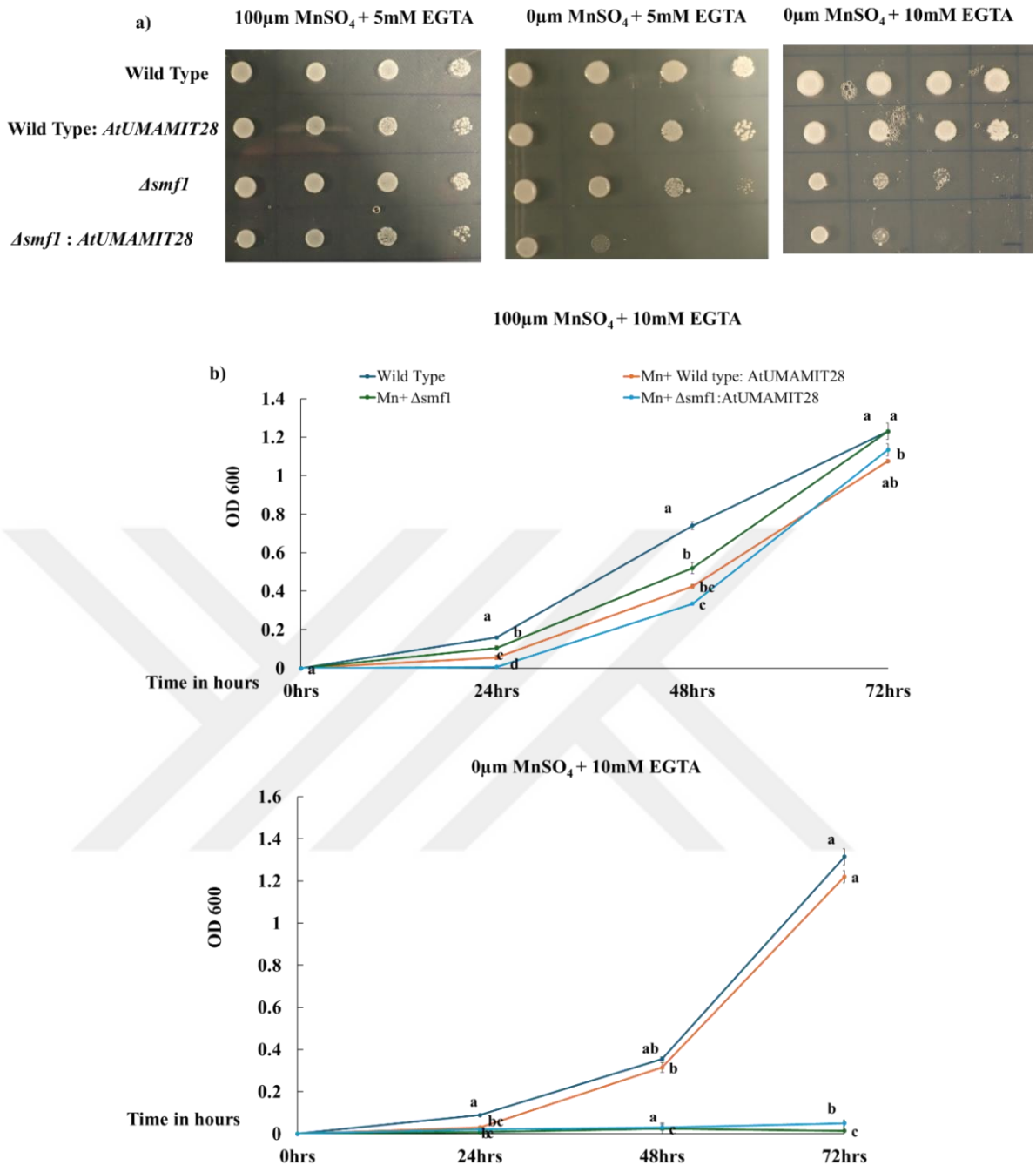

Figure 4.71. *Δsmf1* complementation assay. **a)** The growth assay of the wild type and *Δsmf1* yeast strains (transformed with or without *AtUMAMIT28*) in varied Mn concentrations with or without Mn chelator EGTA on solid media. **b)** The growth assay of the wild type and *Δsmf1* yeast strains (transformed with or without *AtUMAMIT28*) in varied Mn concentrations with Mn chelator EGTA on liquid media. Different letters indicate significant changes among treatments ($p<0.05$).

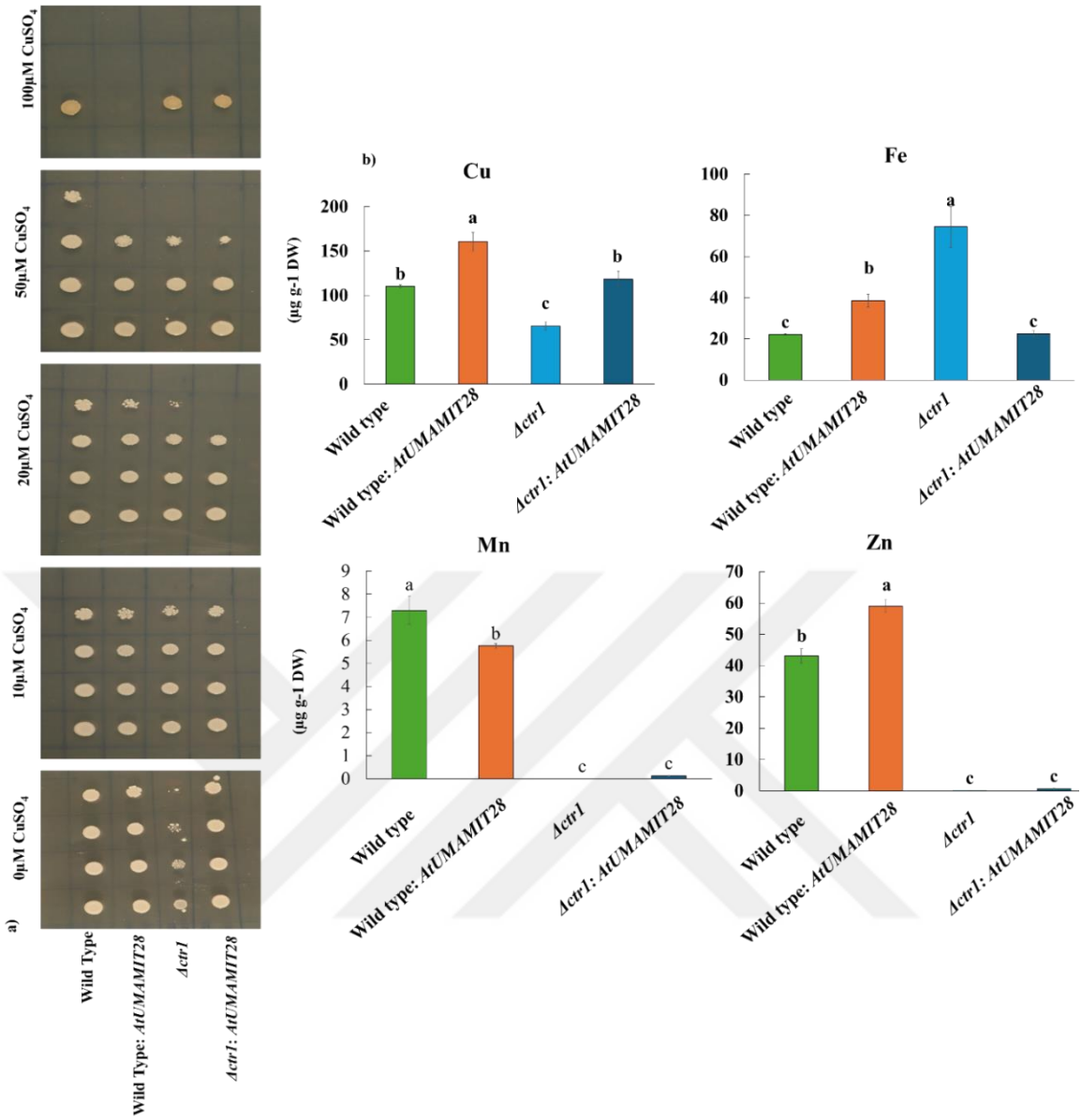

Figure 4.72. *Δctr1*complementation assay. **a)** The growth assay of the wild type and *Δctr1* yeast strains (transformed with or without *AtUMAMIT28*) in varied Cu concentrations on solid media. **b)** The growth assay of the wild type and *Δctr1* yeast strains (transformed with or without *AtUMAMIT28*) in yeast synthetic media without uracil, supplemented with 10µM $CuSO_4$, for 24 hours. Different letters indicate significant changes among treatments ($p<0.05$).

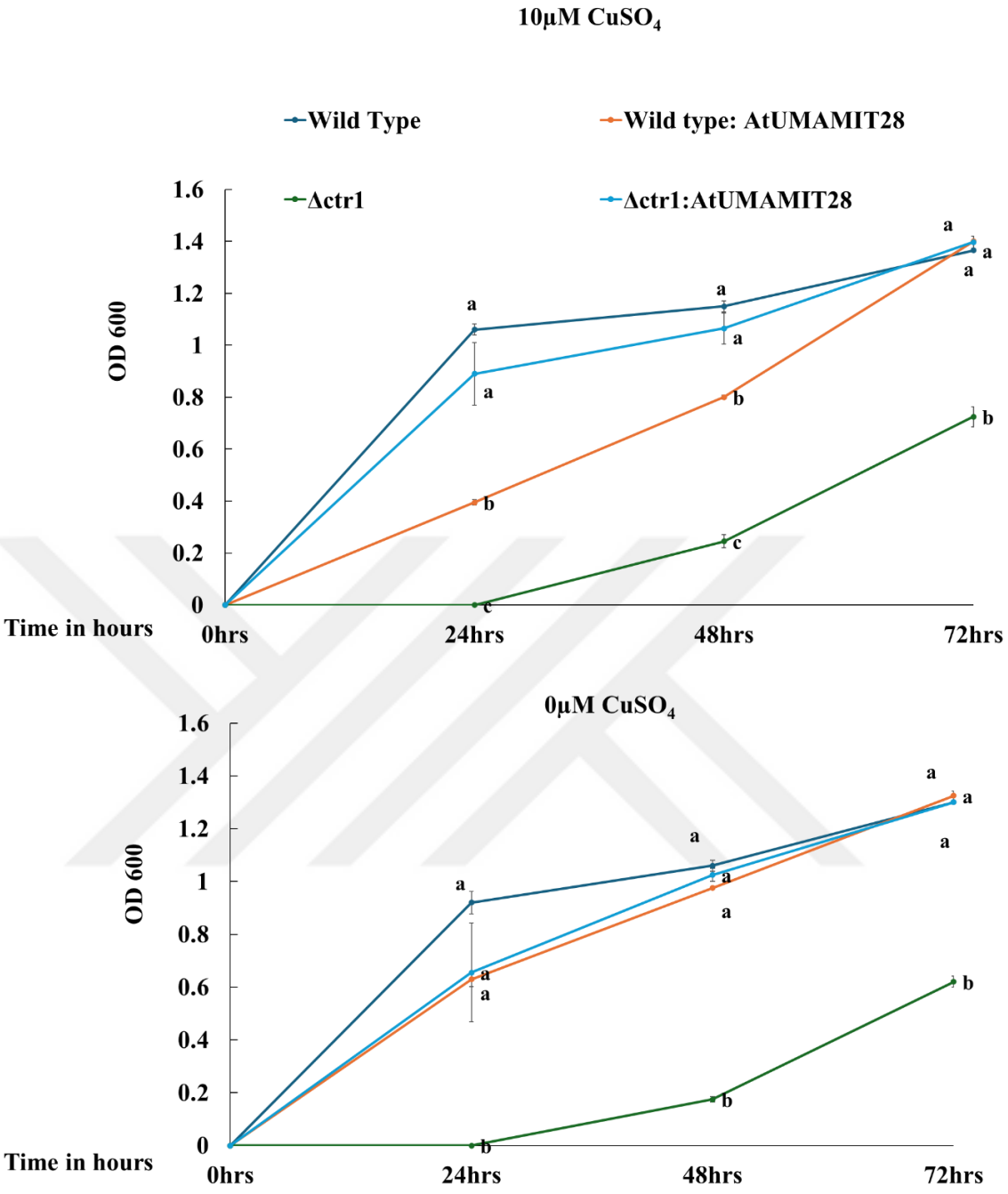

Figure 4.73. Growth rates of wild-type yeast and *Δctr1* mutants, either transformed with *AtUMAMIT28* CDS or with the empty vector *GUS*. Yeast strains were grown in yeast synthetic media without uracil, supplemented with 0 µM or 10µM $CuSO_4$ for 72 hours. Different letters indicate significant changes among treatments ($p<0.05$).

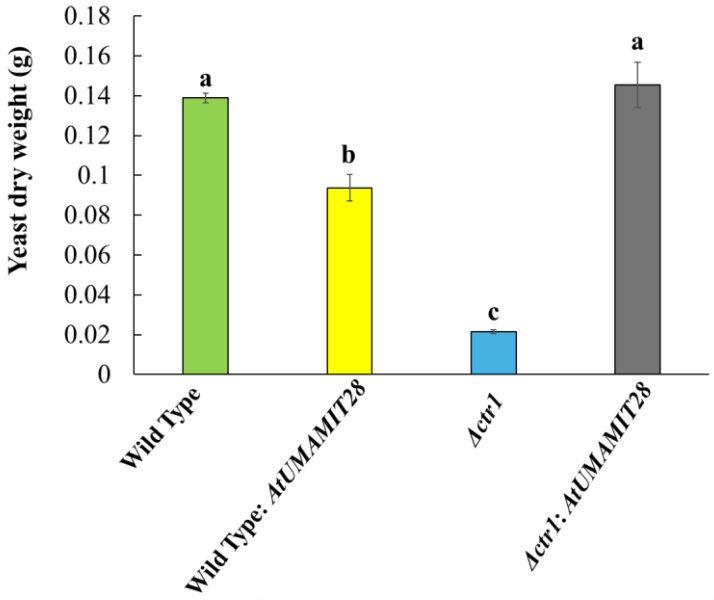

Figure 4.74. Dry weights of wild-type yeast and *Δctr1* mutants, either transformed with *AtUMAMIT28* CDS or with the empty vector *GUS*. The yeast strains were grown in yeast synthetic media without uracil, supplemented with 10 µM $CuSO_4$ for 24 hours. Different letters indicate significant changes among treatments ($p<0.05$).

4.4.12. Yeast complementation assay for Cd resistance or sensitivity in yeast

The wild type, or *Δycf1* yeast strains transformed with At*UMAMIT28* showed slower growth and lower OD values under 20 µM $CdCl_2$ while no differences were observed for the different strains under control conditions (0 µM $CdCl_2$) (Figure 4.75). Metal content analyses showed that *Δycf1* had shown higher Cd levels than the wild type, while the *Δycf1* mutant transformed with *pDR195:AtUMAMIT28* had shown an enhanced Cd uptake.While on the other hand compared to the *Δycf1* the wild type yeast transformed with the *pDR195:AtUMAMIT28* had shown no significant difference in Cd levels compared to the wild type transformed with *pDR195:GUS* (Figure 4.76).

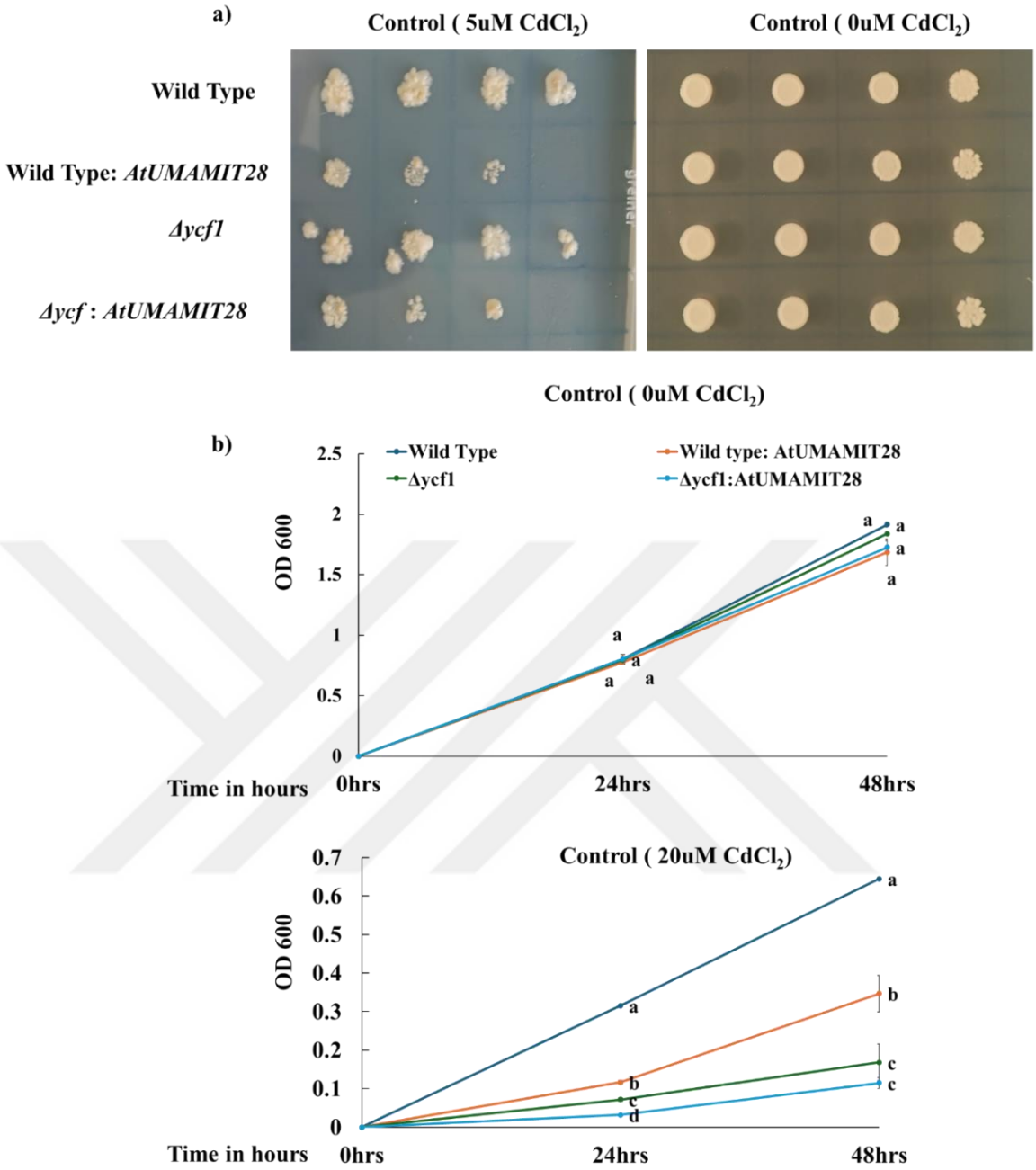

Figure 4.75. *Δycf1* complementation assay. **(a)** Wild type and *Δycf1* yeast strains transformed with *pDR195*:*AtUMAMIT28* or *pDR195:GUS* were grown in -SD media for 48 hours. (**Note**) Yeast on solid media was kept grown for one week in case of Cd stress media since no colonies were observed in the first 2 days **(b)** Wild type and *Δycf1* yeast strains transformed with *pDR195*:*AtUMAMIT28* or *pDR195*:*GUS* were grown in liquid media (-SD media + 20 µM $CdCl_2$ for 48 hours). OD values were recorded every 24 hours. Different letters indicate significant changes among treatments ($p<0.05$).

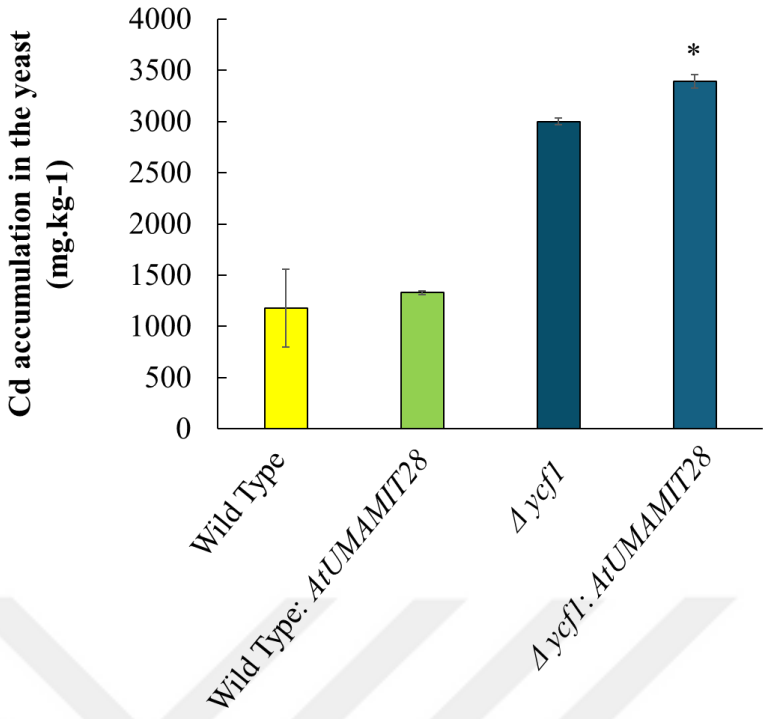

Figure 4.76. Cd content in transgenic yeast and non-transgenic yeast strains. Yeast strains were grown in -SD media + 20 µM $CdCl_2$ for 48 hours and were collected for the ICP-MS analyses.* indicates the significant change compared to the *Δycf1* ($p < 0.05$, Student's t-test)

4.4.13. *AtUMAMIT28* is involved in copper homeostasis in *Arabidopsis thaliana*

Under normal conditions, *umamit28-1* and *AtUMAMIT28* OE lines showed root lengths similar to the wild type. When grown under copper deficiency, Col-0, and *umamit28-1* roots became significantly shorter. Moreover, *umamit28-1* showed shorter root lengths than the wild type while both of the *AtUMAMIT28* OE lines had longer root lengths (Figure 4.77a and c). Additionally, Cu deficiency significantly affected the chlorophyll concentrations in all tested genotypes (Figure 4.77b). *umamit28-1* showed lower chlorophyll levels than the wild type and overexpression lines under Cu deficiency.

AtUMAMIT28 overexpression lines showed higher Cu concentrations in the roots than the wild type and *umamit28-1* mutants under control conditions while *umamit28-1* mutants had lower levels compared to the wild type under Cu deficient conditions. Overall, Cu content in overexpression lines remained higher in both control and Cu-deficient conditions. Interestingly, no significant differences were found for the Cu

concentrations in the leaves of *umamit28-1* mutants compared to the wild type under control conditions while the mutants showed lower levels under Cu deficiency conditions. Meanwhile, overexpression lines showed higher Cu concentrations in the leaves in both conditions (Figure 4.78.). These results indicate that the mutants are unable to uptake or translocate sufficient Cu compared to the wild type and overexpression lines take up more Cu than the wild type under Cu-deficient conditions. These results indicate the role of *AtUMAMIT28* in copper homeostasis in plants.

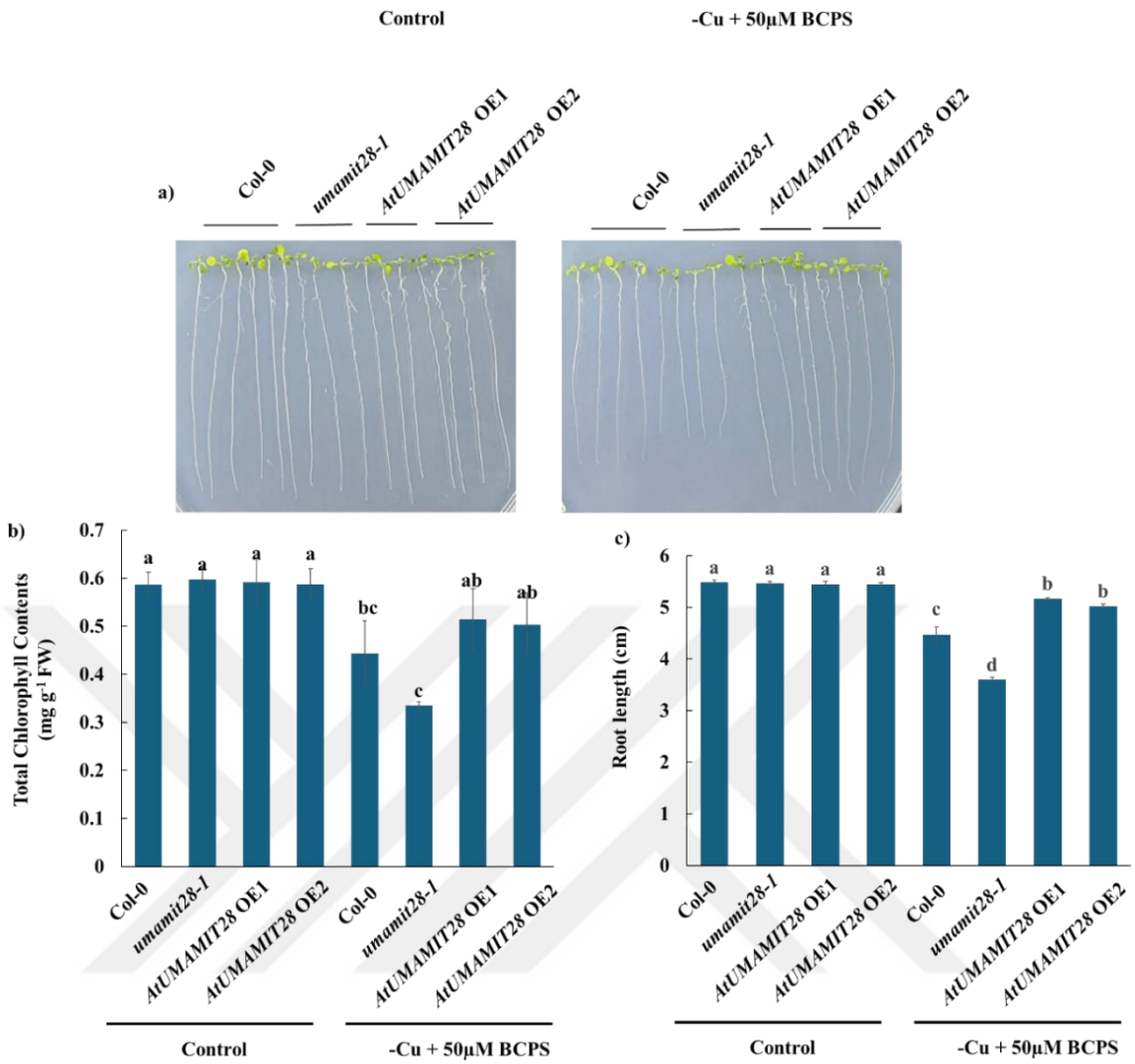

Figure 4.77. Physiological responses of *umamit28-1* and *AtUMAMIT28* OE lines under Cu deficiency. **(a)** Pictures of plants grown under + Cu and - Cu conditions. Plants were grown on control media for 4 days and transferred and grown on + Cu (Control) or - Cu conditions for the next 6 days. **(b)** Total chlorophyll contents of wild type, *umamit28-1* and *AtUMAMIT28* overexpression lines (OE1 and OE2) grown under + Cu and - Cu conditions. **(c)** Root lengths of wild type, *umamit28-1* and *AtUMAMIT28* overexpression lines (OE1 and OE2) grown under + Cu and - Cu conditions. Different letters indicate significant changes among treatments ($p<0.05$).

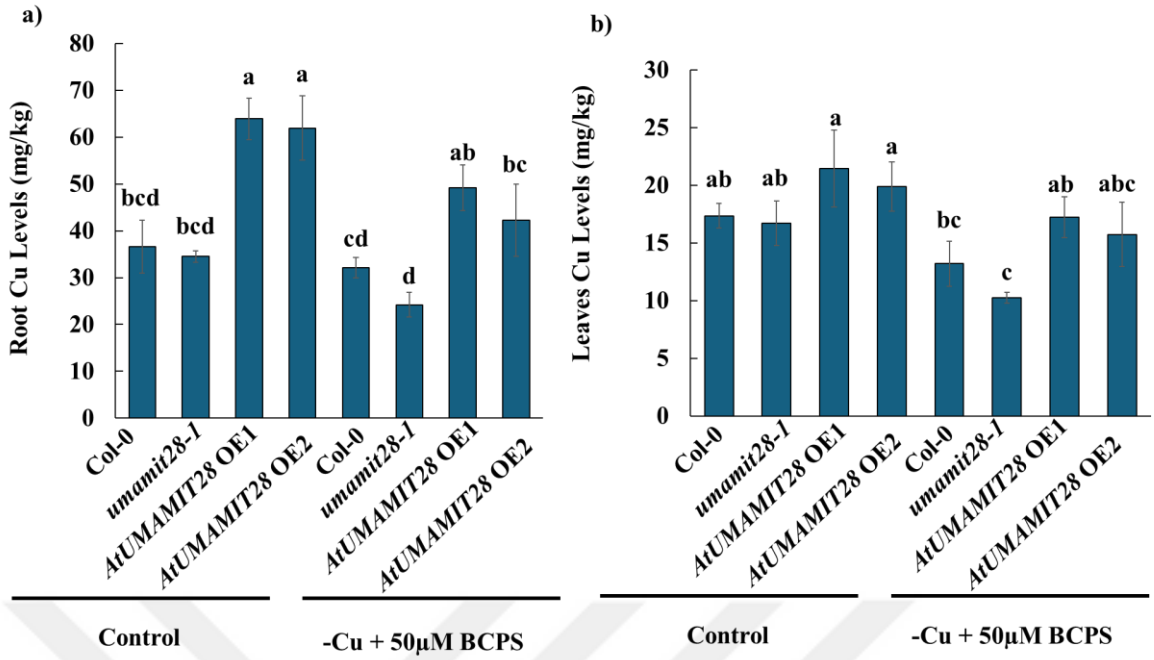

Figure 4.78. Copper levels of *umamit28-1,* and *AtUMAMIT28* OE lines under Cu deficiency. Plants were grown on control media for 4 days and transferred and grown on + Cu (Control) or - Cu conditions for the next 6 days. Different letters indicate significant changes among treatments ($p<0.05$).

Next, the expressions of Cu homeostasis genes were determined in *umamit28-1* and *AtUMAMIT28* OE lines under control and Cu deficiency. The expression of *CITF1* is known to increase under Cu deficiency and its expression levels are considered as a marker for the plants feeling the Cu deficiency (Chia et al., 2023). Under Cu-sufficient conditions, *umamit28-1*, *AtUMAMIT28* OE lines, and wild type showed similar *CITF1* expressions (**Figure 4.79**). *CITF1* expression increased significantly in wild type and *umamit28-1* under Cu deficiency and this increase was significantly higher in *umamit28-1* than in wild type. Similar patterns were observed for the genes involved in the copper uptake and reduction (*COPT1*, *COPT2,* and *FRO5*). These results suggest an important role of *UMAMIT28* in Cu homeostasis, which will further be clear after metal content analyses.

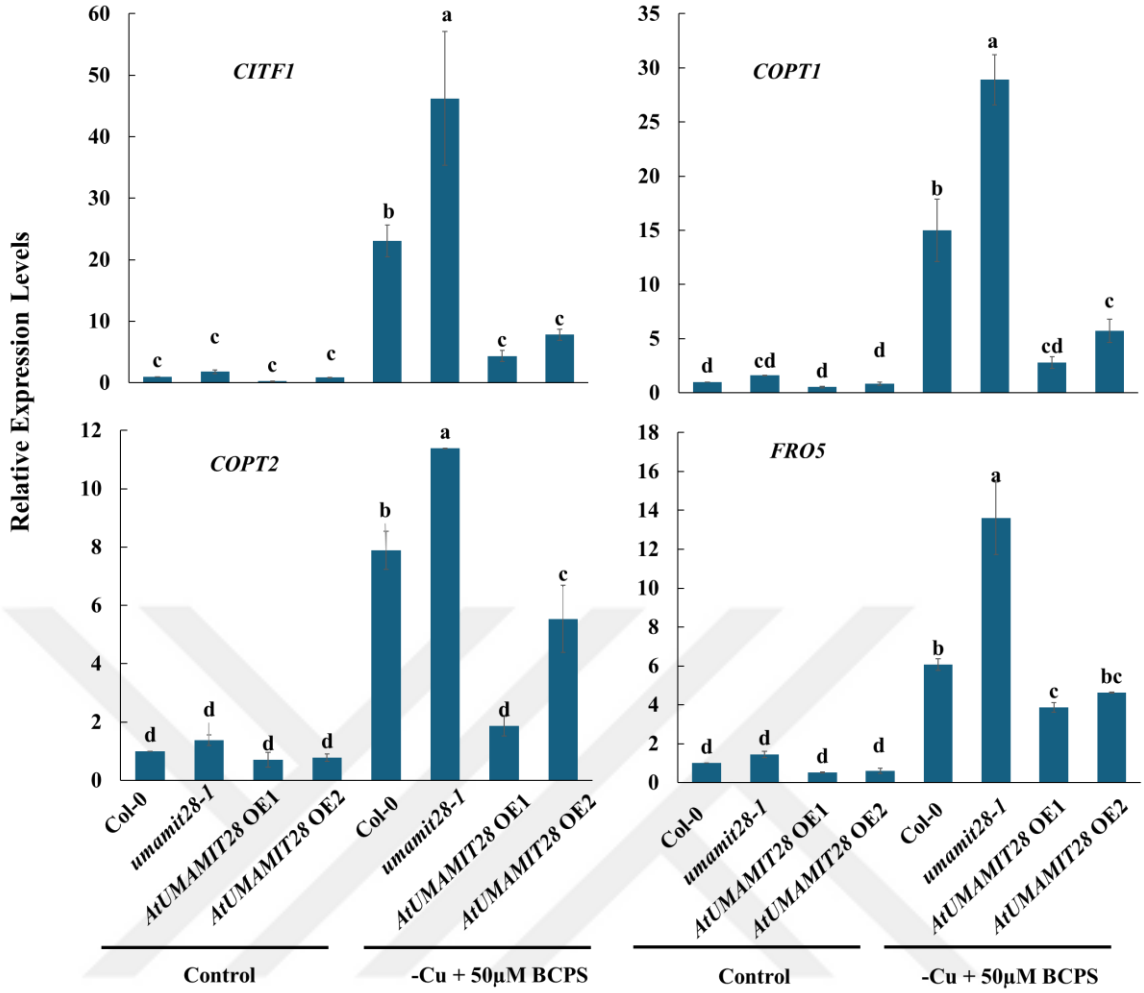

Figure 4.79. Relative expression levels of copper homeostasis and Cu deficiency marker genes against the Wild Type (Col-0) grown under Control (+Cu) conditions. Different letters indicate significant changes among treatments ($p<0.05$).

CHAPTER V

DISCUSSION

Part 1: Effect of iron fertilization on soybean cultivars differing in IDC tolerance

Every year iron deficiency induced by alkalinity exerts a substantial negative impact on soybeans, resulting in significant annual yield losses (Vasconcelos et al. 2014). Iron chelates are applied to overcome the nutritional and yield losses triggered by alkalinity-induced IDC in different crop species. Several studies are present on the optimization of iron fertilizer dosages to correct IDC in soybeans while limited research has been done on the integration of genotypic response to different chelate dosages. This study overwhelms the integration of genetic and agronomic approaches for iron biofortification in soybeans grown on calcareous soils. Nevertheless, it is noteworthy that not all soybean cultivars possess equivalent abilities to efficiently assimilate externally supplied iron. Indeed, discernible genetic variances exist in their utilization of such resources. In the current study, as expected, high pH negatively affected the plant growth attributes in all cultivars while the deleterious effects of high pH-induced iron deficiency were alleviated more efficiently in tolerant cultivars than the sensitive ones with the application of Fe-EDDHA (Figure 4.1). Studies on IDC-alleviation of soybean cultivars by Fe fertilization showed that Fe chelate application from the soil, or leaves can improve the chlorophyll content when plants are grown on calcareous soils (Liesch et al., 2011; Kaiser et al., 2014). Among different sources of iron, Fe-EDDHA was found to be the most effective in alleviating the symptoms of iron deficiency in soybean (Gamble et al., 2014; Bin et al., 2016; Goos., 2021). Notably, this improvement was more significant in soybean cultivars that are more prone to iron deficiency (Wiersma, 2007; Han et al., 2022). These observations can be related to the higher iron levels in the leaves of IDC-tolerant cultivars compared to the sensitive ones. No change or a slight decrease in the photosynthesis rates of tolerant soybean cultivars under high pH is also observed in other studies of soybean (Waters et al., 2018), groundnut (Pattanashetti et al., 2018), potato (Challam et al., 2021), and cowpea (Angira et al., 2022), suggesting the effects of high soil pH on decreased photosynthesis rates is a universal response in plants. The addition of Fe chelates from the soil increased the photosynthesis rates in tolerant cultivars, while no significant change was observed in sensitive cultivars (Figure 4.1 c). Similar results were reported

in sugar beet where iron resupply under Fe deficiency conditions increased the photosynthetic rate (Larbi et al., 2010). It was shown that Fe, Zn, and Mn deficiencies cause drastic effects on the photosynthetic pigment accumulation in the leaves (Roosta et al., 2018). Similar to our observations, divalent metal accumulation also declines in the leaves when grown under high soil pH as the uptake of divalent metals declines with increasing soil pH (Payne et al., 1986). We showed that the leaf Fe content increases following Fe fertilization (Figure 4. 4 a). But even the highest dose of Fe-EDDHA supplementation was not enough to recover the sensitive genotypes back to the control condition. Our observations indicate that the efficiency of iron uptake mechanisms in the tolerant cultivars can be related to the higher Fe contents in the leaves of tolerant cultivars than the sensitive ones.

We observed that the root lengths were increased under high soil pH, which can be related to nutrient foraging as high pH causes iron deficiency. Moreover, Fe-EDDHA supplementation increased the root lengths of IDC-tolerant soybean cultivars while decreasing the root lengths of IDC-sensitive soybean cultivars (Figure 4.2 a). Like our observations, Duan et al. (2023) reported that the *Arabidopsis thaliana* seedlings developed longer primary roots and more lateral roots in neutral and slightly alkaline pH (7.0−8.0) than did the seedlings grown under pH 5.8. In contrast to our results, Robles-Aguilar et al. (2019) showed smaller roots with a reduction in lateral root development in lupin plants under high pH conditions. These discrepancies can be related to the growth of nature and soil requirements of each species as different plant species have different soil quality requirements.

In the current study, all cultivars displayed an increase in FCR activity in response to low iron conditions. However, tolerant cultivars, Arısoy and SA-88, demonstrated a substantial reduction in reductase activity even at minimal iron dosages (Fe-EDDHA 12.5 mg/kg). In contrast, sensitive cultivars, Atakişi and Nova, maintained elevated reductase activities, necessitating higher iron dosages to mitigate iron deficiency symptoms (Figure 4.2 b). Since FCR is the rate-limiting enzyme of Fe uptake from the rhizosphere (Satbhai et al., 2017) and its activity increases under Fe deficiency (Robinson et al., 1999), our observations suggest that higher FCR activities of IDC-sensitive cultivars might be related to limited Fe uptake from the rhizosphere. This observation is supported by a previous study in soybean where the overexpression of *Arabidopsis FERRIC CHELATE*

REDUCTASE2 gene (*FRO2*) increased the Fe accumulation in roots and shoots only when there was enough supplementation of Fe^{3+}-EDDHA (Vasconcelos et al., 2006). Therefore, our results suggest the existence of efficient iron uptake mechanisms in IDC-tolerant soybean cultivars that can easily alter their root morphologies to uptake even the low concentrations of Fe supplementation under low pH conditions. This remarkable adaptation strategy in the roots is also seen under different abiotic stress conditions, such as drought (Ranjan et al., 2022), indicating the essence of the root system in detecting and adapting to changing soil conditions. We showed that the root Fe content increases in parallel to an increase in the Fe fertilizer application and IDC-tolerant cultivars are more efficient in Fe uptake (Figure 4.3 a). A similar trend is observed in soybean plants that overexpress *Arabidopsis FRO2* (Vasconcelos et al., 2006), suggesting that root Fe content is strongly linked with higher FCR activity. To support our observations, some previous studies in soybeans proved that IDC-tolerant genotypes accumulate higher Fe levels in their roots than IDC-sensitive genotypes when grown on calcareous soils (Kaiser et al., 2014: Liesch et al., 2011) while root Fe content increases under Fe fertilization in a dose-dependent manner (Merry et al., 2022). This increase is related to the expression of the genes involved in Fe uptake. We showed that the genes involved in Fe uptake are highly induced in the roots of all cultivars under high soil pH while their expression levels decline after Fe fertilizer application (Fig. 5). Similar to our results, Enomoto et al. (2007) reported that Fe supplementation to iron-deficient tobacco plants leads to low transcript levels of iron reduction and acquisition genes (*FRO* and *IRT1*).

Interestingly, the *GmOPT3* levels remained higher in the leaves upon iron fertilization as well, which indicates that somehow the sensitive cultivars still do not have adequate iron levels and plants are feeling iron deficiency, which can be observed by leaf iron levels in the sensitive cultivars as shown in Figure 6 a. Although higher iron levels were observed in the roots of Arısoy, Sa-88, and Nova under high pH conditions, the expression levels of some iron homeostasis genes remained elevated in the roots. This observation indicates that the long-distance signaling from leaves to the roots may be active since the leaves accumulated lower iron contents under iron-deficient conditions than the control conditions. This scenario can be related to the higher expression of *GmOPT*3 under high pH conditions with no added iron, while iron supplementation increased leaf iron levels, which resulted in the repression of *GmOPT3* in the leaves (compared to soil pH of 8.7 with no added iron) leading to lower expression of other iron homeostasis genes in the

roots. A similar scenario was tried to be explained in *Arabidopsis* under Fe deficiency (Chia et al., 2023; Garcia et al., 2013; Zhai et al., 2014) however, this observation needs further detailed experimentation in soybean.

Ferritins are iron storage proteins, under iron deficiency conditions plants need to utilize already stored iron when they are unable to uptake from the soil. This can be the reason that lower *GmFER* levels were observed in all cultivars under iron-deficient conditions while an increase in the *GmFER* levels was observed under iron supplementation. Noticeably *GmFER* expression did not reach the levels in control except Sa-88, indicating that this cultivar had successfully taken up large amounts of iron from the soil while the other ones had utilized some stored iron in addition to iron uptake from the soil. Similar results were reported by Santos et al. (2016), where plants had lower *FERRITIN* levels under iron deficiency. Taken together, gene expression analyses prove that Fe fertilization affected tolerant cultivars more drastically than sensitive ones at the molecular level.

According to our seed Fe content results, IDC-sensitive cultivars accumulated much lower levels of Fe in their seeds than did the tolerant cultivars under high soil pH. Our results are supported by previous studies in soybean, where tolerant cultivars accumulated higher levels of Fe than moderately tolerant or sensitive cultivars (Moraghan and Helms, 2005; Wiersma, 2012). We found that seed Fe levels increased with increasing Fe supplementation under higher pH. This indicates that plants were able to uptake and translocate the supplied Fe under high pH conditions. An increase in seed iron contents is related to the efficient uptake of added iron in the high-pH soil. Higher seed iron levels were observed in the tolerant cultivars than in the sensitive ones in all treatments (Figure 4.5 a). Moreover, even the highest dosages of Fe-EDDHA supplementation were not enough for IDC-sensitive cultivars to increase their seed Fe content to control levels. These findings suggest that increasing Fe-EDDHA rates in iron-efficient cultivars under high pH conditions could be a potential strategy for enhancing iron biofortification in soybeans cultivated in calcareous soils. Similar results were reported by Wiersma (2005), where higher doses of iron supplementation led to an increase in seed iron content.

Iron plays a vital role in the activity of enzymes like nitrate reductase, nitrite reductase, and glutamate synthase, crucial for nitrogen assimilation (Marschner, 1995). This process converts inorganic nitrogen into amino acids, pivotal for plant growth. This is especially

significant for crops like legumes, which are valuable sources of dietary protein. Overexpression of tobacco *NITRATE REDUCTASE* increased protein content in rice seeds (Zhao et al. 2013). Studies in cucumber (Borlotti et al., 2012) and Arabidopsis (Liu et al., 2015) showed that iron deficiency lowered nitrate reductase activity in both leaves and roots. These studies suggest that reduced nitrate reductase activities due to iron deficiency (high pH treatment with no Fe-EDDHA addition) might have caused the observed low seed protein content in our study. Therefore, adequate iron levels can positively influence the synthesis of essential amino acids, contributing to higher protein content in soybean seeds. Nodulation is one of the primary features of legumes for nitrogen fixation and iron deficiency-suppressed nodule formation ultimately affects nitrogen fixation. For example, higher iron levels have been associated with increased leghemoglobin production and nitrogen fixation in the nodules (Rotaru and Sinclair, 2009; Tang et al., 1990) and may enhance seed protein contents. This suggests that iron availability might indirectly influence seed protein levels by affecting nitrogen fixation, metabolism, and subsequent amino acid production.

100-seed weight, seed size, and seed protein contents showed a positive correlation with seed Fe content (Fig. 5.1), suggesting that seed Fe accumulation influences the yield and protein content in soybean. Opposite to our results, genetic loci responsible for seed size in common bean were found to be independent of iron and zinc levels (Blair et al., 2009). However, stress conditions that cause fluctuations in seed size often result in adjustments to elemental concentrations, although not invariably affecting elemental contents (Wiersma, 2012). Oppositely seed phytic acid, Zn, and Mn levels were negatively correlated with seed Fe levels (Figure 5.1). A negative correlation between the nutrients can be related to the competition between different metals since an increase in the concentration of one metal can lead to an imbalance in the uptake and storage of other metals because of their shared transporters (e.g IRT1) and inter-compartment storage pools within plants. Indeed, the interaction between iron and zinc is well-documented due to their chemical similarity as divalent cations and their interactions with the transporters in the same family. Both metals are essential micronutrients for plants, but their uptake and transport mechanisms can overlap, leading to competition and antagonistic relationships (Rai et al., 2021; Saenchai et al., 2016). This competition for the same transporter can limit the availability of certain metals, even if they are present in sufficient amounts in the soil.

Overall, our findings highlight the positive relationship between 100-seed weight, seed size, and seed protein content with seed Fe accumulation, underscoring the influence of Fe content on soybean yield and protein content. Conversely, the negative correlations observed between seed phytic acid, Zn, and Mn levels with seed Fe levels suggest potential competition among these nutrients, likely due to shared transporters and storage pools within plants. This competition can lead to limitations in the availability of certain metals, even when present in adequate soil concentrations, revealing the intricate interplay of nutrient interactions in plants.

Seed parameters like protein content, phytic acid levels, and micronutrient concentrations have suggested that the efficient biofortification of the soybean grown on calcareous soils by selecting efficient soybean cultivars and implementing higher iron dosages in calcareous soils is necessary. Such measures increased protein and seed iron content, thereby improving biofortification and overall yield in soybean cultivation.

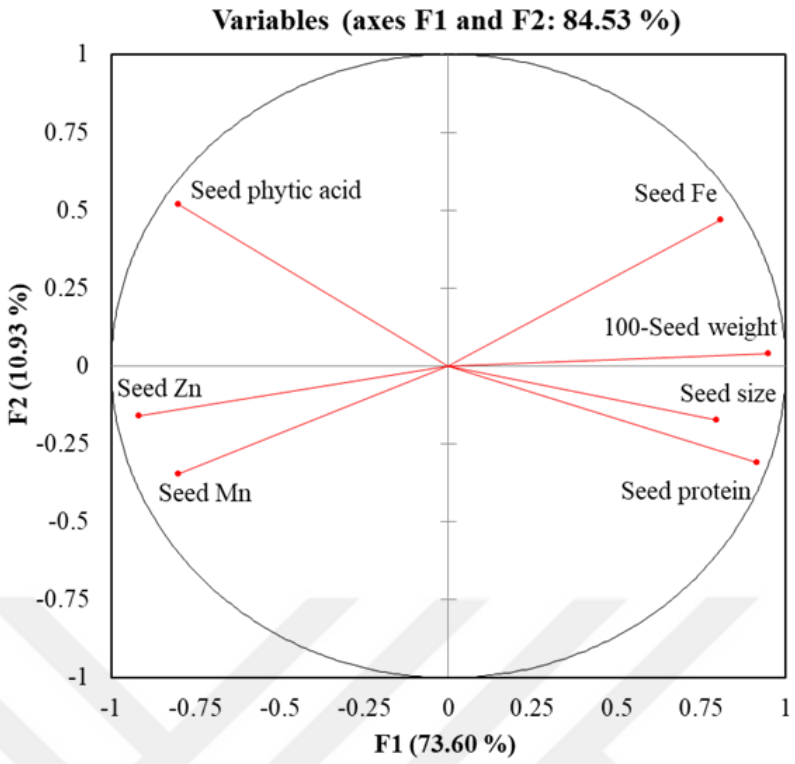

Figure 5.1. Correlation analyses of different seed traits in response to increasing Fe fertilization under high soil pH. Monoplot of the first two axes of PCA executed on measured seed traits. The red lines and letters represent the effect size of different traits.

Part 2: Genome-wide Identification of QTLs Associated with Iron Deficiency Tolerance in Soybean

Herein, the identification of 19 unique regions containing 6493 genes was presented for the first time in soybean (Figure 1) and 3822 unique ortholog genes were obtained in A. thaliana. In silico expression analysis of 3822 unique genes identified 607 of them as differentially expressed under Fe deficiency. To gain a more detailed understanding of their regulation under Fe deficiency, their expression levels in the *bhlh100bhlh101* and *pye1-1* mutants were evaluated, since POPEYE (PYE) is localized to the stele, while basic helix-loop-helix transcription factors bHLH100 and bHLH1001 are localized to the root epidermis and function as a dimer with other bHLH transcription factors including the major Fe deficiency signaling regulator FIT (Gao et al., 2019). The in-silico analysis revealed 10 DEGs affected by both *bHLH100-bHLH1001* and *PYE* (Figure 4.11). GSEA

showed that the core group of genes was linked with Fe deficiency response, while the hierarchical clustering demonstrated their similar expression patterns in different Fe deficiency experiments. Among these genes, the molecular functions of METAL TOLERANCE PROTEIN3 (*MTP3*) and IRON REGULATED PROTEIN2/FERROPORTIN2 (*IREG2/ FPN2*) have already been shown under Fe deficiency. The core group of genes was enriched in GOs linked with Fe tolerance in previous studies (Schwarz and Bauer, 2020). Some additionally enriched GOs include sulfur metabolism. The positive regulatory effect of hydrogen sulfide (Chen et al., 2020) and the involvement of sulfur metabolism in the alleviation of Fe deficiency responses have been demonstrated in plants. Interestingly, these studies demonstrated the necessity of sulfur for proper Fe deficiency tolerance in plants (Robe et al., 2020), and the contribution of hormones, especially auxin and gibberellic acid, to the tolerance mechanisms (Chen et al., 2020). The co-expression gene network analysis identified 6 clusters linked with the core group of genes (Figure 4.12). Clusters 1 and 2 included the genes involved in the Fe signaling networks regulated by *PYE* and FIT/FRU in the root stele and epidermis, respectively, as determined in previous bioinformatic studies (Schwarz and Bauer, 2020). Although these spatially separated signaling networks have been known for a long time, their interdependence has not been shown before. The cluster analysis herein showed that cluster 3 represented a link between the 2 Fe signaling networks, indicating the potential missing link between the 2 most important Fe-signaling components of Fe homeostasis in plant roots. Interestingly, cluster 3 was centered around *GATA12*. By binding to the main sequence of G-A-T-A, GATA transcription factors are classified in the IV group of the zinc finger transcription factor family and function in different pathways (Reyes et al., 2004). Thirty GATA transcription factors have been identified in the Arabidopsis genome and divided into 4 subgroups preserved within themselves. While *GATA12* was found in the first subgroup of GATAs together with *GATA9*, *GATA2*, and *GATA4*, the clustering in this study showed a co-expression of these 4 GATA transcription factors together in cluster 3. It has been reported that GATA transcription factors are controlled by different hormones, and thus play important roles in plant growth and stress responses (Behringer and Schwechheimer, 2015). In a recent study, it was shown that *GATA12* was expressed especially in the root and stem, localized to the nucleus, and negatively affected dormancy (Ravindran et al., 2017). In the same study, it was shown that the activation of *GATA12* was dependent on the presence of gibberellic acid and *GATA12* was activated because of the interaction of the DELLA

transcription factor *RGL2*, which is the main regulator of gibberellic acid signaling, with DOF6, the stress transcription factor. This suggests that the DELLA proteins are one of the possible regulators of GATA transcription factors. In another study, it was shown that the DELLA proteins post-translationally regulate the Fe signaling regulator *FIT* in the roots (Wild et al., 2016). In that study, it was reported that the local distribution of DELLA suppressors responsible for gibberellin signaling was regulated by Fe and contributed to the modulation of the root system architecture. DELLA interacts with *FIT* activity to inhibit it, but DELLA becomes unstable, and unable to release the *FIT* to activate Fe uptake genes in epidermis cells under Fe deficiency. Taken together, the co-expression network analysis conducted in the present study, together with the RT-qPCR results, highlights the importance of the interaction of GATA transcription factors with DELLAs in regulating the stability of FIT (and possibly other bHLH transcription factors involved in Fe signaling) for proper Fe uptake from the rhizosphere in plants. Cluster 1 was centered around *DJC77* (AT2G42750), which is a J domain-containing cochaperone (J protein) that interacts with the chloroplast-localized heat shock protein HSP70 to regulate the binding of HSP70 to folding proteins under stress conditions (Chiu et al., 2013). Interestingly, *DJC77* is highly expressed in the leaves, especially under selenium treatment (Van Hoewyk et al., 2008), and was shown to be mobile from leaves to the roots via the phloem (Thieme et al., 2015), suggesting its potential regulatory effect under mineral imbalances. Cluster 4 included bHLH121, also known as UPSTREAM REGULATOR OF IRT1 (*URI*), which was recently shown to act as a crucial regulator of the Fe deficiency signaling pathway (Gao et al., 2020). The phosphorylated form of URI accumulates under Fe deficiency and forms heterodimers with *bHLH38/39/100/101*. These transcription factors in turn heterodimerize with the FIT and drive the transcription of *IRT1* and *FRO2* to increase Fe uptake. It also interacts with PYE, BTS, and BTSL1. Surprisingly, URI clustered with STA2, ASN1, and AIP1 in cluster 4 instead of clustering together with *FIT*, *FRO2*, *IRT1*, and other bHLHs (Figure 4.12). Moreover, *FIT* was found to be epistatic to *bHLH121*, and FIT overexpression partially rescued the severe phenotype of the *bhlh121* mutant under Fe deficiency (Lei et al., 2020). The expression of *URI* was not affected by Fe availability. This suggests URI as an upstream transcription factor regulating the Fe-signaling pathway depending on the availability of nutrients, especially of Fe, via amino acid metabolism, since cluster 4 was enriched in GOs linked to amino acid metabolism. Taken together, these observations indicate that the core group genes are associated with metal ion transport and Fe deficiency signaling in plants.

Moreover, they expand our understanding of the Fe deficiency signaling network toward the integration of plant hormonal signals. Under Fe deficiency, the root and shoot lengths as well as the FWs decreased significantly compared to the control conditions (Figure 6), which agrees with previous studies done on soybean (Kurtz, 2017; Maqbool, 2018). As Fe is required for chlorophyll biosynthesis, the total chlorophyll content and the chlorophyll index decrease significantly under Fe deficiency in Fe-sensitive soybean genotypes (Maqbool, 2018). Hence, the observations herein are in agreement with the literature. FCR was determined as the major factor affecting the Fe uptake in dicots and the application of Fe deficiency enhances the FCR activity in plants (Jiménez et al., 2019). Herein, a twofold increase was observed in the FCR activity in the roots of the Atakişi plants under Fe deficiency, proving that the plants experienced Fe deficiency in the hydroponics setup. Dicots require the protonation of the rhizosphere for proper solubilization and uptake of Fe. Therefore, they cannot uptake Fe efficiently in alkaline soils (Olsen and Brown, 1980). To understand how high pH affects plant growth, Atakişi plants were also grown under a high pH (9.0) for two weeks. As expected, high pH decreased the chlorophyll content while the root length increased together with root and shoot FWs (Figure 6). The effects of a high pH and Fe deficiency are opposite in terms of root growth (Gheshlaghi et al., 2020), which was also observed in the current study. While the high pH and Fe deficiency caused a decrease in the chlorophyll content in plants (Maqbool, 2018), Fe deficiency showed a more remarkable reduction compared to the high pH application. Interestingly, the high pH did not increase the FCR activity, while Fe deficiency did, suggesting that different molecular mechanisms would be affected by individual stresses. This observation confirms the previously reported mildly acidic pH optimum of *FRO2*-mediated Fe chelate reduction (Tsai et al., 2018). The molecular networks affected by alkalinity (Tsai and Schmidt, 2020) and Fe deficiency have already been studied in plants. However, genes involved in individual networks have not been compared to determine the common genes. Interestingly, the expression levels of some core group genes were significantly induced under both Fe deficiency and high pH, indicating their potential involvement in the common set of genes regulated under both stresses. The identification of these core genes involved in IDC-related QTLs in soybean would enhance our ability to understand molecular mechanisms behind IDC tolerance and sensitivity in soybean and facilitate the development of IDC-tolerant genotypes in the future. Among these genes, *GATA12* stands out with its induced expression levels around 5 and 20 times under Fe deficiency and high pH, respectively (Figure 4.14). Cluster 3,

which was centered around *GATA12*, represented a knob between the 2 Fe signaling networks, indicating the potential missing link between the 2 most important Fe-signaling components of Fe homeostasis in plant roots. Therefore, the potential regulatory roles of the GATA transcription factors in Fe signaling should be investigated in future studies.

Part3: Transcriptomics of IDC-tolerant soybean cultivars in calcareous-alkaline soil

Complicated genetic networks take part in iron homeostasis from its uptake to its translocation and storage to different plant parts, as trans metals play pivotal role in plant growth and development. Although several genes have been identified in Fe homeostasis under deficient and toxic conditions, many still need to be characterized. Until now, several techniques have been employed to identify the genetic players involved in Fe homeostasis in different plant species. Previous studies in soybean involve transcriptomic analyses of near isogenic lines under long- (O'Rourke et al., 2007: Peiffer et al., 2011) and short-term Fe deficiency (Lauter et al., 2020). While on the other hand recent studies related to iron deficiency response transcriptome change in soybeans include a number of soybean genotypes, but these studies involve the early iron deficiency response. Kohlhase et al., 2021 had done RNA sequencing of 18 soybean cultivars root and leaves separately and found a number of genes that have been differentially expressed within 60 minutes of iron deficiency. Current study involves the transcriptomic profiling of two IDC-tolerant soybean cultivars under long term iron deficient conditions (grown under high soil pH conditions) and as a result several differentially expressed genes were identified among both cultivars and tissues (leaves and roots). Here, for the first-time plants were grown under high soil pH triggered iron deficiency conditions for 30 days. After 30 days of growth when the soybean plants reached the V_3 growth stage the top trifoliate leaves and roots samples were collected separately for the transcriptomic analyses. A transcriptomic study of two distinct soybean cultivars revealed the differential expression of many known iron-responsive genes and other gene families and transcription factors potentially involved in iron homeostasis (Appendix 8, Appendix 9). These findings highlight the presence of unexplored genetic potential within the two soybean cultivars, which could be leveraged to enhance iron efficiency and high soil pH-triggered iron deficiency tolerance in future breeding programs for soybean improvement. The results of the study are comprehensively discussed in the following sections.

5.3.1. Up-regulation of genes involved in iron uptake

NRAMP1, *NRAMP2*, *NRAMP3*, and *NRAMP6* were differentially expressed (upregulated) in both soybean cultivars (Appendix 8). NRAMPs (natural resistance-associated macrophage proteins) are the integral membrane transporters that play an essential role in divalent transmetal transport, especially Mn, Cd, and Fe (Cailliatte et al., 2010; Ishimaru et al., 2012; Liu et al., 2022; Li et al., 2021; Wang et al., 2023; Noor et al., 2023).NRAMP1 and NRAMP6, known to have function in metal homeostasis, were differentially expressed (upregulated) in the current study (Appendix 8).

IRT1 is a high-affinity Fe transporter in plants while NRAMP1 cooperates with IRT1 for Fe uptake from the rhizosphere as a low-affinity De transporter under low Fe conditions. Double mutants of *irt1-1nramp1-1* show extreme chlorosis compared to the *irt1-1* single mutants (Castaings et al., 2016). Although both IRT1 and NRAMP1 are divalent metal transporters and are involved in the uptake of Fe^{2+}, *NRAMP1* was induced to promote Fe^{2+} uptake under late Fe deficiency in poplar (Chen et al., 2019). This shows that NRAMP1 may have a major role in late Fe deficiency response in plants. As the current study involves transcriptomic analyses at the late stage of Fe deficiency (almost 30 days), this can be the reason for the differential expression of *NRAMP1* in both cultivars. NRAMP3 and NRAMP4 are vacuolar Fe transporters involved in the Fe export from the vacuole mainly at the germination stage. *nramp3nramp4* double mutants showed no significant difference in the seed Fe content compared to the wild type, however, *nramp3nramp4* mutants showed defective growth and severe chlorosis under Fe deficiency (Bastow et al., 2018), In the current study, induction of *NRAMP3* can be related to the reutilization of the stored Fe in the vacuoles at the late Fe deficiency stage as the severity had been increased after growing the plants at high pH for thirty days. In addition, NRAMP2 may have a similar function at the late Fe deficiency stage since the vacuolar Fe content in *Osnramp2* knockdown lines in rice was found to be higher than in the wild-type plants and the germination of *Osnramp2* was arrested. Conversely, the vacuolar Fe content was lower in the rice plants, overexpressing *NRAMP2*, indicating the role of NRAMP2 in Fe export out of vacuole especially under late Fe deficiency (Li et al., 2021).

AtNRAMP6 is localized to the Golgi/trans-Golgi network and plays a critical role in regulating intracellular Fe homeostasis in Arabidopsis (Li et al., 2019). GUS fusion

tissue-specific expression analysis showed that *AtNRAMP6* is predominantly expressed in the lateral roots and young leaves (the upper three to four leaves) of Arabidopsis. Additionally, the knockout of *AtNRAMP6* impaired lateral root growth without affecting the main root length under Fe-deficient conditions. Moreover, the expression of *AtNRAMP6* increased the sensitivity of the yeast mutant *Δccc1* to high levels of Fe. These results indicate that *AtNRAMP6* is essential for the growth of Arabidopsis in Fe-deficient conditions (Li et al., 2021).

Members of the metal tolerance protein family, namely *MTP8* and *MTP9*, are also differentially expressed in both cultivars (Appendix 8). MTP8 is involved in Fe and Mn homeostasis (Eroglu et al.,2016) while MTP11 is involved in Mn homeostasis (Tsunemitsu et al.,2018) and may have a role in Fe uptake and translocation.

Organelles like mitochondria and chloroplast have high Fe demand because of the active role of Fe in the electron transport chain and other metabolic processes. The proteins found in these processes contain Fe-S clusters and/or haem groups. This suggests that the synthesis of Fe-S clusters and haem is important for the proper functioning of these organelles. Therefore, the need for high Fe demand can be the reason for the differential expression of sulfur assimilation genes in the current study (Appendix 8).

Differential expressions of major transcription factor *FIT* involved in Fe deficiency response were induced under Fe deficiency in both cultivars (Appendix 9). FIT controls the expression of many Fe-responsive genes under Fe-deficient conditions such as *IRT1* and *FRO2* (O'Rourke et al., 2009). Interestingly, 22 members of WRKY transcription factors were differentially expressed in both tissues of two cultivars (Appendix 9). One of the members of the WRKY family, namely WRKY46, is involved in Fe homeostasis as *wrky46-1* and *wrky46-2* mutants were shown to have severe leaf chlorosis and hampered translocation of Fe from roots to the leaves. Thus, WRKY46 plays an important role in roots-to-shoot Fe translocation (Yan et al., 2016). Overexpression of another member of the WRKY family from apples (*Malus xiaojinensis*), *MxWRKY55* in *Arabidopsis thaliana* showed an increase in Fe deficiency tolerance (Han et al., 2020). Keeping in context this, the roles of other WRKY members differentially expressed in our transcriptome data in Fe homeostasis should be investigated further (Appendix 9).

5.3.2. The role of peptide transporters in Fe homeostasis

OPT1, *OPT3,* and *OPT5* were differentially expressed in both cultivars under late Fe deficiency (Appendix 8). OPT3 belongs to the oligopeptide transporter family and null mutation of *OPT3* results in embryo lethality suggesting its role in embryo development (Stacey et al., 2008). It is recognized as a plasma membrane transporter with the ability to transport transition ions in vitro. In *A. thaliana,* OPT3 plays a role in loading Fe into the phloem, facilitating the recirculation of Fe from the xylem to the phloem, and regulating Fe signaling from the shoots to the roots. It also helps in the redistribution of Fe from mature tissues to developing ones, thus playing an important role in the source-to-sink distribution of Fe in plants (Zhai et al., 2014; Mendoza-Cózatl et al., 2014). Recently OPT3 has been reported to have a role in Cu homeostasis as well, *opt3* had shown lower copper levels in the phloem compared to the wild type. Additionally, *opt3* mutants exhibited an enhanced transcriptional response to Cu deficiency in both roots and leaves, marked by increased expression of several key genes, including *CTF1*, *FRO4*, *FRO5*, *COPT2*, and *COPT1*. The application of Cu or Fe to opt3 mutants via the phloem in the leaves led to a downregulation of both Cu- and Fe-deficiency marker genes in the roots. (Chia et al., 2023).

OPT6 is known for the long-distance transport of glutathione (Wongkaew et al., 2018), which is reported to regulate nitric acid-mediated Fe deficiency tolerance in Arabidopsis (Shanmugam et al., 2015). On the other hand, there is no real evidence available explaining the role of OPT1 in Fe transport. In addition to this other members of the oligopeptide family (OPT) include the sub-family named YSL transporters. Members of the YSL (Yellow Stripe-Like) subfamily are specifically involved in the long-distance transport of metal-chelates, thereby playing a crucial role in maintaining metal homeostasis, including essential metals such as Fe, Zn, Cu, Mn, and nickel (Ni) (Kumar et al., 2018). Several YSL transporters, including the OsYSL15, HvYS1, and ZmYS1, are known to have a role in iron transport in barley, rice, and corn (Curie et al., 2001; Murata et al., 2006; Inoue et al., 2009; Kakei et al., 2012). AtYSL1 and AtYSL3 are involved in the translocation of Fe and Cu in *Arabidopsis thaliana* (Waters et al., 2006; Chen et al., 2014).

In addition to the OPT family members, 10 members from the SWEET family of sugar transporters were differentially expressed in our transcriptomics data. Members of the SWEET family have known roles in cold tolerance in plants (Fang et al., 2022: Wang et al.,2018) and can be potential candidates with additional roles in Fe and metal homeostasis. In rice plants, higher levels of endogenous sucrose led to the suppression of genes related to Fe acquisition in the roots, while enhancing the expression of genes associated with Fe transport in the leaves, emphasizing the crucial role of sucrose in modulating the rice plant responses to Fe deficiency (Chen et al.,2018). Recently, short peptides called IMA (Iron Man) were found to be involved in Fe deficiency responses in *Arabidopsis thaliana* (Grillet et al., 2018). Interestingly, 21 members of the UMAMIT amino acid transporter family were differentially expressed in the transcriptomics data with fold changes of more than 2 (Appendix 8). Although UMAMIT transporters have not been associated with metal transport, they may also have a role in the Fe homeostasis at late stages of Fe deficiency in plants similar to the roles of OPTs in Fe homeostasis. UMAMIT family transporters are generally involved in the amino acid transportation in the seeds (Müller et al., 2015).

Because of the redox nature of Fe, it must always be transported in the chelated form in the plant, either with NA, citrate, or others. Soybean does follow some of the established responses to Fe deficiency. It has been proposed that under Fe-deficient conditions, citrate provides a carbon skeleton for chlorotic leaves to allow for sustained growth and respiration (Abadia et al., 2002). Later, *FRD3*, a citrate efflux transporter, was identified as induced under Fe deficiency, and the Fe^{3+}-citrate complex is found to be one of the major forms of Fe in the xylem sap (Durrett et al., 2007). In rice, OsYSL2 was involved in the Fe transport and the phloem-specific expression of *OsYSL2* took part in the Fe transport in the phloem. Electrophysiological studies in *Xenopus laevis* oocytes showed that OsYSL2 transported Fe^{2+}-NA. Keeping in context the nature of Fe and its ability to take part in redox reactions, free Fe can cause damage to membranes. We hypothesized that UMAMIT family transporters can be the potential candidate genes that may have a part in amino acid-chelated iron transportation in plants. UMAMIT family members can bidirectionally transport some amino acids and can transport glutamine (Müller et al., 2015). Furthermore, Alchoubassi et al. (2021) showed that L-glutamine can naturally bind with iron in a study involving the metal chelate analysis of coconut water. Furthermore, L-glutamine analysis in the xylem sap under high pH conditions for all four soybean

cultivars showed an increase in L-glutamine levels in the xylem sap, which shows a decrease when additional iron is supplied in the growth media (Figure 4.39).

Given that Fe can natuarally bind with L-glutamine (Alchoubassi et al.,2021) and UMAMIT family transporters are reported to involve in L-glutamine transportation in plants (Müller et al., 2015), UMAMITs can be the candidate genes responsible for the transportation of Fe-glutamine complex in the plants. Co-expression analysis of *AtUMAMIT28* has shown that it co-expresses with several known iron transporters, and microarray analysis indicates its induction under iron deficiency conditions (Figure 4.40).

Part 4: Characterization of *AtUMAMIT28* in *Arabidopsis thaliana* under transmetal deficiencies

RNA sequencing results of soybean and co-expression analyses of the UMAMIT family in *A. thaliana* revealed that *AtUMAMIT28* may have a potential role in Fe homeostasis in plants. As UMAMIT transporters are L-glutamine transporters (Muller et al., 2015), the xylem sap L-glutamine levels under high pH conditions further supported the hypothesis that *AtUMAMIT28* may be involved in the transport of L-glutamine-Fe complex in plants (Figure 4.39). To understand whether L-glutamine binds with Fe, we have exogenously supplied L-glutamine in the growth media. Interestingly, L-glutamine application significantly hampered the growth of the mutants of Fe homeostasis genes involved in iron uptake (*irt1*), reduction (*fro2*), and translocation indirectly by citrate efflux (*frd3*) compared to the wild-type. Furthermore, after L-glutamine treatments, mutants showed lower chlorophyll contents, and higher FRO/FCR enzyme activities compared to the wild-type(Figure 4.65). In addition, shorter root lengths were observed in the mutants (Figure 4.64). These results indicate that L-glutamine can bind with the Fe in the growth medium *in vivo* making Fe unavailable to the plants. Therefore, we observe much more severe phenotypes of the Arabidopsis mutants of Fe homeostasis genes which may be involved in the direct uptake of L-glutamine from the media.

To test the hypothesis that *AtUMAMIT28* is involved in Fe homeostasis, *umamit28-1* mutant and overexpression (OE) lines were grown on control (Fe sufficient) and Fe deficient media with two additional treatments. *umamit28-1* showed higher FCR enzyme activities in all treatments while OE lines showed lower FCR activities compared to the

mutants and the wild-type (Figure 4.56). These results indicate a possible role of AtUMAMIT28 in Fe uptake through complexation with L-glutamine. In the reduction-based strategy plants, the expression of *FRO2* and the activity of FCR help the plants to reduce Fe^{3+} to Fe^{2+} (Robinson et al., 1999: Jain et al., 2014), which is then taken up by the divalent metal transporter *IRT1* (Quintana et al.,2022). Higher FCR enzyme activities in the mutants showed that plants felt more Fe deficiency, and they tried to reduce Fe^{3+} to Fe^{2+} while OE lines showed lower enzyme activities highlighting that somehow, they can uptake Fe from the recalcitrant pools.

For the leaf and root iron concentration analyses, *umamit28-1* showed lower root iron levels under iron deficiency conditions (no ferrozine), and overexpression lines showed no significant difference in the iron levels compared to the wild type. Under extreme iron-deficient conditions (no iron added + 200 µM ferrozine), overexpression lines showed higher iron concentratşons compared to the wild type and mutants, which can be related to the translocation of iron from leaves to the roots as lower leaf iron levels were found in OE1, while OE2 showed higher iron concentration (Figure 4.58). Seed metal analyses showed that *umamit28-1* and *umamit29-1* accumulated lower levels of Mn, Fe, and Zn in their seeds while no significant differences were found for the overexpression lines compared to the wild type (Figure 4.59).

These results can be related to the yeast complementation assays, where the introduction of the CDS region of *AtUMAMIT28* in the *S. cerevisiae* slowed down the growth of Δ*fet3fet4* (defective in iron uptake), Δ*zrtzrt2* (defective in zinc uptake) and Δ*smf1* (defective in Mn uptake) under recipient metal deficiencies (Figure 4.69-4.71). These results indicate the role of *AtUMAMIT28* in metal export. In *A. thaliana* plants AtUMAMIT28 was found active only later in seed development, starting at the embryo torpedo stage in the innermost layer of the three-layered inner integument, the endothelium (Muller et al., 2015), which indicates the possible role of *At*UMAMIT28 at the late seed development stage. It either has a role in the development process or the export of iron and other divalent metals. Mutant lines showed lower seed Cu content and higher Cu contents were observed in the overexpression lines (Figure 4.59). In addition to this *At*UMAMIT28 had fully complemented the Δ*ctr1* mutant defective in copper uptake and the ICP-OES metal analyses revealed higher Cu contents in the yeast cells expressing the *AtUMAMIT28* (Figure 4.72). While in case of higher Cu concentrations in

media yeast cells expressing the *AtUMAMIT28* had shown toxic symptoms of higher Cu uptake by showing the slower growth (Figure 4.72). These results suggest that *At*UMAMIT28 is a high affinity copper transporter. While Chia et al, 2023 had reported that Δ*ctr1* is partially complemented by the OPT3, disclosing it as low affinity copper transporter.

Copper is an essential metal required for the proper growth and development of plants, being a part of many enzymes. Copper deficiency restricts plant growth ultimately leading to yield losses (Cai et al., 2024). Copper serves as a crucial redox-active cofactor in various plant enzymes. It is integral to the function of numerous proteins, including plastocyanin, cytochrome c oxidase, Cu/Zn superoxide dismutase (CSD), ethylene-binding proteins, laccases, ascorbate oxidase, amine oxidases, plantacyanin, and polyphenol oxidases (Cai et al., 2024). During the last few years recent studies have showed the role of iron transporters in Cu homeostasis as well (Chia et., 2023).When grown under copper-deficient conditions, as compared to wild type Col-0 the *umamit28-1* mutants showed increased sensitivity to Cu deficiency and exhibited shorter root lengths. In contrast, *AtUMAMIT28* overexpression plants displayed longer root lengths than both the wild type and the *umamit28-1* mutant. Cu is an essential metal required for plant growth and development and deficiency of copper leads to attenuation of plant growth (Chen et al., 2022). Keeping in view inhibited root growth in *umamit28-1* can be related to low Cu uptake. Similar results were shown by Shin et al., 2012 where plants sensitive to Cu deficiency had shown smaller root lengths. Furthermore, Martins et al. (2014) also reported that *copt5* mutants had shown shorter root lengths under Cu deficient conditions compared to the wild type. The *copt5* mutants are highly sensitive to copper deficiency because of the dimnished ability to facilitate vacuolar Cu export which is crucial in Cu recycling back to the cytoplasm, which becomes particularly necessary during Cu starvation (Garcia-Molina et al., 2011**)**. Moreover under Cu deficiency conditions *umamit28-1* mutants had shown lower chlorophyll levels and over exoression line had shown higher chlorophyll levels than the wild type. It is reported that in plants around. Because of the poor transport of Cu in the phloem, the typical symptoms of Cu deficiency first appear in young leaves as chlorosis (Xu et al., 2024).

Consitent with the results and increased sensitivity of *umamit28-1* to Cu deficiency the *umamit28-1* mutants had shown mounted expression levels of copper homeostasis genes

in roots (Figure 4.79). CITF1 is a Cu-DEFICIENCY INDUCED TRANSCRIPTION FACTOR1 co-regulates with the major Cu deficiency responsive transcription factor *SPL7.* It regulates the expression of many responsive copper genes including *COPT2*, *FRO4,* and *FRO5*. Under Cu deficiency conditions, *CITF1* expression is upregulated because of the reason it can be used as a marker gene to understand whether plants are under copper deficiency (Chia et al., 2023). Recent studies have shown that OPT3, which is known for its role in iron homeostasis, is also involved in copper homeostasis and mutants of *opt3* showed mounted expression levels of of CITF1 under copper-deficient conditions. Similar results were observed in the current study when grown under Cu-deficient conditions. *umamit28-1* showed higher expression of *CITF1* while the *AtUMAMIT28* overexpression line showed lower expression levels compared to the wild type. This can be related to the increased sensitivity of *umamit28-1* to Cu deficiency and tolerance of AtUMAMIT28 overexpression lines. These results can be related to lower copper levels in mutants and higher copper levels in overexpression lines in comparision with the Col-0 under Cu deficient conditions (Figure 4.78.) Similar patterns were observed for the genes involved in the copper uptake and reduction (*COPT1*, *COPT2,* and *FRO5*). These results are in line with Chia et al. (2023), where mutants of *opt3* (a Cu and iron transporter) had shown higher expression of *COPT1*, *COPT2* and *FRO5*. Metal content analyses of leaf and roots had also shown that *umamit28-1* had lower copper levels and the overexpression line of *ATUMAMIT28* had shown higher Cu levels compared to the wild type (Figure 4.78). These results indicate that AtUMAMIT28 is involved in metal homeostasis in plants and has a role in Cu uptake or translocation.

CHAPTER VI

CONCLUSION

Part1: Effect of iron fertilization on soybean cultivars differing in IDC tolerance

Alkalinity-induced iron deficiency leads to significant yield losses in soybean annually (Vasconcelos et al., 2014). To address this challenge, various strategies are employed, with the application of iron chelates being one of the most successful solutions in calcareous soils. However, the efficiency of iron uptake varies among cultivars due to genotypic differences in iron utilization. Nutrient-efficient genotypes have evolved to thrive in low-nutrient environments (Rengel et al., 2005). Our findings underscore that IDC-tolerant cultivars exhibit enhanced responses to Fe fertilization under high soil pH. In contrast, sensitive cultivars necessitate higher Fe fertilizer dosages to counter the detrimental effects of Fe deficiency. Considering the diverse applications of soybean seeds in food and feed sectors, our results highlight the essential need for integrating genetic and agronomic progress to effectively boost yield while enhancing nutritional quality. Thus, exploring the soybean gene pool to select genotypes that exhibit superior responsiveness to Fe fertilization in alkaline soils is imperative. This holistic approach, combining genetics and agronomy, holds the key to achieving both enhanced crop productivity and improved nutritional value.

Part 2: Genome-wide identification of QTLs associated with iron deficiency tolerance in soybean

Several molecular studies have been performed with IDC-tolerant and sensitive soybean genotypes to find the QTLs linked with IDC in soybean. However, none of these studies have identified the potential genes in these QTL regions and their interactions in Fe uptake in soybean. Herein, 10 core group genes were identified that have not been linked with Fe deficiency responses before. Their interactions with other well-known Fe-signaling components represent the interaction of different nutrient metabolisms and hormonal regulations. Among these 10 core genes, GATA12 stands out as an important integrator of Fe signaling between the epidermis-localized FIT and the stele-localized PYE signaling networks. Overall, these results suggest that the core group genes are induced

by Fe deficiency and high pH in soybean roots and GATA12 should be characterized under Fe deficiency in plants.

Part3: Transcriptomics of IDC-tolerant soybean cultivars in calcareous-alkaline soil

This study explored the response of two soybean cultivars grown under iron deficiency conditions, using RNA sequencing to uncover differentially expressed genes involved in iron homeostasis. Results showed that both known and new potential candidates that were previously unidentified as having a role in iron homeostasis have been differentially expressed. Interestingly 21 transporters from the UMAMIT family have been differentially expressed indicating the possible role of this family in iron homeostasis. These results highlight the complexity of iron regulation in soybeans under low iron available conditions. Results also revealed elevated levels of L-glutamine in the xylem sap, particularly under high pH conditions, where iron becomes less bioavailable to the plant. These results suggest that L-glutamine may also have a role in iron transport. Finally, the findings suggest that in response to iron limitation, soybeans actively lower the pH of the xylem sap, a physiological adaptation that likely enhances iron solubility and transportation.

Part 4: Characterization of *AtUMAMIT28* in *Arabidopsis thaliana* under transmetal deficiencies

AtUMAMIT28 is involved in iron and copper homeostasis in plants. From the yeast complementation assays, it can be concluded that AtUMAMIT28 may also have a role in zinc and manganese homeostasis. Yeast complementation and *in planta* results showed that AtUMAMIT28 is involved in the direct uptake of copper. Results revealed that L-glutamine may have the ability to bind with iron and this can be one of the possible forms of iron translocation within the plant body (Figure 6.1). Further studies are needed to clear the role of L-glutamine-iron complex transportation or storage within the plant body.

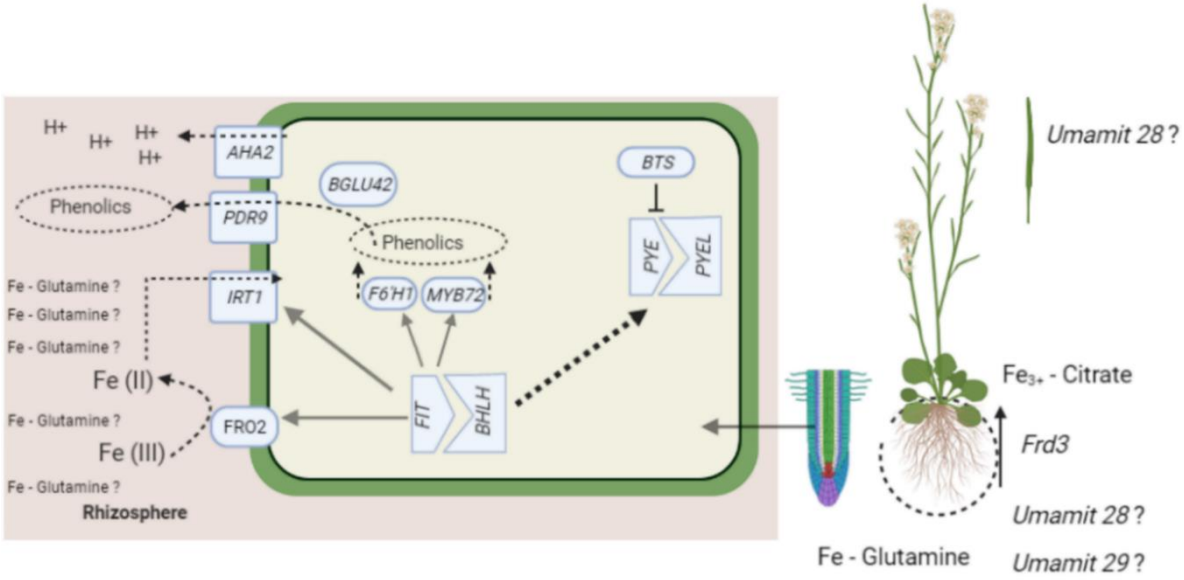

Figure 6.1. The schematic diagram for the potential role of *AtUMAMIT28* in *Arabidopsis thaliana*.

Taken together, this thesis identified a new transcription factor, GATA12, as the candidate regulator of FIT and PYE-based Fe signaling in the roots. Additionally, soybean RNA sequencing results in calcareous-alkaline soils showed that UMAMIT transporters can be potentially important for Fe deficiency tolerance. Among these transporters, AtUMAMIT28 was identified as an important Fe and Cu transporter in plants. Finally, the significance of combining Fe fertilization with genetic selection was demonstrated in soybean plants under alkaline soil conditions.

REFERENCES

Abadía, J., López-Millán, A.F., Rombolà, A. and Abadía, A., "Organic acids and Fe deficiency: a review", ***Plant and Soil***, 241, (75-86), 2002.

Abadía, J., Vázquez, S., Rellán-Álvarez, R., El-Jendoubi, H., Abadía, A., Álvarez-Fernández, A. and López-Millán, A.F., "Towards a knowledge-based correction of iron chlorosis", ***Plant Physiology and Biochemistry***, 49(5), (471-482), 2011.

Aguirre, G. and Pilon, M., "Copper delivery to chloroplast proteins and its regulation", ***Frontiers in plant science***, *6*, p.1250, 2016.

Aksoy, E. and Koiwa, H., "Determination of ferric chelate reductase activity in the Arabidopsis thaliana root", ***Bio-protocol,*** 3(15): e843-e843, 2013.

Aksoy, E., "*Arabidopsis thaliana CARBOXYL-TERMINAL DOMAIN PHOSPHATASE-Like1 (CPL1) Mediates Responses to Iron Deficiency and Cadmium Toxicity"* (**Doctoral dissertation**), 2014.

Aksoy, E., Jeong, I.S. and Koiwa, H., "Loss of function of Arabidopsis C-terminal domain phosphatase-like1 activates iron deficiency responses at the transcriptional level", ***Plant physiology***, 161(1), (330-345), 2013.

Aksoy, E., Maqbool, A., Tindas, İ. and Caliskan, S., "Soybean: A new frontier in understanding the iron deficiency tolerance mechanisms in plants", ***Plant and Soil***, 418(1-2), (37-44), 2017.

Aksoy, E., Yerlikaya, B.A., Ayten, S. and Abudureyimu, B., "Bitkilerde Rizosferden Demir Alım Mekanizmaları", ***Turkish Journal of Agriculture-Food Science and Technology***, 6(12), (1673-1683) 2018.

Alchoubassi, G., Kińska, K., Bierla, K., Lobinski, R. and Szpunar, J., "Speciation of essential nutrient trace elements in coconut water", ***Food Chemistry***, 339, p.127680, 2021.

Alchoubassi, G., Kińska, K., Bierla, K., Lobinski, R. and Szpunar, J., "Speciation of essential nutrient trace elements in coconut water", ***Food Chemistry***, *339*, (127680), 2021.

Am AOCS Approved Procedure Rapid Determination of Oil/Fat Utilizing High Temperature Solvent Extraction", (2005).

Andrés-Colás, N., Carrió-Seguí, A., Abdel-Ghany, S.E., Pilon, M. and Peñarrubia, L., "Expression of the intracellular COPT3-mediated Cu transport is temporally regulated by the TCP16 transcription factor", ***Frontiers in Plant Science***, *9*, p.910, 2018.

Andrés-Colás, N., Carrió-Seguí, A., Abdel-Ghany, S.E., Pilon, M. and Peñarrubia, L., "Expression of the intracellular COPT3-mediated Cu transport is temporally regulated by the TCP16 transcription factor", ***Frontiers in Plant Science***, 9, (910), 2018.

Andrés-Colás, N., Perea-García, A., Puig, S. and Penarrubia, L., "Deregulated copper transport affects Arabidopsis development especially in the absence of environmental cycles", ***Plant physiology***, 153(1), (170-184), 2010.

Angira, B., Zhang, Y., Zhang, Y., Scheuring, C.F., Masor, L., Coleman, J., Singh, B.B., Zhang, H.B., Hays, D.B., Zhang, M. and Khanal, M., "Genetic dissection of iron deficiency chlorosis by QTL analysis in cowpea", ***Euphytica***, *218*(4), (38), 2022.

Aoyama, T., Kobayashi, T., Takahashi, M., Nagasaka, S., Usuda, K., Kakei, Y., Ishimaru, Y., Nakanishi, H., Mori, S. and Nishizawa, N.K., "OsYSL18 is a rice iron (III)–

deoxymugineic acid transporter specifically expressed in reproductive organs and phloem of lamina joints", ***Plant Molecular Biology***, *70*, (681-692), 2009.

Araki, R., Murata, J. and Murata, Y., "A novel barley yellow stripe 1-like transporter (HvYSL2) localized to the root endodermis transports metal–phytosiderophore complexes", ***Plant and Cell Physiology***, *52*(11), (1931-1940), 2011.

Atencio, L., Salazar, J., Lauter, A.N.M., Gonzales, M.D., O'Rourke, J.A. and Graham, M.A., "Characterizing short- and long-term iron stress responses in iron deficiency tolerant and susceptible soybean (Glycine max L. Merr.)", ***Plant Stress***, *2*, (100012), 2021.

Baker, D.E., Rayment, G.E. and Reid, R.E., "Predictive relationships between pH and sodicity in soils of tropical Queensland", ***Communications in soil science and plant analysis***, *14*(11), (1063-1073), 1983.

Banakar, R., Alvarez Fernandez, A., Díaz-Benito, P., Abadia, J., Capell, T. and Christou, P., "Phytosiderophores determine thresholds for iron and zinc accumulation in biofortified rice endosperm while inhibiting the accumulation of cadmium", ***Journal of Experimental Botany***, 68(17), (4983-4995), 2017.

Barberon, M., Dubeaux, G., Kolb, C., Isono, E., Zelazny, E. and Vert, G., "Polarization of IRON-REGULATED TRANSPORTER 1 (IRT1) to the plant-soil interface plays crucial role in metal homeostasis", ***Proceedings of the National Academy of Sciences***, *111*(22), (8293-8298), 2014.

Barton, L.L. and Abadía, J. eds., "*Iron nutrition in plants and rhizospheric microorganisms"*, **Springer Science & Business Media**, 2007.

Bashir, K., Ishimaru, Y., Itai, R.N., Senoura, T., Takahashi, M., An, G., Oikawa, T., Ueda, M., Sato, A., Uozumi, N. and Nakanishi, H., "Iron deficiency regulated OsOPT7 is essential for iron homeostasis in rice", ***Plant molecular biology***, *88*, (165-176), 2015.

Bastow, E.L., Garcia de la Torre, V.S., Maclean, A.E., Green, R.T., Merlot, S., Thomine, S. and Balk, J., "Vacuolar iron stores gated by NRAMP3 and NRAMP4 are the primary source of iron in germinating seeds", ***Plant Physiology***, *177*(3), (1267-1276), 2018.

Behringer, C. and Schwechheimer, C., "B-GATA transcription factors–insights into their structure, regulation, and role in plant development", ***Frontiers in plant science***, 6, (90), 2015.

Bernal, M., Casero, D., Singh, V., Wilson, G.T., Grande, A., Yang, H., Dodani, S.C., Pellegrini, M., Huijser, P., Connolly, E.L. and Merchant, S.S., "Transcriptome sequencing identifies SPL7-regulated copper acquisition genes FRO4/FRO5 and the copper dependence of iron homeostasis in Arabidopsis", ***The Plant Cell***, *24*(2), (738-761), 2012.

Besnard, J., Pratelli, R., Zhao, C., Sonawala, U., Collakova, E., Pilot, G. and Okumoto, S., "UMAMIT14 is an amino acid exporter involved in phloem unloading in Arabidopsis roots", ***Journal of Experimental Botany***, *67*(22), (6385-6397), 2016.

Besnard, J., Zhao, C., Avice, J.C., Vitha, S., Hyodo, A., Pilot, G. and Okumoto, S., "Arabidopsis UMAMIT24 and 25 are amino acid exporters involved in seed loading", ***Journal of experimental botany***, *69*(21), (5221-5232), 2018.

Bin, L.M., Weng, L. and Bugter, M.H., "Effectiveness of FeEDDHA, FeEDDHMA, and FeHBED in preventing iron-deficiency chlorosis in soybean", ***Journal of Agricultural and Food Chemistry***, *64*(44), pp.8273-8281, 2016.

Blair, M.W., Astudillo, C., Grusak, M.A., Graham, R.O.B.I.N. and Beebe, S.E., "Inheritance of seed iron and zinc concentrations in common bean (Phaseolus vulgaris L.)", ***Molecular Breeding***, *23*, (197-207), 2009.

Bock, K.W., Honys, D., Ward, J.M., Padmanaban, S., Nawrocki, E.P., Hirschi, K.D., Twell, D. and Sze, H., "Integrating membrane transport with male gametophyte development and function through transcriptomics", ***Plant Physiology***, 140(4), (1151-1168), 2006.

Borlotti, A., Vigani, G. and Zocchi, G., “Iron deficiency affects nitrogen metabolism in cucumber (Cucumis sativus L.) plants”, ***BMC Plant Biology***, 12, (1-15), 2012.

Briat, J.F., Duc, C., Ravet, K. and Gaymard, F., “Ferritins and iron storage in plants”, ***Biochimica et Biophysica Acta (BBA)-General Subjects***, *1800*(8), (806-814), 2010.

Broadley, M., Brown, P., Cakmak, I., Rengel, Z. and Zhao, F., “Function of nutrients: micronutrients”, **In *Marschner's mineral nutrition of higher plants*** (191-248), 2012.

Brown, A.V., Conners, S.I., Huang, W., Wilkey, A.P., Grant, D., Weeks, N.T., Cannon, S.B., Graham, M.A. and Nelson, R.T., “A new decade and new data at SoyBase, the USDA-ARS soybean genetics and genomics database”, **Nucleic Acids Research**, 49(D1), (D1496-D1501), 2021.

Buckhout, T.J., Yang, T.J. and Schmidt, W., “Early iron-deficiency-induced transcriptional changes in Arabidopsis roots as revealed by microarray analyses”, **BMC genomics**, 10(1), (147), 2009.

Butsai, W., Polthanee, A. and Polpinit, W.K., “Improvement for better nutrition on rice through iron fertilizer applications in acid and alkaline soil under greenhouse conditions”, **In: Proceedings of the 20th National Graduate Studies Research Conference; Khon Kaen, Thailand**. (SDO-1-12), (2019).

Cai, Y. and Liang, G., “CITF1 Functions Downstream of SPL7 to Specifically Regulate Cu Uptake in Arabidopsis”, ***International Journal of Molecular Sciences***, *23*(13), (7239), 2022.

Cai, Y., Li, Y. and Liang, G., “FIT and bHLH Ib transcription factors modulate iron and copper crosstalk in Arabidopsis”, ***Plant, Cell & Environment***, *44*(5), (1679-1691), 2021.

Cai, Y., Ping, H., Zhao, J., Li, C., Li, Y. and Liang, G., “IRON MAN interacts with Cu-DEFICIENCY INDUCED TRANSCRIPTION FACTOR 1 to maintain copper homeostasis”, ***New Phytologist***, *242*(3), (1206-1217), 2024.

Cailliatte, R., Schikora, A., Briat, J.F., Mari, S. and Curie, C., "High-affinity manganese uptake by the metal transporter NRAMP1 is essential for Arabidopsis growth in low manganese conditions", ***The Plant Cell***, *22*(3), (904-917), 2010.

Çalışkan, S., Aytekin, R.İ., Yağız, A.K. and Yavuz, C., "Bazı fasulye (Phaseolus vulgaris L.) çeşitlerinde tam ve kısıtlı sulama uygulamalarının tane kalitesi üzerine etkisi", ***Turkish Journal of Agriculture-Food Science and Technology***, *6*(12), (1853-1859), 2018.

Cao, J., Huang, J., Yang, Y. and Hu, X., "Analyses of the oligopeptide transporter gene family in poplar and grape", ***BMC genomics***, *12*, (1-16), 2011.

Carrió-Seguí, À., Romero, P., Curie, C., Mari, S. and Peñarrubia, L., "Copper transporter COPT5 participates in the crosstalk between vacuolar copper and iron pools mobilization", ***Scientific Reports***, *9*(1), (4648), 2019.

Castaings, L., Caquot, A., Loubet, S. and Curie, C., "The high-affinity metal transporters NRAMP1 and IRT1 team up to take up iron under sufficient metal provision" ***Scientific reports***, *6*(1), (37222), 2016.

Challam, C., Dutt, S., Sudhakar, D., Raveendran, M., Buckseth, T. and Singh, R.K., "Increase in root branching enhanced ferric-chelate reductase activity under iron stress in potato (Solanum tuberosum)", ***Indian J Agric Sci***, 91(11), (1646-9), 2021.

Chao, Z.F. and Chao, D.Y., "Similarities and differences in iron homeostasis strategies between graminaceous and nongraminaceous plants", ***New Phytologist***, 236(5), (1655-1660), 2022.

Charlson, D.V., Bailey, T.B., Cianzio, S.R. and Shoemaker, R.C., "Molecular marker Satt481 is associated with iron-deficiency chlorosis resistance in a soybean breeding population", ***Crop Science***, 45(6), (2394-2399), 2005.

Chen, H.M., Wang, Y.M., Yang, H.L., Zeng, Q.Y. and Liu, Y.J., "NRAMP1 promotes iron uptake at the late stage of iron deficiency in poplars", ***Tree Physiology***, 39(7), (1235-1250), 2019.

Chen, H.M., Wang, Y.M., Yang, H.L., Zeng, Q.Y. and Liu, Y.J., "NRAMP1 promotes iron uptake at the late stage of iron deficiency in poplars", **Tree Physiology**, *39*(7), (1235-1250), 2019.

Chen, J., Zhang, N.N., Pan, Q., Lin, X.Y., Shangguan, Z., Zhang, J.H. and Wei, G.H., "Hydrogen sulphide alleviates iron deficiency by promoting iron availability and plant hormone levels in Glycine max seedlings", ***BMC Plant Biology***, *20*, (1-22), 2020.

Chen, J., Zhang, N.N., Pan, Q., Lin, X.Y., Shangguan, Z., Zhang, J.H. and Wei, G.H., "Hydrogen sulphide alleviates iron deficiency by promoting iron availability and plant hormone levels in Glycine max seedlings", ***BMC Plant Biology***, *20*(1), (1-22), 2020.

Chen, P.F., Chen, L., Jiang, Z.R., Wang, G.P., Wang, S.H. and Ding, Y.F., "Sucrose is involved in the regulation of iron deficiency responses in rice (Oryza sativa L.)", ***Plant cell reports***, 37, (789-798), 2018.

Cheng, L., Yuan, H.Y., Ren, R., Zhao, S.Q., Han, Y.P., Zhou, Q.Y., Ke, D.X., Wang, Y.X. and Wang, L., "Genome-wide identification, classification, and expression analysis of amino acid transporter gene family in Glycine max", ***Frontiers in Plant Science***, *7*, (515), 2016.

Chia, J.C., Yan, J., Rahmati Ishka, M., Faulkner, M.M., Simons, E., Huang, R., Smieska, L., Woll, A., Tappero, R., Kiss, A. and Jiao, C., "Loss of OPT3 function decreases phloem copper levels and impairs crosstalk between copper and iron homeostasis and shoot-to-root signaling in Arabidopsis thaliana", ***The Plant Cell***, *35*(6), (2157-2185), 2023.

Chiu, C.C., Chen, L.J., Su, P.H. and Li, H.M., "Evolution of chloroplast J proteins", ***PLoS One***, *8*(7), (70384), 2013.

Chomczynski, P. and Sacchi, N., "Single-step method of RNA isolation by acid guanidinium thiocyanate-phenol-chloroform extraction", ***Analytical biochemistry***, 162(1), (156-159), 1987.

Chen, G., Li, J., Han, H., Du, R. and Wang, X., "Physiological and molecular mechanisms of plant responses to copper stress", ***International Journal of Molecular Sciences***, 23(21), (12950), 2022.

Colangelo, E.P. and Guerinot, M.L., "The essential basic helix-loop-helix protein FIT1 is required for the iron deficiency response", ***The Plant Cell***, *16*(12), (3400-3412), 2004.

Connorton, J.M., Balk, J. and Rodríguez-Celma, J., "Iron homeostasis in plants–a brief overview", ***Metallomics***, *9*(7), (813-823), 2017.

Conte, S.S. and Walker, E.L., "Genetic and biochemical approaches for studying the yellow stripe-like transporter family in plants", ***Current Topics in Membranes***, 69, (295-322), 2012.

Conte, S.S., Chu, H.H., Chan-Rodriguez, D., Punshon, T., Vasques, K.A., Salt, D.E. and Walker, E.L "Arabidopsis thaliana Yellow Stripe1-Like4 and Yellow Stripe1-Like6 localize to internal cellular membranes and are involved in metal ion homeostasis" **Frontiers in Plant Science**, 4, (283),2013.

Conte, S.S., Chu, H.H., Chan-Rodriguez, D., Punshon, T., Vasques, K.A., Salt, D.E. and Walker, E.L., "Arabidopsis thaliana Yellow Stripe1-Like4 and Yellow Stripe1-Like6 localize to internal cellular membranes and are involved in metal ion homeostasis", ***Frontiers in Plant Science***, 4, (283), 2013.

Cookson, S.J., Van Lijsebettens, M. and Granier, C., "Correlation between leaf growth variables suggest intrinsic and early controls of leaf size in Arabidopsis thaliana", ***Plant, Cell & Environment***, 28(11), (1355-1366), 2005.

Cui, M., Gu, M., Lu, Y., Zhang, Y., Chen, C., Ling, H.Q. and Wu, H., "Glutamate synthase 1 is involved in iron-deficiency response and long-distance transportation in Arabidopsis", ***Journal of Integrative Plant Biology***, 62(12), (1925-1941), 2020.

Cui, Y., Chen, C.L., Cui, M., Zhou, W.J., Wu, H.L. and Ling, H.Q., "Four IVa bHLH transcription factors are novel interactors of FIT and mediate JA inhibition of iron uptake in Arabidopsis", ***Molecular Plant***, *11*(9), (1166-1183), 2018.

Curie, C., Panaviene, Z., Loulergue, C., Dellaporta, S.L., Briat, J.F. and Walker, E.L., "Maize yellow stripe1 encodes a membrane protein directly involved in Fe (III) uptake. *Nature"*, *409*(6818), (346-349), 2001.

Curtis, M.D. and Grossniklaus, U., "A gateway cloning vector set for high-throughput functional analysis of genes in planta", **Plant physiology**, 133(2), (462-469), 2003.

Czechowski, T., Stitt, M., Altmann, T., Udvardi, M.K. and Scheible, W.R., "Genome-wide identification and testing of superior reference genes for transcript normalization in Arabidopsis", ***Plant physiology***, 139(1), (5-17), 2005.

Czechowski, T., Stitt, M., Altmann, T., Udvardi, M.K. and Scheible, W.R., "Genome-wide identification and testing of superior reference genes for transcript normalization in Arabidopsis", ***Plant physiology***, 139(1), (5-17), 2005.

Daniel-Vedele, F. and Caboche, M., "A tobacco cDNA clone encoding a GATA-1 zinc finger protein homologous to regulators of nitrogen metabolism in fungi", ***Molecular and General Genetics MGG***, 240, (365-373), 1993.

Dinesh, A., Rathod, R. and Sreedhar, M., "In silico Identification and Analysis of Iron (Fe) Transporters in Various Plant Species", ***Current Journal of Applied Science and Technology***, 39(38), (14-23), 2020.

Dinkeloo, K., Boyd, S. and Pilot, G., "Update on amino acid transporter functions and on possible amino acid sensing mechanisms in plants", **In *Seminars in cell & developmental biology*** (Vol. 74, pp. 105-113). Academic Press, 2018, February.

Dinneny, J.R., Long, T.A., Wang, J.Y., Jung, J.W., Mace, D., Pointer, S., Barron, C., Brady, S.M., Schiefelbein, J. and Benfey, P.N., "Cell identity mediates the response of Arabidopsis roots to abiotic stress", **Science**, 320(5878), (942-945), 2008.

Divol, F., Couch, D., Conéjéro, G., Roschzttardtz, H., Mari, S. and Curie, C., "The Arabidopsis YELLOW STRIPE LIKE4 and 6 transporters control iron release from the chloroplast", ***The Plant Cell***, 25(3), (1040-1055), 2013.

Donnini, S., Guidi, L., Degl'Innocenti, E. and Zocchi, G., "Image changes in chlorophyll fluorescence of cucumber leaves in response to iron deficiency and resupply", ***Journal of Plant Nutrition and Soil Science***, 176(5), (734-742), 2013.

Du, Q. and Li, W.X., "Iron biofortification in maize by ZmNAC78 is a promising and sustainable way to fight iron-deficiency anaemia", ***Clinical and Translational Medicine****, 14(1),* 2024.

Duan, X., Luo, L., Wang, Z., Wang, W., Ye, C., Jia, L., Xie, Y., Chen, J., Han, Y., Lv, Y. and Qi, W., "Promotion of root development by slightly alkaline pH involves an auxin mediated adaption mechanism", ***Soil Science and Environment***, 2(1), 2023.

Durrett, T.P., Gassmann, W. and Rogers, E.E., "The FRD3-mediated efflux of citrate into the root vasculature is necessary for efficient iron translocation", ***Plant physiology***, 144(1), (197-205), 2007.

Eisen, M.B., Spellman, P.T., Brown, P.O. and Botstein, D., "Cluster analysis and display of genome-wide expression patterns", **Proceedings of the National Academy of Sciences**, 95(25), (14863-14868), 1998.

Elkhouni, A., Rabhi, M., Ivanov, A.G., Krol, M., Zorrig, W., Smaoui, A., Abdelly, C. and Huner, N.P., "Structural and functional integrity of Sulla carnosa photosynthetic apparatus under iron deficiency conditions", ***Plant Biology***, 20(3), (415-425), 2018.

Enomoto, Y., Hodoshima, H., Shimada, H., Shoji, K., Yoshihara, T. and Goto, F., "Long-distance signals positively regulate the expression of iron uptake genes in tobacco roots", **Planta**, 227, (81-89), 2007.

Eroglu, S. and Aksoy, E., "Genome-wide analysis of gene expression profiling revealed that COP9 signalosome is essential for correct expression of Fe homeostasis genes in Arabidopsis", **Biometals**, 30(5), (685-698), 2017.

Eroglu, S., Meier, B., von Wirén, N. and Peiter, E., "The vacuolar manganese transporter MTP8 determines tolerance to iron deficiency-induced chlorosis in Arabidopsis", ***Plant physiology***, 170(2), (1030-1045), 2016.

Fang, T., Rao, Y., Wang, M., Li, Y., Liu, Y., Xiong, P. and Zeng, L., "Characterization of the SWEET gene family in longan (Dimocarpus longan) and the role of DlSWEET1 in cold tolerance", ***International Journal of Molecular Sciences***, 23(16), (8914), 2022.

Festa, R.A. and Thiele, D.J., "Copper: an essential metal in biology", ***Current Biology***, 21(21), (R877-R883), 2011.

Fourcroy, P., Sisó-Terraza, P., Sudre, D., Savirón, M., Reyt, G., Gaymard, F., Abadía, A., Abadia, J., Álvarez-Fernández, A. and Briat, J.F., "Involvement of the ABCG 37 transporter in secretion of scopoletin and derivatives by Arabidopsis roots in response to iron deficiency", **New Phytologist**, 201(1), (155-167), 2014.

Fourcroy, P., Tissot, N., Gaymard, F., Briat, J.F. and Dubos, C., "Facilitated Fe nutrition by phenolic compounds excreted by the Arabidopsis ABCG37/PDR9 transporter requires the IRT1/FRO2 high-affinity root Fe2+ transport system", ***Molecular Plant***, 9(3), (485-488), 2016.

Gamble, A.V., Howe, J.A., Delaney, D., Van Santen, E. and Yates, R., "Iron chelates alleviate iron chlorosis in soybean on high pH soils", ***Agronomy Journal***, 106(4), (1251-1257), 2014.

Gao, F., Robe, K., Bettembourg, M., Navarro, N., Rofidal, V., Santoni, V., Gaymard, F., Vignols, F., Roschzttardtz, H., Izquierdo, E. and Dubos, C., "The transcription factor bHLH121 interacts with bHLH105 (ILR3) and its closest homologs to regulate iron homeostasis in Arabidopsis", **The Plant Cell**, 32(2), (508-524), 2020.

Gao, F., Robe, K., Bettembourg, M., Navarro, N., Rofidal, V., Santoni, V., Gaymard, F., Vignols, F., Roschzttardtz, H., Izquierdo, E. and Dubos, C., "The transcription factor bHLH121 interacts with bHLH105 (ILR3) and its closest homologs to regulate iron homeostasis in Arabidopsis", ***The Plant Cell***, *32*(2), (508-524), 2020.

Gao, F., Robe, K., Gaymard, F., Izquierdo, E. and Dubos, C., "The transcriptional control of iron homeostasis in plants: a tale of bHLH transcription factors?", **Frontiers in plant science**, 10, (6), 2019.

García, M.J., Romera, F.J., Stacey, M.G., Stacey, G., Villar, E., Alcántara, E. and Pérez-Vicente, R., "Shoot to root communication is necessary to control the expression of iron-acquisition genes in Strategy I plants", ***Planta***, 237, (65-75), 2013.

Garcia-Hernandez, M., Berardini, T., Chen, G., Crist, D., Doyle, A., Huala, E., Knee, E., Lambrecht, M., Miller, N., Mueller, L.A. and Mundodi, S., "TAIR: a resource for integrated Arabidopsis data", **Functional & integrative genomics**, 2, (239-253), 2002.

Garcia-Molina, A., Andrés-Colás, N., Perea-García, A., del Valle-Tascón, S., Peñarrubia, L. and Puig, S., "The intracellular Arabidopsis COPT5 transport protein is required for photosynthetic electron transport under severe copper deficiency", ***The Plant Journal***, *65*(6), (848-860), 2011.

Garcia-Molina, A., Andrés-Colás, N., Perea-García, A., Neumann, U., Dodani, S.C., Huijser, P., Peñarrubia, L. and Puig, S., "The Arabidopsis COPT6 transport protein functions in copper distribution under copper-deficient conditions", ***Plant and Cell Physiology***, 54(8), (1378-1390), 2013.

Garcia-Molina, A., Xing, S. and Huijser, P., "A conserved KIN17 curved DNA-binding domain protein assembles with SPL7 to adapt Arabidopsis growth and development to limiting copper availability", ***Plant Physiology***, 2013.

Garcia-Molina, A., Xing, S. and Huijser, P., "A conserved KIN17 curved DNA-binding domain protein assembles with SQUAMOSA PROMOTER-BINDING PROTEIN-LIKE7 to adapt Arabidopsis growth and development to limiting copper availability", ***Plant Physiology***, 164(2), (828-840), 2014.

Garcia-Molina, A., Andrés-Colás, N., Perea-García, A., del Valle-Tascón, S., Peñarrubia, L. and Puig, S., "The intracellular Arabidopsis COPT5 transport protein is required for photosynthetic electron transport under severe copper deficiency", ***The Plant Journal***, *65*(6), (848-860), 2011.

Gautam, C.K., Tsai, H.H. and Schmidt, W., "IRONMAN tunes responses to iron deficiency in concert with environmental pH", ***Plant physiology***, 187(3), (1728-1745), 2021.

Gheshlaghi, Z., Luis-Villarroya, A., Álvarez-Fernández, A., Khorassani, R. and Abadía, J., "Iron deficient Medicago scutellata grown in nutrient solution at high pH accumulates and secretes large amounts of flavins", **Plant Science**, (110664), 2020.

Giehl, R.F. and von Wirén, N., "Root nutrient foraging", **Plant physiology**, 166(2), (509-517), 2014.

Goda, H., Sasaki, E., Akiyama, K., Maruyama-Nakashita, A., Nakabayashi, K., Li, W., Ogawa, M., Yamauchi, Y., Preston, J., Aoki, K. and Kiba, T., "The AtGenExpress hormone and chemical treatment data set: experimental design, data evaluation, model data analysis and data access", **The Plant Journal**, 55(3), (526-542), 2008.

Gong, Q., Zhou, M., Li, X. and Guo, Y., "Transcription factor MYB8 regulates iron deficiency stress response in Arabidopsis", **Plant Science**, 340, (111973), 2024.

Goos, R.J., “Laboratory and greenhouse evaluation of four iron fertilizer sources”, ***Agricultural & Environmental Letters***, *6*(4), (20052), 2021.

Grant, D., Nelson, R.T., Cannon, S.B. and Shoemaker, R.C., “SoyBase, the USDA-ARS soybean genetics and genomics database”, ***Nucleic acids research***, 38, (D843-D846), 2010.

Green, L.S. and Rogers, E.E., “FRD3 controls iron localization in Arabidopsis”, **Plant physiology**, 136(1), (2523-2531), 2004.

Grillet, L., Lan, P., Li, W., Mokkapati, G. and Schmidt, W., “IRON MAN is a ubiquitous family of peptides that control iron transport in plants”, ***Nature plants***, 4(11), (953-963), 2018.

Grillet, L., Mari, S. and Schmidt, W., “Iron in seeds–loading pathways and subcellular localization”, **Frontiers in Plant Science**, 4, (535), 2014.

Gross, J., Stein, R.J., Fett-Neto, A.G. and Fett, J.P., “Iron homeostasis related genes in rice”, ***Genetics and Molecular Biology***, 26, (477-497), 2003.

Han, D., Zhou, Z., Du, M., Li, T., Wu, X., Yu, J., Zhang, P. and Yang, G., “Overexpression of a Malus xiaojinensis WRKY transcription factor gene (MxWRKY55) increased iron and high salinity stress tolerance in Arabidopsis thaliana”, ***In Vitro Cellular & Developmental Biology-Plant***, *56*, (600-609), 2020.

Han, X.G., Bo, Y.A.N.G., Yu, D.B., Xu, C.H., Meng, F.G., Qiang, Q.I.U., Jing, Z.H.A.O., Zhang, M.H., Yan, X.Y. and Zhang, W., “Response of yield and related traits of soybean varieties with different iron efficiency to Fe-EDDHA fertilizer in calcareous iron-deficient soils”, ***Chinese Journal of Oil Crop Sciences***, 44(6), (1329-1336), 2022.

Holt, E.M., Holt, S.L., Tucker, W.F., Asplund, R.O. and Watson, K.J., “Preparation and properties of iron (III)-amino acid complexes. Iron (III)-alanine, a possible ferritin analog”, ***Journal of the American Chemical Society***, 96(8), (2621-2623), 1974.

Horton, P., Park, K.J., Obayashi, T., Fujita, N., Harada, H., Adams-Collier, C.J. and Nakai, K., "WoLF PSORT: protein localization predictor", ***Nucleic acids research***, 35, (W585-W587), 2007.

Hu, R., Fan, C., Li, H., Zhang, Q. and Fu, Y.F., "Evaluation of putative reference genes for gene expression normalization in soybean by quantitative real-time RT-PCR", ***BMC molecular biology***, 10, (1-12), 2009.

Inoue, H., Kobayashi, T., Nozoye, T., Takahashi, M., Kakei, Y., Suzuki, K., Nakazono, M., Nakanishi, H., Mori, S. and Nishizawa, N.K., "Rice OsYSL15 is an iron-regulated iron (III)-deoxymugineic acid transporter expressed in the roots and is essential for iron uptake in early growth of the seedlings", **Journal of Biological Chemistry**, 284(6), (3470-3479), 2009.

Ishimaru, Y., Masuda, H., Bashir, K., Inoue, H., Tsukamoto, T., Takahashi, M., Nakanishi, H., Aoki, N., Hirose, T., Ohsugi, R. and Nishizawa, N.K., "Rice metal-nicotianamine transporter, OsYSL2, is required for the long-distance transport of iron and manganese" ***The Plant Journal***, 62(3), (379-390), 2010.

Ishimaru, Y., Takahashi, R., Bashir, K., Shimo, H., Senoura, T., Sugimoto, K., Ono, K., Yano, M., Ishikawa, S., Arao, T. and Nakanishi, H., "Characterizing the role of rice NRAMP5 in manganese, iron and cadmium transport", ***Scientific reports***, 2(1), p.286, 2012.

Jain, A., Wilson, G.T. and Connolly, E.L., "The diverse roles of FRO family metalloreductases in iron and copper homeostasis", ***Frontiers in Plant Science***, *5*, (100), 2014.

Jean, M.L., Schikora, A., Mari, S., Briat, J.F. and Curie, C., "A loss-of-function mutation in AtYSL1 reveals its role in iron and nicotianamine seed loading", ***The Plant Journal***, *44*(5), (769-782), 2005.

Jeong, J., Merkovich, A., Clyne, M. and Connolly, E.L., "Directing iron transport in dicots: regulation of iron acquisition and translocation", ***Current opinion in plant biology***, 39, (106-113), 2017.

Jian, B., Liu, B., Bi, Y., Hou, W., Wu, C. and Han, T., "Validation of internal control for gene expression study in soybean by quantitative real-time PCR", ***BMC molecular biology***, *9*, (1-14), 2008.

Jiménez, M.R., Casanova, L., Saavedra, T., Gama, F., Suárez, M.P., Correia, P.J. and Pestana, M., "Responses of tomato (L.) plants to iron deficiency in the root zone", ***Folia Horticulturae***, 31(1), (223-234), 2019.

Jiménez, M.R., Casanova, L., Saavedra, T., Gama, F., Suárez, M.P., Correia, P.J. and Pestana, M., "Responses of tomato (L.) plants to iron deficiency in the root zone", ***Folia Horticulturae*****,** 31(1), (223-234), 2019.

Jin, C.W., You, G.Y., He, Y.F., Tang, C., Wu, P. and Zheng, S.J., "Iron deficiency-induced secretion of phenolics facilitates the reutilization of root apoplastic iron in red clover", ***Plant Physiology***, *144*(1), (278-285), 2007.

Jouvin, D., Weiss, D.J., Mason, T.F.M., Bravin, M.N., Louvat, P., Zhao, F., Ferec, F., Hinsinger, P. and Benedetti, M.F., "Stable isotopes of Cu and Zn in higher plants: evidence for Cu reduction at the root surface and two conceptual models for isotopic fractionation processes", ***Environmental science & technology***, *46*(5), (2652-2660), 2012.

Kaiser, D.E., Lamb, J.A., Bloom, P.R. and Hernandez, J.A., "Comparison of field management strategies for preventing iron deficiency chlorosis in soybean", ***Agronomy Journal***, *106*(6), (1963-1974), 2014.

Kakei, Y., Ishimaru, Y., Kobayashi, T., Yamakawa, T., Nakanishi, H. and Nishizawa, N.K., "OsYSL16 plays a role in the allocation of iron", ***Plant molecular biology***, *79*, (583-594), 2012.

Kanehisa, M. and Goto, S., "KEGG: kyoto encyclopedia of genes and genomes", ***Nucleic acids research***, 28(1), (27-30), 2000.

Kearse, M., Moir, R., Wilson, A., Stones-Havas, S., Cheung, M., Sturrock, S., Buxton, S., Cooper, A., Markowitz, S., Duran, C. and Thierer, T., "Geneious Basic: an integrated and extendable desktop software platform for the organization and analysis of sequence data", ***Bioinformatics***, 28(12), (1647-1649), 2012.

Kerkeb, L. and Kramer, U., "The role of free histidine in xylem loading of nickel in Alyssum lesbiacum and Brassica juncea", ***Plant physiology***, 131(2), (716-724), 2003.

Kilian, J., Whitehead, D., Horak, J., Wanke, D., Weinl, S., Batistic, O., D'Angelo, C., Bornberg-Bauer, E., Kudla, J. and Harter, K., "The AtGenExpress global stress expression data set: protocols, evaluation and model data analysis of UV-B light, drought and cold stress responses", ***The Plant Journal***, 50(2), (347-363), 2007.

Kim, J.Y., Loo, E.P.I., Pang, T.Y., Lercher, M., Frommer, W.B. and Wudick, M.M., "Cellular export of sugars and amino acids: role in feeding other cells and organisms", ***Plant Physiology***, 187(4), (1893-1914), 2021.

Kim, S.A. and Guerinot, M.L., "Mining iron: iron uptake and transport in plants", ***FEBS letters***, 581(12), (2273-2280), 2007.

Kim, S.A., LaCroix, I.S., Gerber, S.A. and Guerinot, M.L., "The iron deficiency response in Arabidopsis thaliana requires the phosphorylated transcription factor URI", ***Proceedings of the National Academy of Sciences***, *116*(50), (24933-24942), 2019.

Kim, S.A., Punshon, T., Lanzirotti, A., Li, L., Alonso, J.M., Ecker, J.R., Kaplan, J. and Guerinot, M.L., "Localization of iron in Arabidopsis seed requires the vacuolar membrane transporter VIT1", ***Science***, *314*(5803), (1295-1298), 2006.

Klaumann, S., Nickolaus, S.D., Fürst, S.H., Starck, S., Schneider, S., Ekkehard Neuhaus, H. and Trentmann, O., "The tonoplast copper transporter COPT5 acts as an exporter and

is required for interorgan allocation of copper in Arabidopsis thaliana", ***New Phytologist***, *192*(2), (393-404), 2006.

Klaumann, S., Nickolaus, S.D., Fürst, S.H., Starck, S., Schneider, S., Ekkehard Neuhaus, H. and Trentmann, O., "The tonoplast copper transporter COPT5 acts as an exporter and is required for interorgan allocation of copper in Arabidopsis thaliana", ***New Phytologist***, *192*(2), (393-404), 2011.

Kobayashi, T. and Nishizawa, N.K., "Iron uptake, translocation, and regulation in higher plants", ***Annual review of plant biology***, *63*(1), (131-152), 2012.

Kobayashi, T., "Understanding the complexity of iron sensing and signaling cascades in plants", **Plant and Cell Physiology**, 60(7), (1440-1446), 2019.

Kobayashi, T., Nozoye, T. and Nishizawa, N.K., "Iron transport and its regulation in plants", ***Free Radical Biology and Medicine***, 2018.

Kobayashi, T., Ogo, Y., Itai, R.N., Nakanishi, H., Takahashi, M., Mori, S. and Nishizawa, N.K., "The transcription factor IDEF1 regulates the response to and tolerance of iron deficiency in plants", ***Proceedings of the National Academy of Sciences***, 104(48), (19150-19155), 2007.

Kohlhase, D.R., McCabe, C.E., Singh, A.K., O'Rourke, J.A. and Graham, M.A., "Comparing early transcriptomic responses of 18 soybean (Glycine max) genotypes to iron stress", ***International Journal of Molecular Sciences***, *22*(21), (11643), 2021.

Kohlhase, D.R., McCabe, C.E., Singh, A.K., O'Rourke, J.A. and Graham, M.A., "Comparing early transcriptomic responses of 18 soybean (Glycine max) genotypes to iron stress", ***International Journal of Molecular Sciences***, *22*(21), (11643), 2021.

Koike, S., Inoue, H., Mizuno, D., Takahashi, M., Nakanishi, H., Mori, S. and Nishizawa, N.K., "OsYSL2 is a rice metal-nicotianamine transporter that is regulated by iron and expressed in the phloem", ***The Plant Journal***, *39*(3), (415-424), 2004.

Koiwa, H., Bressan, R.A. and Hasegawa, P.M., "Identification of plant stress-responsive determinants in Arabidopsis by large-scale forward genetic screens", ***Journal of Experimental Botany*****,** *57*(5), (1119-1128), 2006.

Kumar, A., Kaur, G., Goel, P., Bhati, K.K., Kaur, M., Shukla, V. and Pandey, A.K., "Genome-wide analysis of oligopeptide transporters and detailed characterization of yellow stripe transporter genes in hexaploid wheat", ***Functional & integrative genomics***, 19, (75-90), 2019.

Kurtz, S., "Hydroponic Testing of Iron Deficiency Chlorosis in Soybeans", 2017.

Ladwig, F., Stahl, M., Ludewig, U., Hirner, A.A., Hammes, U.Z., Stadler, R., Harter, K. and Koch, W., "Siliques are Red1 from Arabidopsis acts as a bidirectional amino acid transporter that is crucial for the amino acid homeostasis of siliques", ***Plant Physiology***, *158*(4), (1643-1655), 2012.

Lal, M., Singh, K.K., Srinivasan, G., Rathore, L.S., Naidu, D. and Tripathi, C.N., "Growth and yield responses of soybean in Madhya Pradesh, India to climate variability and change", ***Agricultural and Forest Meteorology***, 93(1), (53-70), 1999.

Lamesch, P., Berardini, T.Z., Li, D., Swarbreck, D., Wilks, C., Sasidharan, R., Muller, R., Dreher, K., Alexander, D.L., Garcia-Hernandez, M. and Karthikeyan, A.S., "The Arabidopsis Information Resource (TAIR): improved gene annotation and new tools", ***Nucleic acids research***, 40(D1), (D1202-D1210), 2012.

Lanquar, V., Lelièvre, F., Bolte, S., Hamès, C., Alcon, C., Neumann, D., Vansuyt, G., Curie, C., Schröder, A., Krämer, U. and Barbier-Brygoo, H., "Mobilization of vacuolar iron by AtNRAMP3 and AtNRAMP4 is essential for seed germination on low iron", ***The EMBO journal***, *24*(23), (4041-4051), 2005.

Larbi, A., Morales, F., Abadía, A. and Abadía, J., "Changes in iron and organic acid concentrations in xylem sap and apoplastic fluid of iron-deficient Beta vulgaris plants in response to iron resupply", ***Journal of plant physiology***, 167(4), (255-260), 2010.

Lauter, A.N.M., Rutter, L., Cook, D., O'Rourke, J.A. and Graham, M.A., "Examining short-term responses to a long-term problem: RNA-seq analyses of iron deficiency chlorosis tolerant soybean", ***International Journal of Molecular Sciences***, 21(10), (3591), 2020.

Le, C.T.T., Brumbarova, T., Ivanov, R., Stoof, C., Weber, E., Mohrbacher, J., Fink-Straube, C. and Bauer, P., "Zinc finger of Arabidopsis thaliana12 (ZAT12) interacts with FER-like iron deficiency-induced transcription factor (FIT) linking iron deficiency and oxidative stress responses", ***Plant Physiology***, *170*(1), (540-557), 2016.

Lei, R., Li, Y., Cai, Y., Li, C., Pu, M., Lu, C., Yang, Y. and Liang, G., "bHLH121 functions as a direct link that facilitates the activation of FIT by bHLH IVc transcription factors for maintaining Fe homeostasis in Arabidopsis", ***Molecular plant***, 13(4), (634-649), 2020.

Li, G., Song, H., Li, B., Kronzucker, H.J. and Shi, W., "Auxin resistant1 and PIN-FORMED2 protect lateral root formation in Arabidopsis under iron stress", ***Plant Physiology***, 169(4), (2608-2623), 2015.

Li, J., Wang, Y., Zheng, L., Li, Y., Zhou, X., Li, J., Gu, D., Xu, E., Lu, Y., Chen, X. and Zhang, W., "The intracellular transporter AtNRAMP6 is involved in Fe homeostasis in Arabidopsis", ***Frontiers in plant science***, *10*, (1124), 2019.

Li, L., Zhu, Z., Liao, Y., Yang, C., Fan, N., Zhang, J., Yamaji, N., Dirick, L., Ma, J.F., Curie, C. and Huang, C.F., "NRAMP6 and NRAMP1 cooperatively regulate root growth and manganese translocation under manganese deficiency in Arabidopsis", ***The Plant Journal***, *110*(6), (1564-1577), 2022.

Li, M., Watanabe, S., Gao, F. and Dubos, C., "Iron nutrition in plants: towards a new paradigm?" ***Plants***, *12*(2), (384), 2023.

Li, W. and Lan, P., "The understanding of the plant iron deficiency responses in Strategy I plants and the role of ethylene in this process by omic approaches", ***Frontiers in plant science***, *8*, (40), 2017.

Li, X., Zhang, H., Ai, Q., Liang, G. and Yu, D., "Two bHLH transcription factors, bHLH34 and bHLH104, regulate iron homeostasis in Arabidopsis thaliana", ***Plant physiology***, 170(4), (2478-2493), 2016.

Li, Y., Li, J., Yu, Y., Dai, X., Gong, C., Gu, D., Xu, E., Liu, Y., Zou, Y., Zhang, P. and Chen, X., "The tonoplast-localized transporter OsNRAMP2 is involved in iron homeostasis and affects seed germination in rice", ***Journal of Experimental Botany***, *72*(13), (4839-4852), 2021.

Liang, G., "Iron uptake, signaling, and sensing in plants", ***Plant Communications***, 3(5), 2022.

Liang, H., Sun, H., Shao, C., Qian, J., Lv, B., Zhu, J. and Zhang, Y., "Genome-Wide Prediction and Expression Characterization of the GATA Gene Family under Nitrogen and Phosphate Deficiency in Panax ginseng", ***Horticulturae***, *10*(3), (282), 2024.

Lichtenthaler, H.K., "Chlorophylls and carotenoids: pigments of photosynthetic biomembranes. ***In Methods in enzymology***" (350-382), 1987.

Liesch, A.M., Diaz, D.R., Martin, K.L., Olson, B.L., Mengel, D.B. and Roozeboom, K.L., "Management strategies for increasing soybean yield on soils susceptible to iron deficiency", ***Agronomy Journal***, *103*(6), (1870-1877), 2011.

Lin, S., Cianzio, S. and Shoemaker, R., "Mapping genetic loci for iron deficiency chlorosis in soybean", ***Molecular Breeding***, *3*, (219-229), 1997.

Lin, S.F., Baumer, J., Ivers, D., Cianzio, S. and Shoemaker, R., "Nutrient solution screening of Fe chlorosis resistance in soybean evaluated by molecular characterization", ***Journal of Plant Nutrition***, 23(11-12), (1915-1928), 2000.

Lindsay, W.L. and Schwab, A.P., "The chemistry of iron in soils and its availability to plants", ***Journal of Plant Nutrition***, 5(4-7), (821-840), 1982.

Ling, H.Q., Bauer, P., Bereczky, Z., Keller, B. and Ganal, M., "The tomato fer gene encoding a bHLH protein controls iron-uptake responses in roots", ***Proceedings of the National Academy of Sciences***, 99(21), (13938-13943), 2002.

Lingam, S., Mohrbacher, J., Brumbarova, T., Potuschak, T., Fink-Straube, C., Blondet, E., Genschik, P. and Bauer, P., "Interaction between the bHLH transcription factor FIT and ETHYLENE INSENSITIVE3/ETHYLENE INSENSITIVE3-LIKE1 reveals molecular linkage between the regulation of iron acquisition and ethylene signaling in Arabidopsis", ***The Plant Cell***, 23(5), (1815-1829), 2011.

Liu, T., Zeng, J., Xia, K., Fan, T., Li, Y., Wang, Y., Xu, X. and Zhang, M., "Evolutionary expansion and functional diversification of oligopeptide transporter gene family in rice", ***Rice***, 5, (1-14), 2012.

Liu, W., Huo, C., He, L., Ji, X., Yu, T., Yuan, J., Zhou, Z., Song, L., Yu, Q., Chen, J. and Chen, N., "The NtNRAMP1 transporter is involved in cadmium and iron transport in tobacco (Nicotiana tabacum)", ***Plant Physiology and Biochemistry***, 173, (59-67), 2022.

Liu, W., Karemera, N.U., Wu, T., Yang, Y., Zhang, X., Xu, X., Wang, Y. and Han, Z., "The ethylene response factor AtERF4 negatively regulates the iron deficiency response in Arabidopsis thaliana", **PLoS One**, 12(10), (0186580), 2017.

Liu, W., Li, Q., Wang, Y., Wu, T., Yang, Y., Zhang, X., Han, Z. and Xu, X., "Ethylene response factor AtERF72 negatively regulates Arabidopsis thaliana response to iron deficiency", ***Biochemical and biophysical research communications***, *491*(3), (862-868), 2017.

Liu, X. and Bush, D.R., "Expression and transcriptional regulation of amino acid transporters in plants", ***Amino acids***, 30, (113-120), 2006.

Liu, X., Cui, H., Li, A., Zhang, M. and Teng, Y., "The nitrate transporter NRT1. 1 is involved in iron deficiency responses in Arabidopsis", ***Journal of Plant Nutrition and Soil Science***, 178(4), (601-608), 2015.

Liu, X., Cui, H., Li, A., Zhang, M. and Teng, Y., "The nitrate transporter NRT1. 1 is involved in iron deficiency responses in Arabidopsis", ***Journal of Plant Nutrition and Soil Science***, 178(4), (601-608), 2015.

Liu, X.X., Zhu, X.F., Zheng, S.J. and Jin, C.W., "Beyond iron-storage pool: functions of plant apoplastic iron during stress", ***Trends in Plant Science***, *28*(8), (941-954), 2023.

Livak, K.J. and Schmittgen, T.D., "Analysis of relative gene expression data using real-time quantitative PCR and the 2− ΔΔCT method", **M*ethods***, *25*(4), (402-408), 2001.

Long, T.A., Tsukagoshi, H., Busch, W., Lahner, B., Salt, D.E. and Benfey, P.N., "The bHLH transcription factor POPEYE regulates response to iron deficiency in Arabidopsis roots", **The Plant Cell**, 22(7), (2219-2236), 2010.

López-Millán, A.F., Duy, D. and Philippar, K., "Chloroplast iron transport proteins–function and impact on plant physiology", ***Frontiers in plant science***, *7*, (178), 2016.

López-Millán, A.F., Grusak, M.A., Abadía, A. and Abadía, J., "Iron deficiency in plants: an insight from proteomic approaches", ***Frontiers in plant science***, *4*, (254), 2013.

Lubkowitz, M., "The oligopeptide transporters: a small gene family with a diverse group of substrates and functions?", ***Molecular Plant***, 4(3), (407-415), 2011.

Lucena, C., Romera, F.J., Rojas, C.L., García, M.J., Alcántara, E. and Pérez-Vicente, R., "Bicarbonate blocks the expression of several genes involved in the physiological responses to Fe deficiency of Strategy I plants", ***Functional Plant Biology***, 34(11), (1002-1009), 2007.

Ma, H., Cao, X., Shi, S., Li, S., Gao, J., Ma, Y., Zhao, Q. and Chen, Q., "Genome-wide survey and expression analysis of the amino acid transporter superfamily in potato (*Solanum tuberosum* L.)", ***Plant Physiology and Biochemistry***, 107, (164-177), 2016.

Mai, H.J., Pateyron, S. and Bauer, P., "Iron homeostasis in Arabidopsis thaliana: transcriptomic analyses reveal novel FIT-regulated genes, iron deficiency marker genes and functional gene networks", **BMC Plant Biology**, 16, (1-22), 2016.

Maqbool, A., "Investigation of physiological, biochemical and molecular responses of soybean cultivars under iron deficiency", (Master's thesis, **Niğde Ömer Halisdemir Üniversitesi/Fen Bilimleri Enstitüsü**), 2018.

Maqbool, A., Şahin, A., Bakhsh, A. and Aksoy, E., "Genome-wide identification of QTLs associated with iron deficiency tolerance in soybean reveals GATA12 as the integrator of iron signaling in roots", ***Turkish Journal of Botany***, 47(6), 511-528, 2023.

Marentes, E. and Grusak, M.A., "Iron transport and storage within the seed coat and embryo of developing seeds of pea (Pisum sativum L.)", ***Seed Science Research***, *8*(3), (367-375), 1998.

Mari, S., Bailly, C. and Thomine, S., "Handing off iron to the next generation: how does it get into seeds and what for?", **Biochemical Journal**, 477(1), (259-274), 2020.

Markova, V., Holm, C., Pinborg, A.B., Thomsen, L.L. and Moos, T., "Impairment of the developing human brain in iron deficiency: correlations to findings in experimental animals and prospects for early intervention therapy", ***Pharmaceuticals***, *12*(3), (120), 2019.

Marschner, H., "Mineral nutrition of higher plants**", 2nd (eds) Academic Press**. New York, (15-22,), 1995.

Marschner, H., Römheld, V. and Kissel, M., "Different strategies in higher plants in mobilization and uptake of iron", ***Journal of plant nutrition***, 9(3-7), (695-713), 1986.

Martins, V., Bassil, E., Hanana, M., Blumwald, E. and Gerós, H., "Copper homeostasis in grapevine: functional characterization of the Vitis vinifera copper transporter 1", ***Planta***, *240*, (91-101), 2014.

Matakiadis, T., Alboresi, A., Jikumaru, Y., Tatematsu, K., Pichon, O., Renou, J.P., Kamiya, Y., Nambara, E. and Truong, H.N., "The Arabidopsis abscisic acid catabolic gene CYP707A2 plays a key role in nitrate control of seed dormancy", ***Plant Physiology***, *149*(2), pp.949-960, 2009.

Maurer, F., Naranjo Arcos, M.A. and Bauer, P., "Responses of a triple mutant defective in three iron deficiency-induced basic helix-loop-helix genes of the subgroup Ib (2) to iron deficiency and salicylic acid", ***PLoS One***, 9(6), (e99234), 2014.

McLean, E., Cogswell, M., Egli, I., Wojdyla, D. and De Benoist, B., "Worldwide prevalence of anaemia, WHO vitamin and mineral nutrition information system 1993–2005", ***Public health nutrition***, *12*(4), (444-454), 2009.

Mendoza-Cózatl, D.G., Xie, Q., Akmakjian, G.Z., Jobe, T.O., Patel, A., Stacey, M.G., Song, L., Demoin, D.W., Jurisson, S.S., Stacey, G. and Schroeder, J.I., "OPT3 is a component of the iron-signaling network between leaves and roots and misregulation of OPT3 leads to an over-accumulation of cadmium in seeds", ***Molecular plant***, *7*(9), (1455-1469), 2014.

Mi, H., Muruganujan, A., Ebert, D., Huang, X. and Thomas, P.D., "PANTHER version 14: more genomes, a new PANTHER GO-slim and improvements in enrichment analysis tools", ***Nucleic acids research***, 47(D1), (D419-D426), 2019.

Mizoguchi, M., Umezawa, T., Nakashima, K., Kidokoro, S., Takasaki, H., Fujita, Y., Yamaguchi-Shinozaki, K. and Shinozaki, K., "Two closely related subclass II SnRK2 protein kinases cooperatively regulate drought-inducible gene expression", ***Plant and Cell Physiology***, 51(5), (842-847), 2010.

Moraghan, J.T. and Helms, T.C., "Seed iron in diverse soybean genotypes" ***Journal of plant nutrition***, 28(8), (1453-1463), 2005.

Msilini, N., Attia, H., Rabhi, M., Karray, N., Lachaal, M. and Ouerghi, Z., "Responses of two lettuce cultivars to iron deficiency", ***Experimental Agriculture***, 48(4), (523-535), 2012.

Müller, B., Fastner, A., Karmann, J., Mansch, V., Hoffmann, T., Schwab, W., Suter-Grotemeyer, M., Rentsch, D., Truernit, E., Ladwig, F. and Bleckmann, A., "Amino acid export in developing Arabidopsis seeds depends on UmamiT facilitators", ***Current Biology***, 25(23), (3126-3131, 2015.

Naeve, S.L. and Rehm, G.W., "Genotype× environment interactions within iron deficiency chlorosis-tolerant soybean genotypes", ***Agronomy journal***, 98(3), (808-814), 2006.

Nakashima, K., Fujita, Y., Katsura, K., Maruyama, K., Narusaka, Y., Seki, M., Shinozaki, K. and Yamaguchi-Shinozaki, K., "Transcriptional regulation of ABI3-and ABA-responsive genes including RD29B and RD29A in seeds, germinating embryos, and seedlings of Arabidopsis", ***Plant molecular biology***, 60, (51-68), 2006.

Nepal, M.P. and Benson, B.V., "CNL disease resistance genes in soybeans and their evolutionary divergence", ***Evolutionary Bioinformatics***, *11*, (EBO-S21782), 2015.

Nishimura, N., Yoshida, T., Kitahata, N., Asami, T., Shinozaki, K. and Hirayama, T., ABA-"Hypersensitive Germination1 encodes a protein phosphatase 2C, an essential component of abscisic acid signaling in Arabidopsis seed", ***The Plant Journal***, 50(6), (935-949), 2007.

Noor, I., Sohail, H., Zhang, D., Zhu, K., Shen, W., Pan, J., Hasanuzzaman, M., Li, G. and Liu, J., "Silencing of PpNRAMP5 improves manganese toxicity tolerance in peach (Prunus persica) seedlings", ***Journal of Hazardous Materials***, *454*, (131442), 2023.

Obayashi, T., Kinoshita, K., Nakai, K., Shibaoka, M., Hayashi, S., Saeki, M., Shibata, D., Saito, K. and Ohta, H., "ATTED-II: a database of co-expressed genes and cis elements for identifying co-regulated gene groups in Arabidopsis", ***Nucleic acids research***, *35*, (D863-D869), 2007.

Okamoto, M., Kuwahara, A., Seo, M., Kushiro, T., Asami, T., Hirai, N., Kamiya, Y., Koshiba, T. and Nambara, E., "CYP707A1 and CYP707A2, which encode abscisic acid

8′-hydroxylases, are indispensable for proper control of seed dormancy and germination in Arabidopsis", ***Plant physiology***, *141*(1), (97-107), 2006.

Olsen, R.A. and Brown, J.C., "Factors related to iron uptake by dicotyledonous and monocotyledonous plants. I. pH and reductant", ***Journal of plant nutrition***, 2(6), (629-645), 1980.

O'Rourke, J.A., Charlson, D.V., Gonzalez, D.O., Vodkin, L.O., Graham, M.A., Cianzio, S.R., Grusak, M.A. and Shoemaker, R.C., "Microarray analysis of iron deficiency chlorosis in near-isogenic soybean lines", ***Bmc Genomics***, *8*, (1-13), 2007.

Ortiz-Lopez, A., Chang, H.C. and Bush, D.R., "Amino acid transporters in plants", ***Biochimica et Biophysica Acta (BBA)-Biomembranes***, 1465(1-2), (275-280), 2000.

Palmer, C.M., Hindt, M.N., Schmidt, H., Clemens, S. and Guerinot, M.L., "MYB10 and MYB72 are required for growth under iron-limiting conditions", ***PLoS genetics***, 9(11), (e1003953), 2013.

Pattanashetti, S.K., Pandey, M.K., Naidu, G.K., Vishwakarma, M.K., Singh, O.K., Shasidhar, Y., Boodi, I.H., Biradar, B.D., Das, R.R., Rathore, A. and Varshney, R.K., "Identification of quantitative trait loci associated with iron deficiency chlorosis resistance in groundnut (Arachis hypogaea)", ***Plant Breeding***, *139*(4), (790-803), 2020.

Payne, G.G., Sumner, M.E. and Plank, C.O., "Yield and composition of soybeans as influenced by soil pH, phosphorus, zinc, and copper", ***Communications in soil science and plant analysis***, 17(3), (257-273), 1986.

Peiffer, G.A., King, K.E., Severin, A.J., May, G.D., Cianzio, S.R., Lin, S.F., Lauter, N.C. and Shoemaker, R.C., "Identification of candidate genes underlying an iron efficiency quantitative trait locus in soybean", ***Plant physiology***, 158(4), (1745-1754), 2012.

Peiffer, G.A.," *Utilization of near-isogenic lines to identify genes underlying iron-efficiency QTL*", **Iowa State University**, 2011.

Perea-García, A., Garcia-Molina, A., Andrés-Colás, N., Vera-Sirera, F., Pérez-Amador, M.A., Puig, S. and Peñarrubia, L., "Arabidopsis copper transport protein COPT2 participates in the cross talk between iron deficiency responses and low-phosphate signaling", ***Plant Physiology***, 162(1), (180-194), 2013.

Pike, S., Patel, A., Stacey, G. and Gassmann, W., "Arabidopsis OPT6 is an oligopeptide transporter with exceptionally broad substrate specificity", ***Plant and cell physiology***, 50(11), (1923-1932), 2009.

Printz, B., Lutts, S., Hausman, J.F. and Sergeant, K., "Copper trafficking in plants and its implication on cell wall dynamics", ***Frontiers in plant science***, 7, (601), 2016.

Prity, S.A., El-Shehawi, A.M., Elseehy, M.M., Tahura, S. and Kabir, A.H., "Early-stage iron deficiency alters physiological processes and iron transporter expression, along with photosynthetic and oxidative damage to sorghum", ***Saudi Journal of Biological Sciences***, *28*(8), (4770-4777), 2021.

Pu, Y., Yang, D., Yin, X., Wang, Q., Chen, Q., Yang, Y. and Yang, Y., "Genome-wide analysis indicates diverse physiological roles of the turnip (Brassica rapa var. rapa) oligopeptide transporters gene family", ***Plant diversity***, 40(2), (57-67), 2018.

Quintana, J., Bernal, M., Scholle, M., Holländer-Czytko, H., Nguyen, N.T., Piotrowski, M., Mendoza-Cózatl, D.G., Haydon, M.J. and Krämer, U., "Root-to-shoot iron partitioning in Arabidopsis requires IRON-REGULATED TRANSPORTER1 (IRT1) protein but not its iron (II) transport function", ***The Plant Journal***, 109(4), (992-1013), 2022.

Rai, S., Singh, P.K., Mankotia, S., Swain, J. and Satbhai, S.B., "Iron homeostasis in plants and its crosstalk with copper, zinc, and manganese", ***Plant Stress***, *1*, (100008), 2021.

Rajniak, J., Giehl, R.F., Chang, E., Murgia, I., von Wirén, N. and Sattely, E.S., "Biosynthesis of redox-active metabolites in response to iron deficiency in plants", ***Nature chemical biology***, 14(5), (442-450), 2018.

Ranjan, A., Sinha, R., Singla-Pareek, S.L., Pareek, A. and Singh, A.K., "Shaping the root system architecture in plants for adaptation to drought stress", ***Physiologia plantarum***, 174(2), (13651), 2022.

Ranocha, P., Dima, O., Nagy, R., Felten, J., Corratgé-Faillie, C., Novák, O., Morreel, K., Lacombe, B., Martinez, Y., Pfrunder, S. and Jin, X., "Arabidopsis WAT1 is a vacuolar auxin transport facilitator required for auxin homoeostasis", ***Nature communications***, *4*(1), (2625), 2013.

Ravet, K., Touraine, B., Boucherez, J., Briat, J.F., Gaymard, F. and Cellier, F., "Ferritins control interaction between iron homeostasis and oxidative stress in Arabidopsis", ***The Plant Journal***, 57(3), (400-412), 2009.

Ravindran, P., Verma, V., Stamm, P. and Kumar, P.P., "A novel RGL2–DOF6 complex contributes to primary seed dormancy in Arabidopsis thaliana by regulating a GATA transcription factor", ***Molecular plant***, 10(10), (1307-1320), 2017.

Reddy, I.M. and Mahoney, A.W., "Solution visible difference spectral properties of Fe3+-L-amino acid complexes at pH 6.60", ***Journal of agricultural and food chemistry***, 43(6), (1436-1443), 1995.

Rengel, Z. and Marschner, P., "Nutrient availability and management in the rhizosphere: exploiting genotypic differences", ***New Phytologist***, 168, 2005.

Reyes, J.C., Muro-Pastor, M.I. and Florencio, F.J., "The GATA family of transcription factors in Arabidopsis and rice", ***Plant physiology***, 134(4), (1718-1732), 2004.

Ricachenevsky, F.K. and Sperotto, R.A., "There and back again, or always there? The evolution of rice combined strategy for Fe uptake", ***Frontiers in plant science***, *5*, (189), 2014.

Richter, R., Behringer, C., Zourelidou, M. and Schwechheimer, C., "Convergence of auxin and gibberellin signaling on the regulation of the GATA transcription factors GNC

and GNL in Arabidopsis thaliana", ***Proceedings of the National Academy of Sciences***, *110*(32), (13192-13197), 2013.

Robe, K., Gao, F., Bonillo, P., Tissot, N., Gaymard, F., Fourcroy, P., Izquierdo, E. and Dubos, C., "Sulphur availability modulates Arabidopsis thaliana responses to iron deficiency", ***PLoS One***, 15(8), (0237998), 2020.

Robe, K., Gao, F., Bonillo, P., Tissot, N., Gaymard, F., Fourcroy, P., Izquierdo, E. and Dubos, C., "Sulphur availability modulates Arabidopsis thaliana responses to iron deficiency", ***PLoS One***, 15(8), (e0237998), 2020.

Robinson, N.J., Procter, C.M., Connolly, E.L. and Guerinot, M.L., "A ferric-chelate reductase for iron uptake from soils", ***Nature***, 397(6721), (694-697), 1999.

Robles-Aguilar, A.A., Pang, J., Postma, J.A., Schrey, S.D., Lambers, H. and Jablonowski, N.D., "The effect of pH on morphological and physiological root traits of Lupinus angustifolius treated with struvite as a recycled phosphorus source", ***Plant and soil***, *434*, (65-78), 2019.

Römheld, V. and Marschner, H., "Evidence for a specific uptake system for iron phytosiderophores in roots of grasses", ***Plant physiology***, 80(1), (175-180), 1986.

Roosta, H.R., Estaji, A. and Niknam, F., "Effect of iron, zinc and manganese shortage-induced change on photosynthetic pigments, some osmoregulators and chlorophyll fluorescence parameters in lettuce", ***Photosynthetica*****,** 56, (606-615), 2018.

Saenchai, C., Bouain, N., Kisko, M., Prom-U-Thai, C., Doumas, P. and Rouached, H., "The involvement of OsPHO1; 1 in the regulation of iron transport through integration of phosphate and zinc deficiency signaling", ***Frontiers in plant science***, 7, (396), 2016.

Salzman, R.A., Brady, J.A., Finlayson, S.A., Buchanan, C.D., Summer, E.J., Sun, F., Klein, P.E., Klein, R.R., Pratt, L.H., Cordonnier-Pratt, M.M. and Mullet, J.E., "Transcriptional profiling of sorghum induced by methyl jasmonate, salicylic acid, and

aminocyclopropane carboxylic acid reveals cooperative regulation and novel gene responses", ***Plant Physiology***, *138*(1), (352-368), 2005.

Santos, C.S., Deuchande, T. and Vasconcelos, M.W., "Molecular aspects of iron nutrition in plants", **Progress in Botany,** 81, (125-156), 2020.

Santos, C.S., Roriz, M., Carvalho, S.M. and Vasconcelos, M.W., "Iron partitioning at an early growth stage impacts iron deficiency responses in soybean plants (*Glycine max* L.)", ***Frontiers in Plant Science***, 6, (325), 2015.

Santos, C.S., Serrão, I. and Vasconcelos, M.W., "Comparative analysis of iron deficiency chlorosis responses in soybean (Glycine max) and barrel medic (*Medicago truncatula*)", ***Revista de Ciências Agrárias***, *39*(4), (538-549), 2016.

Sanz, A., Pike, S., Khan, M.A., Carrió-Seguí, À., Mendoza-Cózatl, D.G., Peñarrubia, L. and Gassmann, W., "Copper uptake mechanism of Arabidopsis thaliana high-affinity COPT transporters", ***Protoplasma***, 256(1), (161-170), 2019.

Sanz, A., Pike, S., Khan, M.A., Carrió-Seguí, À., Mendoza-Cózatl, D.G., Peñarrubia, L. and Gassmann, W., "Copper uptake mechanism of Arabidopsis thaliana high-affinity COPT transporters", ***Protoplasma***, *256*(1), (161-170), 2019.

Satbhai, S.B., Setzer, C., Freynschlag, F., Slovak, R., Kerdaffrec, E. and Busch, W., "Natural allelic variation of FRO2 modulates Arabidopsis root growth under iron deficiency", ***Nature communications***, 8(1), (1-10), 2017.

Schaaf, G., Honsbein, A., Meda, A.R., Kirchner, S., Wipf, D. and von Wirén, N., "AtIREG2 encodes a tonoplast transport protein involved in iron-dependent nickel detoxification in Arabidopsis thaliana roots", ***Journal of Biological Chemistry***, *281*(35), (25532-25540), 2006.

Schaaf, G., Ludewig, U., Erenoglu, B.E., Mori, S., Kitahara, T. and Von Wirén, N., "ZmYS1 functions as a proton-coupled symporter for phytosiderophore-and

nicotianamine-chelated metals", ***Journal of Biological Chemistry***, *279*(10), (9091-9096), 2004.

Schenkeveld, W.D.C., Dijcker, R., Reichwein, A.M., Temminghoff, E.J.M. and Van Riemsdijk, W.H., "The effectiveness of soil-applied FeEDDHA treatments in preventing iron chlorosis in soybean as a function of the o, o-FeEDDHA content", ***Plant and Soil***, 303, (161-176), 2008.

Schmidt, H., Günther, C., Weber, M., Spörlein, C., Loscher, S., Böttcher, C., Schobert, R. and Clemens, S., "Metabolome analysis of Arabidopsis thaliana roots identifies a key metabolic pathway for iron acquisition", ***PloS one***, *9*(7), (102444), 2014.

Schmutz, J., Cannon, S.B., Schlueter, J., Ma, J., Mitros, T., Nelson, W., Hyten, D.L., Song, Q., Thelen, J.J., Cheng, J. and Xu, D., "Genome sequence of the palaeopolyploid soybean", ***Nature***, *463*(7278), (178-183), 2010.

Schuler, M., Keller, A., Backes, C., Philippar, K., Lenhof, H.P. and Bauer, P., "Transcriptome analysis by GeneTrail revealed regulation of functional categories in response to alterations of iron homeostasis in Arabidopsis thaliana", ***BMC Plant Biology***, 11, (1-10), 2011.

Schuler, M., Rellán-Álvarez, R., Fink-Straube, C., Abadía, J. and Bauer, P., "Nicotianamine functions in the phloem-based transport of iron to sink organs, in pollen development and pollen tube growth in Arabidopsis", ***The Plant Cell***, 24(6), (2380-2400),2012.

Schwarz, B. and Bauer, P., "FIT, a regulatory hub for iron deficiency and stress signaling in roots, and FIT-dependent and-independent gene signatures", ***Journal of Experimental Botany***, 71(5), (1694-1705), 2020.

Schwarz, B., Azodi, C.B., Shiu, S.H. and Bauer, P., "Putative cis-regulatory elements predict iron deficiency responses in Arabidopsis roots", ***Plant Physiology***, *182*(3), (1420-1439), 2020.

Shanmugam, V., Wang, Y.W., Tsednee, M., Karunakaran, K. and Yeh, K.C., "Glutathione plays an essential role in nitric oxide-mediated iron-deficiency signaling and iron-deficiency tolerance in Arabidopsis", ***The Plant Journal***, *84*(3), (464-477), 2015.

Shoemaker, R.C., Polzin, K., Labate, J., Specht, J., Brummer, E.C., Olson, T., Young, N., Concibido, V., Wilcox, J., Tamulonis, J.P. and Kochert, G., "Genome duplication in soybean (Glycine subgenus soja)", ***Genetics***, *144*(1), (329-338), 1996.

Shultz, J.L., Kurunam, D., Shopinski, K., Iqbal, M.J., Kazi, S., Zobrist, K., Bashir, R., Yaegashi, S., Lavu, N., Afzal, A.J. and Yesudas, C.R., "The Soybean Genome Database (SoyGD): a browser for display of duplicated, polyploid, regions and sequence tagged sites on the integrated physical and genetic maps of *Glycine max*", ***Nucleic Acids Research***, 34, (D758-D765), 2006.

Shin, L.J. and Yeh, K.C., "Overexpression of Arabidopsis ATX1 retards plant growth under severe copper deficiency", ***Plant signaling & behavior***, *7*(9), (1082-1083), 2012.

Sivitz, A.B., Hermand, V., Curie, C. and Vert, G., "Arabidopsis bHLH100 and bHLH101 control iron homeostasis via a FIT-independent pathway", 2012.

Sommer, S.G., Han, E., Li, X., Rosenqvist, E. and Liu, F., "The chlorophyll fluorescence parameter Fv/Fm correlates with loss of grain yield after severe drought in three wheat genotypes grown at two CO_2 concentrations", ***Plants***, 12(3), 436, 2023.

Spielmann, J., Cointry, V., Devime, F., Ravanel, S., Neveu, J. and Vert, G., "Differential metal sensing and metal-dependent degradation of the broad spectrum root metal transporter IRT1", ***The Plant Journal***, 112(5), (1252-1265), 2022.

Stacey, M.G., Koh, S., Becker, J. and Stacey, G., "AtOPT3, a member of the oligopeptide transporter family, is essential for embryo development in Arabidopsis", ***The Plant Cell***, 14(11), (2799-2811), 2002.

Stacey, M.G., Osawa, H., Patel, A., Gassmann, W. and Stacey, G., "Expression analyses of Arabidopsis oligopeptide transporters during seed germination, vegetative growth and reproduction", ***Planta*****,** *223*, (291-305), 2006.

Stacey, M.G., Patel, A., McClain, W.E., Mathieu, M., Remley, M., Rogers, E.E., Gassmann, W., Blevins, D.G. and Stacey, G., "The Arabidopsis AtOPT3 protein functions in metal homeostasis and movement of iron to developing seeds", ***Plant physiology***, 146(2), (589), 2008.

Stringlis, I.A., Yu, K.E., Feussner, K., de Jonge, R., Van Bentum, S., Van Verk, M.C., Berendsen, R.L., Bakker, P.A., Feussner, I. and Pieterse, C.M., "MYB72-dependent coumarin exudation shapes root microbiome assembly to promote plant health", ***Proceedings of the National Academy of Sciences***, *115*(22), (E5213-E5222), 2018.

Su, H., Chu, Y., Bai, J., Gong, L., Huang, J., Xu, W., Zhang, J., Qiu, X., Xu, J. and Huang, Z., "Genome-wide identification and comparative analysis for OPT family genes in Panax ginseng and eleven flowering plants", ***Molecules***, *24*(1), (15), 2018.

Takahashi, M., "Overcoming Fe deficiency by a transgenic approach in rice", ***Plant cell, tissue and organ culture***, *72*, (211-220), 2003.

Tang, C., Robson, A.D. and Dilworth, M.J., "The role of iron in nodulation and nitrogen fixation in Lupinus angustifolius L.", ***New Phytologist***, 114(2), (173-182), 1990.

Tegeder, M., "Transporters for amino acids in plant cells: some functions and many unknowns", ***Current opinion in plant biology***, *15*(3), (315-321), 2012.

Terry, N. and Zayed, A.M., "Physiology and biochemistry of leaves under iron deficiency", **In** ***Iron Nutrition in Soils and Plants: Proceedings of the Seventh International Symposium on Iron Nutrition and Interactions in Plants, June 27–July 2, 1993, Zaragoza, Spain*** (pp. 283-294). Springer Netherlands, 1995.

Thieme, C.J., Rojas-Triana, M., Stecyk, E., Schudoma, C., Zhang, W., Yang, L., Miñambres, M., Walther, D., Schulze, W.X., Paz-Ares, J. and Scheible, W.R., "Endogenous Arabidopsis messenger RNAs transported to distant tissues", **Nature Plants**, 1(4), (1-9), 2015.

Thomine, S., Lelièvre, F., Debarbieux, E., Schroeder, J.I. and Barbier-Brygoo, H., "AtNRAMP3, a multispecific vacuolar metal transporter involved in plant responses to iron deficiency", ***The Plant Journal***, *34*(5), (685-695), 2003.

Thundathil, R.V., Holt, E.M., Holt, S.L. and Watson, K.J., "Preparation and properties of iron (III)-amino acid complexes. 2. The crystal and molecular structure of monoclinic tri-. mu. 3-oxo-triaquohexakis (glycine) triiron (III) perchlorate", ***Journal of the American Chemical Society***, 99(6), (1818-1823), 1977.

Trapnell, C., Roberts, A., Goff, L., Pertea, G., Kim, D., Kelley, D.R., Pimentel, H., Salzberg, S.L., Rinn, J.L. and Pachter, L., "Differential gene and transcript expression analysis of RNA-seq experiments with TopHat and Cufflinks", ***Nature protocols***, *7*(3), (562-578), 2012.

Tsai, H.H. and Schmidt, W., "pH-dependent transcriptional profile changes in iron-deficient Arabidopsis roots", ***BMC genomics***, 21, (1-11), 2020.

Tsai, H.H., Rodriguez-Celma, J., Lan, P., Wu, Y.C., Vélez-Bermúdez, I.C. and Schmidt, W., "Scopoletin 8-hydroxylase-mediated fraxetin production is crucial for iron mobilization", ***Plant Physiology***, 177(1), (194-207), 2018.

Tsuchiya, H., Doki, S., Takemoto, M., Ikuta, T., Higuchi, T., Fukui, K., Usuda, Y., Tabuchi, E., Nagatoishi, S., Tsumoto, K. and Nishizawa, T., "Structural basis for amino acid export by DMT superfamily transporter YddG", ***Nature***, *534*(7607), (417-420), 2016.

Tsunemitsu, Y., Genga, M., Okada, T., Yamaji, N., Ma, J.F., Miyazaki, A., Kato, S.I., Iwasaki, K. and Ueno, D., "A member of cation diffusion facilitator family, MTP11, is required for manganese tolerance and high fertility in rice", ***Planta***, *248*, (231-241), 2018.

Tucker, W.F., Asplund, R.O. and Holt, S.L., “Preparation and properties of Fe3+-amino acid complexes: Crystalline complexes with aliphatic amino acids”, ***Archives of Biochemistry and Biophysics***, *166*(2), (433-438), 1975.

UniProt Consortium, “UniProt: a hub for protein information”, ***Nucleic acids research***, 43(D1), (.D204-D212), 2015.

Van Hoewyk, D., Takahashi, H., Inoue, E., Hess, A., Tamaoki, M. and Pilon-Smits, E.A., “Transcriptome analyses give insights into selenium-stress responses and selenium tolerance mechanisms in Arabidopsis”, ***Physiologia plantarum***, 132(2), (236-253), 2008.

Vasconcelos, M., Eckert, H., Arahana, V., Graef, G., Grusak, M.A. and Clemente, T., “Molecular and phenotypic characterization of transgenic soybean expressing the Arabidopsis ferric chelate reductase gene, FRO2”, ***Planta***, *224*, (1116-1128), 2006.

Vasconcelos, M.W., Clemente, T.E. and Grusak, M.A., “Evaluation of constitutive iron reductase (AtFRO2) expression on mineral accumulation and distribution in soybean (Glycine max. L)”, ***Frontiers in plant science***, *5*, (112), 2014.

Vasconcelos, M.W., Li, G.W., Lubkowitz, M.A. and Grusak, M.A., “Characterization of the PT clade of oligopeptide transporters in rice”, ***The plant genome***, 1(2), 2008.

Vert, G., Grotz, N., Dédaldéchamp, F., Gaymard, F., Guerinot, M.L., Briat, J.F. and Curie, C., “IRT1, an Arabidopsis transporter essential for iron uptake from the soil and for plant growth”, ***The plant cell***, 14(6), (1223-1233), 2002.

Von Wiren, N., Klair, S., Bansal, S., Briat, J.F., Khodr, H., Shioiri, T., Leigh, R.A. and Hider, R.C., “Nicotianamine chelates both FeIII and FeII. Implications for metal transport in plants”, ***Plant physiology***, *119*(3), (1107-1114), 1999.

Wan, Y., King, R., Mitchell, R.A., Hassani-Pak, K. and Hawkesford, M.J., “Spatiotemporal expression patterns of wheat amino acid transporters reveal their

putative roles in nitrogen transport and responses to abiotic stress", ***Scientific Reports***, *7*(1), (5461), 2017.

Wang, L., Yao, L., Hao, X., Li, N., Qian, W., Yue, C., Ding, C., Zeng, J., Yang, Y. and Wang, X., "Tea plant SWEET transporters: expression profiling, sugar transport, and the involvement of CsSWEET16 in modifying cold tolerance in Arabidopsis", ***Plant molecular biology***, 96, (577-592), 2018.

Wang, Z., Zhang, Y., Cao, C., Liu, J., Deng, Y., Zhang, Z. and Wang, C., "TaNRAMP3 is essential for manganese transport in Triticum aestivum", ***Stress Biology***, *3*(1), (41), 2023.

Waters, B.M. and Armbrust, L.C., "Optimal copper supply is required for normal plant iron deficiency responses", ***Plant Signaling & Behavior***, *8*(12), (e26611), 2013.

Waters, B.M., Amundsen, K. and Graef, G., "Gene expression profiling of iron deficiency chlorosis sensitive and tolerant soybean indicates key roles for phenylpropanoids under alkalinity stress", ***Frontiers in plant science***, *9*, (10), 2018.

Waters, B.M., Chu, H.H., DiDonato, R.J., Roberts, L.A., Eisley, R.B., Lahner, B., Salt, D.E. and Walker, E.L., "Mutations in Arabidopsis yellow stripe-like1 and yellow stripe-like3 reveal their roles in metal ion homeostasis and loading of metal ions in seeds", ***Plant Physiology***, *141*(4), (1446-1458), 2006.

Waters, B.M., McInturf, S.A. and Amundsen, K., "Transcriptomic and physiological characterization of the fefe mutant of melon (Cucumis melo) reveals new aspects of iron–copper crosstalk", ***New Phytologist***, *203*(4), (1128-1145), 2014.

Waters, B.M., McInturf, S.A. and Stein, R.J., "Rosette iron deficiency transcript and microRNA profiling reveals links between copper and iron homeostasis in Arabidopsis thaliana", ***Journal of Experimental Botany***, *63*(16), (5903-5918), 2012.

Wiersma, J.V., "High rates of Fe-EDDHA and seed iron concentration suggest partial solutions to iron deficiency in soybean", **Agronomy Journal**, 97(3), (924-934), 2005.

Wiersma, J.V., “Iron acquisition of three soybean varieties grown at five seeding densities and five rates of Fe–EDDHA”, ***Agronomy Journal***, *99*(4), (1018-1028), 2007.

Wiersma, J.V., “Is seed iron concentration predictive of resistance to iron deficiency in soybean?”, ***Crop science***, 52(2), (471-481), 2012.

Wild, M., Davière, J.M., Regnault, T., Sakvarelidze-Achard, L., Carrera, E., Diaz, I.L., Cayrel, A., Dubeaux, G., Vert, G. and Achard, P., “Tissue-specific regulation of gibberellin signaling fine-tunes Arabidopsis iron-deficiency responses”, ***Developmental Cell***, 37(2), (190-200), 2016.

Williams, L.E. and Mills, R.F., “P1B-ATPases–an ancient family of transition metal pumps with diverse functions in plants”, ***Trends in plant science***, 10(10), (491-502), 2005.

Williams, L.E., Pittman, J.K. and Hall, J.L., “Emerging mechanisms for heavy metal transport in plants”, ***Biochimica et Biophysica Acta (BBA)-Biomembranes***, 1465(1-2), (104-126), 2000.

Wintz, H., Fox, T., Wu, Y.Y., Feng, V., Chen, W., Chang, H.S., Zhu, T. and Vulpe, C., “Expression profiles of Arabidopsis thaliana in mineral deficiencies reveal novel transporters involved in metal homeostasis”, ***Journal of Biological Chemistry***, 278(48), (47644-47653), 2003.

Wipf, D., Loqué, D., Lalonde, S. and Frommer, W.B., “Amino acid transporter inventory of the Selaginella genome”, ***Frontiers in plant science***, *3*, (36), 2012.

Wongkaew, A., Asayama, K., Kitaiwa, T., Nakamura, S.I., Kojima, K., Stacey, G., Sekimoto, H., Yokoyama, T. and Ohkama-Ohtsu, N., “AtOPT6 protein functions in long-distance transport of glutathione in Arabidopsis thaliana”, ***Plant and Cell Physiology***, *59*(7), (1443-1451), 2018.

Wu, H., Chen, C., Du, J., Liu, H., Cui, Y., Zhang, Y., He, Y., Wang, Y., Chu, C., Feng, Z. and Li, J., “Co-overexpression FIT with AtbHLH38 or AtbHLH39 in Arabidopsis-

enhanced cadmium tolerance via increased cadmium sequestration in roots and improved iron homeostasis of shoots", ***Plant physiology***, 158(2), (790-800), 2012.

Wu, M., Wu, S., Chen, Z., Dong, Q., Yan, H. and Xiang, Y., "Genome-wide survey and expression analysis of the amino acid transporter gene family in poplar", ***Tree Genetics & Genomes***, *11*, (1-20), 2015.

Wu, X., Wang, T., Song, H., Jia, Y., Ma, Q., Tao, M., Zhu, X. and Cao, S., "The transcription factor WRKY12 negatively regulates iron entry into seeds in Arabidopsis", ***Journal of Experimental Botany***, 74(1), (415-426), 2023.

Wu, Z., Zhang, C., Dai, C. and Ge, Y., "Sufficient sulfur supply promotes seedling growth, alleviates oxidation stress, and regulates iron uptake and translocation in rice", ***Biologia plantarum***, 59(4), (788-792), 2015.

Xiang, Q., Shen, K., Yu, X., Zhao, K., Gu, Y., Zhang, X., Chen, X. and Chen, Q., "Analysis of the oligopeptide transporter gene family in Ganoderma lucidum: structure, phylogeny, and expression patterns", ***Genome***, *60*(4), (293-302), 2017.

Xie, Y., Zhao, J.L., Wang, C.W., Yu, A.X., Liu, N., Chen, L., Lin, F. and Xu, H.H., "Glycinergic–fipronil uptake is mediated by an amino acid carrier system and induces the expression of amino acid transporter genes in Ricinus communis seedlings", ***Journal of Agricultural and Food Chemistry***, 64(19), (3810-3818), 2016.

Xiong, H., Kakei, Y., Kobayashi, T., Guo, X., Nakazono, M., Takahashi, H., Nakanishi, H., Shen, H., Zhang, F., Nishizawa, N.K. and Zuo, Y., "Molecular evidence for phytosiderophore-induced improvement of iron nutrition of peanut intercropped with maize in calcareous soil", ***Plant, Cell & Environment***, *36*(10), (1888-1902), 2013.

Xu, D., Sanden, N.C.H., Hansen, L.L., Belew, Z.M., Madsen, S.R., Meyer, L., Jørgensen, M.E., Hunziker, P., Veres, D., Crocoll, C. and Schulz, A., "Export of defensive glucosinolates is key for their accumulation in seeds", ***Nature***, *617*(7959), (132-138), 2023.

Xu, E., Liu, Y., Gu, D., Zhan, X., Li, J., Zhou, K., Zhang, P. and Zou, Y., "Molecular Mechanisms of Plant Responses to Copper: From Deficiency to Excess", ***International Journal of Molecular Sciences***, *25*(13), (6993), 2024.

Yamasaki, H., Hayashi, M., Fukazawa, M., Kobayashi, Y. and Shikanai, T., "SQUAMOSA promoter binding protein–like7 is a central regulator for copper homeostasis in Arabidopsis", ***The Plant Cell***, *21*(1), (347-361), 2009.

Yan, J., Chia, J.C., Sheng, H., Jung, H.I., Zavodna, T.O., Zhang, L., Huang, R., Jiao, C., Craft, E.J., Fei, Z. and Kochian, L.V., "Arabidopsis pollen fertility requires the transcription factors CITF1 and SPL7 that regulate copper delivery to anthers and jasmonic acid synthesis", ***The Plant Cell***, 29(12), (3012-3029), 2017.

Yan, J.Y., Li, C.X., Sun, L., Ren, J.Y., Li, G.X., Ding, Z.J. and Zheng, S.J., "A WRKY transcription factor regulates Fe translocation under Fe deficiency", ***Plant physiology***, 171(3), (2017-2027), 2016.

Yang, C.L., Huang, Y.T., Schmidt, W., Klein, P., Chan, M.T. and Pan, I.C., "Ethylene response factor109 attunes immunity, photosynthesis, and iron homeostasis in Arabidopsis leaves", ***Frontiers in Plant Science***, 13, (841366), 2022.

Yang, G., Wei, Q., Huang, H. and Xia, J., "Amino acid transporters in plant cells: A brief review", ***Plants***, 9(8), (967), 2020.

Yi, Y. and Guerinot, M.L., "Genetic evidence that induction of root Fe (III) chelate reductase activity is necessary for iron uptake under iron deficiency", ***The Plant Journal***, 10(5), (835-844), 1996.

Yruela, I., "Copper in plants", ***Brazilian journal of plant physiology***, 17, (145-156), 2005.

Zhai, Z., Gayomba, S.R., Jung, H.I., Vimalakumari, N.K., Piñeros, M., Craft, E., Rutzke, M.A., Danku, J., Lahner, B., Punshon, T. and Guerinot, M.L., "OPT3 is a phloem-specific

iron transporter that is essential for systemic iron signaling and redistribution of iron and cadmium in Arabidopsis", ***The Plant Cell***, 26(5), (2249-2264), 2014.

Zhang, C., Hou, Y., Hao, Q., Chen, H., Chen, L., Yuan, S., Shan, Z., Zhang, X., Yang, Z., Qiu, D. and Zhou, X., "Genome-wide survey of the soybean GATA transcription factor gene family and expression analysis under low nitrogen stress", ***PloS one***, 10(4), (e0125174), 2015.

Zhang, C., Huang, Y., Xiao, Z., Yang, H., Hao, Q., Yuan, S., Chen, H., Chen, L., Chen, S., Zhou, X. and Huang, W., "A GATA transcription factor from soybean (Glycine max) regulates chlorophyll biosynthesis and suppresses growth in the transgenic Arabidopsis thaliana", ***Plants***, *9*(8), (1036), 2020.

Zhang, J.C., Wang, X.F., Wang, X.N., Wang, F.P., Ji, X.L., An, J.P., Yang, K., Zhao, Q., You, C.X. and Hao, Y.J., "Abscisic acid alleviates iron deficiency by regulating iron distribution in roots and shoots of apple", ***Scientia Horticulturae***, *262*, (109018), 2020.

ZHANG, N.N., SHANGGUAN, Z.P. and CHEN, J., "Molecular physiological mechanism and regulation of plant responses to iron deficiency stress", ***Journal of Plant Nutrition and Fertilizers***, 24(5), (1365-1377), 2018.

Zhang, X., Zhang, D., Sun, W. and Wang, T., "The adaptive mechanism of plants to iron deficiency via iron uptake, transport, and homeostasis", ***International journal of molecular sciences***, *20*(10), (2424), 2019.

Zhao, C., Pratelli, R., Yu, S., Shelley, B., Collakova, E. and Pilot, G., "Detailed characterization of the UMAMIT proteins provides insight into their evolution, amino acid transport properties, and role in the plant", ***Journal of Experimental Botany***, *72*(18), (6400-6417), 2021.

Zhao, H., Ma, H., Yu, L., Wang, X. and Zhao, J., "Genome-wide survey and expression analysis of amino acid transporter gene family in rice (Oryza sativa L.)", ***PloS one***, *7*(11), (e49210), 2012.

Zhao, X.Q., Nie, X.L. and Xiao, X.G., "Over-expression of a tobacco nitrate reductase gene in wheat (Triticum aestivum L.) increases seed protein content and weight without augmenting nitrogen supplying", ***PloS one***, *8*(9), (e74678), 2013.

Zheng, L., Yamaji, N., Yokosho, K. and Ma, J.F., "YSL16 is a phloem-localized transporter of the copper-nicotianamine complex that is responsible for copper distribution in rice", ***The Plant Cell***, *24*(9), (3767-3782), 2012.

Zheng, L., Ying, Y., Wang, L., Wang, F., Whelan, J. and Shou, H., "Identification of a novel iron regulated basic helix-loop-helix protein involved in Fe homeostasis in Oryza sativa", ***BMC plant biology***, *10*, (1-9), 2010.

Zheng, S.J., "Iron homeostasis and iron acquisition in plants: maintenance, functions and consequences", ***Annals of botany***, *105*(5), (99-800), 2010.

Zimmermann, P., Hirsch-Hoffmann, M., Hennig, L. and Gruissem, W., "GENEVESTIGATOR. Arabidopsis microarray database and analysis toolbox", ***Plant physiology***, 136(1), (2621-2632), 2004.

Zohlen, A. and Tyler, G., "Soluble inorganic tissue phosphorus and calcicole–calcifuge behaviour of plants", ***Annals of Botany***, *94*(3), (427-432), 2004.

APPENDIX

Appendix 1. Details of the QTL regions linked with Fe deficiency in soybean.

QTL name	Parent1	Parent 2	Number of Loci	Reference	Map information			Loci positively assoc with QTL					Nearest sequence-based genetic marker			
					LG	Start	End	Homozygous female	Homozygous male	Heterozygous	Phenotypic R2	P value	5' end	position	3' end	position
Fe effic 1-1	A81356022	PI468916	272	Diers et al., 1992	A2	47.8	49.8	2.6	2.1	2.5	0.17	0.006	BARC-011635-00314	Gm08:6809647	BARC-028361-05840	Gm08:7723315
Fe effic 1-2	A81356022	PI468916	272	Diers et al., 1992	D1a	113.9	115.9	2.9	2.2	2.4	0.31	0.0002	Satt129	Gm01:55166202	BARC-018211-03157	Gm01:56113247
Fe effic 1-3	A81356022	PI468916	272	Diers et al., 1992	D1a	101.3	103.3	2.8	2.3	2.4	0.25	0.0005	Satt407	Gm01:53174848	Sat_160	Gm01:54121486
Fe effic 1-4	A81356022	PI468916	272	Diers et al., 1992	D1a	93.9	95.9	2.7	2.3	2.4	0.11	0.044	BARC-020113-04470	Gm01:52286178	BARC-039805-07589	Gm01:53429616
Fe effic 1-5	A81356022	PI468916	272	Diers et al., 1992	G	23.1	25.1	2.5	2.8	2.4	0.11	0.42	Satt217	Gm18:4713017	Sat_315	Gm18:5348175
Fe effic 2-1	A81356022	PI468916	72	Diers et al., 1992												
Fe effic 3-1	Pride B216 Fe inefficient	A15 Fe efficient	102	Lin et al., 1997	B2	72.8	98.5	2.5	2.11	2.37			Satt122	Gm14:17619136	Sat_424	Gm14:46281808
Fe effic 3-2	Pride B216 Fe inefficient	A15 Fe efficient	102	Lin et al., 1997	B2	93.5	104.7	2.41	2.13	2.4			Satt063	Gm14:45993714	BARC-039667-07534	Gm14:47205629
Fe effic 3-3	Pride B216 Fe inefficient	A15 Fe efficient	102	Lin et al., 1997	G	73	76	2.53	2.37	2.2			BARC-017185-02246	Gm18:50785143	BARC-018441-03188	Gm18:52157617
Fe effic 3-4	Pride B216 Fe inefficient	A15 Fe efficient	102	Lin et al., 1997	N	28.5	30.4	2.43	2.15	2.38			Satt159	Gm03:3197845	BARC-016199-02307	Gm03:5664735

Appendix 1. Details of the QTL regions linked with Fe deficiency in soybean **(Continue)**

Fe effic 4-1	Pride B216 Fe inefficient	A15 Fe efficient	102	Lin et al., 1997	B2	71.1	73.8	5.82	6.8	6.16			BARC-013927-01275	Gm14:16752071	BARC-056587-14511	Gm14:16256888
Fe effic 4-2	Pride B216 Fe inefficient	A15 Fe efficient	102	Lin et al., 1997	I	44	64.9	5.35	6.58	6.31			BARC-029827-06444	Gm20:24177772	Sat_104	Gm20:37789703
Fe effic 4-3	Pride B216 Fe inefficient	A15 Fe efficient	102	Lin et al., 1997	H	60.2	84.1	5.52	6.82	6.29			Sat_334	Gm12:9131428	BARC-049209-10821	Gm12:35692712
Fe effic 5-1	Anoka Fe inefficient	A7 Fe efficient	97	Lin et al., 1997	A1	42	60	2.54	2.75	2.07			BARC-020479-04634	Gm05:32322642	BARC-014463-01558	Gm05:34473339
Fe effic 5-2	Anoka Fe inefficient	A7 Fe efficient	97	Lin et al., 1997	N	58.4	74.5	2.92	1.68	2.35			Sat_033	Gm03:32837825	Satt237	Gm03:38104512
Fe effic 6-1	Anoka Fe inefficient	A7 Fe efficient	97	Lin et al., 1997	I	44	64.9	8.12	5.03	6.86			BARC-029827-06444	Gm20:24177772	Sat_104	Gm20:37789703
Fe effic 6-2	Anoka Fe inefficient	A7 Fe efficient	97	Lin et al., 1997	N	58.4	74.5	5.2	8.04	6.96			Sat_033	Gm03:32837825	Satt237	Gm03:38104512
Fe effic 7-1	Pride B216 Fe inefficient	A15 Fe efficient	102	Lin et al., 1997	G	66.6	73	2.61	2.1	2.28			Satt012	Gm18:49174114	BARC-018441-03188	Gm18:52157617
Fe effic 7-2	Pride B216 Fe inefficient	A15 Fe efficient	102	Lin et al., 1997	N	30.4	42	2.51	1.93	2.13			BARC-044085-08610	Gm03:7805399	BARC-013561-01160	Gm03:33280183
Fe effic 8-1	Pride B216 Fe inefficient	A15 Fe efficient	102	Lin et al., 1997	B2	72.13	98.5	7.88	9.11	8.15			Satt020	Gm14:41294144	Sat_424	Gm14:46281808
Fe effic 8-2	Pride B216 Fe inefficient	A15 Fe efficient	102	Lin et al., 1997	G	66.6	73	7.22	8.29	8.92			Satt012	Gm18:49174114	BARC-018441-03188	Gm18:52157617
Fe effic 8-3	Pride B216 Fe inefficient	A15 Fe efficient	102	Lin et al., 1997	H	60.2	84.1	7.65	9.35	7.93			Sat_334	Gm12:9131428	BARC-049209-10821	Gm12:35692712
Fe effic 8-4	Pride B216 Fe inefficient	A15 Fe efficient	102	Lin et al., 1997	N	30.4	42	7.78	9.56	8.93			BARC-044085-08610	Gm03:7805399	BARC-013561-01160	Gm03:33280183
Fe effic 9-1	Pride B216 Fe inefficient	A15 Fe efficient	99	Lin et al., 2000b	B1	25.2	58.9						Sat_270	Gm11:4234139	BARC-059851-16137	Gm11:24571364
Fe effic 9-2	Pride B216 Fe inefficient	A15 Fe efficient	99	Lin et al., 2000b	B2	93.5	104.7						Satt063	Gm14:45993714	BARC-039667-07534	Gm14:47205629

Appendix 1. Details of the QTL regions linked with Fe deficiency in soybean **(Continue)**

Fe effic 9-3	Pride B216 Fe inefficient	A15 Fe efficient	99	Lin et al., 2000b	G	66.6	73						Satt012	Gm18:49174114	BARC-018441-03188	Gm18:52157617
Fe effic 9-4	Pride B216 Fe inefficient	A15 Fe efficient	99	Lin et al., 2000b	LG	73.4	87.9						BARC-044913-08839	Gm19:43329322	BARC-013505-00505	Gm19:45014383
Fe effic 9-5	Pride B216 Fe inefficient	A15 Fe efficient	99	Lin et al., 2000b	N	30.4	42						BARC-044085-08610	Gm03:7805399	BARC-013561-01160	Gm03:33280183
Fe effic 10-1	Anoka Fe inefficient	A7 Fe efficient	97	Lin et al., 2000b	I	44	64.9						BARC-029827-06444	Gm20:24177772	Sat_104	Gm20:37789703
Fe effic 10-2	Anoka Fe inefficient	A7 Fe efficient	97	Lin et al., 2000b	N	58.4	74.5						Sat_033	Gm03:32837825	Satt237	Gm03:38104512
Fe effic 10-3	Anoka Fe inefficient	A7 Fe efficient	97	Lin et al., 2000b	B2	73	104.7						Sat_189	Gm14:16352945	BARC-039667-07534	Gm14:47205629
Fe effic 11-1	Pride B216 Fe inefficient	A15 Fe efficient	100	Lin et al., 2000a	B2	71.1	73.8	5.82	6.8	6.16		0.0001	BARC-013927-01275	Gm14:16752071	BARC-056587-14511	Gm14:16256888
Fe effic 11-2	Pride B216 Fe inefficient	A15 Fe efficient	100	Lin et al., 2000a	I	44	64.9	5.25	6.58	6.31		0.0001	BARC-029827-06444	Gm20:24177772	Sat_104	Gm20:37789703
Fe effic 11-3	Pride B216 Fe inefficient	A15 Fe efficient	100	Lin et al., 2000a	H	60.2	84.1	5.52	6.82	6.29		0.0001	Sat_334	Gm12:9131428	BARC-049209-10821	Gm12:35692712
Fe effic 12-1	Anoka Fe inefficient	A7 Fe efficient	97	Lin et al., 2000a	I	44	64.9	8.12	5.03	6.86		0.0001	BARC-029827-06444	Gm20:24177772	Sat_104	Gm20:37789703
Fe effic 12-2	Anoka Fe inefficient	A7 Fe efficient	97	Lin et al., 2000a	N	58.4	74.5	5.2	8.04	6.96		0.0001	Sat_033	Gm03:32837825	Satt237	Gm03:38104512
Fe effic 13-1	P9254 Low Fe chlorosis resistance	A97-770012 High Fe chlorosis resistance	24	Charlson et al., 2005	A1	94.95	96.95	2.26	2.4		4.2	0.05	BARC-060051-16321	Gm05:41877400	BARC-018681-02991	Gm05:41347323
Fe effic 13-2	P9254 Low Fe chlorosis resistance	A97-770012 High Fe chlorosis resistance	24	Charlson et al., 2005	L	53.57	55.57	1.94	2.08		11.5	0.01	BARC-059657-15973	Gm19:40154846	Satt156	Gm19:40637071
Fe effic 13-3	P9254 Low Fe chlorosis resistance	A97-770012 High Fe chlorosis resistance	24	Charlson et al., 2005	I	64.62	66.62	2.24	2.18		3.9	0.01	BARC-038869-07359	Gm20:37596189	BARC-030259-06840	Gm20:38262192
Fe effic 14-1	Anoka Fe inefficient	A7 Fe efficient	1219	Peiffer et al., 2012	N	58.38	65.82						Sat_033	Gm03:32837825	BARC-040277-07706	Gm03:36368900

Appendix 2. Experimental details of the studies used in the *in-silico* QTL analyses. [a]

QTL number	QTL name	Reference	Experimental details of the study
9	Fe effic 1-1	Diers et al., 1992	Experiments were conducted in the field on calcareous soil in the summers of 1989 and 1990 for set 1, and in 1990 for the tester set. The test field was at Ames and Humboldt, Iowa. A randomized complete block design was used. The experiment was repeated 3 times in each location. The chlorosis score was recorded at V4 or V5 stages.
1	Fe effic 1-2		
2	Fe effic 1-3		
3	Fe effic 1-4		
13	Fe effic 1-5		
-	Fe effic 2-1		
-	Fe effic 3-1	Lin et al., 1997	The experiment was conducted at Humboldt, Iowa, on calcareous soil in 1993 and 1994. A randomized complete block design was used. The experiment was repeated 3 times in each location. The chlorosis score was recorded at the V4 stage. Chlorophyll contents were measured.
-	Fe effic 3-2		
-	Fe effic 3-3		
4	Fe effic 3-4		
-	Fe effic 4-1		
-	Fe effic 4-2		
-	Fe effic 4-3		
7	Fe effic 5-1		
-	Fe effic 5-2		
-	Fe effic 6-1		
-	Fe effic 6-2		
14	Fe effic 7-1		
5	Fe effic 7-2		
-	Fe effic 8-1		
-	Fe effic 8-2		
-	Fe effic 8-3		
-	Fe effic 8-4		
10	Fe effic 9-1	Lin et al., 2000b	Four periods of nutrient solution evaluations were conducted in the greenhouse at Land O'Lakes Inc., Webster City, Iowa in 1994. A randomized complete block design was used. The experiment was repeated 2 times. Seeds were germinated on peat moss and after 7-8 days, uniform seedlings of each genotype were transplanted to plastic buckets containing 10 liters of nutrient solution. The nutrient solution was prepared with the addition of bicarbonate. The chlorosis score was recorded at V2 and V4 stages. Chlorophyll contents were measured.
-	Fe effic 9-2		
-	Fe effic 9-3		
15	Fe effic 9-4		
-	Fe effic 9-5		
17	Fe effic 10-1		
6	Fe effic 10-2		
12	Fe effic 10-3		
-	Fe effic 11-1	Lin et al., 2000a	Genotypes were evaluated at Humboldt, Iowa, on calcareous soil in 1993 and 1994. Every year, each population was evaluated for Fe efficiency using a randomized complete block design with 3 replications. The chlorosis score was recorded at the V4 stage. Chlorophyll contents were measured.
-	Fe effic 11-2		
11	Fe effic 11-3		
-	Fe effic 12-1		
-	Fe effic 12-2		
8	Fe effic 13-1	Charlson et al., 2005	Genotypes were evaluated for IDC resistance on calcareous soils at two Iowa locations, Ames and Humboldt, Iowa in 2000, 2001, and 2002. The soil pH was around 8.0. A randomized complete block design was used. The experiment was repeated 3 times in each location. The chlorosis score was recorded at the V4 stage.
16	Fe effic 13-2		
18	Fe effic 13-3		
-	Fe effic 14-1	Peiffer et al., 2012	Seeds of each genotype were sown on germination paper for 7 d before seedling transfer to a custom plant holder suspended over a 10-L foil-wrapped plastic bucket. Two replicates containing eight plants were grown under iron stress conditions [50 mM Fe(NO3) 3·9H2O]. Each 10-L bucket contained 2 mM MgSo4·7H2O, 2 mM Mg(NO3)·6H2O, 2.5 mM KNO3, 1 mM CaCl2·2H2O, 4 mM Ca(NO3)2·4H2O, 0.02 mM KH2PO4, 542.5 mM KOH, 217 mM KOH, 20 mM MnCL2·2H2O, 50 mM ZnSO4·7H2O, 50 mM CuSO4·5H2O, 0.2 mM Na2MoO4·2H2O, 1 mM CoSO4·7H2O, 1 mM NiSO4·6H2O, and 10 mM H3BO3. A 3% CO2-air mixture was used to maintain a pH level of 7.8. The greenhouse photoperiod was held constant at 14 h with a 10-h dark period for the entirety of the experiment. Chlorosis score and SPAD readings were recorded on 15th day after transfer into hydroponics at the V3 stage.

[a] All data was obtained from the SoyBase QTL database (https://soybase.org/search/qtllist_by_symbol.php#I).

Appendix 3. Master gene list.

The list can be found on the following link:

https://docs.google.com/spreadsheets/d/1zyxi1MWdLS6sIv80_RGdQNidLoU1b4w5/edit?usp=drive_link&ouid=112896432617768547301&rtpof=true&sd=true

Appendix 4. Differentially expressed genes (DEGs) in *bhlh100bhlh1001* and *pye1-1* mutants.

AGI number	Gene Name	Gene Code	Relative Expression	
DEGs in *bhlh100bhlh1001*			**In *bhlh100bhlh1001***	**In *pye1-1***
AT1G09750	aspartyl protease-like protein	-	-2.30	-
AT1G15670	KISS ME DEADLY 2	*KMD2*	3.14	-
AT1G44800	USUALLY MULTIPLE ACIDS MOVE IN AND OUT TRANSPORTERS 18	*UMAMIT18*	-3.25	-
AT1G48930	GLYCOSYL HYDROLASE 9C1	*GH9C1*	-2.49	-
AT1G49820	S-METHYL-5-THIORIBOSE KINASE	*MTK*	2.25	-
AT1G52820	putative 2-oxoglutarate-dependent dioxygenase	-	-15.67	-
AT1G55210	DIRIGENT PROTEIN 20	*DIR20*	-2.62	-
AT1G68010	HYDROXYPYRUVATE REDUCTASE	*HPR*	2.79	-
AT1G74670	GA-STIMULATED ARABIDOPSIS 6	GASA6	-4.20	-
AT1G76410	RING-H2 FINGER PROTEIN ATL8	*ATL8*	3.99	-
AT1G77760	NITRATE REDUCTASE [NADH] 1	*NIA1*	-3.67	-
AT1G78080	ETHYLENE-RESPONSIVE TRANSCRIPTION FACTOR RAP2-4	*RAP2.4*	2.10	-
AT1G78290	SNF1-RELATED PROTEIN KINASE 2C	*SRK2C*	4.83	-
AT2G15960	hypothetical protein	-	4.91	-
AT2G18050	HISTONE H1-3(HIS1-3)	*HIS1-3*	11.48	-
AT2G18470	PROLINE-RICH EXTENSIN-LIKE RECEPTOR KINASE 4	*PERK4*	-3.51	-
AT2G21100	DIRIGENT PROTEIN 23	-	-3.35	-
AT2G25735	hypothetical protein	-	4.43	-
AT2G35930	E3 UBIQUITIN-PROTEIN LIGASE PUB23	*PUB23*	3.04	-
AT2G38400	ALANINE:GLYOXYLATE AMINOTRANSFERASE 3	*AGT3*	2.09	-
AT2G39200	PROTEIN MILDEW RESISTANCE LOCUS O 12	*MLO12*	2.40	-
AT2G39700	EXPANSIN A4	*EXPA4*	-2.35	-
AT2G39730	RIBULOSE BISPHOSPHATE CARBOXYLASE/OXYGENASE ACTIVASE	*RCA*	2.03	-
AT2G40300	FERRITIN 4	*FER4*	-2.43	-
AT2G41120	hypothetical protein	-	2.01	-
AT2G42250	CYTOCHROME P450, FAMILY 712, SUBFAMILY A, POLYPEPTIDE 1	*CYP712A1*	-7.66	-
AT2G45220	PUTATIVE PECTINESTERASE/PECTINESTERASE INHIBITOR 17	*PME17*	-2.28	-
AT3G03540	NON-SPECIFIC PHOSPHOLIPASE C5	*NPC5*	-4.32	-
AT3G09920	PHOSPHATIDYL INOSITOL MONOPHOSPHATE 5 KINASE	*PIP5K9*	2.32	-
AT3G10740	BIFUNCTIONAL ALPHA-L-ARABINOFURANOSIDASE/BETA-D-XYLOSIDASE	*ASD1*	2.07	-
AT3G13650	DISEASE RESISTANCE-RESPONSIVE, DIRIGENT DOMAIN-CONTAINING PROTEIN	*DIR7*	-2.95	-
AT3G14420	PEROXISOMAL (S)-2-HYDROXY-ACID OXIDASE GLO1	*GLO1*	2.79	-
AT3G14470	NB-ARC DOMAIN-CONTAINING DISEASE RESISTANCE PROTEIN	*RPPL1*	2.03	-
AT3G15353	METALLOTHIONEIN 3	*MT3*	2.25	-
AT3G15510	NAC DOMAIN CONTAINING PROTEIN 2	*NAC2*	3.65	-
AT3G21070	NAD(H) KINASE 1	*NADK1*	2.01	-

Appendix 4. Differentially expressed genes (DEGs) in *bhlh100bhlh1001* and *pye1-1* mutants. (**Continue**)

AT3G49780	PHYTOSULFOKINE 3	*PSK3*	3.65	-
AT3G51860	VACUOLAR CATION/PROTON EXCHANGER 3	*CAX3*	6.71	-
AT3G54700	PHOSPHATE TRANSPORTER 1;7	*PHT1;7*	-2.83	-
AT4G01630	EXPANSIN A17	*EXPA17*	2.10	-
AT4G08290	NODULIN MTN21 /EAMA-LIKE TRANSPORTER FAMILY PROTEIN	-	2.12	-
AT4G10040	CYTOCHROME C-2	*CYTC-2*	-2.10	-
AT4G10310	SODIUM TRANSPORTER HKT1	*HKT1*	4.75	-
AT4G13195	PROTEIN CLAVATA3/ESR-RELATED 44	*CLE44*	2.04	-
AT4G13580	disease resistance-responsive, dirigent domain-containing protein	-	-2.06	-
AT4G19160	hypothetical protein	-	2.32	-
AT4G26010	PEROXIDASE 44	*PRX44*	-2.80	-
AT4G27410	NAC TRANSCRIPTION FACTOR RD26	*RD26*	2.50	-
AT4G28940	phosphorylase superfamily protein	-	-2.06	-
AT4G31330	hypothetical protein	-	6.33	-
AT4G35150	O-methyltransferase family protein	-	-2.39	
AT4G35160	N-ACETYLSEROTONIN O-METHYLTRANSFERASE	*ASMT1*	-2.39	-
AT4G35770	SENESCENCE-ASSOCIATED PROTEIN DIN1	*SEN1*	3.19	-
AT4G36220	FERULIC ACID 5-HYDROXYLASE 1	*FAH1*	-3.69	-
AT4G37220	cold acclimation protein WCOR413	-	2.48	-
AT5G01600	FERRITIN 1	*FER1*	-2.98	-
AT5G01740	Nuclear transport factor 2 (NTF2) family protein	-	-2.19	-
AT5G04000	hypothetical protein	-	2.32	-
AT5G06720	peroxidase 53	*PA2*	-3.78	-
AT5G10180	SULFATE TRANSPORTER 2;1	*SULTR2;1*	-3.82	-
AT5G16110	hypothetical protein	-	2.09	-
AT5G19260	FANTASTIC FOUR 3	*FAF3*	-2.33	-
AT5G24800	BASIC LEUCINE ZIPPER 9	*BZIP9*	2.11	-
AT5G26820	IRON-REGULATED PROTEIN 3	*REG3*	2.60	-
AT5G47550	CYSTEINE PROTEINASE INHIBITOR 5	*CYS5*	-2.20	-
AT5G49780	leucine-rich repeat protein kinase-like protein	-	-2.81	-
AT5G61250	GLUCURONIDASE 1	*GUS1*	2.20	-
AT5G66815	C-TERMINALLY ENCODED PEPTIDE 5	*CEP5*	-5.99	-
AT1G64980	putative nucleotide-diphospho-sugar transferase	-	-	3.53
AT1G77120	ALCOHOL DEHYDROGENASE 1	*ADH1*	-	5.82
AT2G28160	FER-LIKE IRON DEFICIENCY INDUCED TRANSCRIPTION FACTOR	*FIT*	-	2.20

Appendix 4. Differentially expressed genes (DEGs) in *bhlh100bhlh1001* and *pye1-1* mutants. (**Continue**)

AT2G45400	brassinosteroid metabolic pathway protein BEN1	-	-	2.63
AT3G21240	4-coumarate--CoA ligase 2	-	-	2.54
AT3G50930	CYTOCHROME BC1 SYNTHESIS	*BCS1*	-	2.32
AT3G58060	putative metal tolerance protein C3	*MTP8*	-	7.93
AT4G12910	serine carboxypeptidase-like 20	-	-	2.20
AT4G22890	PGR5-like protein 1A	-	-	2.05
AT4G31940	cytochrome P450, family 82, subfamily C, polypeptide 4	-	-	85.8
AT5G13630	magnesium chelatase subunit H	-	-	-2.03
AT5G58650	PLANT PEPTIDE CONTAINING SULFATED TYROSINE 1	*PSY1*	-	2.11
AT5G66985	HYPOXIA RESPONSE UNKNOWN PROTEIN 44	*HUP44*	-	2.18
AT1G77280	adenine nucleotide alpha hydrolases-domain containing protein kinase	-	2.41	3.09
AT2G42750	*DNA J PROTEINC77*	*DJC77*	3.34	3.14
AT3G47340	*GLUTAMINE-DEPENDENT ASPARAGINE SYNTHASE1 / DARK INDUCIBLE6*	*ASN1 / DIN6*	-3.77	-2.08
AT3G50740	*UDP-GLUCOSYL TRANSFERASE 72E1*	*UGT72E1*	2.39	2.16
AT3G58810	*METAL TOLERANCE PROTEIN3 / METAL TOLERANCE PROTEINA2*	*ATMTP3 / MTPA2*	5.74	2.35
AT4G27450	ALUMINUM-INDUCED PROTEIN YGL AND LRDR MOTIFS	*AIP1*	4.03	2.14
AT5G03570	IRON-REGULATED PROTEIN2 / FERROPORTIN2	*IREG2 / FPN2*	5.96	2.52
AT5G07010	*SULFOTRANSFERASE2A*	*ST2A*	2.40	2.50
AT5G25830	*GATA TRANSCRIPTION FACTOR12*	*GATA12*	2.38	2.22
AT5G67370	*CONSERVED IN THE GREEN LINEAGE AND DIATOMS27*	*CGLD27*	6.62	9.21

Appendix 5. Gene Set Enrichment Analysis (GSEA) of core group genes under abiotic stresses.

Gene Set (Number of Genes in the set)	Fe deficiency 10 d [b]	Fe deficiency 1 week [c]	Fe deficiency 24 h [d]	Fe deficiency 24 h [e]	Fe deficiency 72 h [f]	1 µM ABA 3 h [i]	0.5 µM ABA 2 days [g]	100 µM ABA 4 h [h]	300 mM Mannitol 12 h [j]	130 mM NaCl 6 h [j]
	P-value									
Core group (10)	3.2×10^{-5}	2.15×10^{-6}	5.1×10^{-4}	3.42×10^{-5}	4.25×10^{-5}	0.234	0.178	0.189	0.652	0.456
Reference (10)[a]	0.578	0.784	0.415	0.423	0.147	0.254	0.471	0.123	0.156	0.178

GSEA was performed against datasets obtained from GEO accessions GSE40076[b], GSE24348[c], GSE21582[d], GSE15189[e], GSE10576[f], E-MEXP2378[g], and E-MEXP475[h], and NASCArray accessions 176[i], 139[j], and 140[j]. * Indicates a specific gene set significantly enriched ($P<0.05$) in top-ranked genes. [a] A reference gene set contains constitutively expressed genes (Czechowski et al., 2005), and was used as a negative control.

[b] Sivitz, A.B., Hermand, V., Curie, C. and Vert, G., 2012. Arabidopsis bHLH100 and bHLH101 control iron homeostasis via a FIT-independent pathway. PloS one, 7(9), p.e44843.

[c] Schuler M et al. (2011) Transcriptome analysis by GeneTrail revealed regulation of functional categories in response to alterations of iron homeostasis in Arabidopsis thaliana. Bmc Plant Biology 11.

[d] Long TA et al. (2010) The bHLH Transcription Factor POPEYE Regulates Response to Iron Deficiency in Arabidopsis Roots. Plant Cell 22: 2219-2236.

[e] Buckhout TJ et al. (2009) Early iron-deficiency-induced transcriptional changes in Arabidopsis roots as revealed by microarray analyses. Bmc Genomics 10, 147.

[f] Dinneny JR et al. (2008) Cell identity mediates the response of Arabidopsis roots to abiotic stress. Science 320: 942-945

[g] Mizoguchi M et al. (2010) Two Closely Related Subclass II SnRK2 Protein Kinases Cooperatively Regulate Drought-Inducible Gene Expression. Plant and Cell Physiology 51: 842-847.

[h] Nishimura N et al. (2007) ABA-Hypersensitive Germination1 encodes a protein phosphatase 2C, an essential component of abscisic acid signaling in Arabidopsis seed. Plant Journal 50: 935-949.

[i] Goda H et al. (2008) The AtGenExpress hormone and chemical treatment data set: experimental design, data evaluation, model data analysis and data access. Plant Journal 55: 526-542.

[j] Kilian J et al. (2007) The AtGenExpress global stress expression data set: protocols, evaluation and model data analysis of UV-B light, drought and cold stress responses. Plant Journal 50: 347-363.

Appendix 6. Cluster analysis of the co-expression network of ten core genes.

AGI	Gene code	AGI	Gene code	AGI	Gene code	AGI	Gene code
Cluster 1		**Cluster 2**		**Cluster 4**		**Cluster 5**	
AT1G01520	*REV3*	AT1G01580	*FRO2*	AT1G03090	*MCCA*	AT1G06160	*ERF59*
AT1G10960	*FD1*	AT1G07560	-	AT1G06570	*PDS1*	AT1G07090	*LSH6*
AT1G23020	*FRO3*	AT1G09560	*GLP5*	AT1G10070	*BCAT2*	AT1G13110	*CYP71B7*
AT1G24580	-	AT1G11540	-	AT1G10585	*BHLH163*	AT1G15125	-
AT1G48300	*DGAT3*	AT1G14185	-	AT1G11260	*STP1*	AT1G16500	-
AT2G20920	-	AT1G18910	*BTSL2*	AT1G21400	-	AT1G21050	-
AT2G37200	-	AT1G29280	*WRKY65*	AT1G21920	*MRF1*	AT1G27020	-
AT2G42750	*DJC77*	AT1G73120	-	AT1G22890	*STMP2*	AT1G64170	*CHX16*
AT3G15780	-	AT1G74770	*BTSL1*	AT1G22890	*STMP2*	AT2G16380	-
AT3G17770	-	AT1G77920	*TGA7*	AT1G51780	*ILL5*	AT2G44490	*BGLU26*
AT3G18290	*BTS*	AT2G01880	*PAP7*	AT1G54100	*ALDH7B4*	AT3G04720	*PR4*
AT3G21360	-	AT2G02680	-	AT1G64660	*MGL*	AT3G04880	*DRT102*
AT3G47640	*PYE*	AT2G28160	*FIT*	AT1G71230	*CSN5*	AT3G23550	*DTX18*
AT4G00030	*FBN9*	AT2G28960	-	AT1G75450	*CKX5*	AT3G26200	*CYP71B22*
AT4G16370	*OPT3*	AT2G28970	-	AT1G79700	*WRI4*	AT3G50740	*UGT72E1*
AT4G25700	*BCH1*	AT2G35270	*GIK*	AT1G80920	*TOC12*	AT4G06746	*RAP2.9*
AT4G27990	*YLMG1-2*	AT2G43060	*IBH1*	AT2G02710	*PLP*	AT4G32290	-
AT4G31390	*ABC1K1*	AT3G04570	*AHL19*	AT2G05540	-	AT4G36920	*AP2*
AT4G38225	-	AT3G07720	-	AT2G17880	*DJC24*	AT5G07580	*ERF106*
AT5G03560	-	AT3G12820	*MYB10*	AT2G18700	*TPS11*	AT5G12170	*CLT2*
AT5G04150	*BHLH101*	AT3G12900	*S8H*	AT2G25900	*TZF1*	AT5G61160	*ACT1*
AT5G05250	-	AT3G13760	-	AT2G30600	-		
AT5G11840	*YCF36*	AT3G44510	-	AT2G31810	*AIP1*	**Cluster 6**	
AT5G13740	*ZIF1*	AT3G46330	-	AT2G38240	*JOX4*	AT1G05170	-
AT5G42760	-	AT3G47040	-	AT2G38400	*AGT3*	AT1G07590	-
AT5G44000	-	AT3G47200	-	AT2G41810	-	AT1G17550	*NHL29*
AT5G53450	*ORG1*	AT3G47210	-	AT2G45170	*ATG8E*	AT1G52080	-
AT5G67330	*NRAMP4*	AT3G51350	-	AT2G47700	*RFI2*	AT1G76380	-
AT5G67370	*CGLD27*	AT3G58810	*MTP3*	AT3G06380	*TLP9*	AT1G77280	-
		AT3G61410	-	AT3G10020	-	AT1G80300	*NTT1*
Cluster 3		AT3G44510		AT4G07820	*CAP*	AT3G15450	*AT2G32430*
AT1G01570	-	AT4G14780	-	AT3G19860	*URI*	AT2G41000	-
AT1G06980	-	AT4G16780	*HB2*	AT3G45060	*NRT2.6*	AT3G03790	*RCC1*
AT1G32760	-	AT4G19690	*IRT1*	AT3G45300	*IVDH*	AT3G09560	*PAH1*
AT2G19660	-	AT4G31940	*CYP82C4*	AT3G61060	*PP2-A13*	AT3G15450	-
AT2G28250	*NCRK*	AT5G03570	*FPN2*	AT4G15610	-	AT3G56320	*NTP7*

AT2G40620	*BZIP118*	AT5G25820	-	AT4G21680	*NRT1.8*	AT4G23050	-
AT2G45050	*GATA2*	AT5G33355	-	AT4G24040	*TRE1*	AT4G29130	*HXK1*
AT3G19370	-	AT5G43520	-	AT4G27450	-	AT5G04830	*NTF2*
AT3G58120	*BZIP61*	AT5G45070	*PP2-A8*	AT4G35770	*DIN1*	AT5G11260	*HY5*
AT3G60220	*TL4*	AT5G49850	-	AT4G37770	*ACS8*	AT5G51040	*SDHAF2*
AT3G60530	*GATA4*	AT5G56080	*NAS2*	AT4G37990	*CAD8*	AT5G53760	*MLO11*
AT4G03190	*GRH1*	AT5G63930	-	AT5G05600	*JOX2*	AT5G54800	*GPT1*
AT4G32890	*GATA9*			AT5G07010	*STA2*	AT5G60170	-
AT4G35030	-			AT5G10625	-		
AT5G02260	*EXP9*			AT5G13330	*RAP2.6L*		
AT5G02550	-			AT5G15330	*SPX4*		
AT5G04820	*OFP13*			AT5G16410	-		
AT5G05890	*UGT76C5*			AT5G19120	-		
AT5G14690	-			AT5G20250	*DIN10*		
AT5G22740	*CSLA2*			AT5G21170	*KINβ1*		
AT5G25830	*GATA12*			AT5G21940	-		
AT5G58000	*RTN21*			AT5G22920	*RZPF34*		
				AT5G28770	*BZIP63*		
				AT5G35750	*HK2*		
				AT5G43830	-		
				AT5G49450	*BZIP1*		
				AT5G56870	*BGLA4*		
				AT5G64410	*OPT4*		
				AT5G65207	-		

Appendix 7. Gene ontology enrichment of clusters obtained in co-expression analysis. Only the top 5 enriched GO terms are shown.

GO term	Fold Enrichment	raw P value
Cluster 1		
cellular response to iron ion starvation	> 100	1.39E-07
cellular iron ion homeostasis	> 100	8.93E-08
iron ion homeostasis	71.26	3.73E-07
cellular transition metal ion homeostasis	66.58	4.83E-07
transition metal ion homeostasis	53.44	4.40E-08
Cluster 2		
iron import into cell	> 100	1.37E-05
nickel cation transport	> 100	1.37E-05
iron ion import across plasma membrane	> 100	1.37E-05
regulation of iron ion transport	> 100	3.96E-07
iron ion transmembrane transport	> 100	7.25E-07
Cluster 3		
circadian rhythm	78.78	2.72E-04
positive regulation of cellular biosynthetic process	38.21	2.98E-08
cell differentiation	30.11	3.53E-06
cellular developmental process	26.53	5.83E-06
response to light stimulus	25.67	6.63E-06
Cluster 4		
valine biosynthetic process	> 100	1.95E-04
leucine metabolic process	59.09	2.52E-05
branched-chain amino acid metabolic process	43.77	1.61E-07
cellular response to nutrient levels	16.30	2.22E-06
response to starvation	14.54	4.20E-06
Cluster 5		
response to ethylene	25.43	2.27E-04
innate immune response	9.80	1.62E-03
secondary metabolic process	8.65	2.24E-02
defense response	6.86	6.52E-04
hormone-mediated signaling pathway	1.60	4.14E-02
Cluster 6		
primary root development	41.54	2.45E-02
response to far red light	31.88	3.16E-02
gibberellic acid mediated signaling pathway	30.46	3.30E-02
phosphorylation	4.51	1.07E-02
carbohydrate derivative transmembrane transporter activity	23.23	3.42E-03

Appendix 8. Transporters found in the GO enrichments analysis.

Gene number G.max	Arabidopsi Orthologs number	Gene code/ Description	Gene Name	E- value
GLYMA.05G194600	AT5G09220	*AAP2*	amino acid permease 2	0.00E+00
GLYMA.06G088200	AT1G10010	*AAP8*	amino acid permease 8	4.00E-166
GLYMA.13G119000	AT1G02520	*ABCB11/ MDR8*		0.00E+00
GLYMA.17G041200	AT3G62150	*ABCB21/PGP21*	P-GLYCOPROTEIN 21	0.00E+00
GLYMA.02G218400	AT1G58340	*ABS4, ZF14, BCD1, ZRZ*	BUSH-AND-CHLOROTIC-DWARF	0
GLYMA.11G101900	AT3G22910	*ACA13*	auto-inhibited Ca2+ ATPase 13	0
GLYMA.11G048300	AT4G37640	*ACA2*	calcium ATPase 2	0.00E+00
GLYMA.01G193600	AT2G22950	*ACA7*	auto-regulated Ca2+-ATPase 7	0.00E+00
GLYMA.01G007100	AT4G29140	*ADP1/ABS3*	ALTERED DEVELOPMENT PROGRAM 1	5.00E-96
GLYMA.15G208600	AT5G57090	*AGR1*	AGRAVITROPIC ROOT	4.00E-61
GLYMA.13G065400	AT3G47950	*AHA4*	H(+)-ATPase 4	0

Appendix 8. Transporters found in the GO enrichments analysis **(Continue)**

GLYMA.04G129200	AT5G04930	*ALA1*	aminophospholipid ATPase 1	0.00E+00
GLYMA.02G129500	AT1G68710	*ALA9*	AMINOPHOSPHOLIPID ATPASE 9	0.00E+00
GLYMA.13G275500	AT3G23560	*ALF5*	ABERRANT LATERAL ROOT FORMATION 5	1.00E-71
GLYMA.20G221400	AT4G13510	*AMT1;1*	ARABIDOPSIS THALIANA AMMONIUM TRANSPORT 1	3.00E-149
GLYMA.10G167800	AT1G64780	*AMT1;2*	ammonium transporter 1;2	0.00E+00
GLYMA.07G088200	AT3G51895	*AST12/SULTR3;1*	sulfate transporter 3;1	0.00E+00
GLYMA.13G360000	AT1G23090	*AST91/SULTR3;3*	SULFATE TRANSPORTER 91	0.00E+00
GLYMA.19G263100	AT4G13420	*ATHAK5*	ARABIDOPSIS THALIANA HIGH AFFINITY K+ TRANSPORTER 5	1.00E-140
GLYMA.01G113400	AT2G45960	*ATHH2/ PIP1;2*	PLASMA MEMBRANE INTRINSIC PROTEIN 1B	1.00E-176
GLYMA.15G015200	AT1G79900	*ATMBAC2*	ARABIDOPSIS MITOCHONDRIAL BASIC AMINO ACID CARRIER 2	1.00E-70
GLYMA.20G170400	AT4G10380	*AtNIP5;1/ NLM6 involve in boron uptake*	NOD26-LIKE INTRINSIC PROTEIN 5;1	5.00E-113
GLYMA.08G120100	AT4G18910	*ATNLM2/NIP1;2*	NOD26-LIKE INTRINSIC PROTEIN 2	NOD26-LIKE INTRINSIC PROTEIN 2

Appendix 8. Transporters found in the GO enrichments analysis **(Continue)**

GLYMA.17G115300	AT2G26690	*ATNPF6.2*		0
GLYMA.10G296600	AT4G21680	*AtNPF7.2*	NRT1/ PTR FAMILY 7.2	0
GLYMA.13G323800	AT5G60780	*ATNRT2.3*	nitrate transporter 2.3	0.00E+00
GLYMA.18G141900	AT1G12940	*ATNRT2.5/NRT2.5*	nitrate transporter2.5	0
GLYMA.12G232000	ATCG00120	*ATPA*	ATP synthase subunit alpha	0.00E+00
GLYMA.13G204800	AT4G04640	*ATPC1*	Arabidopsis chloroplast ATP synthase	0.00E+00
GLYMA.12G231900	ATCG00130	*ATPF*	ATPase F subunit.	7.00E-53
GLYMA.10G005400	AT5G46050	*ATPR3*	ARABIDOPSIS THALIANA PEPTIDE TRANSPORTER 3	8.00E-134
GLYMA.17G152300	AT2G24220	*ATPUP5*	PURINE PERMEASE 5	0.003
GLYMA.12G030100	AT2G21120	*AVI2/ENOR3*	ANTIVIRAL RNAI-DEFECTIVE 2/ENHANCER OF RDR6 3	7.00E-158
GLYMA.06G005000	AT4G38730	*AVI2H*	ANTIVIRAL RNAI-DEFECTIVE 2H	2.00E-156
GLYMA.01G216600	AT1G71870	*BIGE1A/MATE45*	MULTIDRUG AND TOXIC COMPOUND EXTRUSION 45	1.00E-148

Appendix 8. Transporters found in the GO enrichments analysis **(Continue)**

GLYMA.03G222300	AT2G47160	*BOR1*	REQUIRES HIGH BORON 1	0.00E+00
GLYMA.06G071200	AT3G62270	*BOR2*	REQUIRES HIGH BORON 2	0.00E+00
GLYMA.15G011200	AT1G15460	*BOR4*	REQUIRES HIGH BORON 4	0
GLYMA.01G055700	AT1G74810	*BOR5*	REQUIRES HIGH BORON 5	8.00E-12
GLYMA.13G358800	AT5G46800	*BOU*	A BOUT DE SOUFFLE	3.00E-38
GLYMA.09G118900	AT4G21120	*CAT1*	CATIONIC AMINO ACID TRANSPORTER 1	5.00E-156
GLYMA.19G116500	AT1G58030	*CAT2*	CATIONIC AMINO ACID TRANSPORTER 2	0.00E+00
GLYMA.17G148600	AT3G10600	*CAT7*	cationic amino acid transporter 7	1.00E-177
GLYMA.02G226500	AT3G13320	*CAX2*	cation exchanger 2	3.00E-93
GLYMA.18G063200	AT3G51860	*CAX3*	Cation Exchanger 3	2.00E-133
GLYMA.14G193400	AT5G01490	*CAX4*	cation exchanger 4	1.00E-135
GLYMA.19G066700	AT5G17860	*CAX7*	calcium exchanger 7	7.00E-33

Appendix 8. Transporters found in the GO enrichments analysis **(Continue)**

GLYMA.19G117200	AT5G17850	*CCX2*	CATION/CA2+EXCHANGER2	3.00E-122
GLYMA.06G138300	AT5G44650	*CEST*	CHLOROPLAST PROTEIN-ENHANCING STRESS TOLERANCE	0.15
GLYMA.12G008100	AT2G13620	*CHX15*	cation/hydrogen exchanger 15	1.00E-83
GLYMA.09G228400	AT3G52080	*chx28*	ation/hydrogen exchanger 28	0.00E+00
GLYMA.19G089800	AT5G40890	*CLCA/CLC-A*	CHLORIDE CHANNEL A	0
GLYMA.16G057600	AT3G27170	*CLC-B*	Chloride channel B	0.00E+00
GLYMA.02G059200	AT5G66650	*CMCU*	CHLOROPLAST-LOCALIZED MITOCHONDRIAL CALCIUM UNIPORTER	3.00E-98
GLYMA.04G076400	AT2G24610	*CNGC14*	CYCLIC NUCLEOTIDE-GATED CHANNEL 14	0.00E+00
GLYMA.07G263300	AT4G22120	*CSC1*	CALCIUM PERMEABLE STRESS-GATED CATION CHANNEL 1	0.00E+00
GLYMA.13G356000	AT3G16240	*DELTA-TIP*	DELTA TONOPLAST INTEGRAL PROTEIN	0.00E+00
GLYMA.04G092100	AT2G22500	*DIC1 /UCP5*	DICARBOXYLATE CARRIER 1	2.00E-141
GLYMA.02G040700	AT4G24570	*DIC2*	dicarboxylate carrier 2	3.00E-110

Appendix 8. Transporters found in the GO enrichments analysis **(Continue)**

GLYMA.02G090100	AT2G04040	*DTX1*	detoxification 1	2.00E-173
GLYMA.14G078000	AT1G47530	*DTX33*	MATE efflux family protein	1.00E-163
GLYMA.20G162000	AT4G25640	*DTX35*	detoxifying efflux carrier 35	0
GLYMA.16G198700	AT5G52050	*DTX50*	DETOXIFICATION EFFLUX CARRIER 50	1.00E-161
GLYMA.10G239000	AT5G19700	*ELS1*	EARLY LEAF SENESCENCE 1	9.00E-159
GLYMA.17G115600	AT4G32400	*EMB42/SHS1/BT1*	ARABIDOPSIS THALIANA BRITTLE 1	7.00E-108
GLYMA.20G206900	AT1G35350	*ERD1/XPR1/SYG1*		4.00E-151
GLYMA.15G091600	AT1G30360	*ERD4*	early-responsive to dehydration 4	0.00E+00
GLYMA.04G252000	AT2G41705	*FEX*	FLUORIDE EXPORT PROTEIN	6.00E-45
GLYMA.12G237400	AT3G08040	*FRD3*	FERRIC REDUCTASE DEFECTIVE 3	0.00E+00
GLYMA.12G013200	AT3G47420	*G3Pp1/ PS3*	GLYCEROL-3-PHOSPHATE PERMEASE 1/PHOSPHATE STARVATION-INDUCED GENE 3	0.00E+00
GLYMA.09G223700	AT4G25220	*G3Pp2*	GLYCEROL-3-PHOSPHATE PERMEASE 2	0.00E+00

Appendix 8. Transporters found in the GO enrichments analysis **(Continue)**

GLYMA.09G096500	AT2G13100	*G3Pp5*	glycerol-3-phosphate permease 5	0
GLYMA.02G275800	AT3G20320	*GD2/ABCI15/TGD2*	TRIGALACTOSYLDIACYLGLYCEROL2	9.00E-51
GLYMA.16G061800	AT5G11210	*GLR2.5*	glutamate receptor 2.5	1.00E-118
GLYMA.07G226500	AT2G29110	*GLR2.8*	glutamate receptor 2.8	0.00E+00
GLYMA.13G039200	AT1G21360	*GLTP2*	glycolipid transfer protein 2	4.00E-78
GLYMA.08G312400	AT5G54800	*GPT1*	GLUCOSE 6-PHOSPHATE/PHOSPHATE TRANSLOCATOR 1	0.00E+00
GLYMA.15G105900	AT1G61800	*GPT2*	PHOSPHATE TRANSLOCATOR 2	0.00E+00
GLYMA.07G130100	AT4G10310	*HKT1*	HIGH-AFFINITY K+ TRANSPORTER 1	6.00E-80
GLYMA.19G140000	AT1G63440	*HMA5*	heavy metal atpase 5	0.00E+00
GLYMA.05G132900	AT5G44790	*HMA7/ AtHMP51*	HEAVY METAL ASSOCIATED PROTEIN 51	0.00E+00
GLYMA.08G013600	AT5G21930	*HMA8*	HEAVY METAL ATPASE 8	5.00E-115
GLYMA.17G067300	AT4G12400	*Hop3*	Hop3	0.55

Appendix 8. Transporters found in the GO enrichments analysis **(Continue)**

GLYMA.11G066500	AT2G43330	*INT1*	INOSITOL TRANSPORTER 1	7.00E-55
GLYMA.10G099900	AT1G51340	***Involve in citrate transport***	-	7.00E-175
GLYMA.08G232100	AT5G46240	*KAT1*	POTASSIUM CHANNEL IN ARABIDOPSIS THALIANA 1	0
GLYMA.14G126500	AT2G26650	*KT1*	K+ transporter 1	0.00E+00
GLYMA.18G136500	AT1G70300	*KUP6*	K+ uptake permease 6	0.00E+00
GLYMA.19G076800	AT5G40780	*LHT1*	lysine histidine transporter 1	0
GLYMA.16G062500	AT1G24400	*LHT2*	lysine histidine transpoter 2	0.00E+00
GLYMA.19G083900	AT3G01760	*LHT6*	lysine-histidine-like transporter 6	0.00E+00
GLYMA.12G023100	AT4G35180	*LHT7*	LYS/HIS TRANSPORTER 7	1.00E-23
GLYMA.02G238500	AT1G09575	*MCU1*	MITOCHONDRIAL CALCIUM UPTAKE1	6.00E-99
GLYMA.14G207400	AT1G57610	*MCU2*	MITOCHONDRIAL CALCIUM UPTAKE2	1.00E-66
GLYMA.18G012700	AT3G28345	*MDR13*	multi-drug resistance 13	0.00E+00

Appendix 8. Transporters found in the GO enrichments analysis **(Continue)**

GLYMA.15G005200	AT3G19640	*MGT4*	Magnesium Transporter 4	1.00E-21
GLYMA.19G087200	AT5G20090	*MPC1*	MITOCHONDRIAL PYRUVATE CARRIER 1	6.00E-43
GLYMA.16G146700	AT5G14040	*MPT3*	MITOCHONDRIAL PHOSPHATE TRANSPORTER 3	1.00E-168
GLYMA.10G227400	AT3G59140	*MRP14*	MULTIDRUG RESISTANCE-ASSOCIATED PROTEIN 14	0
GLYMA.16G172600	AT3G13080	*MRP3*	MULTIDRUG RESISTANCE PROTEIN 3	0.00E+00
GLYMA.16G172500	AT1G04120	*MRP5*	MULTIDRUG RESISTANCE-ASSOCIATED PROTEIN 5	0.00E+00
GLYMA.20G165000	AT3G21250	*MRP6*	MULTIDRUG RESISTANCE-ASSOCIATED PROTEIN 6	0
GLYMA.08G190700	AT3G13100	*MRP7*	MULTIDRUG RESISTANCE-ASSOCIATED PROTEIN 7	0.00E+00
GLYMA.03G101000	AT3G60160	*MRP9*	MULTIDRUG RESISTANCE-ASSOCIATED PROTEIN 9	0.00E+00
GLYMA.09G122600	AT2G39450	*MTP11*	MTP11	2.00E-129
GLYMA.14G206600	AT3G58060	*MTP8*		2.00E-113
GLYMA.12G181900	AT2G27810	*NAT12*	NUCLEOBASE-ASCORBATE TRANSPORTER 12	0.00E+00

Appendix 8. Transporters found in the GO enrichments analysis **(Continue)**

GLYMA.13G272000	AT1G53210	*NCL*	Na+/Ca2+ exchanger	0.00E+00
GLYMA.20G247400	AT5G19640	*NFP7.1*		0.00E+00
GLYMA.09G238200	AT5G37820	*NIP4;2/NLM5*	NOD26-LIKE INTRINSIC PROTEIN 4;2/NODULIN- 26-LIKE MAJOR INTRINSIC PROTEIN 5	5.00E-65
GLYMA.05G162500	AT4G19030	*NLM1/NIP1;1*	NOD26-LIKE INTRINSIC PROTEIN 1;1/ NOD26-LIKE MAJOR INTRINSIC PROTEIN 1	2.00E-112
GLYMA.05G155500	AT5G37810	*NLM4/NIP4;1*	NOD26-LIKE INTRINSIC PROTEIN 4;1/NOD26-LIKE MIP 4	1.00E-91
GLYMA.18G259500	AT3G06100	*NLM8/NIP7;1/NLM6*	NOD26-LIKE INTRINSIC PROTEIN 7;1	6.00E-46
GLYMA.17G096200	AT5G62680	*NPF2.11/GTR2*	GLUCOSINOLATE TRANSPORTER-2	0
GLYMA.05G030300	AT5G28470	*NPF2.8 /FST1*	FLAVONOL SOPHOROSIDE TRANSPORTER 1	5.00E-48
GLYMA.13G116900	AT1G27040	*NPF4.5*	NRT1/ PTR FAMILY 4.5	1.00E-109
GLYMA.05G029900	AT1G69850	*NPF4.6*	NRT1/ PTR FAMILY 4.6	0
GLYMA.18G033900	AT1G22540	*NPF5.10*		5.00E-111
GLYMA.17G139400	AT1G12110	*NPF6.3/NRT1*	NRT1/ PTR FAMILY 6.3/Nitrate transporter 1	0

Appendix 8. Transporters found in the GO enrichments analysis **(Continue)**

GLYMA.18G260000	AT3G54140	*NPF8.1*	NRT1/ PTR FAMILY 8.1	5.00E-162
GLYMA.03G165900	AT5G01180	*NPF8.2*	NRT1/ PTR FAMILY 8.2	9.00E-175
GLYMA.05G136300	AT2G02040	*NPF8.3/PTR2*	PEPTIDE TRANSPORTER 2	0.00E+00
GLYMA.09G237600	AT2G02020	*NPF8.4/PTR4*	NRT1/ PTR FAMILY 8.4, PEPTIDE TRANSPORTER 4	4.00E-119
GLYMA.04G220700	AT1G62200	*NPF8.5/PTR6*	NRT1/ PTR FAMILY 8.5/PEPTIDE TRANSPORTER 6	2.00E-132
GLYMA.06G115800	AT1G80830	*NRAMP1*	NATURAL RESISTANCE-ASSOCIATED MACROPHAGE PROTEIN 1	5.00E-67
GLYMA.05G101700	AT1G47240	*NRAMP2*	NRAMP METAL ION TRANSPORTER 2	0.00E+00
GLYMA.17G165200	AT2G23150	*NRAMP3*	NATURAL RESISTANCE-ASSOCIATED MACROPHAGE PROTEIN 3	0.00E+00
GLYMA.07G023600	AT5G67330	*NRAMP4*	NATURAL RESISTANCE ASSOCIATED MACROPHAGE PROTEIN 4	2.00E-105
GLYMA.08G218200	AT1G15960	*NRAMP6*	NRAMP METAL ION TRANSPORTER 6	0
GLYMA.08G037200	AT1G52190	*NRT1.11*	NITRATE TRANSPORTER 1.11	0.00E+00
GLYMA.14G138200	AT3G16180	*NRT1.12*	nitrate transporter 1.12	7.00E-177

Appendix 8. Transporters found in the GO enrichments analysis **(Continue)**

GLYMA.17G153300	AT1G32450	*NRT1.5*	NITRATE TRANSPORTER 1.5	0
GLYMA.01G200100	AT1G69870	*NRT1.7/AtNPF2.13/NPF2.13*	NITRATE TRANSPORTER 1.7	4.00E-90
GLYMA.11G195200	AT5G60770	*NRT2.4*	ARABIDOPSIS THALIANA NITRATE TRANSPORTER 2.4	0.00E+00
GLYMA.09G166400	AT1G73220	*OCT1,*	ORGANIC CATION/CARNITINE TRANSPORTER1	4.00E-55
GLYMA.16G216500	AT1G79360	*OCT2,*	ORGANIC CATION TRANSPORTER 2	1.00E-96
GLYMA.02G149300	AT1G16390	*OCT3,*	ORGANIC CATION/CARNITINE TRANSPORTER 3	0.00E+00
GLYMA.02G301800	AT5G55930	*OPT1*	ARABIDOPSIS THALIANA OLIGOPEPTIDE TRANSPORTER 1	0.00E+00
GLYMA.19G142200	AT5G55930	*OPT1*	OLIGOPEPTIDE TRANSPORTER 1	9E-54
GLYMA.07G267800	AT4G16370	*OPT3*	OLIGOPEPTIDE TRANSPORTER	0
GLYMA.14G028700	AT4G26590	*OPT5*	OLIGOPEPTIDE TRANSPORTER 5	9E-52
GLYMA.20G066800	AT4G04340	*OSCA1*	INDUCED CA2+ INCREASE 1	0.00E+00
GLYMA.13G220900	AT4G02900	*OSCA1.7*		7.00E-92

Appendix 8. Transporters found in the GO enrichments analysis **(Continue)**

GLYMA.06G139500	AT3G28390	*PGP18/*	P-GLYCOPROTEIN 18	8.00E-24
GLYMA.02G130200	AT1G68740	*PHO1*	PHO1	0.00E+00
GLYMA.10G004800	AT3G23430	*PHO1*	phosphate 1	0.00E+00
GLYMA.18G261900	AT1G26730	*PHO1;H3*	PHO1 homolog 3	0.00E+00
GLYMA.13G040200	AT5G43350	*PHT1;1/PT1*	PHOSPHATE TRANSPORTER 1	0.00E+00
GLYMA.02G005800	AT5G43370	*PHT1;2/PHT2*	PHOSPHATE TRANSPORTER 2	0
GLYMA.10G006700	AT5G43360	*PHT1;3/PHT3*	PHOSPHATE TRANSPORTER 3	0
GLYMA.20G204100	AT2G38940	*PHT1;4*	phosphate transporter 1;4	0
GLYMA.19G164300	AT2G32830	*PHT1;5/ PHT5*	phosphate transporter 1;5	0.00E+00
GLYMA.10G186500	AT5G43340	*PHT1;6/PHT6*	phosphate transporter 1;6	0
GLYMA.03G162800	AT3G54700	*PHT1;7*	phosphate transporter 1;7	0.00E+00
GLYMA.07G222700	AT1G20860	*PHT1;8*	PHOSPHATE TRANSPORTER 1;8	1.00E-48

Appendix 8. Transporters found in the GO enrichments analysis **(Continue)**

GLYMA.10G036800	AT1G76430	*PHT1;9*	phosphate transporter 1;9	2.00E-164
GLYMA.18G228700	AT4G11810	*PHT5;2*	transports Pi into the vacuole	0.00E+00
GLYMA.16G158200	AT2G39210	*PIC30*	PICLORAM RESISTANT30	0.00E+00
GLYMA.18G241000	AT5G16530	*PIN5*	PIN-FORMED 5	2.00E-121
GLYMA.09G251600	AT5G15100	*PIN8*	PIN-FORMED 8	2.00E-64
GLYMA.11G097800	AT3G61430	*PIP1*	PLASMA MEMBRANE INTRINSIC PROTEIN 1	2.00E-14
GLYMA.12G023700	AT3G53420	*PIP2A*	PLASMA MEMBRANE INTRINSIC PROTEIN 2	7.00E-15
GLYMA.14G153900	AT4G35100	*PIP3*	PLASMA MEMBRANE INTRINSIC PROTEIN 3	5.00E-47
GLYMA.01G174400	AT4G36670	*PLT6/PMT6*	POLYOL/MONOSACCHARIDE TRANSPORTER 6	3.00E-168
GLYMA.11G066100	AT2G16120	*PMT1*	POLYOL/MONOSACCHARIDE TRANSPORTER 1	4.00E-138
GLYMA.11G066000	AT3G18830	*PMT5*	POLYOL/MONOSACCHARIDE TRANSPORTER 5	5.00E-146
GLYMA.02G106100	AT3G05290	*PNC1*	PEROXISOMAL ADENINE NUCLEOTIDE CARRIER 1	1.00E-162

Appendix 8. Transporters found in the GO enrichments analysis **(Continue)**

GLYMA.17G088500	AT5G33320	*PPT*	PHOSPHATE/PHOSPHOENOLPYRUVATE TRANSLOCATOR	2.00E-171
GLYMA.10G032700	AT2G39890	*PROT1*	Proline transporter 1	1.00E-54
GLYMA.11G226000	AT3G55740	*PROT2*	PROLINE TRANSPORTER 2	0
GLYMA.05G069700	AT1G44750	*PUP11*	purine permease 11	7.00E-06
GLYMA.03G058300	AT2G38170	*RCI4*	RARE COLD INDUCIBLE 4.	2.00E-116
GLYMA.U038600	AT1G58520	*RXW8*		0.00E+00
GLYMA.06G116900	AT1G21650	*SECA2/ANU1*	SECA2/ANU1	0
GLYMA.20G032500	AT4G25350	*SHB1*	SHORT HYPOCOTYL UNDER BLUE1	0.00E+00
GLYMA.10G229300	AT1G62280	*SLAH1*	SLAC1 HOMOLOGUE 1	6.00E-58
GLYMA.09G126900	AT4G27970	*SLAH2*	SLAC1 homologue 2	0.00E+00
GLYMA.16G173600	AT5G24030	*SLAH3*	SLAC1 HOMOLOGUE 3	2.00E-147
GLYMA.10G249500	AT5G26340	*STP13*	STP13	0.00E+00
GLYMA.05G228400	AT1G77210	*STP14*	sugar transport protein	0.00E+00

Appendix 8. Transporters found in the GO enrichments analysis **(Continue)**

GLYMA.01G238800	AT4G02050	*STP7*	sugar transporter protein 7	0.00E+00
GLYMA.16G156800	AT1G71880	*SUC1*	SUCROSE-PROTON SYMPORTER 1	0.00E+00
GLYMA.12G076800	AT1G22710	*SUC2*	SUCROSE-PROTON SYMPORTER 2	0.00E+00
GLYMA.02G075000	AT2G14670	*SUC8*	sucrose-proton symporter 8	0.00E+00
GLYMA.11G238500	AT4G08620	*SULTR1;1*	sulphate transporter 1;1	2.00E-177
GLYMA.08G207100	AT1G78000	*SULTR1;2,SEL1*	SELENATE RESISTANT 1, SULFATE TRANSPORTER 1;2	0.00E+00
GLYMA.08G138600	AT1G22150	*SULTR1;3*	sulfate transporter 1;3	0.00E+00
GLYMA.14G169700	AT1G22150	*SULTR1;3*	sulfate transporter 1;3	0
GLYMA.18G018900	AT5G10180	*SULTR2;1*	SULFATE TRANSPORTER 2;1	0.00E+00
GLYMA.11G238400	AT1G77990	*SULTR2;2*	SULPHATE TRANSPORTER 2;2	0.00E+00
GLYMA.07G006500	AT4G02700	*SULTR3;2*	sulfate transporter 3;2	0.00E+00
GLYMA.15G014000	AT3G15990	*SULTR3;4*	sulfate transporter 3;4	0

Appendix 8. Transporters found in the GO enrichments analysis **(Continue)**

GLYMA.09G188700	AT5G19600	*SULTR3;5*	SULFATE TRANSPORTER	0.00E+00
GLYMA.03G072700	AT5G13550	*SULTR4;1*	sulfate transporter 4.1	7E-33
GLYMA.13G037900	AT1G21460	*SWEET1*	SWEET1	3.00E-106
GLYMA.06G167000	AT5G50790	*SWEET10*	SWEET10	8.00E-35
GLYMA.08G360500	AT5G50790	*SWEET10*	SWEET10	4E-75
GLYMA.05G202600	AT5G23660	*SWEET12*	SWEET12	1.00E-54
GLYMA.18G301200	AT5G23660	*SWEET12*	SWEET12	1E-84
GLYMA.08G010000	AT5G50800	*SWEET13*	SWEET13	6.00E-96
GLYMA.18G301100	AT5G13170	*SWEET15*	SWEET15	1E-103
GLYMA.09G043200	AT3G16690	*SWEET16*	SWEET16	4.00E-64
GLYMA.15G149800	AT4G15920	*SWEET17*	SWEET17	5.00E-82
GLYMA.15G210400	AT3G14770	*SWEET2*	SWEET2	9.00E-90

Appendix 8. Transporters found in the GO enrichments analysis **(Continue)**

GLYMA.19G009900	AT5G62850	*SWEET5*	SWEET5	1.00E-87
GLYMA.08G025100	AT4G10850	*SWEET7*	SWEET7	4.00E-26
GLYMA.17G080400	AT5G39040	*TAP2/ALS1*	ALUMINUM SENSITIVE 1	0.00E+00
GLYMA.01G157300	AT4G35300	*TMT2*	TONOPLAST MONOSACCHARIDE TRANSPORTER2	3.00E-64
GLYMA.07G144200	AT3G54110	*UCP1*	ARABIDOPSIS THALIANA PLANT UNCOUPLING MITOCHONDRIAL PROTEIN 1	3.00E-180
GLYMA.19G126400	AT2G40900.1	*UMAMIT11*	USUALLY MULTIPLE ACIDS MOVE IN AND OUT TRANSPORTERS 11	1E-138
GLYMA.19G173800	AT2G37460.1	*UMAMIT12*	USUALLY MULTIPLE ACIDS MOVE IN AND OUT TRANSPORTERS 12	5E-174
GLYMA.08G182900	AT5G13670	*UMAMIT15*	USUALLY MULTIPLE ACIDS MOVE IN AND OUT TRANSPORTERS 15	8.00E-69
GLYMA.02G032600	AT4G08300	*UMAMIT17*	USUALLY MULTIPLE ACIDS MOVE IN AND OUT TRANSPORTERS 17	6.00E-06
GLYMA.04G250700	AT1G21890	*UMAMIT19*	USUALLY MULTIPLE ACIDS MOVE IN AND OUT TRANSPORTERS 19	4.00E-67
GLYMA.15G227700	AT1G21890.1	*UMAMIT19*	USUALLY MULTIPLE ACIDS MOVE IN AND OUT TRANSPORTERS 19	2E-108
GLYMA.06G111800	AT4G08290	*UMAMIT20*	USUALLY MULTIPLE ACIDS MOVE IN AND OUT TRANSPORTERS 20	4.00E-41

Appendix 8. Transporters found in the GO enrichments analysis **(Continue)**

GLYMA.08G146100	AT5G64700	*UMAMIT21*	USUALLY MULTIPLE ACIDS MOVE IN AND OUT TRANSPORTERS 21	1.00E-131
GLYMA.05G187900	AT1G43650	*UMAMIT22*	USUALLY MULTIPLE ACIDS MOVE IN AND OUT TRANSPORTERS 21	2.00E-75
GLYMA.15G049900	AT1G68170	*UMAMIT23*	USUALLY MULTIPLE ACIDS MOVE IN AND OUT TRANSPORTERS 23	5.00E-86
GLYMA.15G049700	AT1G25270	*UMAMIT24*		4.00E-09
GLYMA.08G182500	AT1G09380	*UMAMIT25*	USUALLY MULTIPLE ACIDS MOVE IN AND OUT TRANSPORTERS 25	2.00E-73
GLYMA.05G121900	AT1G11460	*UMAMIT26*	USUALLY MULTIPLE ACIDS MOVE IN AND OUT TRANSPORTERS 26	0.001
GLYMA.09G284000	AT4G01440	*UMAMIT31*	USUALLY MULTIPLE ACIDS MOVE IN AND OUT TRANSPORTERS 31	2.00E-112
GLYMA.05G160100	AT3G30340	*UMAMIT32*	USUALLY MULTIPLE ACIDS MOVE IN AND OUT TRANSPORTERS 32	1.00E-127
GLYMA.17G069200	AT4G28040	*UMAMIT33*	USUALLY MULTIPLE ACIDS MOVE IN AND OUT TRANSPORTERS 33	8.00E-86
GLYMA.06G149400	AT4G30420	*UMAMIT34*	USUALLY MULTIPLE ACIDS MOVE IN AND OUT TRANSPORTERS 34	1.00E-33
GLYMA.06G123200	AT1G60050	*UMAMIT35*		1.00E-14
GLYMA.02G032400	AT5G40240	*UMAMIT40*	USUALLY MULTIPLE ACIDS MOVE IN AND OUT TRANSPORTERS 40	5.00E-69

Appendix 8. Transporters found in the GO enrichments analysis **(Continue)**

GLYMA.02G032500	AT5G40210	*UMAMIT42*	USUALLY MULTIPLE ACIDS MOVE IN AND OUT TRANSPORTERS 42	1.00E-66
GLYMA.20G203100	AT5G07050	*UMAMIT9*	USUALLY MULTIPLE ACIDS MOVE IN AND OUT TRANSPORTERS 9	7.00E-51
GLYMA.02G220500	AT4G27870	*VIT*	Vacuolar iron transporter	2.00E-11
GLYMA.05G121600	AT1G21140	*VTL1*	Vacuolar Iron Transporter-Like 1	1.00E-63
GLYMA.20G166100	AT1G76800	*VTL2*	VACUOLAR IRON TRANSPORTER-LIKE 2	4.00E-86
GLYMA.13G206700	AT5G17630	*XPT*	XYLULOSE 5-PHOSPHATE/PHOSPHATE TRANSLOCATOR	1.00E-98
GLYMA.10G172900	AT4G24120	*YSL1*	YELLOW STRIPE LIKE 1	0.00E+00
GLYMA.03G149300	AT2G48020	*ZIF2*	Zinc-Induced Facilitator 2	2.00E-111
GLYMA.06G313500	AT5G13750	*ZIFL1*		2.00E-59
GLYMA.13G186600	AT3G43790	*ZIFL2*	zinc induced facilitator-like 2	0
GLYMA.15G262800	AT3G12750	*ZIP1*	zinc transporter 1 precursor	1.00E-124
GLYMA.07G223200	AT1G31260	*ZIP10*	zinc transporter 10 precursor	2.00E-139

Appendix 8. Transporters found in the GO enrichments analysis **(Continue)**

GLYMA.13G338300	AT1G55910	*ZIP11*	zinc transporter 11 precursor	2.00E-124
GLYMA.15G036300	AT5G59520	*ZIP2*	ZRT/IRT-LIKE PROTEIN 2	2.00E-30
GLYMA.20G063100	AT1G05300.1	*ZIP5*	zinc transporter 5 precursor	5E-96
GLYMA.20G123300	AT1G15150.1			6E-161
GLYMA.04G097900	AT5G65380	-	-	8.00E-146
GLYMA.11G026300	AT4G23030	-	-	5.00E-162
GLYMA.01G084800	AT1G25530	-	-	0
GLYMA.10G267700	AT1G15170	-	-	3.00E-120
GLYMA.11G166900	AT5G15240	-	-	8.00E-57
GLYMA.02G302100	AT5G55950	-	-	3.00E-168
GLYMA.17G225100	AT1G72820	-	-	5.00E-71
GLYMA.11G066300	AT2G18480	-	-	1.00E-17

Appendix 8. Transporters found in the GO enrichments analysis **(Continue)**

GLYMA.10G267600	AT1G15160	-	-	2.00E-32
GLYMA.02G260300	AT3G56200	-	-	2.00E-14
GLYMA.04G036100	AT5G62730	-	-	2E-128
GLYMA.13G319900	AT1G08230	-	-	2.00E-101
GLYMA.04G175900	AT1G18940	-	-	4.00E-62
GLYMA.04G089000	AT5G49130	-	-	2E-115
GLYMA.06G145200	AT2G40460	-	-	6.00E-53
GLYMA.10G203700	AT2G16980	-	-	2.00E-68
GLYMA.12G099300	AT3G21690	-	-	2.00E-174
GLYMA.01G091800	AT2G03260	-	-	1.00E-119
GLYMA.20G135300	AT1G49960	-	-	0
GLYMA.20G123400	AT1G71140	-	-	1.00E-155

Appendix 8. Transporters found in the GO enrichments analysis **(Continue)**

GLYMA.09G235200	AT3G29060	-	-	0.00E+00
GLYMA.15G262400	AT1G16310	-	-	0.00E+00
GLYMA.08G076300	AT3G43660	-	-	8.00E-64
GLYMA.02G237600	AT1G79520	-	-	2.00E-90
GLYMA.10G267300	AT1G15150	-	-	2.00E-180
GLYMA.19G167000	AT5G46040	-	-	0.00E+00
GLYMA.06G317200	AT5G61520	-	-	6.00E-144
GLYMA.11G252400	AT5G16740	-	-	2.00E-143
GLYMA.04G102100	AT2G04080	-	-	5.00E-49
GLYMA.04G019200	AT1G47670	-	-	0.00E+00
GLYMA.04G069500	AT5G25430	-	-	0.00E+00
GLYMA.11G223900	AT2G37900	-	-	0.00E+00

Appendix 8. Transporters found in the GO enrichments analysis **(Continue)**

GLYMA.10G183300	AT2G03240	-	-	1E-131
GLYMA.11G042000	AT3G54450	-	-	2E-114
GLYMA.15G107100	AT1G61890	-	-	0
GLYMA.16G142100	AT2G23790	-	-	2.00E-114
GLYMA.15G274600	AT2G38330	-	-	7.00E-83
GLYMA.20G031700	AT1G69480	-	-	0.00E+00
GLYMA.06G091100	AT2G38510	-	-	0
GLYMA.11G226200	AT3G11320	-	-	0
GLYMA.15G099600	AT5G18840	-	-	9.00E-49
GLYMA.18G293200	AT1G66760	-	-	2.00E-145
GLYMA.14G077100	AT5G42610	-	-	2.00E-89
GLYMA.17G088800	AT3G06450	-	-	0.00E+00

Appendix 8. Transporters found in the GO enrichments analysis **(Continue)**

GLYMA.12G181100	AT5G41800	-	-	6.00E-66
GLYMA.11G166500	AT3G28960	-	-	1.00E-152

Appendix 9. Transcription Factors found in the GO enrichments analysis.

G.max Number	Family	Arabidopsis Ortholog number	Name	Full name	E-value
GLYMA_03G231600	AHL	AT5G49700	AHL17	AT-HOOK MOTIF NUCLEAR LOCALIZED PROTEIN 17	6.00E-17
GLYMA_14G066800	AHL	AT4G14465	AHL20	AT-HOOK MOTIF NUCLEAR-LOCALIZED PROTEIN 20	1.00E-42
GLYMA_04G091600	AHL	AT1G14490	AHL28	AT-HOOK MOTIF NUCLEAR LOCALIZED PROTEIN 28	8.00E-49
GLYMA_03G231400	AHL	AT2G45430	AHL22	AT-HOOK MOTIF NUCLEAR-LOCALIZED PROTEIN 22	8.00E-16
GLYMA_20G222000	AHL	AT3G04570	AHL19	AT-HOOK MOTIF NUCLEAR-LOCALIZED PROTEIN 19	2.00E-51
GLYMA_10G008400	AHL	AT4G12050	AHL26	AT-HOOK MOTIF NUCLEAR LOCALIZED PROTEIN 26	7.00E-38
GLYMA_12G184400	alpha/beta-Hydrolases	AT3G44510			1.00E-112
GLYMA_17G076000	ARR-B	AT2G25180	ARR12	response regulator 12	8.00E-106
GLYMA_02G217800	BHLH	AT5G65640	bHLH093	BETA HLH PROTEIN 93	6.00E-78
GLYMA_09G060200	BHLH	AT5G57150			2.00E-84
GLYMA_07G092700	BHLH	AT1G73830	BEE3	BR enhanced expression 3	2.00E-61

Appendix 9. Transcription Factors found in the GO enrichments analysis **(Continue)**

GLYMA_19G132500	BHLH	AT3G56970	bHLH38	BASIC HELIX-LOOP-HELIX 38	1.00E-47
GLYMA_08G152500	BHLH	AT2G42280	FBH4	FLOWERING BHLH 4	1.00E-39
GLYMA_14G071400	BHLH	AT1G75390	bZIP44	basic leucine-zipper 44	2.00E-38
GLYMA_04G199900	BHLH	AT5G50915	bHLH137	BASIC HELIX-LOOP-HELIX 137	2.00E-54
GLYMA_07G055200	BHLH	AT1G01260	bHLH13/JAM2	BASIC HELIX-LOOP-HELIX 137/jasmonate Associated MYC2 LIKE 2	8.00E-152
GLYMA_05G201700	BHLH	AT3G23690	BHLH 77	BASIC HELIX-LOOP-HELIX 77	2.00E-43
GLYMA_16G201400	BHLH	AT4G25410	bHLH126	BASIC HELIX-LOOP-HELIX 126	7.00E-38
GLYMA_16G020500	BHLH	AT4G00870	BHLH14		1.00E-69
GLYMA_09G183500	BHLH	AT1G18400	bHLH44/ BEE1	BASIC HELIX-LOOP-HELIX 44/ BR ENHANCED EXPRESSION 1	3.00E-60
GLYMA_08G009100	BHLH	AT5G50915	bHLH137	BASIC HELIX-LOOP-HELIX 137	2.00E-51
GLYMA_13G284400	BHLH	AT3G20640	bHLH123	BASIC HELIX-LOOP-HELIX 123	3.00E-76
GLYMA_16G156700	BHLH	AT1G61660	bHLH112	BASIC HELIX-LOOP-HELIX 112	1.00E-54

Appendix 9. Transcription Factors found in the GO enrichments analysis **(Continue)**

GLYMA_03G130600	BHLH	AT3G56980	bHLH39	BASIC HELIX-LOOP-HELIX 39	2.00E-46
GLYMA_03G130400	BHLH	AT2G41240	BHLH100	basic helix-loop-helix protein 100	1.00E-36
GLYMA_12G178500	BHLH	AT2G28160	BHLH029/ FIT	BASIC HELIX-LOOP-HELIX PROTEIN 29	2.00E-93
GLYMA_U035800	BHLH	AT4G20970	bHLH162	BASIC HELIX-LOOP-HELIX PROTEIN 162	1.00E-24
GLYMA_15G166800	BHLH	AT5G57150	bHLH35	BASIC HELIX-LOOP-HELIX PROTEIN 35	2.00E-75
GLYMA_01G019700	BHLH	AT5G10570	bHLH61	BASIC HELIX-LOOP-HELIX PROTEIN 61	8.00E-75
GLYMA_05G234500	BHLH	AT1G25330	bHLH75/CES/HAF	helix-loop-helix protein75/CESTA/ HALF FILLED	2.00E-46
GLYMA_19G132600	BHLH	AT5G04150	BHLH101	helix-loop-helix protein101	5.00E-13
GLYMA_16G023900	BHLH	AT2G46510	bHLH17/ATAIB	helix-loop-helix protein17/ABA-INDUCIBLE BHLH-TYPE TRANSCRIPTION FACTOR	1.00E-86
GLYMA_09G204500	BHLH	AT1G32640	bHLH6/ MYC2/JAI1	MYC2/ JASMONATE INSENSITIVE 1	8.00E-167
GLYMA_06G165700	BHLH	AT5G48560	BHLH78/ CIB2	CRY2-interacting bHLH 2	1.00E-43
GLYMA_13G322100	BHLH	AT2G16910	AMS	ABORTED MICROSPORES	1.00E-20

Appendix 9. Transcription Factors found in the GO enrichments analysis **(Continue)**

GLYMA_17G058600	BHLH	AT4G29930	bHLH 27	helix-loop-helix protein 27	3.00E-67
GLYMA_02G233300	BHLH	AT1G29270	-	-	4.00E-08
GLYMA_10G281800	BHLH	AT1G63650	EGL3	ENHANCER OF GLABRA 3	5.00E-16
GLYMA_17G131800	BHLH	AT1G10610	-	-	1.00E-20
GLYMA_09G278100	BHLH	AT4G09820	BHLH42/TT8	BHLH42/TRANSPARENT TESTA 8	1.00E-04
GLYMA_03G247100	bZIP	AT5G28770	bZIP63	BASIC LEUCINE ZIPPER 63	3.00E-62
GLYMA_02G058900	bZIP	AT4G36740	HB40	HOMEOBOX PROTEIN 40	1.00E-40
GLYMA_08G115300	bZIP	AT4G34590	BZIP11	BASIC LEUCINE-ZIPPER 11	1.00E-33
GLYMA_19G244800	BZIP	AT3G54620	BZIP25	BASIC LEUCINE ZIPPER 25	4.00E-38
GLYMA_14G217200	bZIP	AT4G38900	bZIP29	basic leucine-zipper 29	4.00E-65
GLYMA_17G253200	bZIP	AT2G18160	BZIP2	BASIC LEUCINE-ZIPPER 2	5.00E-18
GLYMA_04G029600	BZIP	AT1G75390	bZIP44	basic leucine-zipper 44	9.00E-16

Appendix 9. Transcription Factors found in the GO enrichments analysis **(Continue)**

GLYMA_16G021000	BZIP	AT3G61890	HB-12	HOMEOBOX 12	4.00E-62
GLYMA_U029500	BZIP	AT3G49760	bZIP5	basic leucine-zipper 5	4.00E-15
GLYMA_01G195800	BZIP	AT2G22850	bZIP6	basic leucine-zipper 6	9.00E-21
GLYMA_17G255800	BZIP	AT2G21230	bZIP30	basic leucine-zipper 30	6.00E-60
GLYMA_12G227700	BZIP	AT3G58120	BZIP61	BZIP61	2.00E-50
GLYMA_19G037900	BZIP	AT3G30530	BZIP42	basic leucine-zipper 42	5.00E-51
GLYMA.19G145300	BZIP	AT5G06839	bZIP65	bZIP65	8.00E-172
GLYMA_13G266600	BZR	AT1G78700	BEH4	BES1/BZR1 homolog 4	2.00E-119
GLYMA_08G366900	C2H2	AT1G67030	ZFP6	zinc finger protein 6	5.00E-27
GLYMA_19G214600	C2H2	AT5G06650	GIS2	GLABROUS INFLORESCENCE STEMS 2	6.00E-15
GLYMA_01G036600	C2H2	AT1G68360	GIS3	LABROUS INFLORESCENCE STEMS 3	1.00E-15
GLYMA_02G029100	C2H2	AT1G80730	ZFP1	zinc-finger protein 1	2.00E-09

Appendix 9. Transcription Factors found in the GO enrichments analysis **(Continue)**

GLYMA_03G157400	C2H2	AT5G66730	ENY/IDD1	ENHYDROUS/ INDETERMINATE DOMAIN 1	3.00E-106
GLYMA.20G117800	C2H2	AT1G68360	GIS3	GLABROUS INFLORESCENCE STEMS 3	7.00E-36
GLYMA_07G093900	Calmodulin binding proteins	AT5G57580	-	-	2.00E-107
GLYMA_15G206100	CBF	AT2G24300	CBF	calmodulin binding protein	0
GLYMA_17G092700	CBF	AT5G62570	CBP60a	calmodulin-binding protein 60a	3.00E-150
GLYMA_05G158200	Dof	AT1G29160	COG1	COGWHEEL1	1.00E-52
GLYMA_11G239000	EIL	AT5G10120	TEIL	transcription factor TEIL	3.00E-107
GLYMA_04G217400	ERF	AT2G33710	-	-	4.00E-23
GLYMA_07G025800	ERF	AT5G25190	ESE3	ethylene and salt inducible 3	0
GLYMA_10G007100	ERF	AT3G23230	ERF98/TDR1	ETHYLENE RESPONSE FACTOR 98	9.00E-42
GLYMA_19G164100	ERF	AT3G23240	ERF1	ETHYLENE RESPONSE FACTOR 1	3.00E-41
GLYMA_19G248900	ERF	AT2G31230	ERF15	ETHYLENE RESPONSE FACTOR 15	2.00E-36
GLYMA_13G151900	ERF	AT2G36450	HRD	HARDY	4.00E-22

Appendix 9. Transcription Factors found in the GO enrichments analysis **(Continue)**

GLYMA_11G188200	ERF	AT4G25490	CBF1	C-REPEAT/DRE BINDING FACTOR 1	2.00E-49
GLYMA_13G123000	ERF	AT3G23220	ERF95	ETHYLENE RESPONSE FACTOR 95	1.00E-22
GLYMA_14G106200	ERF	AT1G19210	ERF17	ETHYLENE RESPONSE FACTOR 17	4.00E-38
GLYMA_10G067000	ERF	AT5G51990	CBF4	C-REPEAT-BINDING FACTOR 4	2.00E-38
GLYMA_08G035000	ERF	AT5G11590	TINY2	TINY2	2.00E-48
GLYMA_12G086200	ERF	AT4G25470	CBF2	C-REPEAT/DRE BINDING FACTOR 2	8.00E-45
GLYMA_13G166700	ERF	AT1G15360	SHN1/WIN1	WAX INDUCER 1	1.00E-62
GLYMA_05G049900	ERF	AT1G63030	DDF2	DWARF AND DELAYED FLOWERING 2	2.00E-37
GLYMA_02G132500	ERF	AT2G33710	-	-	2.00E-25
GLYMA_01G231000	ERF	AT1G33760	ERF022	ETHYLENE RESPONSE FACTOR022	1.00E-34
GLYMA_01G225000	ERF	AT1G64380	-	-	2.00E-51
GLYMA_12G117000	ERF	AT5G44210	ERF-9	ERF DOMAIN PROTEIN 9	6.00E-31

Appendix 9. Transcription Factors found in the GO enrichments analysis **(Continue)**

GLYMA_10G193400	ERF	AT4G13620	-	-	1.00E-55
GLYMA_19G026000	ERF	AT5G19790	RAP2.11	related to AP2 11	8.00E-22
GLYMA_20G168500	ERF	AT1G43160	RAP2.6	related to AP2 6	2.00E-09
GLYMA_20G155200	ERF	AT5G52020	-	-	1.00E-28
GLYMA_02G080200	ERF	AT5G50080	ERF110	ethylene response factor 110	8.00E-27
GLYMA_05G186700	ERF	AT5G64750	ABR1	ABA REPRESSOR1	5.00E-32
GLYMA_13G112400	ERF	AT1G74930	ORA47	ORA47	2.00E-48
GLYMA_11G014200	ERF	AT1G71450	FUF1	FYF UP-REGULATING 321 FACTOR 1	3.00E-64
GLYMA_03G111700	ERF	AT2G44840	ERF13	ETHYLENE-RESPONSIVE ELEMENT BINDING FACTOR 13	9.00E-50
GLYMA_18G206600	ERF	AT2G40340	ERF48	ETHYLENE-RESPONSIVE ELEMENT BINDING FACTOR 48	9.00E-28
GLYMA_15G025100	ERF	AT4G25480	CBF3	C-REPEAT BINDING FACTOR 3	1.00E-24
GLYMA_19G163900	ERF	AT5G51190	ERF105	ethylene response factor 105	1.00E-19

Appendix 9. Transcription Factors found in the GO enrichments analysis **(Continue)**

GLYMA_09G147200	ERF	AT5G25810	ERF040	ETHYLENE RESPONSE FACTOR 40,	2.00E-21
GLYMA_17G047300	ERF	AT5G21960	ERF016	ETHYLENE RESPONSE FACTOR 016	6.00E-37
GLYMA_20G155100	ERF	AT2G35700	ERF38	ERF FAMILY PROTEIN 38	7.00E-32
GLYMA_17G131900	ERF	AT1G12610	DDF1	DWARF AND DELAYED FLOWERING 1	7.00E-47
GLYMA_20G197000	ERF	AT4G39780	-	-	2.00E-27
GLYMA_15G077100	ERF	AT1G28370	ERF11	ERF DOMAIN PROTEIN 11	4.00E-21
GLYMA_02G067600	ERF	AT5G13910	LEP	LEAFY PETIOLE	7.00E-30
GLYMA_13G236500	ERF	AT3G15210	ERF4	ETHYLENE RESPONSIVE ELEMENT BINDING FACTOR 4	1.00E-21
GLYMA_15G085400	ERF	AT4G23750	CRF2/TMO3	CYTOKININ RESPONSE FACTOR 2/TARGET OF MONOPTEROS 3	2.00E-08
GLYMA_03G116700	ERF	AT2G44940	ERF34	ETHYLENE-RESPONSIVE TRANSCRIPTION FACTOR 34	1.00E-50
GLYMA_19G104200	ERF	AT5G61890	ERF114	ETHYLENE RESPONSE FACTOR 114	9.00E-30
GLYMA_18G281400	ERF	AT5G13330	Rap2.6L	related to AP2 6l	8.00E-27

Appendix 9. Transcription Factors found in the GO enrichments analysis **(Continue)**

GLYMA_03G162600	ERF	AT5G43410	ERF96	ETHYLENE RESPONSE FACTOR 96	5.00E-21
GLYMA_01G216000	ERF	AT1G01250	-	-	8.00E-15
GLYMA_10G239400	ERF	AT4G32800	ERF043	ETHYLENE RESPONSE FACTOR 43	2.00E-22
GLYMA_06G085700	ERF	AT3G16280	ERF036	ETHYLENE RESPONSE FACTOR 36	1.00E-47
GLYMA_17G174900	ERF	AT4G11660	HSF7/HSFB2B	HEAT SHOCK TRANSCRIPTION FACTOR B2B/ HEAT SHOCK FACTOR 3	6.00E-49
GLYMA_10G007000	ERF	AT1G06160	ERF59	ETHYLENE RESPONSIVE FACTOR 59	1.00E-31
GLYMA_15G180000	ERF	AT4G31060	-	-	1.00E-28
GLYMA_11G053800	ERF	AT4G36920	AP2/ FL1	FLOWER 1	5.00E-107
GLYMA_03G191800	ERF	AT1G12630	-	-	2.00E-25
GLYMA_10G194200	ERF	AT5G07580	ERF106	ethylene response factor	9.00E-33
GLYMA_16G147500	ERF	AT5G07310	ERF115	ETHYLENE RESPONSE FACTOR 115	2.00E-27
GLYMA_06G058400	ERF	AT1G21910	DREB26	DEHYDRATION RESPONSE ELEMENT-BINDING PROTEIN 26	1.00E-26

Appendix 9. Transcription Factors found in the GO enrichments analysis **(Continue)**

GLYMA_10G239300	ERF	AT2G25820	ESE2	ethylene and salt inducible 2	2.00E-15
GLYMA_20G196400	ERF	AT5G47220	ERF2	ETHYLENE RESPONSIVE ELEMENT BINDING FACTOR 2	2.00E-30
GLYMA_03G017300	ERF	AT4G11140	CRF1	cytokinin response factor 1	3.00E-11
GLYMA_04G201900	ERF	AT2G47520	ERF71	ETHYLENE RESPONSE FACTOR 71	3.00E-14
GLYMA_06G148400	ERF	AT3G16770	ERF72	ETHYLENE RESPONSE FACTOR 72	7.00E-16
GLYMA_08G257300	ERF	AT4G34410	ERF109	ETHYLENE RESPONSE FACTOR 109	7.00E-19
GLYMA_16G199000	ERF	AT4G16750	ERF39	ETHYLENE RESPONSE FACTOR 39	1.00E-16
GLYMA_09G072000	ERF	AT4G06746	RAP2.9	RELATED TO AP2 9	4.00E-22
GLYMA_08G202300	ERF	AT3G60490	ERF35	ETHYLENE-RESPONSIVE TRANSCRIPTION FACTOR 35	2.00E-38
GLYMA_20G195900	ERF	AT5G47230	ERF5	ETHYLENE RESPONSIVE ELEMENT BINDING FACTOR- 5	9.00E-37
GLYMA_02G006200	ERF	AT4G17490	ERF6	ETHYLENE RESPONSIVE ELEMENT BINDING FACTOR 6	4.00E-19
GLYMA_02G261700	ERF	AT5G05410	DREB2	DEHYDRATION-RESPONSIVE ELEMENT BINDING PROTEIN 2	1.00E-29

Appendix 9. Transcription Factors found in the GO enrichments analysis **(Continue)**

GLYMA_07G212400	ERF	AT4G27950	CRF4	cytokinin response factor 4	9.00E-19
GLYMA_13G060600	ERF	AT1G72360	ERF73	ETHYLENE RESPONSE FACTOR 73	7.00E-12
GLYMA_19G192400	ERF	AT1G77200	-	-	4.00E-16
GLYMA_08G216600	ERF	AT5G11190	SHN2	shine2	3.00E-19
GLYMA_05G062100	ERF	AT4G36900	RAP2.10	RELATED TO AP2 10	1.00E-23
GLYMA_03G162500	ERF	AT4G17500	ERF100	ETHYLENE RESPONSE FACTOR	4.00E-17
GLYMA_07G078600	ERF	AT5G53290	CRF3	cytokinin response factor 3	2.00E-09
GLYMA_03G162400	ERF	AT5G61600	ERF104	ETHYLENE RESPONSE FACTOR 104	9.00E-05
GLYMA_16G079600	ERF	AT3G61630	CRF6	cytokinin response factor 6	1.00E-29
GLYMA_01G232000	ERF	AT1G71520	-	-	5.00E-38
GLYMA_03G162700	ERF	AT4G18450	-	-	1.00E-17
GLYMA_10G036600	ERF	AT5G61590	ERF107/DEWAX	ETHYLENE RESPONSE FACTOR 107/DECREASE WAX BIOSYNTHESIS, DEWAX	7.00E-20

Appendix 9. Transcription Factors found in the GO enrichments analysis **(Continue)**

GLYMA_02G006300	ERF	AT1G03800	ERF10	ETHYLENE RESPONSE FACTOR 10	4.00E-14
GLYMA_14G123900	ERF	AT2G4631	CRF5	cytokinin response factor 5	3.00E-31
GLYMA_19G163700	ERF	AT1G53910	RAP2.12	related to AP2 12	2.00E-13
GLYMA_04G057700	ERF	AT2G23340	DEAR3	DREB and EAR motif protein 3	2.00E-24
GLYMA_05G049800	ERF	AT3G50260	ERF011/CEJ1/DEAR1	COOPERATIVELY REGULATED BY ETHYLENE AND JASMONATE 1	1.00E-11
GLYMA_10G036700	ERF	AT1G22190	RAP2.4/WIND2	WRKY DNA-BINDING PROTEIN 72	5.00E-12
GLYMA_13G123100	ERF	AT1G28360	ERF12	ERF DOMAIN PROTEIN 12	2.00E-10
GLYMA_12G226600	ERF	AT1G53170	ERF8	ETHYLENE RESPONSE FACTOR 8	1.00E-20
GLYMA_17G145400	ERF	AT2G20880	ERF53	ERF domain 53	4.00E-13
GLYMA_19G178200	ERF	AT2G28550	TOE1/RAP2.7	TARGET OF EARLY ACTIVATION TAGGED/RELATED TO AP2.7	1.00E-107
GLYMA_20G203700	ERF	AT5G18560	PUCHI	PUCHI	1.00E-10
GLYMA_17G219700	ERF	AT4G28140	ERF54	ETHYLENE RESPONSIVE FACTOR54	2.00E-19
GLYMA_18G051500	ERF	AT4G27950	CRF4	cytokinin response factor 4	0.98

Appendix 9. Transcription Factors found in the GO enrichments analysis **(Continue)**

GLYMA_08G145300	ERF	AT5G25390	SHN3	shine3	8.00E-20
GLYMA_05G200100	ERF	AT1G75490	-	-	3.00E-13
GLYMA_11G036400	ERF	AT1G46768	RAP2.1	related to AP2 1	2.00E-19
GLYMA_07G017300	ERF	AT1G22810	ERF019	ERF019	1.00E-19
GLYMA_16G164800	ERF	AT2G22200	-	-	9.00E-14
GLYMA_14G147500	ERF	AT1G77640	-	-	2.00E-25
GLYMA_17G143900	ERF	AT3G57600	-	-	3.00E-19
GLYMA_04G067200	ERF	AT3G20310	ERF7	ETHYLENE RESPONSE FACTOR 7	5.00E-12
GLYMA.09G052900	ERF	AT3G15210	ERF 4	Ethylene response factor 4	3.00E-12
GLYMA.07G250100	ERF	AT5G13910	LEP	Leafy petiole	4.00E-34
GLYMA.17G024300	ERF	AT4G06746	RAP2.9	RAP2.9	3.00E-13
GLYMA_17G127500	GRAS	AT1G66350	RGL1	RGA-like 1	4.00E-75

Appendix 9. Transcription Factors found in the GO enrichments analysis **(Continue)**

GLYMA_06G26 5500	GRAS	AT5G48150	PAT1	phytochrome a signal transduction 1	9.00E-178
GLYMA_04G15 0500	GRAS	AT1G14920	RGA2	GIBBERELLIC ACID INSENSITIVE, RESTORATION ON GROWTH ON AMMONIA 2	1.00E-141
GLYMA_12G13 7700	GRAS	AT1G50600	SCL5	scarecrow-like 5	4.00E-165
GLYMA_13G28 5400	GRAS	AT2G04890	SCL21	SCARECROW-like 21	1.00E-163
GLYMA_02G07 4800	GRAS	AT3G54220	SGR1/SCR	SCARECROW/SHOOT GRAVITROPISM 1	1.00E-50
GLYMA_11G15 0200	GRAS	AT1G50420	SCL3	scarecrow-like 3	5.00E-150
GLYMA_07G15 4300	GRAS	AT5G66770	GRAS 32	SCARECROW gene regulator	4.00E-13
GLYMA_13G08 1700	GRAS	AT4G08250	-	-	6.00E-121
GLYMA_12G21 6100	GRAS	AT4G17230	SCL13	SCARECROW-like 13	7.00E-133
GLYMA_09G13 3600	GRAS	AT5G52510	SCL8	SCARECROW-like 8	5.00E-104
GLYMA_12G19 7300	GRAS	AT3G49950	GRAS 18	GRAS 18	5.00E-120
GLYMA_04G25 1900	GRAS	AT5G41920	SCL23	SCARECROW-LIKE 23	8.00E-54

Appendix 9. Transcription Factors found in the GO enrichments analysis **(Continue)**

GLYMA_06G213100	GRAS	AT3G03450	RGL2	RGA-like 2	3.00E-129
GLYMA_17G162800	GRAS	AT5G67411	-	-	1.00E-68
GLYMA_05G103400	GRAS	AT4G37650	SGR7	SHOOT GRAVITROPISM 7	4.00E-44
GLYMA_13G304900	GRAS	AT2G37650	-	-	3.00E-35
GLYMA_17G007600	GRAS	AT1G21450	SCL1	SCARECROW-like 1	7.00E-124
GLYMA_10G038500	GRAS	AT2G01570	RGA/RGA1	REPRESSOR OF GA1-3 1	9.00E-51
GLYMA_08G146900	GRAS	AT1G55580	SCL18	SCARECROW-LIKE 18	2.00E-43
GLYMA_13G345700	GRAS	AT1G63100	SCL28	SCL28	2.00E-31
GLYMA_18G123500	Homeobox	AT1G69780	HB13	HOMEOBOX 13	1.00E-105
GLYMA_11G035900	Homeobox	AT4G16780	HB2	HOMEOBOX PROTEIN 2	1.00E-93
GLYMA_02G171300	Homeobox	AT5G06710	HAT14	HOMEOBOX FROM ARABIDOPSIS THALIANA	1.00E-64
GLYMA_13G102800	Homeobox	AT3G60390	HAT3	homeobox-leucine zipper protein 3	9.00E-46

Appendix 9. Transcription Factors found in the GO enrichments analysis **(Continue)**

GLYMA_14G09 1000	Homeobox	AT4G37790	ABIG1/HAT22	ABA INSENSITIVE GROWTH 1/ homeobox-leucine zipper protein 22	1.00E-43
GLYMA_02G05 6100	Homeobox	AT2G18350	ZHD6	HOMEOBOX PROTEIN 24	8.00E-59
GLYMA_12G07 7800	Homeobox	AT2G27990	BLH8/PNF	BEL1-LIKE HOMEODOMAIN 8/ POUND-FOOLISH	3.00E-76
GLYMA_07G26 3600	Homeobox	AT4G08150	BP1/KNAT1/BP	BREVIPEDICELLUS/ BREVIPEDICELLUS 1/ KNOTTED-LIKE FROM ARABIDOPSIS THALIANA	7.00E-88
GLYMA_15G16 8800	Homeobox	AT2G22800	HAT9	HAT9	1.00E-49
GLYMA_02G02 2300	Homeobox	AT3G01470	HD-ZIP-1/HAT5	HOMEOBOX 1/HOMEOBOX 1	9.00E-45
GLYMA_09G10 9700	Homeobox	AT5G47370	HAT2	HAT2	8.00E-50
GLYMA_09G17 0500	Homeobox	AT4G24660	MEE68/HB22	MATERNAL EFFECT EMBRYO ARREST 68/HOMEOBOX PROTEIN 22	2.00E-41
GLYMA_07G10 7200	Homeobox	AT5G60480	HB26	HOMEOBOX PROTEIN 26	8.00E-34
GLYMA_07G23 0200	Homeobox	AT1G69600	HB29	HOMEOBOX PROTEIN 29	4.00E-51
GLYMA_19G15 9500	HSF	AT3G22830	HSFA6B	HEAT SHOCK TRANSCRIPTION FACTOR A6B	4.00E-93
GLYMA_01G18 5800	HSF	AT4G36990	HSF4	HEAT SHOCK FACTOR 4	3.00E-78

Appendix 9. Transcription Factors found in the GO enrichments analysis **(Continue)**

GLYMA_10G029600	HSF	AT3G51910	HSFA7A	HEAT SHOCK TRANSCRIPTION FACTOR A7A	3.00E-84
GLYMA_10G244000	HSF	AT2G26150	HSFA2	HEAT SHOCK TRANSCRIPTION FACTOR A2	3.00E-91
GLYMA_10G066100	HSF	AT5G03720	HSFA3	HEAT SHOCK TRANSCRIPTION FACTOR A3	7.00E-94
GLYMA_04G052000	HSF	AT5G16820	HSF3	HEAT SHOCK FACTOR 3	1.00E-68
GLYMA_05G095900	HSF	AT5G62020	HSFB2A	HEAT SHOCK TRANSCRIPTION FACTOR B2A	2.00E-36
GLYMA_03G135800	HSF	AT2G41690	HSFB3	HEAT SHOCK TRANSCRIPTION FACTOR B3	7.00E-65
GLYMA_19G137800	HSF	AT2G41690	HSFB3	HEAT SHOCK TRANSCRIPTION FACTOR B3	1.00E-62
GLYMA_01G143500	HSF	AT1G32330	ATHSFA1D/HSFA1D	HEAT SHOCK TRANSCRIPTION FACTOR A1D	8.00E-33
GLYMA_13G180200	HSF	AT5G43840	HSFA6A	HEAT SHOCK TRANSCRIPTION FACTOR A6A	5.00E-31
GLYMA_02G036900	KN	AT1G23380	KNAT6	KNOTTED1-LIKE HOMEOBOX GENE 6	6.00E-115
GLYMA_19G034600	MADS	AT1G26310	AGL10	AGAMOUS-LIKE 10	1.00E-71
GLYMA_20G154200	MADS-Box	AT5G62165	AGL42	AGAMOUS-like 42	7.00E-73

Appendix 9. Transcription Factors found in the GO enrichments analysis **(Continue)**

GLYMA_04G159300	MADS-Box	AT5G60910	AGL8	AGAMOUS-LIKE 8	2.00E-105
GLYMA_04G036700	MYB	AT3G50060	MYB77	myb domain protein 77	7.00E-58
GLYMA_09G169300	MYB	AT1G17950	MYB52	myb domain protein 52	4.00E-84
GLYMA_04G242200	MYB	AT1G73410	MYB54	MYB DOMAIN PROTEIN 54	1.00E-61
GLYMA_16G218900	MYB	AT1G69560	MYB105	MYB DOMAIN PROTEIN 105	5.00E-60
GLYMA_19G118500	MYB	AT1G26780	MYB117	MYB DOMAIN PROTEIN 117	6.00E-65
GLYMA_06G036800	MYB	AT5G67300	MYB 44	MYB DOMAIN PROTEIN 44	3.00E-57
GLYMA_06G121200	MYB	AT5G17800	MYB56	MYB56	2.00E-57
GLYMA_03G203000	NFY	AT5G06510	NF-YA10	nuclear factor Y, subunit A10	6.00E-52
GLYMA_15G118800	NF-Y	AT4G14540	NF-YB3 |	uclear factor Y, subunit B3	2.00E-72
GLYMA_15G153900	NF-Y	AT2G47810	:NF-YB5	nuclear factor Y, subunit B5	2.00E-54
GLYMA_15G129900	NF-Y	AT1G30500	NF-YA7	nuclear factor Y, subunit A7	4.00E-49

Appendix 9. Transcription Factors found in the GO enrichments analysis **(Continue)**

GLYMA_09G023800	NF-Y	AT2G34720	NF-YA4	nuclear factor Y, subunit A4	1.00E-45
GLYMA_12G236800	NF-Y	AT5G12840	NF-YA1	NUCLEAR FACTOR Y, SUBUNIT A1	2.00E-35
GLYMA_10G186800	NF-Y	AT1G04370	ERF97	ETHYLENE-RESPONSIVE ELEMENT BINDING FACTOR 14	1.00E-21
GLYMA_13G107900	NF-Y	AT1G72830	NF-YA3	NUCLEAR FACTOR Y, SUBUNIT A3	7.00E-40
GLYMA_12G217200	NF-Y	AT1G54830	NF-YC3	nuclear factor Y	6.00E-31
GLYMA_20G186200	RAV	AT1G68840	RAV2/EDF2	ETHYLENE RESPONSE DNA BINDING FACTOR 2/ RAV2	9.00E-129
GLYMA_14G053900	SCREAM	AT2G40435	-	-	1.00E-55
GLYMA.18G090500	SWIB/ MDM2	AT4G26810	-	-	1.00E-55
GLYMA_07G080300	TCP	AT2G45680	TCP9	TCP domain protein 9	2.00E-71
GLYMA_05G013300	TCP	AT3G18550	TCP18	TCP18	3.00E-19
GLYMA_17G132400	TCP	AT5G51910	TCP19	TCP domain protein 19	2.00E-66
GLYMA_12G228300	TCP	AT1G53230	TCP3	CYCLOIDEA AND PCF TRANSCRIPTION FACTOR 3	2.00E-42

Appendix 9. Transcription Factors found in the GO enrichments analysis **(Continue)**

GLYMA_18G242000	WRKY	AT5G56270	WRKY2	WRKY DNA-binding protein 2	5.00E-95
GLYMA_14G103100	WRKY	AT1G80840	WRKY40	WRKY DNA-binding protein 40	2.00E-73
GLYMA_18G238200	WRKY	AT4G01250	WRKY22	WRKY DNA-binding protein 22	9.00E-67
GLYMA_15G003300	WRKY	AT4G31800	WRKY18	WRKY DNA-binding protein 18	2.00E-81
GLYMA_08G218600	WRKY	AT2G25000	WRKY60	WRKY DNA-BINDING PROTEIN 60	3.00E-30
GLYMA_04G218700	WRKY	AT5G64810	WRKY51	WRKY DNA-BINDING PROTEIN 51	2.00E-42
GLYMA_07G023300	WRKY	AT4G22070	WRKY31	WRKY DNA BINDING PROTEIN 31	2.00E-25
GLYMA_10G138300	WRKY	AT4G04450	WRKY42	WRKY DNA-binding protein 42	3.00E-75
GLYMA_01G222300	WRKY	AT5G52830	WRKY27	WRKY DNA-BINDING PROTEIN 27	1.00E-21
GLYMA_19G177400	WRKY	AT2G37260	WRKY44	WRKY DNA-BINDING PROTEIN 44	1.00E-105
GLYMA_17G011400	WRKY	AT1G62300	WRKY6	WRKY6	8.00E-117
GLYMA_03G002300	WRKY	AT1G66550	WRKY67	WRKY DNA-binding protein 67	1.00E-18

Appendix 9. Transcription Factors found in the GO enrichments analysis **(Continue)**

GLYMA_19G221700	WRKY	AT4G01720	WRKY47	WRKY DNA-BINDING PROTEIN 47	2.00E-72
GLYMA_05G096500	WRKY	AT2G23320	WRKY15	WRKY DNA-binding protein 15	6.00E-73
GLYMA_03G176600	WRKY	AT2G03340	WRKY3	WRKY DNA-binding protein 3	4.00E-75
GLYMA_08G021900	WRKY	AT4G11070	WRKY41	WRKY DNA-binding protein 2	1.00E-73
GLYMA_15G186300	WRKY	AT5G15130	WRKY72	WRKY DNA-BINDING PROTEIN 72	2.00E-31
GLYMA_19G094100	WRKY	AT5G13080	WRKY75	WRKY DNA-binding protein 75	8.00E-58
GLYMA_13G370100	WRKY	AT1G68150	WRKY9	WRKY DNA-binding protein 9	5.00E-24
GLYMA_09G080000	WRKY	AT1G18860	WRKY61	WRKY DNA-BINDING PROTEIN 61	2.00E-31
GLYMA_14G102900	WRKY	AT1G64000	WRKY56	RKY DNA-binding protein 56	3.00E-19
GLYMA_08G011300	WRKY	AT3G01970	WRKY45	WRKY DNA-BINDING PROTEIN 45	9.00E-41
GLYMA_13G063100	ZHD	AT3G28917	MIF2	mini zinc finger 2	2.00E-23
GLYMA_02G058500		AT3G50700	IDD2	indeterminate(ID)-domain 2	4.00E-108

Appendix 9. Transcription Factors found in the GO enrichments analysis **(Continue)**

GLYMA_17G010200		AT1G62360	SHL	SHOOT MERISTEMLESS	2.00E-127
GLYMA_19G208900		AT1G03840	MGP/IDD3	INTERDETERMINATE DOMAIN 3/ MAGPIE	3.00E-107
GLYMA_13G203700		AT3G57670	WIP2	WIP domain protein 2	6.00E-120
GLYMA_01G129700		AT3G56220	-	-	1.00E-45
GLYMA_04G200500		AT3G26744	ICE1/SCRM/ATICE1	INDUCER OF CBP EXPRESSION 1/SCREAM/INDUCER OF CBF EXPRESSION 1	2.00E-120
GLYMA_02G144400		AT4G02670	IDD12	indeterminate(ID)-domain 12	2.00E-111
GLYMA_08G274200		AT1G12860	ICE2/SCRM2	NDUCER OF CBF EXPRESSION 2/ SCREAM 2	3.00E-29

Appendix 10. Oppositely expressing genes between two cultivars under high pH growth conditions.

Gene (Glyma Number)	AGI Number	Name	Tissue	Fold Change	
				Arısoy	Sa-88
GLYMA_09G282900	AT2G29090	*CYP707A2*	Roots	2.08	-2.64
GLYMA_07G265500	-	-	Roots	2.08	-2.53
GLYMA_04G109500	AT5G17680	-	Roots	2.14	-3.99
GLYMA_11G030800	AT1G12240	*AtVI2 , FRUCT4*	Roots	4.18	-2.50
GLYMA_17G177000	AT3G50610	*CEP9*	Roots	4.36	-3.45
GLYMA_14G019500	AT1G79440	*ALDH5F1 ,ENF1*	Roots	-2.52	2.094
GLYMA_01G131100	AT2G30970	*ASP1*	Leaves	5.10	-3.42
GLYMA_12G200400	AT4G10270	*WIP4*	Leaves	2.99	-3.00
GLYMA_15G274200	AT1G70890	*MLP43*	Leaves	3.32	-2.13
GLYMA_18G082700	AT3G07040	*RPM1*	Leaves	5.16	-2.2
GLYMA_18G208300	AT2G15480	*UGT73B5*	Leaves	2.94	-2.29
GLYMA_19G192400	AT2G36450	*HRD, Hardy*	Leaves	3.52	-3.07
GLYMA_03G252500	AT3G04290	*LT1*	Leaves	-3.23	4.45
GLYMA_17G132800	AT4G22920	*ATNYE1*	Leaves	-3.99	2.71
GLYMA_17G191800	-	-	Leaves	-4.52	2.87

CURRICULUM VITAE

Amir Maqbool was born on He completed his higher secondary education from Afterwards he joined Bahauddin Zakariya University, Multan Pakistan in 2011 for his undergraduate studies. He completed his B.Sc (Hons) in Agriculture from Department of Plant Breeding And Genetics, Faculty of Agricultural Sciences and Technologies in September 2015. Afterwards he enrolled in the Graduate School of Natural and Applied Sciences, Department of Agricultural Genetic Engineering at Niğde Ömer Halisdemir University, Niğde, Türkiye to pursue his master's education under the Supervision of Assistant Professor Dr. Emre Aksoy. During his master thesis research, he worked on 'Physiological Biochemical and Molecular Response of Different Soybean Cultivars Under Iron Deficiency'. Afterwards he has done doctorate (Ph.D.) in Agricultural Genetic Engineering under the Supervision of Assistant Professor Dr. Emre Aksoy. Amir Maqbool boasts nearly eight years of experience in the intricate realm of metals homeostasis in plants. His research primarily focuses on identification of novel metal transporters in plants and developing crop plants efficient in the uptake of essential metals required for plant growth. Furthermore, Maqbool extends his research pursuits to unravelling the intricacies of metal homeostasis in yeast, alongside an avid exploration of bioremediation strategies leveraging microorganisms. Through the strategic integration of interdisciplinary methodologies, Maqbool aspires to the development of novel fertilizers and plant varieties proficient in the efficient uptake of essential metals, thereby contributing to the advancement of agricultural sustainability and productivity. He knows English, Urdu, Turkish and Punjabi languages.

PUBLICATIONS FROM THESIS

SCI INDEX:

Maqbool, A., Şahin, A., Bakhsh, A. and Aksoy, E., 2023. Genome-wide identification of QTLs associated with iron deficiency tolerance in soybean reveals GATA12 as the integrator of iron signaling in roots. ***Turkish Journal of Botany***, *47*(6), pp.511-528.

SCIENTIFIC CONFERENCES

Amir MAQBOOL, Erdem ANIL, Sevgi CALISKAN and Emre AKSOY, **"**Transcriptomic Analysis of Two IDC-Tolerant Soybean Varieties Revealed a Sub-family of UMAMIT Amino Acid Transporters are Linked to Iron Uptake and Translocation in Plants" **EMBO Workshop** Virtual 26-27 April 2021. (**Oral Presentation**)

Amir MAQBOOL, Sevgi CALISKAN and Emre AKSOY, "Iron Deficiency Chlorosis in Soybean: Efforts in Turkey to Counter This Threat" **2021 Soybean Breeder's Workshop Feb. 22-24,2021.** (**Oral Presentation**)

Amir MAQBOOL, Sevgi CALISKAN and Emre AKSOY, "Evaluating the effects of iron fertilization on IDC (Iron Deficiency Chlorosis) tolerant and sensitive soybean cultivars under high pH conditions". **Turkcose 2021, ID170 (Poster Presentation)**

Amir MAQBOOL, Allah BAKSH and Emre AKSOY, "In Silico analysis of QTLs associated with iron efficiency in soybean lead to identification of GATA transcription factors involved in iron homeostasis" **2022 Soybean Breeder's Workshop (Oral Presentation)**

Amir MAQBOOL, Sevgi CALISKAN, Sebastien THOMINE and Emre AKSOY "Transcriptomics Insights of IDC Tolerant Soybean Varieties under High pH Indicates a Sub-family of Amino Acid Transporters are Linked to Iron Homeostasis in Plants" **30 August-2 September 2022**, **STSM CA-19116 'Trace Metals Metabolism in Plants' Ankara, Turkey (Oral Presentation)**

Amir MAQBOOL, Sebastien THOMINE and Emre AKSOY, **"Roles of Amino Acid Transporters for Metal Transport in Plants and Yeast"** In Vitro Biology Meeting, June 10 – 14, 2023 Hilton Norfolk the Main – Norfolk, Virginia (Virtual Participation) **(Oral Presentation)**

Amir MAQBOOL, Sebastien THOMINE and Emre AKSOY, "RNA-Seq Analyses of Iron Deficiency Chlorosis Tolerant Soybean Varieties Indicates a Sub-family of Amino Acid Transporters are Linked to Iron Homeostasis in Plants" **April 13-14, 2023**, **STSM CA-19116 'Trace Metals Metabolism in Plants' Smolenice Castle near Bratislava, Slovakia (Oral Presentation)**